Inactivation mechanisms of *Geobacillus* and *Bacillus* spores during high pressure thermal sterilization

vorgelegt von
Diplom-Ingenieur
Alexander Mathys

von der Fakultät III – Prozesswissenschaften
der Technischen Universität Berlin

zur Erlangung des akademischen Grades
Doktor der Ingenieurwissenschaften
- Dr.-Ing. -
genehmigte Dissertation

Promotionsausschuss:
Vorsitzender: Prof. Dr. Dipl.-Ing. Frank-Jürgen Methner
1. Berichter: Prof. Dr. Dipl.-Ing. Dietrich Knorr
2. Berichter: Dr. Dipl.-Ing. Volker Heinz
Tag der wissenschaftlichen Aussprache: 04.04.2008

Berlin 2008
D-83

Dedicated to my family, to the friends I have and to the friend I lost…

Zusammenfassung

Hochdrucksterilisation als neuartige Technologie kann minimal behandelte Produkte höchster Qualität im Vergleich zur thermischen Konservierung erzeugen. Bisher gelang keine erfolgreiche Einführung in die Lebensmittelindustrie, oft begründet durch die wenig bekannten Inaktivierungsmechanismen hoch resistenter bakterieller Sporen. Diese Studie entwickelt und verwendet neue analytische Werkzeuge zur wesentlichen Verbesserung des Verständnisses dieser Mechanismen unter Druck- und Temperaturbedingungen. Biophysikalische Analysen zeigten, dass die oft gefundene lag-Phase („Schulterformation") bei thermischer Inaktivierung durch Kinetiken erster Ordnung mit Berücksichtigung der Sporenagglomerationsgröße beschrieben werden kann. Zwei limitierende Fälle der mathematischen Modellierung wurden unterschieden: dreidimensionale Kugelpackung für maximale und zweidimensionale Kreispackung für minimale Sporenanzahl bei einem bestimmten Agglomerat. Physiologische Analysen detektierten für druckbehandelte Sporen vier Sub-Populationen durch Durchflusszytometrie, für welche ein Drei-Schritt-Model der Inaktivierung vorgeschlagen wurde. Das Model beinhaltet die Keimung und nachfolgender Hydrolyse des Sporencortex, einen unbekannten Schritt und letztendlich die Inaktivierung mit Abbau der inneren Membran. Chemische und thermodynamische Analysen von verwendeten Puffersystemen lieferten unterschiedliche Verschiebungen des Dissoziationsgleichgewichtes unter Druck- und Temperaturbedingungen. Hitze- und Druckinaktivierung bakterieller Sporen bei verschiedenen pH-Werten in ACES- und Phosphatpuffer bestätigten die modellierten Daten. Die Entwicklung einer Temperaturregelung für eine innovative Hochdruckanlage ermöglichte ideal adiabatische Prozessbedingungen und isotherme Haltezeiten, optimal für die Untersuchung des detaillierten Inaktivierungsmechanismus bei Ultra-Hochdruckbehandlung. Maximale Inaktivierungsraten wurden bei 700 - 800 MPa erreicht, wobei die beobachtete Sporenstabilisierung bei 1100 MPa mit einer kumulativen Verteilung der letalen Effekte, hypothetisch hervorgerufen durch unterschiedliche Keimungsreaktionen, beschrieben wurde. Exemplarisch wurden die generierten Daten zur Analyse industrieller Sterilisationsprozesse verwendet. Ein erweitertes Verständnis der mechanistischen Sporeninaktivierung verbessert die Möglichkeiten einer Kommerzialisierung des vorgestellten Prozesses.

Abstract

High pressure thermal sterilization is an emerging technology that can produce uniform, minimally processed foods of high quality, better than heat treatment alone. At present, it has not yet been successfully introduced into the food industry, possibly due to the less known inactivation mechanism of high resistant bacterial spores. This study developed and used new analytical tools, to improve the understanding of spore mechanisms at high pressures and temperatures.

Biophysical analyses showed that the lag phase often found in thermal spore inactivation ("shoulder formation") can sufficiently be described by first-order inactivation kinetics, when the spore agglomeration size is considered. Two limiting cases have been discriminated in mathematical modeling: three-dimensional, spherical packing for maximum spore count and two dimensional, circular packing for minimum spore count of a particular agglomerate.

Physiological analyses using flow cytometry detected four distinct sub-populations for pressure treated spores, which could be described by a three step model of inactivation. The model involves a germination step following hydrolysis of the spore cortex, an unknown step, and finally an inactivation step with physical compromise of the spore's inner membrane.

Chemical and thermodynamical analyses of commonly used buffer solutions resulted in different shifts of the dissociation equilibrium under pressure and temperature. Heat and pressure inactivation of bacterial spores at different initial pH-values in ACES and phosphate buffer confirmed the data modeled.

The development of a temperature control system for an innovative high pressure unit allowed ideal adiabatic process conditions and isothermal dwell times, which provided an excellent tool to study the spore inactivation mechanisms at ultra-high pressures in detail. Highest inactivation rates were found within 700 - 800 MPa. Spore stabilization at 1100 MPa was explained by using a cumulative lethal effect distribution, which was hypothetically produced by different germination reaction pathways at various pressure levels. The generated data were exemplarily incorporated into analyses of industrial sterilization processes. An improved understanding of the mechanisms of spore inactivation will aid in the food safety assessment of high pressure thermal sterilization in particular, and also assist in the commercialization of this novel process, facilitating adoption by industry.

Acknowledgements

I would like to thank Prof. Dr. Dietrich Knorr for the continuous confidence, scientific advice and, especially, for the great independence he gave to me. Very special thanks to Dr. Volker Heinz for his amazing supervision, inspiration and very helpful discussions. My gratitude is also expressed to Prof. Dr. Frank-Jürgen Methner, for being part of the evaluation committee during the thesis defense. I gratefully acknowledge Belinda Chapman, Michelle Bull and all people of Food Science Australia in North Ryde, Australia for their excellent cooperation and support during my stay there.

This research was supported by the German Ministry of Economics and Technology (BMBF, Grant No. 0330089A), the European Project NovelQ (015710-2 NOVELQ), Food Science Australia, the Commonwealth Scientific and Industrial Research Organization Food Futures National Research Flagship, the German Institute of Food Technology (DIL) and the German Armed Forces Scientific Institute for Protection Technologies-NBC Protection (E/E590/7Z014/3F071).

Thanks to the diploma students Rainer, Kai, Thomas, Markus and Daniel for your support and your activities! Special thanks to Dr. Stefan Töpfl and Dr. Roman Buckow for their advices and many valuable discussions. This thesis has been also possible thanks to the collaboration and discussions with the scientists: Dr. Carole Tonello, Dr. Oliver Schlüter, Dr. Alexander Angersbach, Friedel Schwartz, Dr. Bärbel Niederwöhrmeier, Dr. Hans-Jürgen Marschall, Prof. Dr. Helmar Schubert, Dr. Peter Nünnerich, Dr. Kai Knoerzer, Prof. Dr. Chris Michiels, Antje Fröhlig and many others, to whom I express my thanks.

I also would like to express my gratitude to the colleagues at the Berlin University of Technology, Department of Food Biotechnology and Food Process Engineering, specially, to my room mate Dipl.-Ing. Stefan Boguslawski, Dr. Cornelius Luscher, Irene Hemmerich, Martin Bunzeit, Sophie Uhlig and Gisela Martens for their patience and support. Thanks to my friend Dr. P-Bonny Soh Bejeng Ndikung, who made an excellent and patient work reviewing the English version of the text.

Particular thanks to my parents Christine and Alfonso as well as to my brother Jimmy (FOW!), who gave me everything I need, every time and everywhere.

Thank you very much Danja, for your love and endless support!

Index

List of abbreviations

A	Helmholtz Energy [kJ kg^{-1}]
A_A	Cross-sectional area of a spore agglomerate [μm^2]
A_{spore}	Cross-sectional area of an individual spore [μm^2]
A^-	Base
AC/DC	Alternating / direct current
ACES	N-(2-Acetamido)-2-aminoethanesulfonic acid
ATP	Adenosine 5'-triphosphate
ATCC	American Type Culture Collection
CE diameter	Diameter of a circle with the same area as the particle [µm]
CFU	Colony forming units
CLE	Cortex lytic enzyme
D	Decimal reduction time at specific temperature [min or s]
DNA	Desoxyribonucleic acid
DPA	Pyridine-2,6-dicarboxylic acid or Dipicolinic acid
E_a	Activation energy [kJ mol^{-1}]
F	F-value, equivalent time at reference T for a specific z-value [min]
F_A	Change of agglomeration distribution
FPIA	Flow picture image analysis
FT-IR	Fourier transform infrared spectroscopy
G	Gibbs free energy [kJ kg^{-1}]
GAM	Gifu anaerobic agar medium
GFP	Green fluorescent protein
H	Enthalpy [kJ kg^{-1}]
$\Delta_r H^0$	Standard molar enthalpy [kJ mol^{-1}]
HA	Acid
HP	High pressure
HPF	High power field
I	Ion strength
K	Equilibrium constant
K_a	Acid dissociation constant
K_W	Ion product of water [(mol $kg^{-1})^2$]
LD_{50}	Lethal dose at which 50% of subjects will die
N	Species concentration
N_0	Initial species concentration
N_A	Sum of all agglomerates after the treatment
N_{A0}	Sum of all agglomerates before the treatment
NAS	Nutrient agar + 0.1% w/v starch
NIST	National Institute of Standard and Technology
P	Pressure
PBS	Phosphate buffer system
PE	Polyethene
PEF	Pulsed electric field
PET	Poly(ethylene terephthalate)
PI	Propidium iodide
PID	Proportional-integral-derivative
PLC	Programmable logic controller
PTFE	Polytetrafluoroethylene
R	Correlation coefficient
R_m	Molar gas constant, 8.3145 [cm^3 MPa K^{-1} mol^{-1}]
R^2	Coefficient of determination
RNA	Ribonucleic acid
RNAP	Ribonucleic acid polymerase
S	Entropy [kJ kg^{-1} K^{-1}]
SASP	Small acid soluble protein

SDW	Sterile distilled water
T	Temperature [°C or K]
$T(t)_p$	T(t) for pressure holding times [°C]
U	Internal energy [kJ kg^{-1}]
V	Volume [m^3]
V_A	Volume of a spore agglomerate [μm^3]
V_{spore}	Volume of an individual spore [μm^3]
ΔV	Reaction volume at atmospheric pressure [cm^3 mol^{-1}]
$\Delta V_{intrinsic}$	Volume change because of alteration in binding length and angle [cm^3 mol^{-1}]
$\Delta V_{solvational}$	Volume change because of solvational properties [cm^3 mol^{-1}]
$\Delta V^{\#}$	Activation volume of the reaction [cm^3 mol^{-1}]
3D ORM	Three-fold dynamic optical back-reflection measurement
a_w	Water activity
b	Weibull parameter b
c_p	Specific heat [kJ kg^{-1} K^{-1} or J kg^{-1} K^{-1}]
d	Derivate
i	Spore number per agglomerate
k	Rate constant [min^{-1} or s^{-1}]
k´	Empirical rate constant [min^{-1} or s^{-1}]
lg	log_{10}
n	Reaction order
n	Weibull parameter
p	Pressure [MPa]
p	Survival probability
pH	Decadic logarithm of the activity of hydroxonium ions
pK_a	Decadic logarithm of acid dissociation constant
pOH	Decadic logarithm of the activity of hydroxide ions
q	Heat energy [kJ kg^{-1}]
q	Inactivation probability
q_0	Agglomeration size distribution
q(T)	Volume power of heat source (T) [W m^{-3}]
r	Radius
t	Time [min or s]
t_0	Heating up time [s]
t_{exp}	Experimental holding time [s]
t_{real}	Real holding time [s]
v	Specific volume [m^3 kg^{-1}]
w	Volumetric work [kJ kg^{-1}]
z	z-value at specific pressure (°C), dT for decimal D-value reduction
z_i	Number of elementary charges of the ion i
α_p	Isobaric expansion coefficient [K^{-1}]
β_T	Isothermal compressibility [MPa^{-1}]
γ_i	Activity coefficients for molecule i
Δ	Increment or gradient
ε	Relative static permittivity [-]
η	Dynamic viscosity [µPa s or mPa s]
λ	Thermal conductivity [mW m^{-1} K^{-1} or W m^{-1} K^{-1}]
μ	Chemical potential
ν_i	Velocity of the reaction i
ρ	Density [kg m^{-3}]
σ	Sigma factor, protein subunit
∂	Partial derivative
[]	Concentration of every molecule

Microorganisms and methods for Table 2.1

A	*Alicylobacillus*
B	*Bacillus*
C	*Clostridium*
G	*Geobacillus*
Acy	*A. acidoterrestris*
am	*B. amyloliquefaciens*
ant	*B. anthracis*
bot	*C. botulinum*
cer	*B. cereus*
co	*B. coagulans*
la	*C. laramie*
li	*B. licheniformis*
meg	*B. megaterium*
pas	*C. pasteurianum*
per	*C. perfringens*
pol	*B. polymyxa*
pum	*B. pumilis*
sa	*C. saccharolyticum*
sh	*B. sphaericus*
sp	*C. sporogenes*
st	*G. stearothermophilus*
sub	*B. subtilis*
te	*C. tertium*
ty	*C. tyrobutyricum*
G	germination
I	inactivation
b	biochemical
m	microbiological

Figure list

Table list

1. Introduction

The application of isostatic high pressure as emerging technology in food processing has steadily increased during the past 10 years (Figure 1.1) and in 2007, 110 industrial installations existed worldwide with volumes ranging from 35 to 420 L and an annual production volume of more than 120,000 tons (Tonello Samson, C., 2007, NC Hyperbaric, Spain, personal communication). Most of the vessel volume is used for meat and vegetable products, which are interesting for sterilization processes.

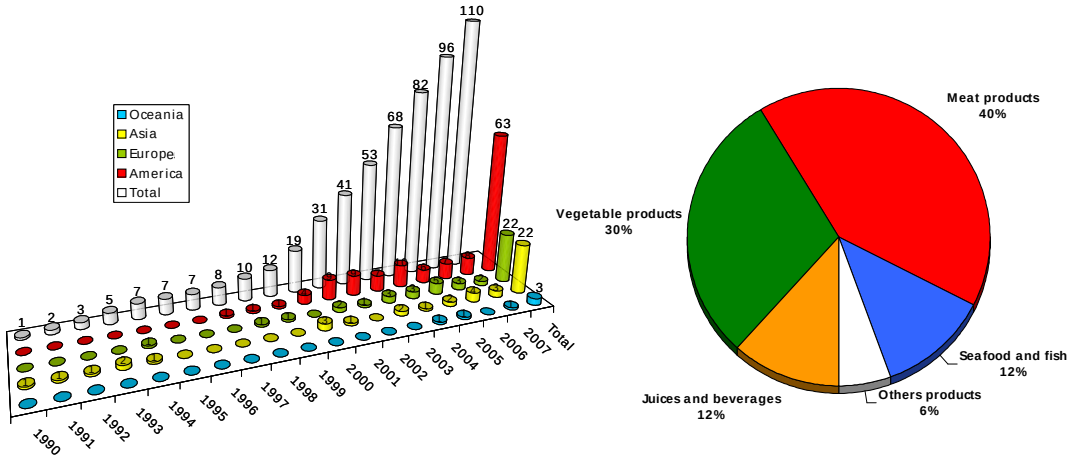

Figure 1.1: HP machines in the world and total vessel volume versus food industries (Tonello Samson, C., 2007, NC Hyperbaric, Spain, personal communication).

High pressure thermal processing as combined technique can homogeneously heat up and cool down products, and it allows the accurate control of the treatment intensity required for bacterial spore inactivation (Heinz & Knorr, 2002). Apart from consumer benefit like enhanced product quality, a key advantage of sterilization under high pressure is its applicability to packed food, making obsolete efforts to prevent recontamination or an aseptic filling process (Toepfl, Mathys, Heinz & Knorr, 2006). Industrial equipments exist with volumes up to 50 L, 700 MPa maximum working pressure and initial temperatures of up to 95 °C (Uhde High Pressure Technologies GmbH, Hagen, Germany; Avure Technologies, Kent, WA, USA).

Although it is widely accepted that sterilization under high pressure is environmentally friendly and can retain the fresh-like characteristics of foods better than heat treatment, it has not yet been successfully introduced into the food industry- possibly due to the less known inactivation mechanisms of high resistant bacterial spores.

Spore germination and subsequent growth can cause food spoilage (e.g. *Geobacillus stearothermophilus*) and potential toxin formation (e.g. *Clostridium botulinum*), which may ultimately lead to food-borne diseases. Botulism derived from the Latin word for sausage "botulus", is rare but extremely dangerous. The neurotoxin A from *C. botulinum* has a lethal dose LD_{50} for humans of 1 ng kg^{-1} (Morin & Kozlovac, 2000). Infant botulism is the most common type of botulism and may occur in children in the first year of life, when *C. botulinum* spores populate the intestines, germinate and produce toxins. The toxin can lead to the feared paralysis of respiratory muscles, which ultimately leads to death (BfR, 2001). Hence, probably stabilized dormant *C. botulinum* spores are also a risk factor. Another worse scenario is pulmonary anthrax, because of the germination of *B. anthracis* in lung macrophage (Guidi-Rontani, Weber-Levy, Labruyere & Mock, 1999). From the financial point of view, the effects of food spoilage or one case of botulism could result in expensive recalls, destroy public confidence in the company's products or at worst, lead to bankruptcy.

Consequently, for microbiological safety and control of this emerging technology, new methodologies for detailed investigations of the heat and pressure effects on bacterial spores are required. The main objective of this basic study was the development and application of new analytical tools to clarify the mechanistic relationships during spore inactivation under high pressure and temperature. Using particle analyzing systems, thermodynamical calculations or approaches and an innovative high pressure sterilization unit, a fundamental assessment of spore inactivation mechanisms and non-linear $\log_{10}$ reductions was performed. Most of the generated data are universal applicable and can also be used for other sterilization techniques.

2. Literature review and background

2.1. Spore inactivation by high pressure- A literature overview

The evolution of high pressure processing started with the development of cannons for the military. A summary of the early cannon development that aimed to contain high pressure is given by Crossland (1995). Based on this research vessel designs for laboratory experiments became available and first measurements of the compressibility of water (Perkins, 1820) and other fluids (Perkins, 1826) were performed. First use of high pressure for biological studies was presented by Regnard (1884) and Certes (1884). Regnard studied the effects of pressures ranging up to 100 MPa on a wide variety of aquatic organisms. Royer (1895) reported as the first the pressure inactivation of bacteria. The first high pressure experiments with microorganisms in a food sample were performed by Hite (1899). Investigations of bacterial spores under pressure followed in 1903 by Chlopin and Tammann, which found that bacterial spores were resistant to hydrostatic pressure. This was also reported by Hite, Giddings and Weakley in 1914 and confirmed in more detail by experiments with different spore strains at pressures from about 300 to 1200 MPa (Larson, Hartzell & Diehl, 1918). Larson et al. (1918) were the first to show the differences in the inactivation of vegetative and sporulated cells of *Bacillus subtilis* at high applied pressure up to 1200 MPa. In 1932, the survival of *B. subtilis* spores after treatment with 1750 MPa for 45 minutes at ambient temperature was found by Basset and Macheboeuf (1932). Extensive research was performed in the following years and an overview of bacterial spore inactivation and / or germination by high pressure is given in Table 2.1.

Table 2.1: Bacterial spore inactivation and germination by high pressure: A literature overview [adapted from Heinz and Knorr (2002) and updated]

Reference	*Organism*		*Treatment*		*Type*	*Method*	*Medium*	*Comments*
	Bacillus	*Clostridium*	*Pressure [MPa]*	*Temperature [°C]*				
Chlopin & Tammann, 1903	ant		0.1-300	0-40	I	m	Nutrient broth	Spore formers are highly resistant; lethal pressure effect increases at higher T
Hite et al., 1914	sub		< 700	Room	I	m	Different foods e.g. fruits	Pressure tolerance of spore was inferred
Larson et al., 1918	sub		300-1200	Room	I	m	Infusorial earth	Still survivors after 14 h at 1200 MPa
Basset et al., 1932	sub		< 1750	Room	I	m		Rapid inactivation of vegetative form; survival of spores up to 1750 MPa and 45 min
Johnson & Zobell, 1948	sub		0.1-60	25-94	I	m	Buffer pH 7 Water	1 lg at 60 MPa/94°C/30 min; 4 lg at 0.1 MPa/94°C/30 min
Timson & Short, 1965	sub		0.1-800	-30-100	I	m	Milk	Spore can survive phase transitions of water, survivors after 700 MPa/100°C /30 min
Clouston & Wills, 1969	pum		0.1-170	25	l/G	m/b	Water Buffer pH 6/8	2 lg at 170 MPa/25°C/270 min; 4.5 lg with simultaneous irradiation
Clouston & Wills, 1970	pum		80-100	25	l/G	m	Buffer pH 6/8	Less than 1 lg at 80 MPa/25°C/100 min
Gould & Sale, 1970	sub, cer co , pum		25-100	20-80	G	m	Water	At 50 and 100 MPa, germination optimum at 50°C
Sale et al., 1970	co, cer, sub	sp	0.1-800	25-75	l/G	m/b	Buffer pH 8	6 lg after (70°C/30 min) + (300 MPa/75°C/120 min)
Murrel & Wills, 1977	sub, pum, cer		50-70	25-44	l/G	m	Buffer pH 6/8	1 lg at 63 MPa /41°C/40 min; germination optimum at 63 MPa/ 50°C
Bender & Marquis, 1982	meg		30-100	24-60	G	m	Buffer pH 6/8	>30 MPa/45°C can induce germination
Butz et al., 1990	st		200-300	40-60	I	m	Salt solution	2.5 lg at 60°C/300 MPa and 360 min
Mallidis & Drizou, 1991	st		1-30	117-128	I	m	Water	5 lg at 10 MPa/123°C/3 min
Taki et al., 1991	li		600	60	I	m	Buffer pH 7	Inactivation at 600 MPa/ 60°C/20 min
Seyderhelm & Knorr, 1992	st		0.1-600	20-90	I	m	Water	6 lg at 350 MPa/80°C/30 min
Hayakawa et al., 1994a	st		0.1-800	20-70	I	m	Water	6 lg at 600 MPa/70°C/ 6 x 5 min oscillatory treatment

continues…

Table 2.1: continued

Reference	*Organism*		*Treatment*		*Type*	*Method*	*Medium*	*Comments*
	Bacillus	*Clostridium*	*Pressure [MPa]*	*Temperature [°C]*				
Hayakawa et al., 1994b	st		0.1-800	20-70	l	m	Water	6 lg at 600 MPa/70°C/6 x 5 min oscillatory treatment
Nishi et al., 1994	lic, sub, pol		50-200	25-60	l/G	m	Milk nutrient broth	6 lg after (200 MPa/60°C/10 min) + (incub. 37°C/60 min) + (6 5°C/30 min)
Okazaki et al., 1994	sub		0.1-500	25-111	l	m	Buffer pH 7	4 lg at 400 MPa/100°C/10 min
Sojka & Ludwig, 1994	sub		20-500	40-80	l/G	m	Germination Medium	>8 lg at 50°C/6 x 30 min/cycling between 150 and 500 MPa
Fornari et al., 1995	cer, li, co, st		200-900	20-70	I	m	PBS buffer pH 7	cer: 5 lg 20°C, 200 MPa/ 1 min+900 MPa/ 1 min li:complete inactivation 800 MPa/5 min /60°C st:complete inactivation 700 MPa /5 min / 70°C co:4 lg at 900 MPa / 5 min / 70°C
Crawford et al., 1996		sp	410-820	80	l	m	Chicken	2 lg at 680 MPa/80°C/20 min and 6 lg with subsequent irradiation (3 kGy)
Gola et al., 1996	cer, li, st, co	sp	300-900		l	m	Buffer pH 7 Truffle cream	st: 5 lg at 700 MPa/70°C/5 min li: 6 lg at 700 MPa/70°C/3 min sp: 2 lg at 900 MPa/80°C/10 min
Ludwig at al., 1996	sub		0.1-500	4-70	l/G	m/b	Physio. NaCl	4.5 lg at 500 MPa/70°C/15 min; 8 lg by oscillation: 70°C/ 7x (1 min/500 MPa + 1 min/ 0.1 MPa)
Kakugawa et al., 1996	st		0.1-400	50-120	l	m	Buffer pH 7	5 lg at 150 MPa/90°C/30 min
Nakayama et al., 1996	sub, st, lic, meg, co		200-1000	5-10	l	m	Water	Less than 1 lg inactivation at 1000 MPa/10°C/40 min
Okazaki et al., 1996	sub, co	sp	0.1-400	35-110	l	m	Buffer pH 7	sub: 6 lg at 400 MPa/65°C/15 min; co: 6 lg at 400 MPa/110°C/18 min; sp: 6 lg at 400 MPa/110°C/18 min
Roberts & Hoover, 1996	co		400	25-70	l	m	Buffer pH 4-7	6 lg at 400 MPa/70°C/30 min/ pH 4/ + Nisin
Arroyo et al., 1997	cer, sub		100-400	10, 20	I	m	Tryptone soy broth	No significant reduction at 400 MPa
Heinz, 1997	sub		0.1-600	5-80	l/G	m/b	Ringer solution	6 lg at 150 MPa/70°C/30 min; depending on the p-T level germination is either initiated/ inhibited
Hölters et al., 1997	sub/st		0.1-500	30-70	G	m/b	Physio. NaCl	Germination at 60 MPa/30°C or 30 MPa/ 50°C

continues...

Table 2.1: continued

Reference	*Organism*		*Treatment*		*Type*	*Method*	*Medium*	*Comments*
	Bacillus	*Clostridium*	*Pressure [MPa]*	*Temperature [°C]*				
Marquis, 1997	meg		100	25	l	m	Aqueous H_2O_2 solutions	0 lg at 100 MPa/25°C/3 h; 5.5 lg at 100 MPa/25°C/3 h i n the presence of 1% H_2O_2
Sojka & Ludwig, 1997	sub		0.1-520	30-50	G	m/b	Physio. NaCl	> 50 MPa/ >30°C can induce germination
Wuytack et al., 1997	sub		100	40	G	m/b	Water	Rate of pressure-induced germination in mutant spores is decreased
Hayakawa et al., 1998	st		30-200	5-100	l	m	Buffer pH 7	6 lg at 200 MPa/95°C/60 min + rapid decompression (1.5 ms) 1 lg at 30 MPa/95°C/720 min + rapid decompression (1.5 ms)
Heinz & Knorr, 1998	sub		50-300	10-70	l/G	m/b	Water	6 lg at 150 MPa/70°C/30 min
Herdegen & Vogle, 1998	sub		0.1-700	40-80	l	m	Peptone solution pH 7	5 lg at (500 MPa/20°C/15 min) + (0.1 MPa/37°C/30 min) + (600 MPa/20°C/15 min)
Mills et al., 1998		sp	60-600	20-80	l	m	Water	2 lg at 0.1 MPa/80°C/10 min + 400 Ma/60°C/70 min
Raso et al., 1998a	cer		250-690	25-60	l/G	m	Buffer pH 7	8 lg at 690 MPa/60°C/1 min (sporulation at 37°C) 6 lg at 690 MPa/60°C/15 min (sporulation at 20°C)
Rovere et al., 1998	cer, li, st, co	bot, sp	700-900	50-70	l	m	Beff broth, Buffer pH 7	At 700 MPa/70°C/5 min: cer, 5 lg; li, 6 lg; st, 5 lg; co, 1 lg at 800 MPa/88°C/9 min: bot, 3 lg,
Wuytack et al., 1998	sub		100-600	40-55	l/G	m/b	Buffer pH 7	3 lg at (600 MPa/40°C/60 min) + (0.1 MPa/55°C/10 min)
Hölters et al., 1999		pas	0.1-500	30-60	l/G	m/b	Physio. NaCl	2 lg at 420 MPa/60°C/75 min 4 lg by oscillation: 60°C/6x(10 min/40 MPa + 5 min/0.1 MPa)
Reddy et al., 1999		bot	689-827	35-60	l	m	Buffer pH 7	5 lg at 827 MPa/40°C/10 min 5 lg at 227 MPa/50°C/5 min

continues...

Table 2.1: continued

Reference	*Organism*		*Treatment*		*Type*	*Method*	*Medium*	*Comments*
	Bacillus	*Clostridium*	*Pressure [MPa]*	*Temperature [°C]*				
Rovere et al., 1999		sp	600-1200	90-110	I	m	Meat broth	D(90°C) at 400/ 600/ 800/ 1200 MPa: 76.9/ 16.7/ 5.3/ 4.38 min D(110°C) at 0.1/ 400/ 600/ 800 MPa: 13.3/ 6.1/ 1.3/ 0.7 min
Wuytack et al., 1999	sub		0.1-600	20-80	I/G	m/b	Various aqueous media	6 lg 500 MPa/ 60°C/ 30 min, different germina tion mechanisms at 100 MPa and 600 MPa use of fluorescent GFP-containing spores
Capellas et al., 2000	sub		60, 500	25, 40	I/G	m	Goat's milk fresh cheese	5 lg 60 MPa/40°C/210 min+ 500 MPa/40°C/15 min 2.7 lg with the same treatment at 25°C
Furukawa et al., 2000	sub		200-400	25-55	I/G	m	Water	>6 lg at 300 MPa/55°C/ 6 cycle a 5 min >4.5 lg at 400 MPa/55°C/1 cycle and 30 min
Meyer, 2000	cer	sp	2 x 690	90	I	m	macaroni cheese	Sterilization after two-pulse treatment 2 x 1 min
Meyer et al., 2000	cer, sub, st	sp	621, 690, 966	60, 90, 105	I	m	food pH > 4.5 fat<10%,a_w>0.8	2 or more cycles 621 MPa/ 105°C lead to sterility with 10 E+6/g spore load
Okazaki et al., 2000	sub, st, co	sp	0.1-400	35-120	I/G	m	PBS buffer(pH 7)	6 lg at 400 MPa/110°C/ B.co (17 min), C.sp(7 min) 4 lg at 400 MPa/113°C/ 10 min B.st wit h tailing
Shearer et al., 2000	sub, cer, co Acy	sp	392	45°C	I/G	m/b	mil k, beef, apple tomato juice	Sucrose laurate(> 1%)+ 392 MPa 45°C ,1 0-15 min lead to 3- 5.5 lg reduction laurate is inhibitory not lethal on spores
Stewart et al., 2000	sub	sp	404	25-90	I	m	Citrate buffer +Nisin +Sucr. laurate	sp at 25°C/30 min/ pH 4 (2.5 lg) pH 7(<0.5 lg) sub at pH 6-7/15 min/ 70°C (5 lg) 25°C(<0.5 lg) +/- synergism of HP/ pH/ Nisin/ sucr. laurate
Wilson & Baker, 2000	sub, st	sp	51-827	75-90	I	m	Meat emulsion	Treatment: 621 MPa/98°C/5 min >5 lg (sp), > 9 lg (sub), > 10 lg (st)
Wuytack et al., 2000	sub		100-600	40	G	m	Water	Different pathway for germination at 100 and 600 MPa
Ananta et al., 2001	st		50-600	60-120	I	m	Mashed broccoli Cocoa mass	6 lg at 600 MPa/80°C/60 min in mash. broccoli 6 lg 600 MPa/90°C/45mi n in cocoa mass
Furukawa et al., 2001	sub, li		200	25-65	I	m	NaCl solution	4 lg(li) at 65°C/180 min; 6 lg(sub) at 65°C/90 m in 1 lg more after filtration and HP
Meyer, 2001	cer	sp	345-965	70-100	I	m	Different food	Two or more cycles of ultra-high pressure were combined with temperature treatment

continues...

Table 2.1: continued

Reference	*Organism*		*Treatment*		*Type*	*Method*	*Medium*	*Comments*
	Bacillus	*Clostridium*	*Pressure [MPa]*	*Temperature [℃]*				
Moerman et al., 2001	sub, st		50- 400	20- 80	I	m	Fried minc. pork Mash.potatoes	sp 5 lg at 400 MPa/80℃/ 60 min in pork sp 5 lg at 400 MPa/80℃/ 60 min in potatoes
Wuytack and Michiels, 2001	sub		100, 600	40	I/G	m/b	Buffer pH 3 - 8	Higher inactivation if first pressure treated at neutral pH + then exposed to low pH for 1 h sensitive to heat inactivation at low pH
De Heij et al., 2002	st		700	121	I	m	Tryptone soy broth	6 lg after 2 x 700MPa/ 121℃/ 90 s
Fujii et al., 2002	cer		500-600	20-40	I	m	Water+argon	Pressure resistance of *B. cereus* spores was affected by a strong 'water ordering' effect
Furukawa et al., 2002	sub		100	45-75	I	m	Water	>6 lg after120 min with different initial concentrations; higher No=higher resistance
Lee et al., 2002	Acy		0.1-621	22,45,71,90	I	m	Apple juice	4 lg 41℃/207 MPa/10 min, 6 lg 71℃/207 MPa and 5 min, 6 lg at 90℃/414 MPa/1 mi n
Krebbers et al., 2002	natural flora		700, 860	75, 85	I	m	Basil	Below detection line after 2 x 950 MPa/75℃/30 s or 2 x 700 MPa/85℃/30 s, initial 4 lg/g spores
Paidhungat et al., 2002	sub		100, 550	Room	G	m/b	KPO_4 (pH 7.4) Water	100 MPa activation of germinant receptors 550 MPa opens channels for DPA release
Balasubramiam et al., 2003	sub		827	50, 70	I	m	PBS, pH 7	Effect of pressure transmitting fluids, sodium benzoate highest dT/dp; 8 lg 827 MPa,70℃
De Heij et al., 2003	st, sub		300-800	84–122	I	m	Tryptone soy broth	6 lg 700 MPa/ 90℃/3 min in standard steel ves sel 10 lg at 700 MPa/ 90℃/ 3 m in in isolated vessel
Farkas et al., 2003	sub		300, 600	Room	I/G	m/b	Nutrient broth	Germination of recombinant sub was accompanied by the emergence of bioluminescence
Furukawa et al., 2003	sub		200-500	25-55	I/G	m	Water	>6 lg at 300 MPa/55℃/6 cycle a 5 min >6 lg at 500 MPa/45℃/1 cycle and 30 min
Igura et al., 2003	sub		100-300	50	I	m	Distilled water	Sporulated at 30℃ highest resistance, increased after demineralization
Kalchayanand et al., 2003		sp,la,per,te	345	60	I/G		Roast beef +Biopreservat.	la alone-extended shelf-life for 84 days at 4℃; with mixture of clostridial spores for 42 days
Krebbers et al., 2003	st		300,500,700	20, 80 90 initial T	I	m	in meat balls in tomato puree	6 lg at 700 MPa/ 20℃/ 2 min 6 lg pulse 2 x 700 MPa/ 80℃/ 30 s
Lopez-Pedemonte … 2003	cer		60-400				Cheese	2.4 lg after 60 MPa/30℃/210 min and 400 MPa/30℃/15 min+Nisin

continues…

Table 2.1: continued

Reference	*Organism*		*Treatment*		*Type*	*Method*	*Medium*	*Comments*
	Bacillus	*Clostridium*	*Pressure [MPa]*	*Temperature [°C]*				
März, 2003	sub	sp	600	60-90	I	m	Salt solution	1-2 lg of sp 600 MPa/ 60°C/ 300 min 6 lg of sp at 600 MPa/ 90°C/ 180 min
Oh and Moon, 2003	cer		0.1-600	20-60	I/G	m/b	Suspension	B. cer sporulated at pH 6 showed more resistance than at pH 7 or pH 8
Reddy et al., 2003		bot	417-827	60-75	I	m	PBS pH 7.0 crabmeat blend	2-3 lg at 827 MPa/ 75°C/ 20 min in PBS same lg reduction in crab meat -->no protection
Watanabe et al., 2003	st, co, sub, cer li		0.1-200 + CO_2	35-95	I	b	Water	HP+CO_2 resulted in 5 lg at 30 MPa/95°C/120 min
Wilson and Baker, 2003	sub, st	sp	500-900	75-130	I	m, b	Phosphate Meat	Mixed spore culture (sub, st, sp) was inactivated 6 lg at 621 MPa/85°C/1 min
Ardia, 2004	st		200-1400	90-130	I	m	PBS, ACES Buffer pH7/ 6	8 lg in p,T diagram up to 1400 MPa/170°C for 3 different holding times(10, 30, 60 s) in PBS and 20 s holding time at pH 6 and 7 in ACES
Ardia et al., 2004a	Acy		0.1-700	initial 80-95	I	m	Orange juice	6 lg in p,T diagram for 5 holding times(10-30 min)
Clery-Barraud et al., 2004	ant		280-500	20-75	I	m		D(75°C) at 0.1/500 MPa: 348/4 min; D(20°C) at 500:160 min
Kalchayanand et al., 2004		te, per, la sp	138-483	25, 50	I/G	m/b	0.1% peptone pediocin AcH nisin A	483 MPa/ 50°C/ 5 min- te: 2.5 l g reduction per, la, sp: 0.1-0.2 lg reduction antimicrobial compound after HP
Margosch et al., 2004a	sub, cer, li, am		200-800	initial 60-80	I/G	m/b	Mashed carrots	>6 lg to no reduction, large resistance variation inact.=2 stage mechanism without germination *B. amyloliquefaciens* suggested target organism
Margosch et al., 2004b	sub, cer, li, am	bot	600-800	80-116	I	m/b	Mashed carrots	5.5 lg to no reduction at 600 MPa/ 80°C/ 1 s inact.=2 stage mechanism without germination *C. botulinum* TMW 2.357 most resistant *B. amyloliquefaciens* suggested target organism
Matser et al., 2004	naturally flora		900	initial 90°C	I/ G	m	Vegetables	>3 lg; all under detection limit of ~1 lg, defined as sterility;2 pressure pulses
Rodriguez et al., 2004	st	bot	400-827	60-75; 92-110	I	m	PBS pH 7.0 (bot) dest.Water (st)	st- z(T) = 34.5°C, z(p)= 370 MPa;model for steady and transient process conditions
Van Opstal et al., 2004	cer		0-600	30-60	I/G	m	Milk	6 lg-500 MPa/ 60°C/ 30 min or two-step treatment 200 MPa/ 45°C/ 30 min and then 60°C/ 10 min

continues...

Table 2.1: continues

Reference	*Organism*		*Treatment*		*Type*	*Method*	*Medium*	*Comments*
	Bacillus	*Clostridium*	*Pressure [MPa]*	*Temperature [°C]*				
Van Schepdael et al., 2004	st, sub		600-950	60-90	I	m	Tryptone soy	5.7 lg of B.st. at 60°C/950 MPa B. sub. at 90°C/700 MPa below detec tion limit
Aoyama et al., 2005a	sub, li, cer, co		60	40	I/G	m	PBS GAM broth	60 MPa/ 40°C/ 24 h sub -PBS: 1.6 lg; GAM broth: 5 lg li, cer, co- GAM broth, 1-3 lg
Aoyama et al., 2005b	sub		0.1-300	20-70	I/G	m	PBS glucose broth	Induction germination started at 10 MPa/ 40°C/1 h 2 lg at 20 MPa/ 60°C/ 1 h in broth 5 lg (PBS and broth) at 300 MPa/ 60°C/ 30 m in
Black et al., 2005	sub		150	initial 37°C	G	m/b	50 mM Tris -HCl pH 7.5	Detection of germinated spores with Syto16 and Flow Cytomerty;effects on pressure germination
De Heij et al., 2005	st, sub	bot, sp	400-800	70–110	I	m	Broth	st D(105°C) at 800 MPa = 20 s
Koutchma et al., 2005	st	sp	600-800;688 in 35 L vessel	91-121	I	m	PBS, Scrambled Egg patties	4.5 lg of C.sp at 800 MPa/108°C/3 min, z(p)~21 °C in PBS, >6 lg at 688 MPa/121°C/3 min in patties >6 lg of B.st at 688 MPa/108°C/5 min in p atties
Moerman, 2005	sub, st	sp, ty, sa	400	20, 50	I	m	Pork Marengo	20°C/30 min sub 1 lg, st 0.2 lg, sp ty sa 0.7 l g 50°C/30 min sub 4 lg, st 1.5 lg, sp ty sa ~3 lg
Farid, 2006	st		0.1 - 87	90 - 125	I	m	Water Milk	Heating a liquid food product to a temperature of 95°C will generate pressure of 700 bar 90 min leads to an inactivation of 4 lg
Gao et al., 2006a	st		432-768	63-97	I	m	Milk buffer	Optima at 86°C/625 MPa/ 14 min-->6 lg Response surface methodology (RSM)
Gao et al., 2006b	sub		323-668	63-97	I	m	Milk buffer	Optima at 87°C/576 MPa/ 13 min-->6 lg Response surface methodology
Islam et al., 2006	sub, coa, st		100	65-85	I	m	Potage, ketchup pH 4/ 7	4-8 lg dependent on pH (4 higher) higher inactivation in potage than ketchup
Lee et al., 2006	Acy		207,414,621	22,45,71,90	I/G	m	Apple juice 17, 35, 70°Brix	17.5°Brix 2 lg at 45°C, 5 lg at 71 and 90°C 30°Brix no effect at 45°C, 2 and 4lg at 71, 90°C 70°Brix, no inactivation
Margosch et al., 2006	am	bot	0.1-1400	70-120 const.	I	m	Tris-His buffer pH 4, 5.15, 6	p,T-diagram for 5 lg reduction of C.bot (pH 5.15) Isothermal conditions, tailing under pressure 4 lg reduction of B.am at 800 MPa/100°C
Patazca et al., 2006	st		500-700	92-111	I	m	Water	D(T,p) values 29.4 to 108.8 s at 92°C, 17 - 76 s at 100°C, 6.1 to 51 s at 111°C within 500-700 MPa

continues…

Table 2.1: continued

Reference	*Organism*		*Treatment*		*Type*	*Method*	*Medium*	*Comments*
	Bacillus	*Clostridium*	*Pressure [MPa]*	*Temperature [℃]*				
Rajan et al., 2006a	am		500-700	95-121	I	m	Egg patty mince	6.8 lg at 600 MPa/121℃/~1.7 min and 700 MPa at 110℃/ 3 min; z (700 MPa) = 28.6℃; z (12 1℃) = 332 M Pa
Rajan et al., 2006b	st		400-700	105	I	m	Egg patty mince Water	4 lg at 700 MPa/ 105℃/ 5 min no inactivation difference in patties and water
Reddy et al., 2006		bot	551-827	40-100	I	m	Crabmeat blend PBS (pH 7)	>6 lg at 827 MPa/ 75℃/ 20 min in both media Crabmeat blend provided no protection
Sasagawa et al., 2006	sub		700	55℃	I/G	m	Orange juice PBS, Acetate	PEF+ HP, 7.1 lg in acetate buffer with pH 3.3 HP main lethal effect, HP 6 lg in orange juice
Scurrah et al., 2006	cer, co, li, pum		600	25, 75-95 initial T	I	m	Skim milk 9.5 % (w,w)	No inactivation to 6 lg at 600MPa/initial 72℃/1min high variability between species
Subramanian et al., 2006	am, sh	ty	700	121	I	m/b	Distilled water	Inactivation determined by FT-IR spectroscopy, adaquate comparison to plate count between 0-8 lg inactivation after different dwell times
Ahn et al., 2007	am, sh	sp, ty	700	105, 121	I	m	Deionized water	sp, ty 6 lg at 700 MPa/ 105, 121℃(2, 0.2 mi n) am 6 lg at 700 MPa/ 105, 121℃(3, 0. 2 min)
Black et al., 2007c	sub		150, 500	50-76	G	m/b	Tris/HCl buffer pH 7.5	Germination detected by flow cytometry (Syto 16) 500 MPa no nutrient-germinantion, but DPA
Mathys et al., 2007a	li		150, 600	10, 37, 77	I/G	m/b	Citrate buffer Nutrient broth	3 step mechanisms of inactivation detected by flow cytometry(PI,S16) with unknown population
Shigeta et al., 2007	sub, cer, pol		20-100	40	I/G	m	PBS glucose broth	60 MPa/ 40℃/ 30-60 min 5 lg germination with nutrients; 2-3 lg without nutrients
Subramanian et al., 2007	sh, am	ty	700	121	I	m	TSB, clostridial medium	Biochemical changes were studied by FT-IR 121℃ no changes in the DPA content pressure leads to release of DPA
Vepachedu et al., 2007	sub		150, 500	Room	G	m/b	Buffer	SpoVAproteins involved in DPA release,perhaps SpoVA proteins component of DPA channel
Mathys et al., 2008	st		500,600,900	80	I	m/b	PBS, ACES buffer (pH 5-8)	Different dissociation equilibrium shifts in buffer with effect on inactivation, up to 1.5 lg different

Organism: sub, *B. subtilis*; st, *G. stearothermophilus*; cer, *B. cereus*; li, *B. licheniformis*; meg, *B. megaterium*; pum, *B. pumilis*; co, *B. coagulans*; pol, *B. polymyxa*; ant, *B. anthracis;* am, *B. amyloliquefaciens*; sh, *B. sphaericus*; Acy, *Alicylobacillus acidoterrestris*; sp, *C. sporogenes*; pas, *C. pasteurianum*; bot, *C. botulinum*; ty, *C. tyrobutyricum*; sa, *C. saccharolyticum*; la, *C. laramie*; per, *C. perfringens*; te, *C. tertium* .
Type (of experiment): I, inactivation; G, germination.
Methodology used: m, microbiological; b, biochemical.
Comments: lg = $\log_{10}$.

Summarizing this literature overview some milestones in high pressure thermal sterilization can be pointed out. After the pioneer work in the beginning of the 20th century, spore germination was detail studied by Clouston and Wills (1969; 1970), as well as Gould and Sale (1970), which showed that low pressures below 200 MPa can trigger spore germination. In 1974 D. C. Wilson presented the synergistic effect of pressure and temperature on spore inactivation at the 34th IFT Annual Meeting, which was also discussed in peer-reviewed publications later by Mallidis and Drizou (1991), as well as Seyderhelm and Knorr (1992). Pressure cycling, as sterilization method came into favor in 1994 with the work from Sojka and Ludwig (1994) as well as Hayakawa et al. (1994a; 1994b), but failed because of high resistant sub-populations and concern in terms of industrial process conditions. Hence, most of the performed studies used one pressure cycle. For a short time it seemed that a combination process with spore germination at pressures below 200 MPa and an additional moderate heat treatment could open up the way to success. However, also this idea failed because a small population of spores in the sample could not be germinated. The following studies investigated some other combinations with electroporation (Kalchayanand, Sikes, Dunne & Ray, 1994) or food additives (Kalchayanand et al., 1994; Roberts & Hoover, 1996). Extensive studies were carried out in the following years, where varied spore resistances led to different results. Matrix effects, different target organisms and properties of the spore suspensions as well as methodic problems complicated also the reproducibility of the suggested sterilization processes. In this matter, basic studies on spores in simple matrices started with ideal adiabatic process conditions and isothermal dwell times in a wide range of pressure and temperature to clarify the detailed inactivation mechanism (Ardia, 2004; Margosch, Ehrmann, Buckow, Heinz, Vogel & Gänzle, 2006). These basic studies will lead to better process conditions or combinations of this "emerging" technology, which are essential to ensure food safety and consumer health.

2.2. High isostatic pressure

2.2.1. Thermodynamics of high isostatic pressure

The fundamental behavior of a thermodynamic system is summarized in the four laws of thermodynamics:

The zeroth law states that if two systems are in equilibrium with a third, they are in equilibrium with each other. It essentially states that the equilibrium relationship is an equivalence relation.

The first law is the law of conservation of energy, where dU is the increase in internal energy of the system, dq is the amount of heat energy added to the system and dw is the amount of volumetric work done on the system (e.g. pressurization),

$$dU = dw + dq + \sum_{i=1}^{j} \mu_i dN_i \qquad (2.1)$$

with the chemical potential μ and the number of particles N of type *i* in the system. The last term can be removed, if the closed system has just one single component (j=1).

The second law summarizes the tendency of intensive thermodynamic properties, such as pressure, temperature, etc., to equalize as time goes by, or dS≥0, where *S* is the entropy of the system. The heat term is generally related to the entropy by:

$$dq = TdS \qquad (2.2)$$

Combining the first and the second law of thermodynamics (Equation 2.1 and 2.2), where the term –pdV represents the change of volumetric work dw, one achieves an equation which is convenient for situations involving variations in internal energy, with changes in volume V and entropy:

$$dU = -pdV + TdS \qquad (2.3)$$

The third law of thermodynamics states that at the absolute zero of temperature, the entropy is at a minimum and all thermodynamic processes cease.

During pressure build-up all these fundamental relationships have to be considered in their functional relationship with temperature and pressure.

By using the thermodynamic potentials,

Internal energy	U(S, V)
Enthalpy	H(S, p)
Helmholtz free energy	A(T, V)
Gibbs function of free energy	G(T, p)

the fundamental equations are expressed as:

$$dU(S,V) = -pdV + TdS \tag{2.4}$$

$$dH(S,p) = Vdp + TdS \tag{2.5}$$

$$dA(T,V) = -SdT - pdV \tag{2.6}$$

$$dG(T,p) = Vdp - SdT \tag{2.7}$$

The Gibbs function of free energy dG(T, p) (Equation 2.7) is the fundamental equation for a system where pressure and temperature are the independent variables.

For the case of a single component system, there are three standard material properties of which all others may be derived:

According to the first fundamental theorem of thermodynamics and for a constant pressure, heat capacity c_p is usually defined as:

$$c_p \equiv \left(\frac{\partial H}{\partial T}\right)_p = T\left(\frac{\partial S}{\partial T}\right)_p \tag{2.8}$$

The isobaric coefficient of thermal expansion can be defined as (Bridgman 1912),

$$\alpha_p \equiv \frac{1}{V}\left(\frac{\partial V}{\partial T}\right)_p = \frac{1}{\rho}\left(\frac{\partial \rho}{\partial T}\right)_p \tag{2.9}$$

with the density ρ.

Isothermal compressibility as an intrinsic physical property of the material is defined by Equation 2.10 (Bridgman, 1912) and exhibits a high variability in gases, liquids and solids,

$$\beta_T \equiv \frac{1}{v}\left(\frac{\partial v}{\partial p}\right)_T = \frac{1}{\rho}\left(\frac{\partial \rho}{\partial p}\right)_T \tag{2.10}$$

with the specific volume v.

These properties are seen to be the three possible second derivative of the Gibbs free energy with respect to temperature and pressure.

On the base of the first law of thermodynamics (Equation 2.1) and incorporation of the isothermal compressibility (Equation 2.10) the volumetric work dw from A to B can be expressed as:

$$\int_A^B dw = \int_A^B pv\beta_T dp \qquad (2.11)$$

By using the second law of thermodynamics (Equation 2.2), which derives a relation for enthalpy, entropy and temperature,

$$\left(\frac{\partial H}{\partial T}\right)_p = T\left(\frac{\partial S}{\partial T}\right)_p \qquad (2.12)$$

the adiabatic-isentropic heating of a system can be obtained by combining Equation 2.12 with the basic equations for the compressibility of a system (Equation 2.10) and specific heat capacity at constant pressure (Equation 2.8):

$$\left(\frac{\partial T}{\partial p}\right)_S = \frac{\beta_T T}{c_p \rho} \qquad (2.13)$$

A temperature rise is accompanied by a dissipation of heat within and through the pressure vessel, which is dependent on the vessel size, rate of compression, heat transfer parameters as well as initial and boundary conditions.

The phase transition between two states of matter can be characterized by the Clausius-Clapeyron relation (Equation 2.14), which can give a relation of the temperature dependence of the melting pressure.

$$\frac{dp}{dT} = \frac{\Delta H}{T\Delta V} \qquad (2.14)$$

Chemical reactions under pressure and temperature are dependent on both parameters. An adequate equation on the temperature dependence of the rate constant k was first published by Arrhenius (1889) in Equation 2.15,

$$\left(\frac{\partial \ln k}{\partial T}\right)_p = -\frac{E_a}{R_m T^2} \qquad (2.15)$$

where E_a represents the activation energy (kJ mol^{-1}) and R_m the molar gas constant with 8.3145 cm^3 MPa K^{-1} mol^{-1}.

Eyring (1935a; 1935b) derived a similar expression (Equation 2.16) for the pressure dependence of k,

$$\left(\frac{\partial \ln k}{\partial p}\right)_T = -\frac{\Delta V^{\#}}{R_m T} \qquad (2.16)$$

with the activation volume of the reaction $\Delta V^{\#}$ [$cm^3\,mol^{-1}$].

Limitations of Equation 2.16 are the pressure dependence of $\Delta V^{\#}$ and the order of reaction, which might vary at different pressure levels.

2.2.2. Effects on relevant systems

2.2.2.1. Water

Water is essential to all known forms of life. It represents the major component of most food systems and is typically used as the pressure transmitting medium. Extensive data and formulations of the main thermodynamic properties of water are available of the "International Association for the Properties of Water and Steam" (IAPWS) and in the database from the "National Institute of Standards and Technology" (NIST). Most of the time, data and formulations are valid up to 1000 MPa. In this work, data were extrapolated up to 1400 MPa.

After compression of 1 kg water up to 1400 MPa, a maximum volumetric work of 128 kJ kg^{-1} at 140 °C is performed on the system according to Equation 2.11. In Figure 2.1 the specific volumetric work w in pure water, in the pressure and temperature landscape, is presented. The high pressure and low temperature dependence resulted from the functional relationships of the isothermal compressibility $\beta_T(p, T)$ (Figure 2.4 d) and the specific volume v(p, T) (Figure 2.2 b).

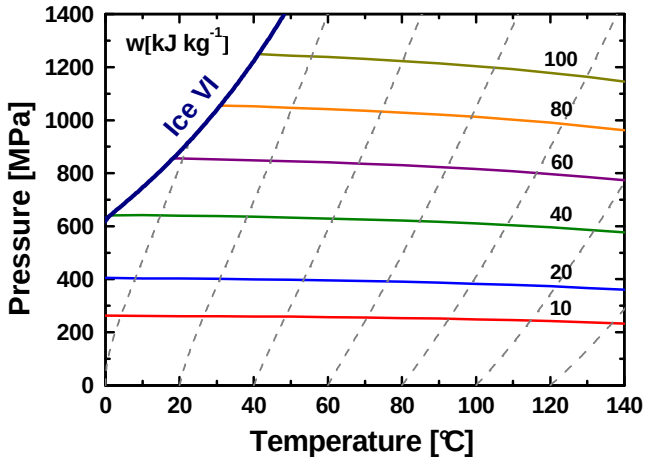

Figure 2.1: Specific volumetric work w [kJ kg^{-1}] in pure water with adiabatic lines due to compression (--) of water in the p-T landscape according to Equation 2.11 with the isothermal compressibility $\beta_T(p,T)$ (Figure 2.4 d) and the specific volume v(p,T) (Figure 2.2 b).

Bridgman (1911; 1912) was the first to determine the phase diagram of water as function of temperature and pressure. The phase transition lines of water and its different ice modifications, according to Bridgman, are shown in Figure 2.2 a. At present, 12 different crystal structures plus two amorphous states are known. At the transition from the liquid to the solid state Ice I represents a specialty since only this ice modification shows a positive volume change ΔV.

In Figure 2.2 b the density ρ (NIST) of pure water with adiabatic lines due to compression (Equation 2.13) in the p-T landscape is shown. At high pressures the compressibility decreases and there is a volume contraction of 10%, 17% or 23% at 400 MPa, 800 MPa or 1400 MPa, respectively. Lower initial temperatures have significantly lower (approx. 2 K / 100 MPa) temperature increases due to compression than higher starting temperatures (up to 5 K / 100 MPa over 80 °C).

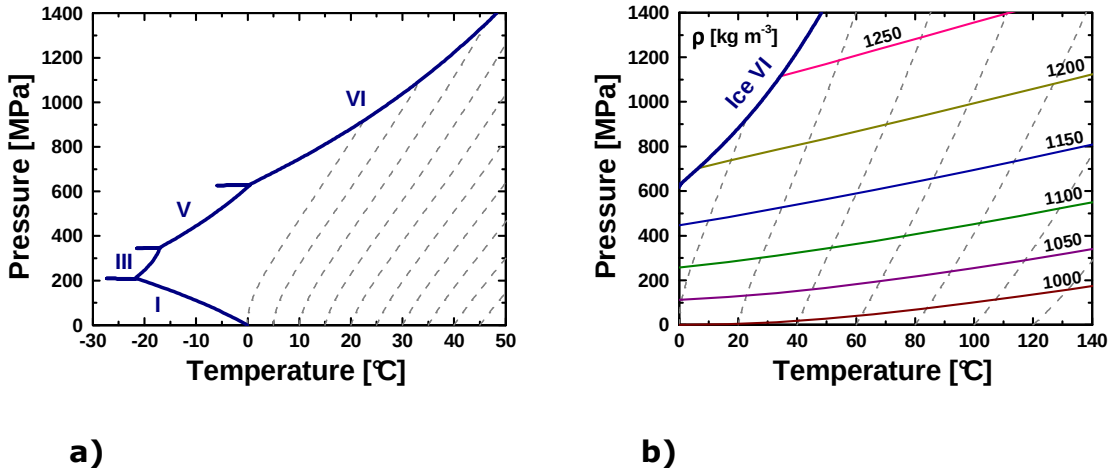

Figure 2.2: a) Phase diagram (Bridgman 1911, 1912) with different ice modifications and b) density ρ [kg m^{-3}] with adiabatic lines due to compression (--) of water in the p-T landscape (NIST). The volume contraction of water at 400 MPa, 800 MPa or 1400 MPa with 50 °C is 10%, 17% or 23%, respectively.

Figure 2.3 shows the p-T landscape of fundamental thermodynamic parameters with adiabatic lines due to compression of water (NIST) with a) internal energy U, b) enthalpy H, c) Helmholtz free energy A, d) Gibbs free energy G and e) entropy S. Iso-entropy and adiabatic lines are equal, because adiabatic processes are reversible. According to the second fundamental theorem of thermodynamic dS during reversible processes is zero.

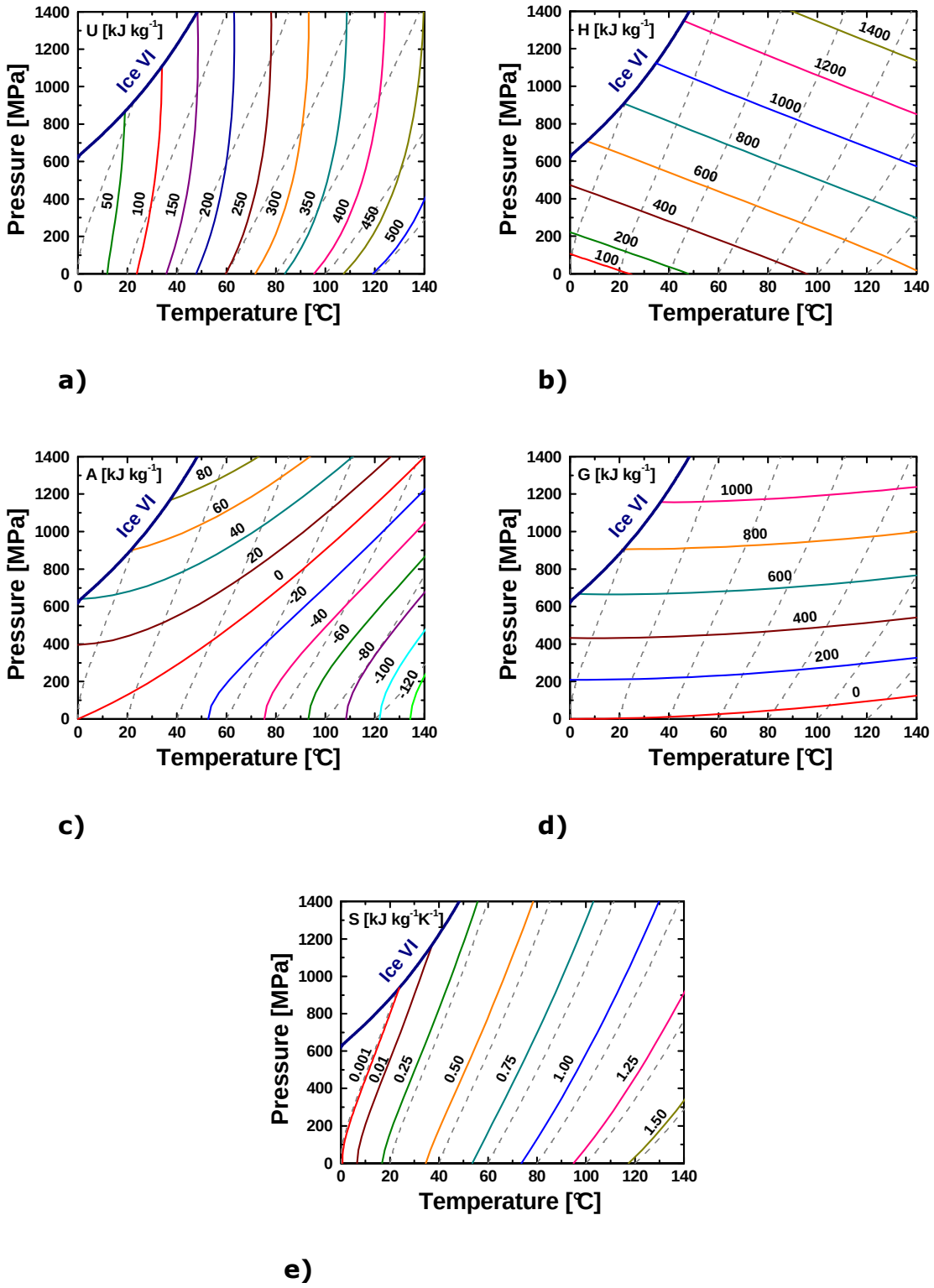

Figure 2.3: a) Fundamental thermodynamic parameter with adiabatic lines due to compression (--) of water in the p-T landscape (NIST) with a) internal energy U, b) enthalpy H, c) Helmholtz free energy A, d) Gibbs free energy G and e) entropy S.

Figure 2.4 presents the p-T landscape of material properties with adiabatic lines due to compression of water after NIST with a) isobaric heat capacity c_p, b) relative static permittivity ε, c) isobaric thermal expansion coefficient α_p and d) isothermal compressibility β_T.

The heat capacity shows a strong decrease when increasing the pressure but features only a very small change from 500 MP between 30-60 °C (Figure 2.4 a).

The relative static permittivity ε has importance in the calculation of ionic reactions and shows noticeable changes with pressure and temperature (Figure 2.4 b).

The thermal expansion coefficient α_p and the coefficient of compressibility β_T are most important in the calculation of adiabatic heating as a result of compression. β_T shows an extensive decrease with pressure at all temperatures.

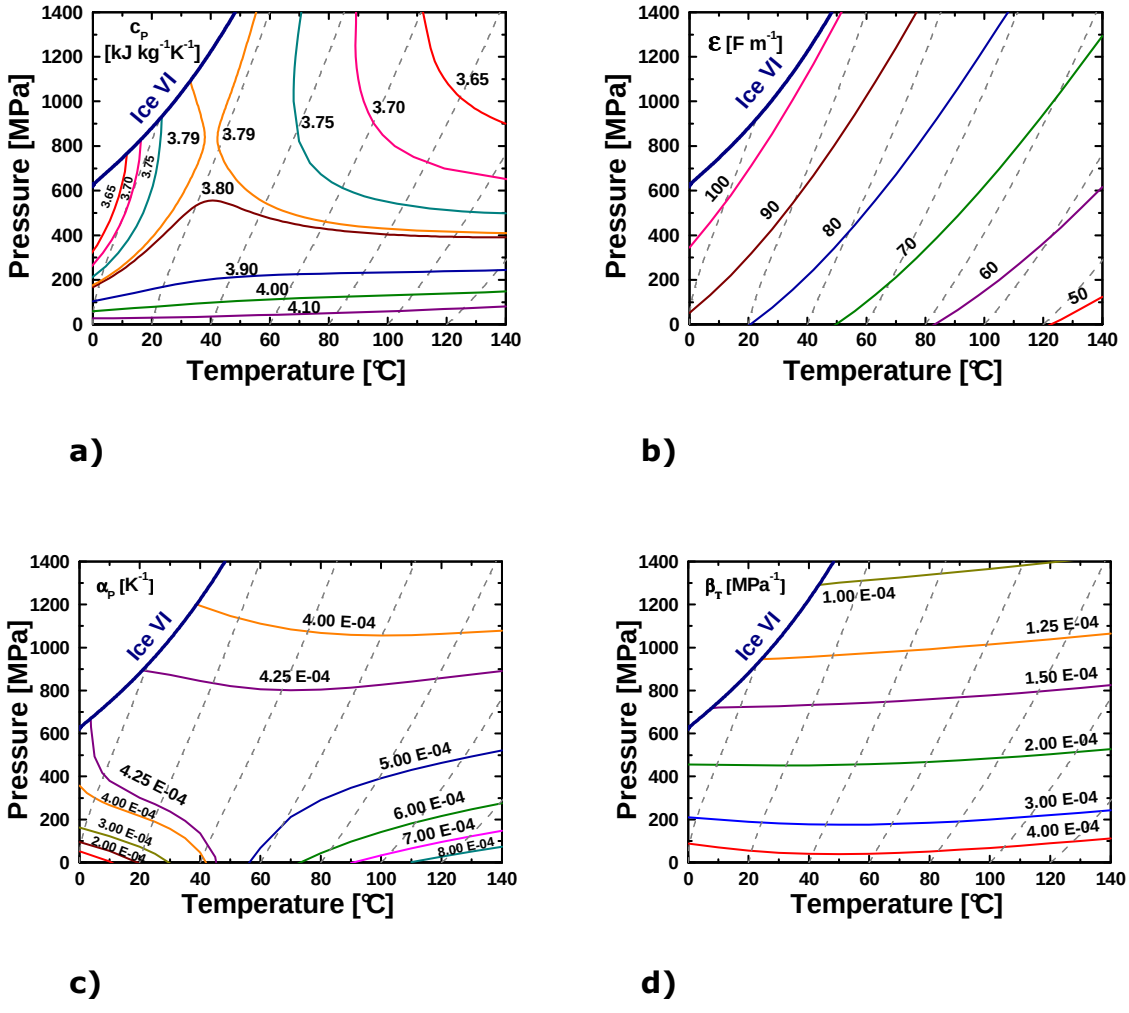

Figure 2.4: Material properties with adiabatic lines due to compression (--) of water in the p-T landscape after NIST with a) isobaric heat capacity c_p, b) relative static permittivity ε, c) thermal expansion coefficient α_p and d) isothermal compressibility β_T.

Figure 2.5 shows the p-T landscape of transport properties with adiabatic lines due to compression of water after NIST with a) thermal conductivity λ and b) dynamic viscosity η. The thermal conductivity has a strong pressure dependence and improves the heat transfer in and to the product during pressure build-up as well as dwell time. At molecular processes the dynamic viscosity η (Figure 2.5 b) has an important role and shows strong temperature dependence.

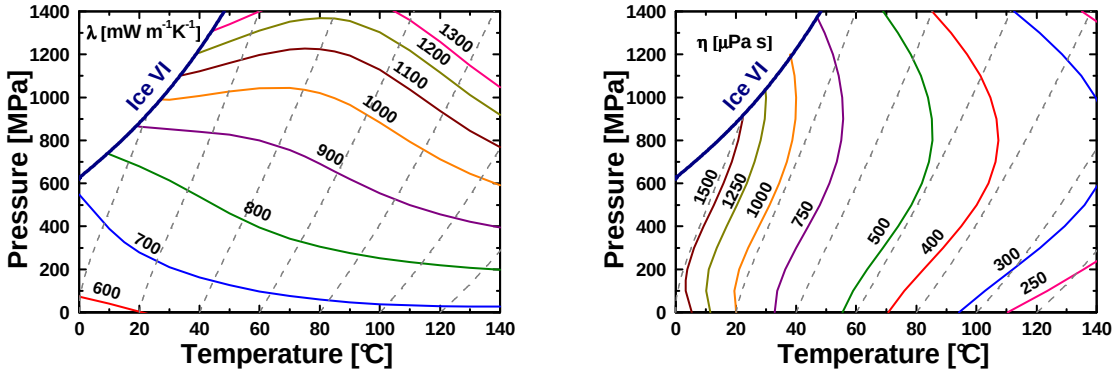

Figure 2.5: a) Transport properties with adiabatic lines due to compression (--) of water in the p-T landscape after NIST with a) thermal conductivity λ and b) dynamic viscosity η.

2.2.2.2. Dissociation reactions

The thermodynamic background of a typical dissociation reaction in diluted solution is described in Equation 2.17,

$$HA + H_2O \leftrightarrow A^- + H_3O^+ \qquad (2.17)$$

with an acid HA, water H_2O, the conjugate base A^- and hydroxonium H_3O^+.

The equilibrium constant K is a quantity characterizing a chemical equilibrium in a chemical reaction. The law of mass action is an useful tool in determining the concentration of various reactants and products in a system where chemical equilibrium occurs (Equation 2.18),

$$K = \frac{\gamma_{H_3O^+} \cdot \gamma_{A^-}}{\gamma_{HA} \cdot \gamma_{H_2O}} \cdot \frac{[A^-] \cdot [H_3O^+]}{[HA] \cdot [H_2O]} \qquad (2.18)$$

with the activity coefficients γ_i (correction factors) and concentration of every molecule i. A good approximation of the activity coefficients in aqueous solutions

can be estimated by the limiting Debye-Hueckel law (Debye & Hueckel, 1923) in Equation 2.19,

$$\log_{10} \gamma_i = -1.825 \cdot 10^6 \cdot z_i \cdot \sqrt{\frac{I \cdot \rho}{\varepsilon^3 \cdot T^3}} \quad (2.19)$$

with the number of elementary charges z_i of the ion i and the ion strength I. The relative static permittivity ε shows noticeable changes with pressure and temperature (Figure 2.4 b), which leads to varying activity coefficients γ_i.

The concentration of water remains essentially unchanged throughout dissociation, because it is very large (55.5 M) in relation to the other concentrations in the expression. Therefore the term for the concentration of water is omitted from the general equilibrium constant expression. This assumptions leads to the acid dissociation constant K_a (Equation 2.20),

$$K_a = \frac{\gamma_{H_3O^+} \cdot \gamma_{A^-}}{\gamma_{HA}} \cdot \frac{[A^-] \cdot [H_3O^+]}{[HA]} \quad (2.20)$$

which is a specific type of equilibrium constant that indicates the extent of dissociation of hydroxonium from an acid. Because this constant differs for each acid and varies over many degrees of magnitude, the acidity constant is often represented by the additive inverse of its common logarithm, represented by the symbol pK_a (Equation 2.21).

$$pK_a = -\log_{10}(K_a) \quad (2.21)$$

The activity of hydroxonium is a key in describing thermodynamic and kinetic properties of processes occurring in aqueous solutions and can vary over a wide range, too. Consequently it is common to express the activity of hydroxonium in a logarithmic form as pH (Equation 2.22),

$$pH = -\log_{10}\left(\gamma_{H_3O^+} \cdot \frac{[H_3O^+]}{1\ mol\ L^{-1}}\right) \quad (2.22)$$

where 1 mol L^{-1} makes the parameter dimensionless. During shift of dissociation equilibria the pH-value would be changed with all reaction partners (Equation 2.17), but no change of the concentration difference on one site occurs during the reaction. For example in water at 0.1 MPa and 20 °C with nearly equal hydroxonium and hydroxide ($[OH^-]$) concentrations there would be neutral conditions ($[H^+] = [OH^-]$). Under pressure there are increased hydroxonium and hydroxide concentrations, but still "neutral" conditions. Consequently, the pH-

shift alone can not exactly describe the dissociation equilibrium shift and thus the pK_a-shift is used.

By using the regression equation from Marshall and Frank (1981), the negative logarithm of the ion product K_w ([mol kg^{-1}]^2) of water substance (Equation 2.23) can be calculated with a deviation of ± 0.01 at < 200 °C, ± 0.02 at ≤ 374 °C, ± 0.3 at > 374 °C and ± 0.05 - 0.3 at high pressures.

$$-\log_{10}(K_W) = -\log_{10}\left(\left[H_3O^+\right]\cdot\left[OH^-\right]\right) \qquad (2.23)$$

The modeled dissociation equilibrium shift in pure water showed large variations with pressure and temperature (Figure 2.6). Especially the high temperature area is a matter of particular interest for the application of supercritical water in food technology (Figure 2.6 a). After extrapolation up to 1400 MPa (Figure 2.6 b), an estimation about the K_W-characteristics at the current technical limit for spore inactivation studies could be given. To obtain the pH or pOH-value, the negative logarithm of K_W has to be divided by two (according to Equation 2.23).

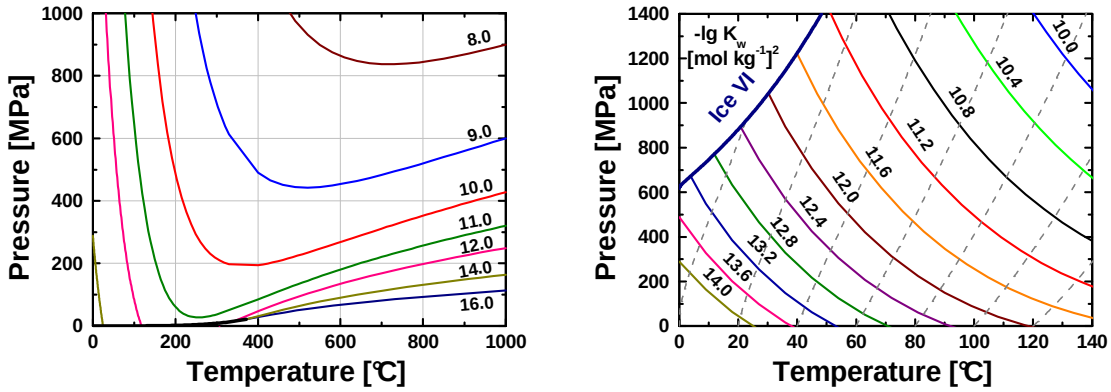

Figure 2.6: Dissociation equilibrium shift (negative logarithm of the ion product K_W [mol kg^{-1}]^2) in pure water under different p-T conditions up to 1000 MPa and 1000 °C (a) and with adiabatic lines (--) up to 140 °C extrapolated up to 1400 MPa (b) (according to Marshall and Franck, 1981).

For any equilibrium reaction the pressure and temperature dependence of the equilibrium constant is described by Planck's equation (Planck, 1887) (Equation 2.24),

$$\left(\frac{d\ln(K)}{dp}\right)_T = \frac{\Delta V}{R_m \cdot T} \quad (2.24)$$

where T is the absolute temperature (K) and ΔV the reaction volume at atmospheric pressure ($cm^3\ mol^{-1}$).

The reaction volume ΔV is equal to the difference of the partial volumes of products and reactants. It includes the volume change because of alteration in binding length and angle $\Delta V_{intrinsic}$ as well as solvational properties $\Delta V_{solvational}$ (Equation 2.25).

$$\Delta V = \Delta V_{\text{int}\,rinsic} + \Delta V_{solvational} \quad (2.25)$$

In this study, 2-amino-2-hydroxymethylpropane-1,3 diol (Tris), N-(2-Acetamido)-2-aminoethanesulfonic acid (ACES), *N*,*N*`-1,2-ethenediyl-methanimidamid (Imidazole) and phosphate (2nd, PBS), acetic acid (Acetate) and citric acid (2nd, Citrate) buffer were applied. The associated dissociation reactions in Equation 2.26- 2.31,

$$TrisH^+ + H_2O \leftrightarrow Tris + H_3O^+ \quad (2.26)$$

$$ACES^-H^+ + H_2O \leftrightarrow ACES^- + H_3O^+ \quad (2.27)$$

$$\text{Im}\,idazoleH^+ + H_2O \leftrightarrow \text{Im}\,idazole + H_3O^+ \quad (2.28)$$

$$H_2PO_4^- + H_2O \leftrightarrow HPO_4^{-2} + H_3O^+ \quad (2.29)$$

$$CH_3COOH + H_2O \leftrightarrow CH_3COO^- + H_3O^+ \quad (2.30)$$

$$Citrate^- + H_2O \leftrightarrow Citrate^{-2} + H_3O^+ \quad (2.31)$$

with a simplified Tris-, ACES-, Imidazole- and Citrate-molecule, show the different formation of charges in direction of the products. Charge formation leads to a volume contraction (Drude & Nernst, 1894) and consequently negative reaction volumes (ΔV) occur during reactions with charge formation.

Hamann (1982) found a relationship between the thermodynamic acid dissociation constant K_a and high pressure up to 1000 MPa in Equation 2.32,

$$\ln\left(K_a(p)\right) = \ln(K_a) - \frac{p \cdot \Delta V}{R \cdot T \cdot \left(1 + b \cdot p\right)} \quad (2.32)$$

with b = 9.2 x 10^{-4} MPa^{-1}.

After calculation of $K_a(p)$ it is possible to obtain the pressure dependence of the pK_a-value, respectively (Equation 2.33):

$$pK_a(p) = -0.4343 \cdot \ln(K_a(p)) \quad (2.33)$$

2.2.2.3. Pressure transmitting fluids

For industrial processes water is the main used pressure transmitting medium. However, at very high pressure level a phase transition could occur (Figure 2.2 a) e.g. during decompression. For other potential fluids the rheological behavior is one of the most critical points in the design of high-pressure standards. Unfortunately, the effect of pressure on the viscosity of liquids can be very strong and this reduces the effective pressure domain covered by each liquid (Vergne, 1994). Bis-(2 -ethylhexyl) sebacate (trivial name sebacate) has been shown to be valuable as a pressure transmitting fluid (Vergne, 1990; 1994). This is because it does not have relaxation effects over long periods of time (Wisniewski, Machowski & Komorowski, 1995) and has good lubricant properties (Alsaad, Bair, Sanborn & Winer, 1978). Vergne (1994) has discussed alternative fluids, but concluded that there is a lack of data for such potential media. Sebacate belongs to the diesters and is a middle-chain hydrocarbon (Wisniewski et al., 1995). In Figure 2.7 the phase diagram according to the data of Wisniewski et al. (1995) and the adiabatic lines due to compression measured by Ardia (2004) are shown. Phase transitions could cause a delay in the pressure transmission and a blockage of the transmission connections. No phase transitions in the pressure and temperature range of interest can be identified in Figure 2.7.

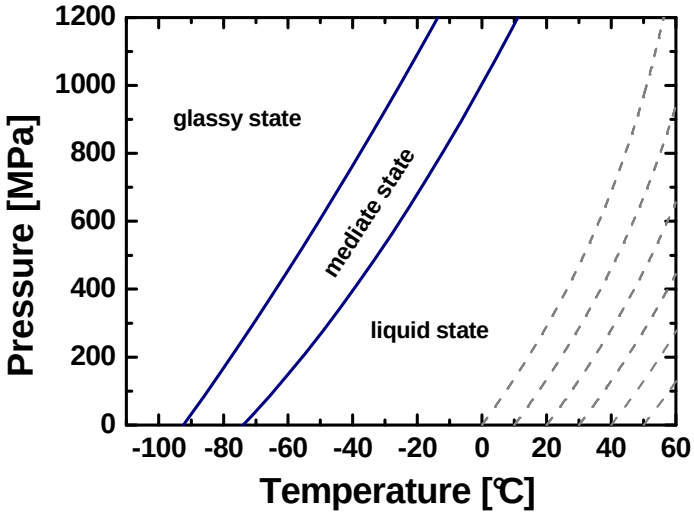

Figure 2.7: Phase diagram (Wisniewski et al., 1995) with adiabatic lines due to compression (--, Ardia, 2004) of sebacate in the p-T landscape.

For the thermodynamic characterization and calculation of transport phenomena the fluid density in dependence of pressure and temperature has to be known (Figure 2.8 a; ASME, 1953). Unfortunately, extensive data has rarely been addressed. As mentioned, the strong viscosity increase because of pressure build-up is one of the most important points. In Figure 2.8 b the data from Izuchi and Nishibata (1986) and Vergne (1994) are presented. No other property of sebacate shows so dramatically the effect of pressure.

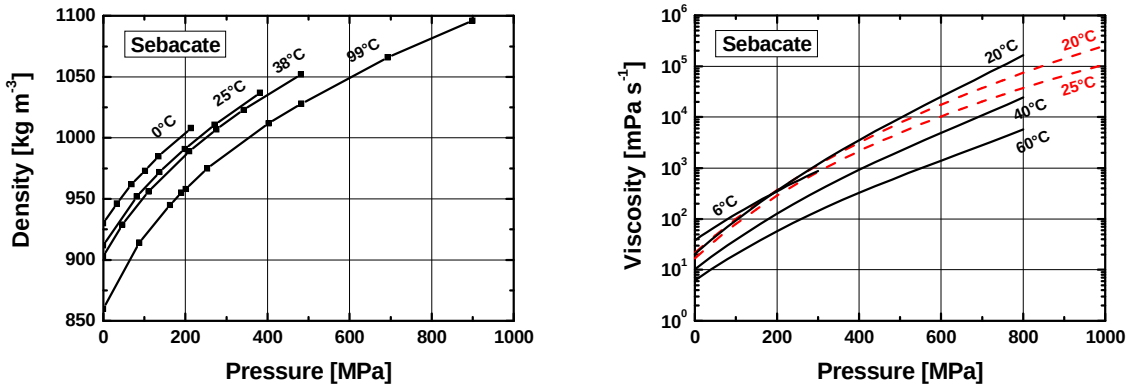

Figure 2.8: a) Density (ASME, 1953) and b) dynamic viscosity (lines Izuchi & Nishibata, 1986 ; dashed lines Vergne, 1994) of sebacate at elevated temperature as a function of different pressure level.

Ardia (2004) reported delays in reaching the desired ultra-high pressure levels from approximately 1100 MPa to 1400 MPa with sebacate, because of pressure-relaxation phenomena through the capillary tube. Hence, pressure treatments at pressure levels higher than 1200 MPa were performed by heating the capillary connector at 100 °C during the pressure build-up. In Figure 2.9 the relaxation effect for a pressure cycle up to 1400 MPa is presented. In particular, the difference between the two pressure signals showed a delay of approximately 30 seconds to reach the maximum pressure.

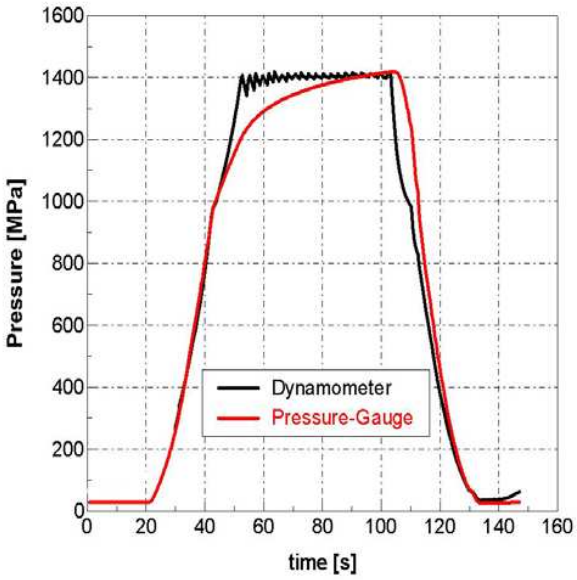

Figure 2.9: Difference between two pressure signals, depending on the increase of viscosity and rapid thermal equilibration in the high pressure capillary connection. The red line accounts for the pressure-transducer measurement in the micro-vessel while the black line is referred to the measurement provided by the dynamometer at the intensifier (Ardia, 2004).

2.2.2.4. Proteins

High pressure induced reversible or irreversible changes of the protein native structure (Heremans, 1982; Cheftel, 1992) are similar to the changes occurring at heat and in the presence of chemicals, but the residual molecular structure can vary significantly. Knorr, Heinz and Buckow (2006) published a detailed review regarding the changes of the protein structure under pressure and temperature.

For analyzing the pressure and temperature landscape of proteins, a two-state transition is assumed which is at equilibrium at the phase transition line (Figure 2.10, e.g. transition from native to denatured). Transition phenomena can be modeled using an empirical approach with a thermodynamic background considering the three-dimensional free energy landscape in response to pressure and temperature (Figure 2.10).

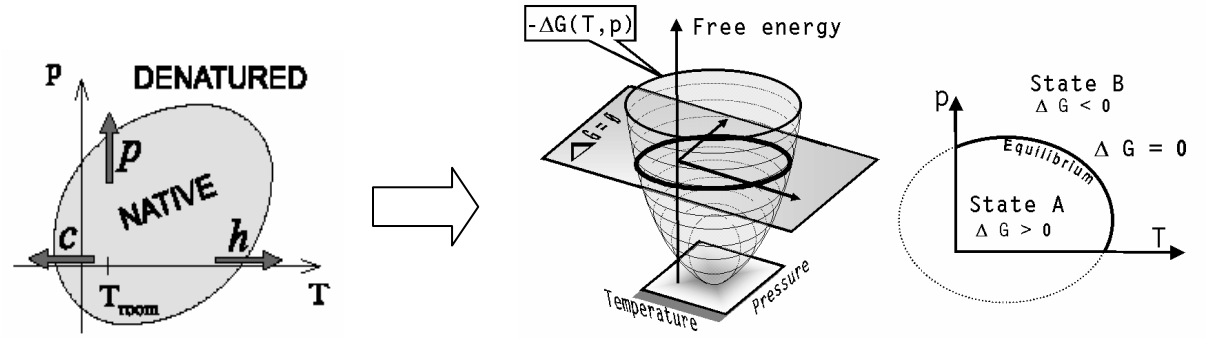

Figure 2.10: Relation between cold (c), pressure (p) and heat (h) denaturation of proteins (Smeller, 2002) and three-dimensional free energy landscape in response to pressure and temperature (Heinz & Knorr, 2002).

In Gibbs function of free energy (Equation 2.7) pressure and temperature are the independent variables. Integration of Equation 2.7 using a Taylor series expansion up to second order terms (Smeller, 2002) yields Equation 2.34:

$$\Delta G = \Delta G_0 + \Delta V_0 (p - p_0) - \Delta S_0 (T - T_0) + (\Delta\beta / 2)(p - p_0)^2 - (\Delta c_p / 2T_0)(T - T_0)^2 + \Delta\alpha (p - p_0)(T - T_0) \quad (2.34)$$

where Δ denotes the change of the corresponding parameter during unfolding. This quadratic two-variable approximation of the difference in Gibbs free energy yields to an ellipsoidal phase transition line in the pressure and temperature landscape at equilibrium conditions (ΔG=0 in Figure 2.10) (Zhang, Peng, Jonas & Jonas, 1995). This model can be treated as a general approach, where state A and state B could denote molecular or physicochemical states. In the case of spore inactivation, state A may be represent the recoverable and B the not recoverable spores, respectively. The transition line would run along the equilibrium ΔG=0 in an elliptical shape at various pressure and temperature conditions (Heinz & Knorr, 2002).

2.3. Process parameters and technical aspects

2.3.1. Fundamental parameters

Two different concepts of high pressure processing have been developed for different kinds of foods (Figure 2.11). By using an internal intensifier (Figure 2.11 b) the maximum size of the particulates is limited by the rating of valves and pumps. However, this solution is more suitable for sterilization processes,

because the cold inflow of pressure medium in the batch system (Figure 2.11 a) during pressurization may produce unwanted temperature inhomogeneities. In any case batch and continuous systems have the potential for high pressure thermal sterilization processes with respective treatment parameters.

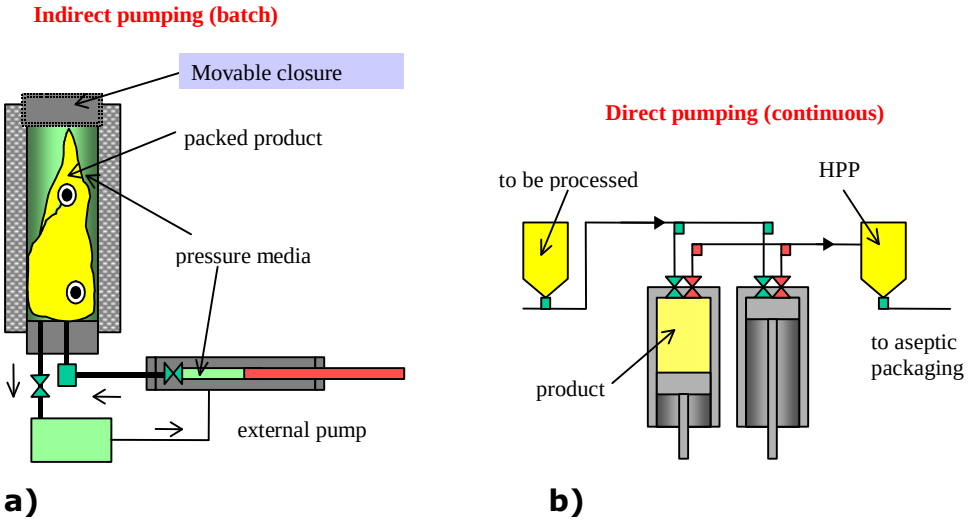

Figure 2.11: Two concepts of high pressure processing: a) indirect (batch) and b) direct (continuous) pumping (Rovere, 2002).

Both concepts shown in Figure 2.11 include an intensifier, where the simplest practical system is a single-acting, hydraulically driven pump. The two main parts of an intensifier are the low pressure and the high pressure cylinder. A double-acting arrangement enables a continuous, uniform flow. While one of the double-acting pistons is delivering, the other cylinder is being charged during its intake stroke (Figure 2.12).

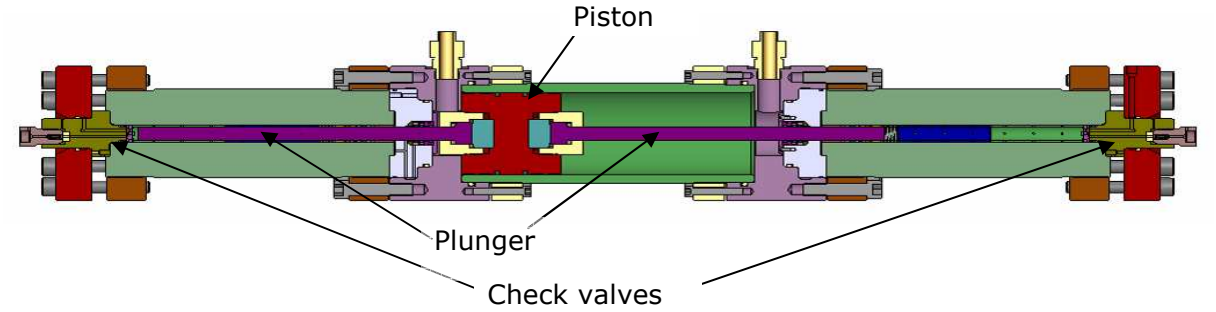

Figure 2.12: Double-acting intensifier (Hernando, A., 2007, NC Hyperbaric, Spain, personal communication).

As pressure level is the same in each volume element the heat of compression is homogeneously distributed and improves microbial inactivation. Thus the process efficiency can be maximized. Instantaneous adiabatic heating can be utilized to reach the sterilizing end-temperature quickly and can result in a new approach to food sterilization with a significant improvement in food quality. Additional heat flow across the boundary of the system must be taken into account as a transient temperature field, thermal equilibration will occur during pressure holding time between the warmest point in the center of the product and the metal high pressure vessel. It is noteworthy that after pressure release the product will return to its initial temperature or even below, an aspect of most interest for processing of high quality foods. In contrast to liquid food, where the heat transfer can be improved by application of heat exchangers with large area and heat recovery rates of above 90 % are obtained, preservation of particulate food or packaged food requires long times for heat transfer or a large temperature gradient. Over-processing and fouling at the inner surface of the packaging may inhibit increasing the treatment temperature. Industrial scale systems for sterilization of cans therefore are limited to heat recovery rates in the range of 50% (Toepfl et al., 2006).

As an example of the reduction in spore resistance to heat, Heinz and Knorr (2002) compared the inactivation data at 800 MPa of Rovere et al. (1999) with the generally accepted botulinum cook at ambient pressure (Stumbo, 1948). By using the F-value concept (Equation 2.35) it is possible to compare the thermal effect of treatments where the temperature is a function of time T(t), N_0 is the initial count and N is the survival count.

$$F \equiv \int_0^t 10^{\frac{T(t)-T_{ref}}{z}} dt = D_{ref} \log_{10}\left(\frac{N}{N_0}\right) \qquad (2.35)$$

In Figure 2.13 a, both decimal reduction times (D-value) converge at 121.1 °C (= 250° Fahrenheit, Figure 2.13 a) and this level has been chosen as the reference (ref) temperature T_{ref} for calculation of the F-value in Figure 2.13 b. The z-value represents the temperature increase required to reduce the D-value by 1 $\log_{10}$. In the food canning industry it is common to use 121.1 °C as T_{ref} and a z-value of 10 °C, which is derived from the slope in Figure 2.13 a. For the inactivation data at 800 MPa of Rovere et al. (1999) z yields 18 °C. An F-value of 2.4 min is equivalent to a 12 log-cycle reduction of *C. botulinum* with D_{ref} = 0.2

min (F = 36 min for *G. steraothermophilus* with D_{ref} = 3 min) and is regarded as the minimum thermal load that must be applied to every part of the product.

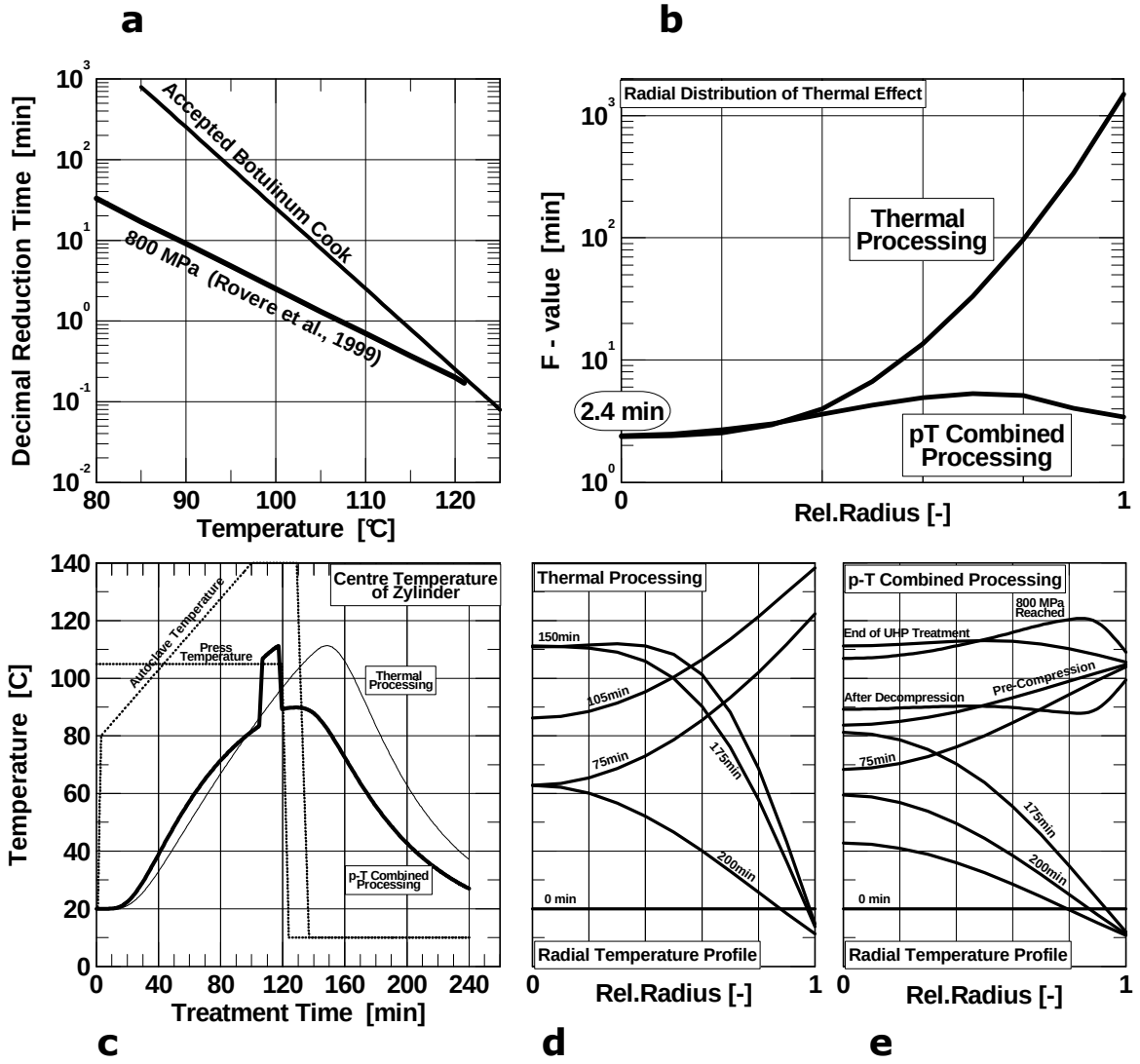

Figure 2.13: Comparison between conventional and p-T combined sterilization; rel. Radius 0=centre, 1=periphery of container (Heinz & Knorr, 2002).

In immiscible products the temperature increase of the center is delayed by the limitations in heat conduction of the outer layers. Heinz and Knorr (2002) simulated the time course of the core temperature of a cylindrical package (diameter: 10 cm) for conventional thermal treatment with heating from 80 °C to 140 °C and 30 min holding time in Figure 2.13 c. The product was then cooled to 10 °C. After calculation of the F-value of the thermal process profile, which is typical for canning, the same thermal load of 2.4 min was obtained for the pressure assisted process. The authors also compared the radial temperature

profiles derived from Equation 2.35 (Figure 2.13 d and e), where the temperature increase after 90 minutes of conventional heating was produced by the heat of compression at the initial phase of a 800 MPa high pressure treatment (Figure 2.13 c). The heat of compression increased the temperature homogeneously throughout the product (Figure 2.13 d), avoiding an overprocessing of the boundary layer, which is expressed by a local F-value of more than 1000 min (Figure 2.13 b) (Heinz & Knorr, 2002).

The (transient) energy input of these processing techniques is compared in Figure 2.14 at two different points of time (Toepfl et al., 2006). Ref 1 is defined as the time (105 min, Figure 2.13 c) when the core temperature of both techniques is equal. Ref 2 is defined as the moment when no additional energy will be transferred into the product anymore. For the high pressure process this corresponds to the end of compression, for thermal processing the beginning of cooling. For the heating of both samples, both purely thermal processes, a heat recovery of 50% can be assumed, same as for the rest of the thermal process. The specific energy input required for a sterilization of cans can be reduced from 300 to 270 kJ kg^{-1} when applying a high pressure treatment. In case of HPP, an energy recovery rate up to 50% can be estimated when a twin-vessel-system or a pressure storage is used. Making use of energy recovery, a specific energy input of 242 kJ kg^{-1} would be required for sterilization, corresponding to an energy reduction of 20%. It has to be noted that these calculations are based on the energy required for compression work (Equation 2.11).

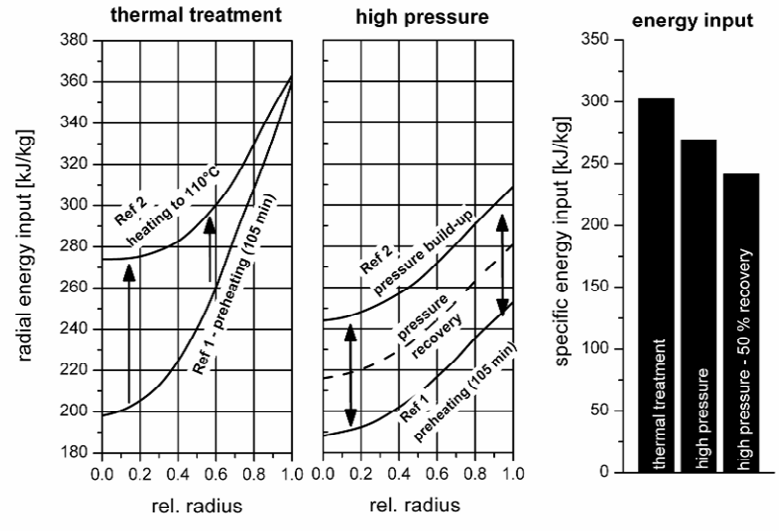

Figure 2.14: Comparison of radial specific energy input of a thermal and a combined thermal and HP sterilization for the process shown in Figure 2.13 c (Toepfl et al., 2006).

At present, the high investment costs as well as cost-intensive maintenance and service of high pressure equipment inhibit a broad industrial exploitation, although numerous applications for high hydrostatic pressure food processing have been shown (Figure 1.1).

2.3.2. Adiabatic heating

Considering that during compression all compressible materials change their temperature an adiabatic heating will occur in isentropic systems. This temperature rise is a result of the inner friction that occurs when fluids are compressed adiabatically to extreme pressures. A general expression for the temperature increase upon compression in adiabatic-isentropic-situations is given in Equation 2.13. The thermo-physical properties β, ρ and c_p are pressure-temperature dependent. If these properties are known the calculation of the thermal profile during the compression phase is possible. Different media show different adiabatic heating (Ardia, 2004), which could be obtained for some fluid food systems with the help of equations for estimating thermophysical properties of mixtures of pure substances. For example, different water and sucrose solutions can be used as a model system for orange juice (Ardia, Knorr & Heinz, 2004b). Some adiabatic heat of compression profiles are shown in Figure 2.15, where n-hexane and sebacate are pressure transmitting media. The lack of thermodynamic data for real foods under high pressure conditions has limited the possibilities to study and calculate the temperature increase during compression. So far, mainly empirical measurements can demonstrate the differences of the adiabatic heating in real food systems (Table 2.2).

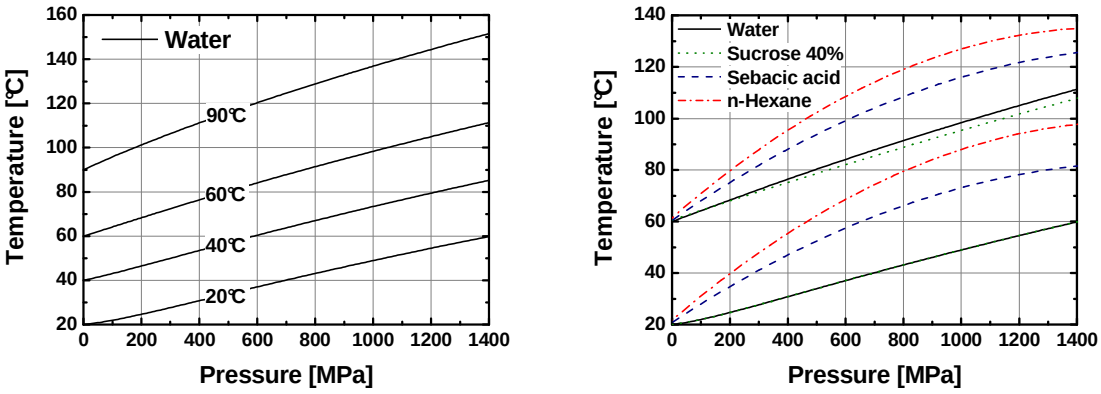

Figure 2.15: Adiabatic heat of compression in water, sucrose solution with 40% solid content, sebacate and n-hexane (Ardia, 2004).

The main component in most foods is water and thus, the thermodynamic properties of water can be utilized to estimate the temperature increase upon compression of high moisture foods. The compression heating in fat containing foods could be up to three times higher than for water (Ting, Balasubramaniam & Raghubeer, 2002). In a situation in which organic solvents or oils are used as pressure transmitting media and the food matrix has high water content, a difference in compression temperature increase between the food and the medium would occur. The transfer of heat from the pressure transmitting medium into the product could be utilized to increase the temperature of the food system during and after the adiabatic heating.

Table 2.2: Adiabatic heat of compression in different food systems (Ting et al., 2002)

Substances at 25 °C	**Temperature increase per 100 MPa [°C]**
Water	~3,0
Mashed potato	~3,0
Orange juice	~3,0
Tomato salsa	~3,0
2%-Fat milk	~3,0
Salmon	~3,2
Chicken fat	~4,5
Beef fat	~6,3
Olive oil	From 8,7 to <6,3[a]
Soy oil	From 9,1 to <6,2[a]

[a] *Substances exhibited decreasing T as pressure increased*

2.3.3. Temperature peaks

High initial sample temperatures before pressure build-up and the resulting adiabatic heating during pressurization may result in temperature peaks in high pressure processing. This "over-processing" has an effect on all food relevant studies, especially at higher temperatures. The impact of non-isothermal dwell times under pressure is exemplified in Figure 2.16, with a sterilization process at 600 MPa and 110 °C (nutrient agar as sample). Two different experimental designs resulted in different thermal loads during pressure treatment, where the red dashed line represents a profile with too high initial temperature before pressure build-up in comparison with an adequate sample temperature profile (black line). The arrows show the time, when final pressure (600 MPa) is reached (Figure 2.16 a). More than 50 % of the F-value in a process at 600 MPa, 110 °C and 3 minutes holding time could be produced by a temperature peak with 117 °C in the initial phase after pressure build-up (Figure 2.16 b).

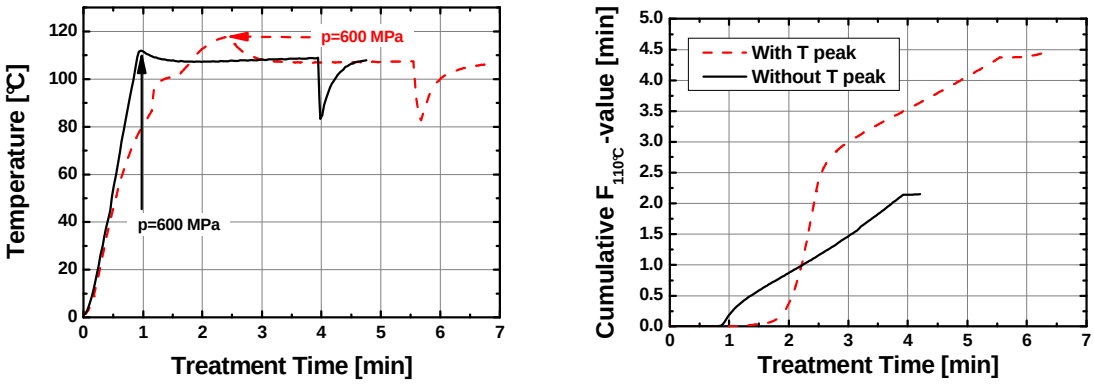

a) **b)**

Figure 2.16: Comparison of different sample temperature profiles (a) and the resulted cumulative $F_{110\ °C}$ –values (b, according to Equation 2.35 with z= const. =10 °C) of the whole sterilization process with 110 °C final thermostat temperature, 600 MPa and 3 min holding time.

Rajan et al. (2006a) compared the inactivation of *Bacillus amyloliquefaciens* at isothermal and non-isothermal conditions under pressure. They found differences of more than 1.5 $\log_{10}$ inactivation after 7 min holding time at 105 °C. At higher inactivation rates these non-isothermal conditions would have an higher impact. To avoid temperature peaks, the initial temperature has to be set to the special

type of food, because of the differences of the adiabatic heating (Figure 2.15, Table 2.2).

2.3.4. Temperature heterogeneities

Thermal heterogeneities in the sample volume during high pressure treatment affect all food relevant studies and are strongly dependent on the vessel design. Ardia et al. (2004b) modeled the temperature heterogeneities in a PET container with a diameter of 80 mm, a length of 100 mm and a wall thickness of 0.5 mm (Figure 2.17). *A. acidoterrestris* spore inactivation in orange juice was estimated as a function of punctual pressure and temperature values. Figure 2.17 shows the prediction of the temperature distribution and the inactivation kinetics of *A. acidoterrestris* spores in orange juice, at two different locations in the sample. The simulation of *A. acidoterrestris* spores was performed in a range of pressures from 0.1 to 800 MPa and an initial temperature of 50 °C. It was shown that the adiabatic heating of the product at the inner side-wall of the PET bottle (B) was characterized by lower temperatures compared to the center (A, dT/dp ~30 K), because of the heat flux to the "cold" metallic vessel (T ~50 °C). These temperature heterogeneities led to a difference in the spore inactivation level of approximately -6 $\log_{10}$ between the center and the inner side-wall of the bottle.

Modeling with the help of "Computational Fluid Dynamics" enables the investigation of three-dimensional temperature fields during high pressure treatment (Hartmann, 2002; Hartmann & Delgado, 2002; Hartmann, Delgado & Szymczyk, 2003; Hartmann & Delgado, 2004; Kitsubun, Hartmann & Delgado, 2005; Farid, 2006; Knoerzer, Juliano, Gladman, Versteeg & Fryer, 2007). Hartmann et al. (2003) investigated the influence of heat and mass transport effects on the uniformity of a high pressure induced inactivation. The geometry of the high pressure vessel with 6.3 L volume is shown in Figure 2.18 a. After 480 s pressure treatment at 40 °C (~ 313 K) temperature and velocity inhomogeneities in different package positions as well as within the packages were observed (Figure 2.18b). If the fluid motion is of very low intensity (e.g. if the food is highly viscous), thermal heterogeneities may be preserved and can give rise to process-non-uniformities (Hartmann et al., 2003).

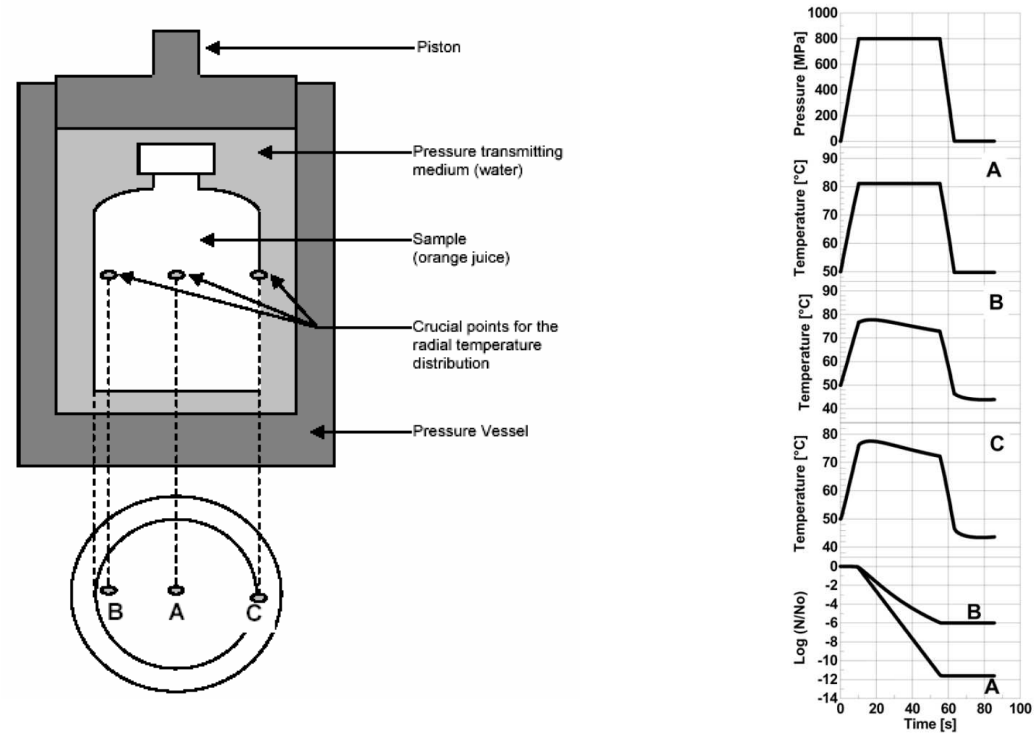

Figure 2.17: Schematic view of the geometry of the product sample used for the numerical simulation and the three points where the adiabatic heating has been predicted: A) center of the sample; B) inner layer of the sample container; C) sample container (PET). Simulation of adiabatic heat and inactivation kinetics of *A. acidoterrestris* spores in the crucial points of the sample, the center (A), the inner layer of the product sample (B) and the PET container (C) (Ardia et al., 2004b).

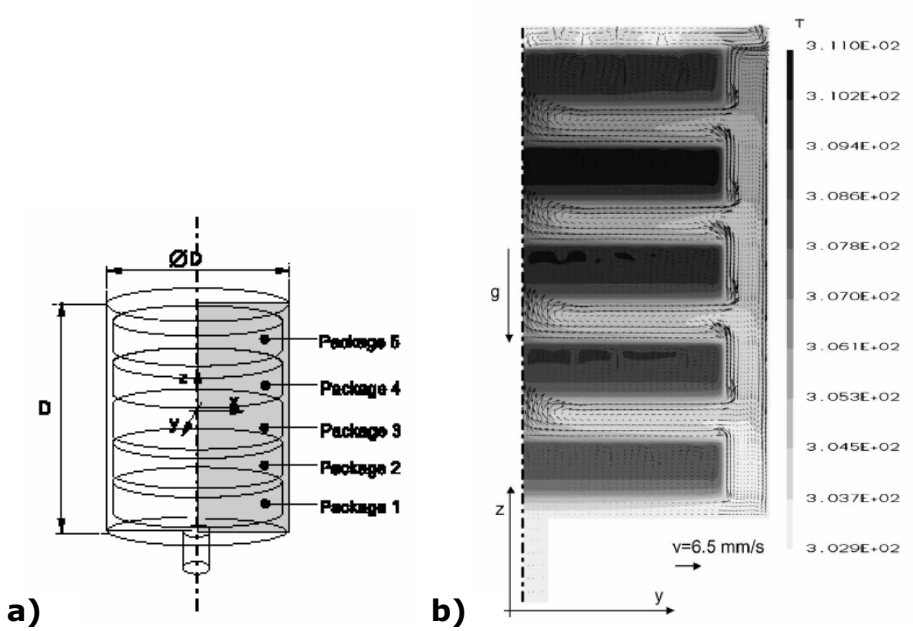

Figure 2.18: Geometry of a 6.3 L high pressure vessel (a) and temperature and velocity field after 480 s at 400 MPa (b) (Hartmann et al., 2003).

2.3.5. Scale up analysis

Every scale up produces changes in basic parameters, which have to be taken into account in the analysis of the process. The simultaneous effect of pressure and temperature could strongly decrease at inhomogeneities of one parameter during the treatment. At higher vessel volumes a higher specific volumetric work and energy consumption has to be considered (Figure 2.1). Different temperature distributions after 960 s at 530 MPa for a micro- and lab-scale chamber are shown in Figure 2.19 (Hartmann et al., 2003). After a scale up analysis for packed material (Figure 2.18 a) in two different pressure vessel volumes (0.8 and 6.3 L), significant differences average temperature profiles were observed (Figure 2.19). In this approach the modeling showed that the effective process intensity (combination of pressure and temperature) increased with the geometrical scale of the high pressure vessel. Consequently, process cycles could be shortened since the effective process intensity has increased (Hartmann et al., 2003).

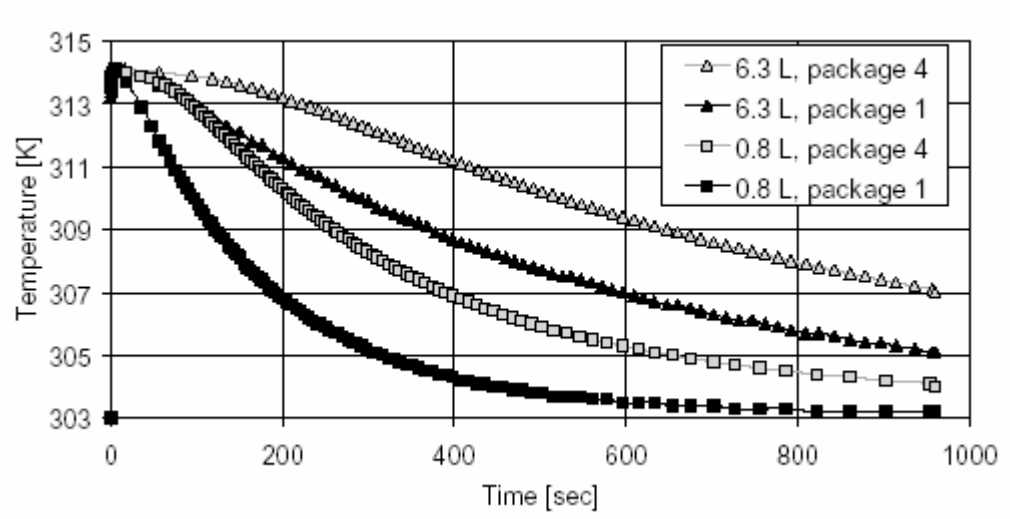

Figure 2.19: Average temperature in package 1 and 4 (Figure 2.18) for 0.8 L and 6.3 L volume versus time (Hartmann et al., 2003).

Knoerzer et al. (2007) developed a model to predict the flow and temperature fields during a sterilization process inside a pilot scale (35 L) vessel without carrier, with metal composite carrier and with a Polytetrafluoroethylene (PTFE) carrier. The model agreed well with experimental results and temperature uniformity was achieved when a PTFE carrier was inserted, acting as a barrier for

flow and heat transfer. After simulation of a high pressure sterilization process at 600 MPa and approx. 121 °C more than 94.6% of the PTFE carrier volume achieved a 12 $\log_{10}$ reduction or more according to the F-value concept (Equation 2.35 with z = 10 °C, T_{ref} = 121.1 °C and $D_{121.1\,°C}$ = 0.21 min for *C. botulinum*). It has to be taken into the account, that only thermal inactivation was modeled.
It can be concluded, that non-uniform temperature conditions can influence the result of high pressure processes (Hartmann & Delgado, 2002; Hartmann et al., 2003; Ardia et al., 2004b; Knoerzer et al., 2007).

2.4. *Bacillus* and *Geobacillus* endospores

2.4.1. Scientific classification

Bacterial endospores were first described by Ferdinand J. Cohn in 1872 and 1876 by Robert Koch in the pathogen, *Bacillus anthracis.* Cohn demonstrated the heat resistance of endospores with *B. subtilis,* and Koch described the developmental cycle of spore formation with *B. anthracis.*
In this study, *Bacillus* and *Geobacillus* spores were investigated. The genus *Bacillus* includes in total 303 species and subspecies (DSMZ, 2008) and is classified as:

Kingdom: Bacteria
Division: Firmicutes
Class: Bacilli
Order: Bacillales
Family: Bacillaceae
Genus: *Bacillus*

Bacillus stearothermophilus has been excluded from the genus *Bacillus* and reallocated to a new genera, *Geobacillus* (Nazina, Tourova, Poltaraus, Novikova, Grigoryan, Ivanova et al., 2001). The genus *Geobacillus* includes in total 19 species and subspecies (DSMZ, 2008).
Endospores have proven to be the most durable type of cell found in nature, and they can remain viable for extremely long periods of time e.g. hundreds millions of years (Cano & Borucki, 1995; Vreeland & Rosenzweig, 2000).

2.4.2. Life cycle of spore forming bacteria

The life cycle of bacterial spores can be divided into five processes with multiplication, possible vegetative cell agglomeration, sporulation, possible spore agglomeration and germination (Figure 2.20). Vegetative cell multiplication is characterized by symmetric division of single organisms into two daughter cells with identical morphological and genetical characteristics. The possible vegetative cell agglomeration has been observed several times under the microscope. It can have the same effect like spore agglomeration (Chapter 2.4.7) on different analysis, e.g. particle analysis (flow cytometry) or plate count. All spore relevant mechanisms of the life cycle are discussed in the following chapters

2.4.3. Sporulation

Many authors have recently studied and reviewed the process of spore formation (e.g. Heinz & Knorr, 2002; Phillips & Strauch, 2002; Piggot & Losick, 2002; Errington, 2003; Barák, 2004; Piggot & Hilbert, 2004; Setlow, 2007). The formation of endospores is a complex and highly-regulated form of development in a relatively simple cell, in which more than 125 genes are involved (Stragier & Losick, 1996). Approximately 7 hours are required to produce high resistant bacterial spores with extensive changes in morphology and physiology of the cells during this transition. Sporulation of *Bacillus* species is induced by starvation for carbon and / or nitrogen and initiated by phosphorylation of the master transcription regulator, Spo0A. Spo0A-phosphate activates expression of genes encoding two sigma (σ) factors that associate with RNA polymerase (RNAP) (Setlow, 2007). Sigma-factors σ are protein subunits, where the associated sigma-factor determines the binding specificity of RNAP to certain promoter regions, enhancing transcription of specific sub-sets of genes involved in specific processes (Haldenwang, 1995; Gruber & Gross, 2003), e.g. sporulation.

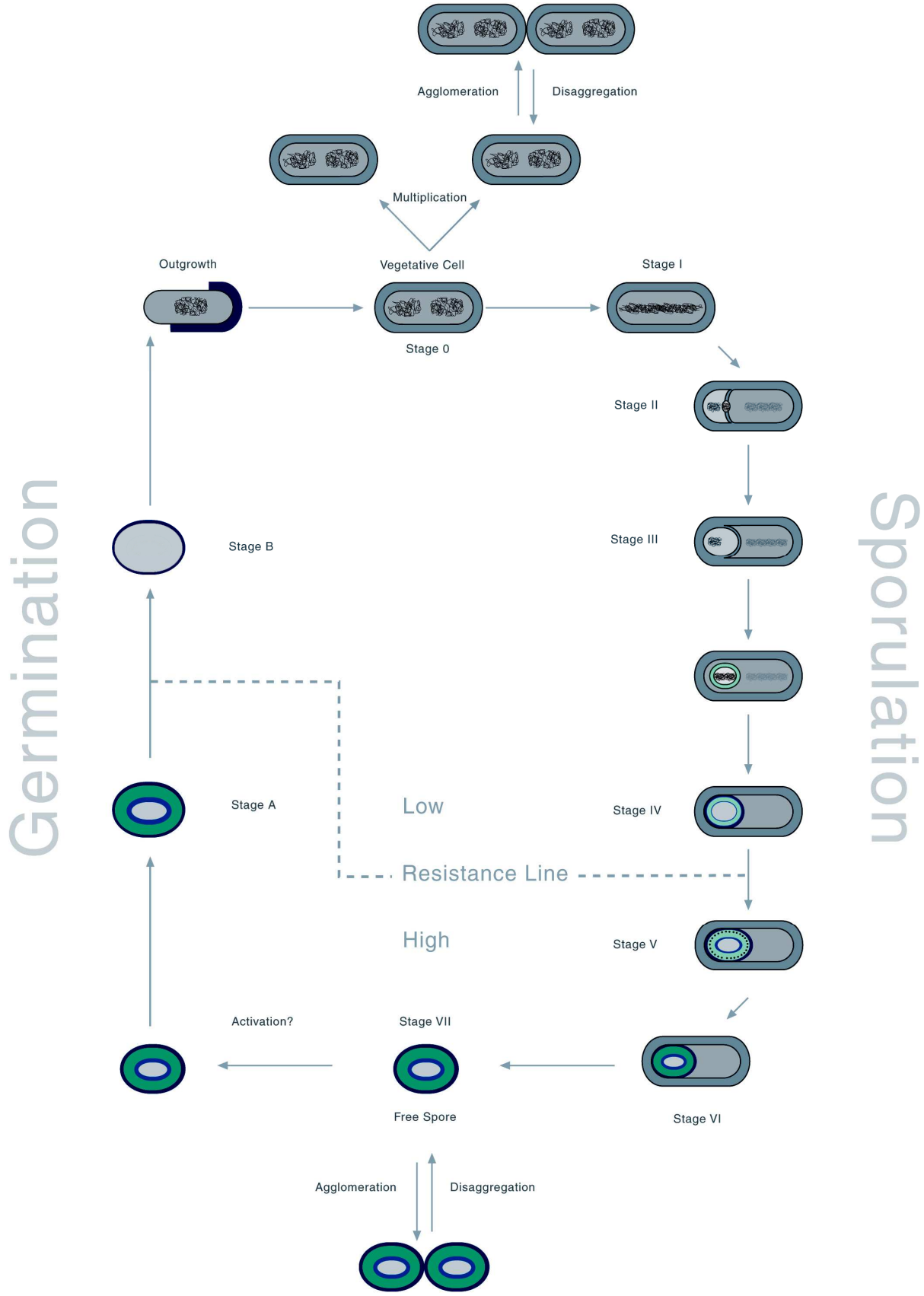

Figure 2.20: Life cycle of bacterial spores (Aiba & Toda, 1966; Heinz & Knorr, 2002; Setlow, 2003).

The process of spore formation can be divided into eight defined stages (0-VII), represented in Figure 2.20. This classification is mainly based on microscopic observation. After induction of sporulation, the vegetative cell (stage 0) begins spore development, when the DNA coils along the central axis of the cell (stage I). It follows the separation of the DNA and division of the cell into two compartments of unequal size but with an identical set of chromosomes (stage II). Then, the forespore or pre-spore is engulfed by the mother cell membrane (stage III). After activation and / or synthesis of additional σ factors, σ^F and σ^G drive the forespore gene expression (Wang, Setlow, Conlon, Lyond, Imamura, Sato et al., 2006) as well as σ^E and σ^K drive mother cell gene expression (Setlow, 2007). The mother cell membrane grows around the forespore compartment, which is already surrounded by an intact membrane. The synthesis of a thick peptidoglycan cortex between the outer and inner forespore membranes initiates the formation of the cortex and the germ cell wall (stage IV) and is accompanied by a large decrease in volume and water content of the forespore. The loss of ions and the simultaneous decrease in pH by approximately 1 unit marked the beginning of the water removal. Before stage IV is reached, small acid soluble proteins (SASP), which play an important role in DNA protection, can be detected. The uptake of considerable quantities of divalent cations like Ca^{2+}, Mg^{2+}, or Mn^{2+} and pyridine-2,6-dicarboxylic acid (DPA), which is synthesized in the mother cell, decreases the water content even further. As water is removed from the spore, the final DPA concentration exceeds its saturation level and it is assumed that DPA-Ca^{2+} complexes are generated. In this stage (V) the protoplast developes an increasing heat resistance and a bright appearance of the spore in phase contrast illumination can be observed. From now the spore is extremely resistant to physical stress like heat, pressure, or radiation, and to the attack of chemical agents or enzymes (Heinz & Knorr, 2002) (Figure 2.20). A very significant fact for possible agglomerations is that a complex proteinaceous coat with coat proteins from the mother cell is layered on the outer surface of the spore (stage VI). *B. cereus* spores as well as some other species have a large external balloon-like layer termed the exosporium. This outer proteinaceous coat and / or exosporium leads to the specific hydrophobicity of bacterial spores (Wiencek, Klapes & Foegeding, 1990), which is very important for spore interactions as well as for the selection of packing materials and surfaces to

prevent bacterial adhesion. The release of the spore (stage VII) occurs during the mother-cell lyses in a process of programmed cell death (Figure 2.20).

The conditions of the whole sporulation process have strong influence on the resistance of bacterial spores (Raso, Palop, Bayarte, Condon & Sala, 1995; Raso, Barbosa-Cánovas & Swanson, 1998a; Melly, Genest, Gilmore, Little, Popham, Driks et al., 2002; Igura, Kamimura, Islam, Shimoda & Hayakawa, 2003). Large biological variations could be observed, which have an impact on every inactivation process. Raso et al. (1995) found that *B. licheniformis* spores, sporulated at 52 °C, showed ten-fold higher heat resistant than those sporulated at 30 °C. The same properties have been observed by Melly et al. (2002) with *B. subtilis* spores. This increase of heat resistance at higher sporulation temperatures could account for the frequent failures of sterilization processes of canned vegetables, during hot seasons in warmer regions.

Wright, Hoxey, Sope & Davies (1995) have screened 29 strains of *B. stearothermophilus* after sporulation on four different media. Only five strains produced spores with the characteristic high resistance, linear semi-logarithmic survivor curves and high growth index, which is typical for a potential biological indicator. Raso et al. (1998a) found spores prepared at 20 or 30 °C to be more resistant to pressure inactivation than those sporulated at > 30 °C after a treatment at 690 MPa and 60 °C for 30 s. Melly et al. (2002) did a detailed investigation on the effect of the sporulation temperature on *Bacillus subtilis* spore resistance and spore composition. The temperature of sporulation affects the pressure resistance and also results in significant alterations in the spore coat and cortex composition. Igura et al. (2003) sporulated *Bacillus subtilis* at 30, 37, and 44 °C and investigated the effect of minerals on the resistance. Spores sporulated at 30 °C had the highest resistance to treatments with high hydrostatic pressure (100 to 300 MPa, 55 °C, 30 min). Pressure resistance increased after demineralization of spores and decreased after remineralisation of spores with Ca^{2+} or Mg^{2+}, but not with Mn^{2+} or K^{+}. This may suggest that Ca^{2+} or Mg^{2+} are involved in the activation of cortex-lytic enzymes during germination. Furthermore, *B. cereus* spores sporulated at pH 6.0 were more resistant to pressures up to 600 MPa than those sporulated at pH 8.0 (Oh & Moon, 2003).

The precise conditions for the formation of bacterial spores have a large effect on many spore properties and the increased pressure resistance with lower sporulation temperature is the opposite as found for heat resistance.

2.4.4. Germination

The loss of resistance properties is the crucial step during the spore germination process (Figure 2.20), which is of highest importance for sterilization techniques and research. Recently, the germination of spores have been studied and reviewed extensively (Heinz & Knorr, 2002; Moir, Corfe & Behravan, 2002; Setlow, 2003; Moir, 2006). Therefore, only a brief summary is given here.
Germination can be divided into nutrient and non-nutrient mechanisms, where the main involved systems are the nutrient germinants, germinant receptors, the ion and DPA channels as well as the cortex lytic enzymes (CLEs). The receptor proteins are encoded by the *gerA* operons homologs expressed in the forespore late in sporulation and located at the inner membrane of the spore. Before the germinant interacts with the receptor, there is a possible activation (e.g. by heat shock), which can potentiate the germination (Figure 2.20). However, the mechanism of spore activation is still not fully understood (Paidhungat & Setlow, 2002), and several hypothesis have been published (Aiba & Toda, 1966; Mathys, Heinz, Schwartz & Knorr, 2007b). Setlow (2003) reviewed the further steps in detail and gave an order of action for physiological mechanisms and structure alterations (Figure 2.20-2.21). As first H^+ ions, monovalent cations and Zn^{2+}, probably from the spore core, were released in stage A (Figure 2.20). Especially the H^+ release increases the internal pH-value of the spore from 6.5 to 7.7, which enables enzyme actions (Jedrzejas & Setlow, 2001) once the spore core hydration is high enough. In the next step DPA (10% of spore dry weight) and its associated divalent cations (e.g. Ca^{2+}) are release. This event triggers CwlJ (CLE) action as the released Ca^{2+}–DPA flows past this enzyme. Two crucial cortex lytic enzymes have been identified. CwlJ is DPA-responsive and located at the cortex-coat junction. SleB is a lytic transglycosylase. It is present at the inner spore membrane and in outer layers. SleB is more resistant to wet heat than CwlJ (Moir, 2006). After the replacement of DPA by water, core hydration and heat sensitivity is increased. It follows the hydrolysis of the spore's peptidoglycan cortex in stage B (Figure 2.20) as wells as further water uptake and swelling of

the spore core, which leads to the expansion of the germ cell wall (Setlow, Melly & Setlow, 2001) and a loss of dormancy. From now protein mobility in the core returns and enzyme activity is possible (Setlow et al., 2001; Cowan, Koppel, Setlow & Setlow, 2003). During all these mechanisms no detectable energy metabolism (Paidhungat & Setlow, 2002) takes place. SASP, which protect the spore DNA (Setlow, 2007), are degraded and hydrolyzed by enzyme action in the outgrowth phase (Figure 2.20). It follows a macromolecular synthesis and escape from the spore coats. For an individual spore these events may take only few minutes, but because of significant variation of spores, these mechanisms may take much longer for the whole population (Setlow, 2007).

For a better differentiation of nutrient and non-nutrient spore germination Setlow (2003) developed a reaction / interaction model, which is shown in Figure 2.21. Alkylamines can activate Ca^{2+}–DPA release by effects at the spore's inner membrane and do not require any germinant receptors. Exogenous Ca^{2+}–DPA is probably released from other neighboring spores activates CwlJ, which leads to cortex hydrolysis and hydration. Lysozymes can also cause cortex lysis (Setlow, 2003).

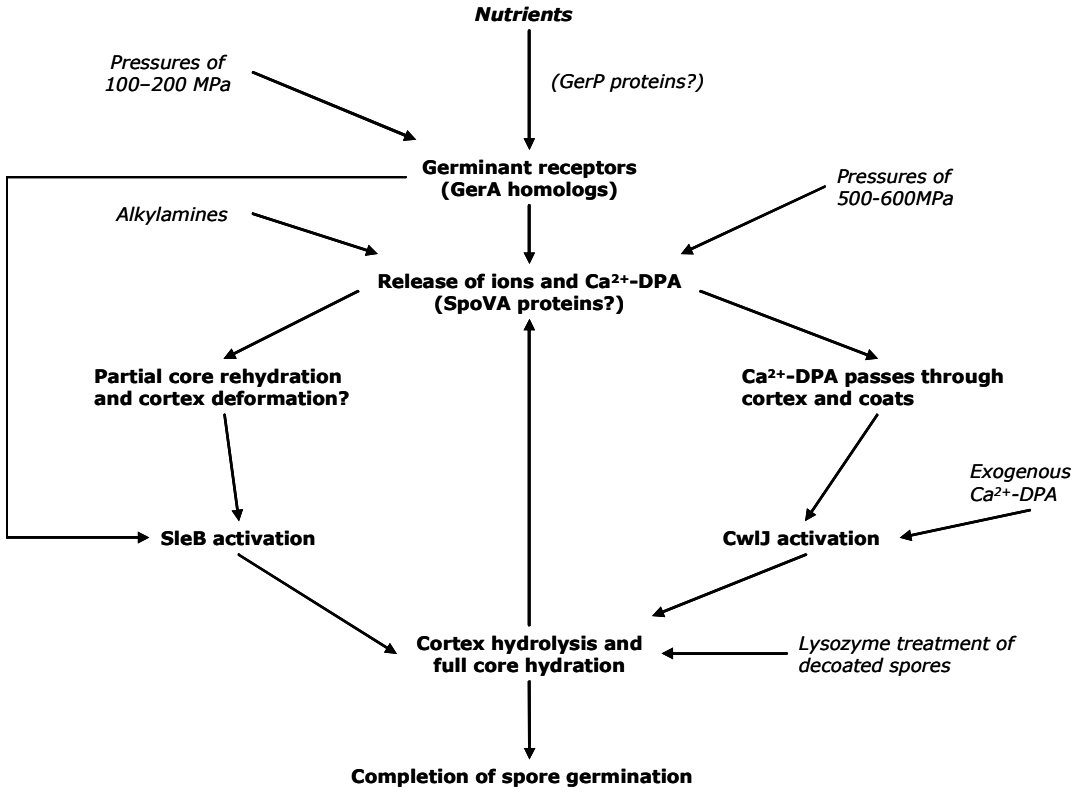

Figure 2.21: Reaction / interaction model for nutrient and non-nutrient spore germination in *B. subtilis* (Setlow, 2003).

For this thesis the main interesting non-nutrient germination is the pressure induced germination. Pressures between 100 - 200 MPa activate the germinant receptors, which lead to pathways similar to nutrient germination. The whole reaction and / or kinetic depends strongly on temperature (Heinz & Knorr, 1998). Heinz and Knorr (1998) assumed that pressure and temperature can trigger the de-immobilization of CLE activities and cause inactivation of the same enzymes by structural unfolding, which probably completely inhibits the CLE activity. Very high pressures of 500-600 MPa open the Ca^{2+}-DPA channels (Paidhungat, Setlow, Daniels, Hoover, Papafragkou & Setlow, 2002), which may result in an incomplete germination process (Wuytack, Boven & Michiels, 1998; Paidhungat et al., 2002).

2.4.5. Resistance

The extreme resistance of bacterial endospores to physical and chemical treatments is related to a number of factors, which reprersents a significant problem for the food industry. Main factors for resistance are the very high core dehydration, impermeability of coat layers and membranes, and the presence of SASPs. Spore resistance can vary with different treatments, because of different target sites. The DNA is the main target of γ-radiation, UV-light, freezing, desiccation and chemicals. However, the DNA-α/β-type SASP complex protects the spore against radiation or UV-light, stabilizes the helix structure during drying and freezing, as well as increases the resistance to small molecules, like formaldehyde (Loshon, Genest, Setlow & Setlow, 1999). Chemicals are mainly excluded by the complex permeability barrier, but small molecules may penetrate the spore and attack the DNA. During thermal treatment, proteins are the main targets instead of the DNA, because general mutagenesis or DNA damage have not been observed (Fairhead, Setlow & Setlow, 1993). Again, the DNA-α/β-type SASP complex leads to one of the highest thermal stabilities in nature (Setlow, 2007). Divalent cations such as Ca^{2+}, Mn^{2+} ,Mg^{2+} and DPA have a synergistic effect on stability. Ca^{2+}-DPA protects the spore DNA against wet and dry heat, desiccation and hydrogen peroxide, but actually sensitizes DNA in spores to UV radiation (Douki, Setlow & Setlow, 2005; Setlow, Atluri, Kitchel, Koziol-Dube & Setlow, 2006). Further, there might be a direct correlation

between core water content and thermal stability. Due to the low water content, molecular motions are inhibited and macromolecules are stabilized (Heinz & Knorr, 2002).

In 1974, Wilson was the first who presented the the synergistic effect of pressure and temperature on spore inactivation. Mallidis and Drizou (1991) and later Seyderhelm and Knorr (1992) investigated this synergistic effect on *Bacillus stearothermophilus* spore inactivation. Many authors followed, where Heinz and Knorr (2002) suggested a system to compare the effect of pressure on the heat resistances of the endospores investigated. In Figure 2.22 the thermal resistances of spores from different organisms at 400 MPa and ambient pressure (Stumbo, 1948; Navani, Scholfield & Kibby, 1970; Kakugawa, Okazaki, Yamauchi, Morimoto, Yoneda & Suzuki, 1996; Okazaki, Kakugawa, Yamauchi, Yoneda & Suzuki, 1996; Rovere et al., 1999) were compared (Heinz & Knorr, 2002).

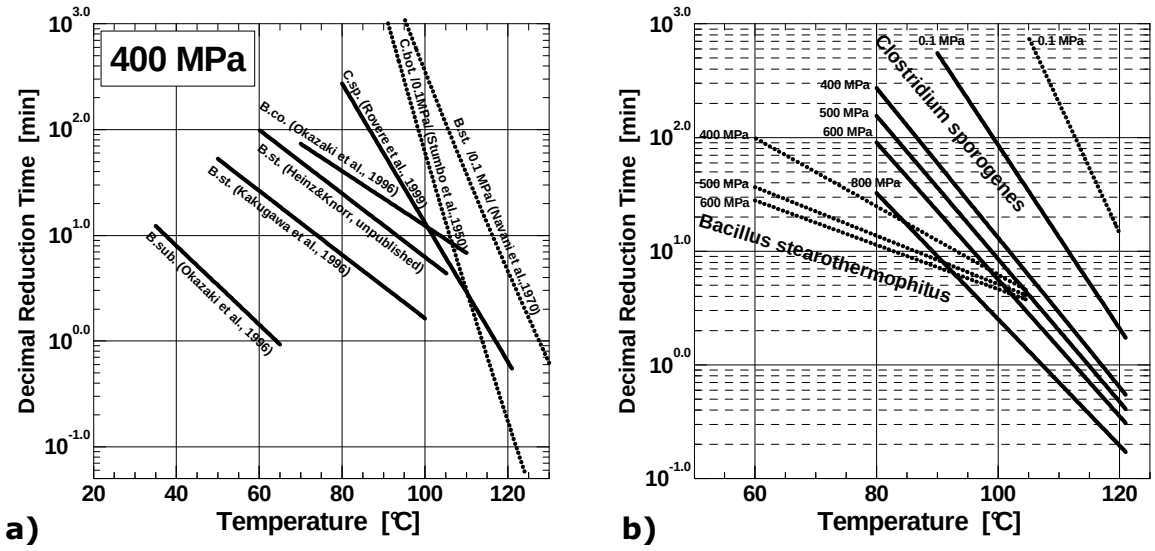

Figure 2.22: a) Thermal resistances of endospores at 400 MPa [B.sub. (*Bacillus subtilis*); B.st (*Bacillus stearothermophilus*); B.co. (*Bacillus coagulans*); C.sp. (*Clostridium sporogenes*)] compared to ambient pressure [B.st (*Bacillus stearothermophilus*); C.bot (*Clostridium botulinum*): dotted lines] and b) thermal resistances of *Clostridium sporogenes* in beef broth (Rovere et al., 1999) and *Bacillus stearothermophilus* in mashed broccoli in dependence of the applied pressure (Heinz & Knorr, 2002).

It is also possible to compare the effect of different pressure levels on the thermal resistance in one graph (Figure 2.22 b). Heinz and Knorr (2002) used thermal resistances of *Clostridium sporogenes* in beef broth (Rovere et al., 1999) and *Bacillus stearothermophilus* in mashed broccoli (Ananta, Heinz, Schlüter &

Knorr, 2001) in dependence of the applied pressure. A reduction of the D-value can be obtained either by a temperature or pressure rise (Heinz & Knorr, 2002). However, these diagrams are based on linear $\log_{10}$ reductions and first order kinetics, although experimental deviations (shoulder and tailing) have been observed. Other modeling approaches lead to further comparison systems of literature data, for example the p-T-diagram.

2.4.6. Predictive modeling

Mathematical modeling is frequently used in food microbiology to quantify the effect of environmental conditions on growth or destruction of microbial populations. Having the quantitative knowledge of the surviving organisms, when exposed to alterations in the habitat, offers a useful tool particularly for those concerned with the preservation of foods. The different inactivation theories have been mainly grouped into "mechanistic" and "vitalistic" models (Watson, 1908; Lee & Gilbert, 1918).

2.4.6.1. The mechanistic conception

The central background of the mechanistic conception is that the process of destruction "is an orderly time process presenting a close analogy to a chemical reaction" (Lee & Gilbert, 1918). Consequently, inactivation of bacterial spores would be defined as a pseudo first-order molecular transformation. The theory explains the progressive heat inactivation by the discrete and random action of energy transferring collisions. If the number of target sites (=microorganisms) is higher, collisions are more probable to happen. Further it is assumed that there is a general similarity of resistance between the different individuals of a population (Lee & Gilbert, 1918). Chick (1910) first described the reduction of the logarithmic number of bacterial cells in response to chemical agents or heat to be a linear function of time t.

$$\ln\left(\frac{N}{N_0}\right) = -k \cdot t \quad \text{or} \quad \log\left(\frac{N}{N_0}\right) = \frac{-k \cdot t}{2.303} \tag{2.36}$$

The slope k obtained from linear regression analyses of the survival count N relative to the initial number of microorganisms (N/N_0) plotted logarithmically versus time formed the basis for evaluation concepts of thermal processes with variable treatment temperatures (e.g. F-value). First application occurred when Esty and Meyer (1922) developed the concept of setting process performance criteria for heat treatment of low-acid canned food products to reduce the risk of botulism. Apart from this empirical finding, Equation 2.36 can be derived from integrating the following linear first order differential equation:

$$\frac{dN}{dt} = -k \cdot N \qquad (2.37)$$

The interpretation of Equation 2.37 yields that the decrease in survivor count with time (dN/dt) is proportional to the number of remaining survivors N itself.
This theory served well for detailed investigations of spore inactivation, where additional parameters affecting the inactivation of spores were included (Fernandez, Gomez, Ocio, Rodrigo, Sanchez & Martinez, 1995; Gonzalez, Lopez, Mazas, Gonzales & Bernardo, 1995) or intermediate steps (e.g. activation and/ or germination) were incorporated with a system of first order differential equations (Rodriguez, Smerage, Teixeira & Busta, 1988; Abraham, Debray, Candau & Piar, 1990). By using the Arrhenius equation (Equation 2.15) the temperature dependency of corresponding rate constants was found to be appropriately described. This approach has been the theoretical basis of the growing canning industry (Ball, 1923) and the wide use at industrial sterilization processes showed the universal application. However, experimental deviations were observed early (Esty & Meyer, 1922; Aiba & Toda, 1966; Cerf, 1977). Whether Equation 2.37 can also serve as a general rule for thermal inactivation of microorganisms is still under discussion. Many authors have challenged its general applicability because of the frequently observed deviations from the log-linear shape of the inactivation kinetics (Casolari, 1994). An occurring initial lag phase ("shoulder"), as well as a leveling-off at longer treatment times ("tailing") cannot be accurately described and thermal preservation concepts based on Equation 2.36 may fail.
Modifying Equation 2.37 by using an empirical reaction order n leads to Equation 2.38, the n^{th} order reaction model (Kessler, 1996):

$$\frac{dN}{dt} = -k \cdot N^n \qquad (2.38)$$

This expression describes non-linear $\log_{10}$ reductions and enables the use of Arrhenius equation (Equation 2.15) for the temperature dependence or Eyrings equation (Equation 2.16) for the pressure dependence of the corresponding rate constant k. The reaction order n can be regressively determined and has no mechanistic background. By using a functional relationship for k(p, T) it is possible to create iso-kinetic lines in the pressure and temperature landscape (p-T diagram).

2.4.6.2. The vitalistic conception

The vitalistic approach is based on the assumption that individuals in a population are not identical (Lee & Gilbert, 1918). It considers the biological diversity of microbial resistance within a microbial population against different kind of external stress. Consequently, it is assumed that the survival curve is the cumulative form of a temporal distribution of lethal events. By using this interpretation, survival curves can be described by the Weibullian Power Law (Equation 2.39),

$$\log_{10}\left(\frac{N}{N_0}\right) = -b \cdot t^n \qquad (2.39)$$

with the Weibull parameters b and n. Equation 2.39 was first formulated by Rosin and Rammler (1933) in a similar mathematical form. The authors observed that the particle size frequency distribution of coal-dust can be described adequately with this expression, which was used for modeling of microbiological inactivation curves later (Heinz & Knorr, 1996; Heinz, 1997; Peleg & Cole, 1998). In this context, the probability density function reflects the distribution of critical times for inactivation (Van Boekel, 2002).

In a summary about modeling approaches of Heldman and Newsome (2003) van Boekel compared different theories for the description of the initial lag phase ("shoulder") during spore inactivation. After comparison and evaluation by the Akaike criterion and a Bayesian posterior probability test of the Shull and Sapru models (both based on first-order kinetics), the stochastic Peleg model, and the "double Weibull", the two empirical model performed best (Heldman & Newsome, 2003). Fernández, Salmerón, Fernández and Martínez (1999) found that the prediction of thermal inactivation of *Bacillus cereus* spores was closer to the

experimental data, when using the Weibull distribution (Equation 2.39) instead of the log-linear model (Equation 2.36). Anderson, McClure, Baird-Parker and Cole (1996) obtained similar results with thermal inactivation data of *Clostridium botulinum* 213B.

However, Watson (1908) noted that the vitalistic conception could be wrong, because a very high amount of the spores would have a low resistance, instead of following the normal distribution that would be expected from natural biological variability. Cerf (1977) stated that tails or concavities upward could be artefacts. Kellerer (1987) mentioned that the vitalistic theory ignores the stochastic basis for the inactivation transformation (Maxwell- Boltzman distribution of speed of molecules or random radiation "hits" on DNA). Teixeira and Rodriquez (Heldman & Newsome, 2003) concluded that empirical (curve-fitting) models generally should not be used for modeling of microbial inactivation.

2.4.7. Agglomerations

The effectiveness of thermal treatments is often verified by challenge tests using foods that have been spiked with highly concentrated microbe suspensions. Due to preparation, storage and handling of those suspensions the clumping and the formation of aggregates can hardly be avoided (Aiba & Toda, 1966; Bueltermann, 1997; Furukawa, Narisawa, Watanabe, Kawarai, Myozen, Okazaki et al., 2005; Mathys et al., 2007b). This phenomenon is well known, Aiba and Toda (1966) first reported the effect of spore agglomerations on inactivation. However, the importance for the quantitative assessment of survivors in inactivation experiments has rarely been addressed. Its importance becomes evident by the following. Agglomerates always produce one colony per each plate. Consequently, agglomerates of unknown cell numbers are always counted as one spore until all spores in the agglomerate are inactivated. Beyond this agglomeration and disintegration can change the colony forming units per milliliter. In this context Aiba and Toda (1966) as well as Bueltermann (1997) developed a model for the discussed phenomenon.

The following assumptions were made in Bueltermanns model:

- thermal inactivation is similar to the target theory (Lea, 1955) for the inactivation of bacterial spores subjected to irradiation,
- all spores are under the same temperature and time conditions,
- inactivation underlying first order reaction with the rate constant k or k(t),
- inactivation of a single spore in an agglomerate is independent on the size of the agglomerate, and
- the number of spores i from an agglomerate represent the size of the agglomerate.

Under quasi-isothermal conditions the survival probability p of a single spore is:

$$p(t) = e^{-k \cdot t} \quad \textit{with } k=\textit{const} \tag{2.40}$$

Alternatively the inactivation probability q would be:

$$q(t) = 1 - p(t) = 1 - e^{-k \cdot t} \tag{2.41}$$

By the time all i spores in the agglomerate will be inactivated the agglomerate would form one colony on the agar plate. The probability in this case is

$$p_i(t) = \frac{N(t)}{N_0} = 1 - [q(t)]^i = 1 - (1 - e^{-k \cdot t})^i \tag{2.42}$$

Many other models, ranging from the inactivation of bacterial to mammalian cells, describe such initial zero destruction rate with the same mathematical approach (Alper, Gillies & Elkind, 1960; Bender & Gooch, 1962; Powers, 1962; Tyler & Dipert, 1962). Figure 2.23 shows the resulting inactivation curves with different numbers of spores i in one agglomerate.

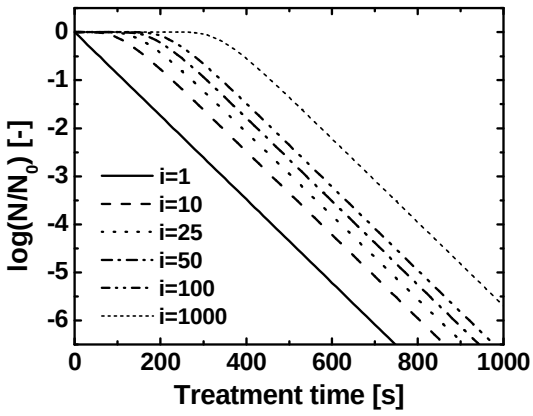

Figure 2.23: Influence of aggregate size on spore inactivation kinetics with the spore number per agglomerate i using a D-value of 115 s.

Under non quasi-isothermal conditions the term $e^{-k \cdot t}$ from Equation 2.40 can either be transformed into

$$e^{-\int_0^t k(t)dt} \quad with \;\; k(t) = k_0 \cdot e^{-\frac{E_a}{R_m \cdot T(t)}} \tag{2.43}$$

with the temperature dependence on time T(t) (Arrhenius, 1889)
or into

$$e^{-\int_0^t \frac{\ln(10)}{D(t)}dt} \quad with \;\; D(t) = D_{ref} \cdot 10^{\frac{T_{ref} - T(t)}{z}} \tag{2.44}$$

by using the z-value concept, with the D-value dependent on time D(t), the reference D-value D_{ref} and temperature T_{ref} as well as the z-value.
At a given agglomeration size distribution $q_0(i)$, the single survival probability for every agglomerate can be calculated. When agglomerates of all sizes are summed up the whole survival rate is received by

$$\log_{10} \frac{N(t)}{N_0} = \log_{10} \left(\sum_{i=1}^{i_{max}} q_0(i) \cdot p_i(t) \right) \tag{2.45}$$

including the survival probability $p_i(t)$ of an agglomerate with i spores.
In case of changing agglomeration size distribution, because of disintegration and / or further agglomeration processes, the factor F_A has been introduced

$$F_A = \frac{N_A}{N_{A0}} \tag{2.46}$$

with the sum of all agglomerates before (N_{A0}) and after (N_A) the treatment. Then F_A has to be integrated into Equation 2.45:

$$\log_{10} \frac{N(t)}{N_0} = \log_{10} \left(\sum_{i=1}^{i_{max}} F_A \cdot q_0(i) \cdot p_i(t) \right) \tag{2.47}$$

With the help of F_A an increase of the CFU mL^{-1}, similar to "activation", at the beginning of the treatment can be described.
In literature there are no data available about spore agglomeration under high pressure.
The main reason for spore agglomerations seems to be the outer proteinaceous coat and / or the spore exosporium. These layers may lead to the specific hydrophobicity of bacterial spores, which affects the bacterial adhesion and "clumbing behavior" (Doyle, Nedjat-Haiem & Singh, 1984; Wiencek et al., 1990). The hydrophobicity can be changed by heat treatment (Craven & Blankenship, 1987; Wiencek et al., 1990; Furukawa et al., 2005).

2.4.8. Hypothesized mechanism of spore inactivation

Spore inactivation, either by high pressure or combined high pressure and heat, is partly attributed to germination (Clouston & Wills, 1969; Raso et al., 1998a; Knorr, 1999; Mathys, Chapman, Bull, Heinz & Knorr, 2007a). Ardia (2004) investigated the pressure and temperature effect on inactivation independently and discussed the spore inactivation mechanisms at very high pressure. The author compared the behavior under high pressure of CLEs from the spore coat with bacterial spores (Figure 2.24). He assumed that the CLEs, which catalyze the cortex breakdown and so the access of water to the spore core, are pressure unstable under a certain range of pressure-temperature conditions $(p\text{-}T)_1$. At this stage, temperature is leading the inactivation process and an increase of pressure has no consequence. The main effect of pressure is to squeeze water inside of the spore cortex. Without active CLEs, the spore cortex can only be re-hydrated and subsequently inactivated by ultra high pressure of minimal 800 MPa (Ardia, 2004).

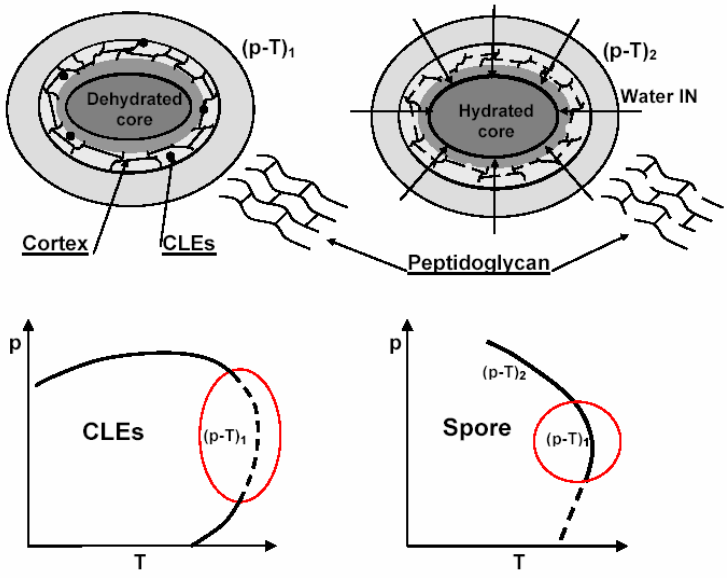

Figure 2.24: Hypothesized mechanism of spore inactivation. It is assumed that at $(p\text{-}T)_1$ the lytic-enzymes which are responsible for the cortex breakdown are inactivated by the pressure-temperature intensity of the treatment, while at $(p\text{-}T)_2$, higher pressure levels require lower temperature to achieve the same degree of inactivation (Ardia, 2004).

The phenomenon of spore stabilization at ultra high pressure has been reported later by other authors (Margosch et al., 2006; Patazca, Koutchma & Ramaswamy, 2006; Rajan et al., 2006a; Ahn, Balasubramaniam & Yousef,

2007). Margosch et al. (2006) mentioned that bacterial spores are very complex and the behavior of a single protein, which shows also stabilization areas under pressure, can hardly be described as determinative for inactivation unless it is required for a vital function (e.g. as a structural or protective component).

2.5. Matrix effects

2.5.1. Medium constituents

Medium constituents such as carbohydrates, proteins and lipids can have a protective effect on microorganisms (Simpson & Gilmour, 1997). Different media such as milk offer a protective effect to vegetative cells (Hauben, Bernaerts & Michiels, 1998; Black, Huppertz, Kelly & Fitzgerald, 2007a). However, Van Opstal et al. (2004) detected a higher $\log_{10}$ reduction of *B. cereus* spores at 300 or 600 MPa in milk compared to phosphate buffer, because of a higher level of spore germination in milk. Other media like meat batter (fried minced pork), mashed potatoes (Moerman, Mertens, Demey & Huyghebaert, 2001) or crabmeat (Reddy, Solomon, Tezloff & Rhodehamel, 2003; Reddy, Tetzloff, Solomon & Larkin, 2006) showed no improved inactivation of spores or any protection effects.

A low water activity protects microorganisms against the effects of high pressure (Oxen & Knorr, 1993; Palou, Lopez-Malo, Barbosa-Canovas, Welti-Chames & Swanson, 1997) and Timson and Short (1965) found spores of *B. subtilis* to be protected from pressure effects by glucose and NaCl. Addition of sucrose (Taki, Awao, Toba & Mitsuura, 1991; Raso, Gongora-Nieto, Barbosa-Canovas & Swanson, 1998b) or glycerol (Taki et al., 1991) increased the spore resistance to inactivation. The improved resistance can be attributed to incomplete germination in the absence of water (Black, Setlow, Hocking, Stewart, Kelly & Hoover, 2007b). Lee et al. (2006) demonstrated, that the effect of high pressure combined with heat against spores of *A. acidoterrestris* was highly dependent on the apple juice concentration, where 17.5 °Brix resulted in 5 $\log_{10}$ reductions but 30 °Brix just in 2 $\log_{10}$ reduction at 71 °C and combined pressure. The effects of medium constituents on sporulation can also have an effect on pressure and / or thermal resistance.

2.5.2. Food additives

Food additives such as nisin, lysozyme, pediocin AcH, lacticin 3147, bovine lactoferrin and lactoferricin can induce additive or synergistic effects with high pressure inactivation in different media e.g. whey, skim milk and buffer systems (Kalchayanand et al., 1994; Hauben, Wuytack, Soontjens & Michiels, 1996; Roberts & Hoover, 1996; Kalchayanand, Sikes, Dunne & Ray, 1998; Garcia-Graells, Masschalck & Michiels, 1999; Morgan, Ross, Beresford & Hill, 2000; Masschalck, Van Houdt & Michiels, 2001; Masschalk, Van Houdt, Van Haver & Michiels, 2001). However, combined spore inactivation is much more complex in comparison to vegetative cell destruction. It seemed that pressure inactivation of *B. cereus* and *B. coagulans* spores is enhanced in the presence of the emulsifier sucrose laurate (< 1%) in milk and beef (Shearer, Hoover, Dunne & Sikes, 2000). The authors noted that the emulsifier inhibited spore outgrowth and delivered not a lethal effect, because of the difference in CFU on enumeration media and agar supplemented with sucrose laurate. However, Stewart et al. (2000) found a 6 $\log_{10}$ reduction of *B. subtilis* in McIlvaine's buffer at 404 MPa, 45 °C for 15 min with 0.1% sucrose laurate.

Nisin (1.56 mg L^{-1}) and lysozyme were combined with pressure by Lopez-Pedemonte et al. (2003). It was possible to increase the *B. cereus* inactivation in cheese with nisin, but not with lysozyme. Four clostridial species *C. perfringens, C. sporogenes, C. tertium*, and *C. laramie* were inactivated by a combination of nisin, pediocin, and treatment at 345 MPa for 5 min at 60 °C in roast beef (Kalchayanand, Dunne, Sikes & Ray, 2003). After high pressure processing in combination with either pediocin or nisin the shelf-life of the roast beef inoculated with a mixture of clostridial spores was doubled in comparison to only pressure treated samples (42 d at 4 °C).

It has to taken into account, that carboxylic acids show enhanced dissociation under high pressure (analogue Equation 2.29-2.31). The effect of these food additives would decrease, because undissociated acid forms are believed to be the active antimicrobial entities (Eklund, 1989; Earnshaw, Appleyard & Hurst, 1995).

2.5.3. pH-value

A combination of pH-value, temperature and pressure can act synergistically (Zipp & Kauzmann, 1973) leading to increased microbial inactivation. During the first phase of basic inactivation studies buffer systems to achieve constant pH-values and medium properties are commonly used. However, the dissociation equilibrium in water and buffer solutions varies with pressure and temperature (Distèche, 1959; North, 1973; Marshall & Franck, 1981; Hamann, 1982; Kitamura & Itoh, 1987; Quinlan & Reinhart, 2005; Bruins, Matser, Janssen & Boom, 2007). The change of the pK_a-value may play a major role in different sensitive reactions, but its behavior has rarely been investigated. Distèche (1959) developed one of the first pH electrodes that can be used up to 150 MPa. At present, the dissociation equilibrium shift cannot be measured in solid food, but few optical measurement methods during pressure treatment up to 250 MPa (Hayert, Perrier-Cornet & Gervais, 1999; Quinlan & Reinhart, 2005) and 450 MPa (Stippl, Delgado & Becker, 2002; 2004) have been developed for in situ pH measurement of liquids. However, these experimental methods are limited and not suitable for the investi,gation of combined thermal and pressure effects. Due to the shift of dissociation equilibria during heating and / or compression, the results of inactivation experiments are prone to error, if not designed correctly. Different authors showed that there is a strong pH dependence of spore inactivation during thermal treatment (Sognefest, Hays, Wheaton & Benjamin, 1948; Loewick & Anema, 1972; Alderton, Ito & Chen, 1976; Cameron, Leonard & Barrett, 1980; Hutton, Koskinen & Hanlin, 1991). The same dependence was observed during high pressure inactivation. Clouston and Wills (1969) found different logarithmic reduction of *B. licheniformis* spores in water and phosphate buffer after low pressure inactivation up to 170 MPa. Timson and Short (1965) observed higher destruction of *Bacillus subtilis* at pH 6 than at pH 8. Spores of *C. sporogenes* and *B. coagulans* were also more sensitive to high pressure inactivation (400 MPa) at pH 4.0 than at pH 7.0 (Roberts & Hoover, 1996; Stewart et al., 2000). Another example for the influence of the pH-value has been presented by Ardia (2004). The iso-kinetic line of spores suspended in ACES at pH 6.0 showed a threshold temperature level (113 °C), where an increase of pressure was not producing an improvement of the inactivation

reaction. Wuytack & Michiels (2001) found that highest levels of *B. subtilis* spore inactivation were achieved when spores were high pressure treated (100 to 600 MPa/ 40 °C) at neutral pH and then exposed to low-pH conditions for 1 h. This was explained by an inhibition of the pressure-induced germination at low pH-values. It was also reported that the pH-value of the sporulation medium can also influence the resistance of spores (Oh & Moon, 2003).

3. Materials and Methods

3.1. *Geobacillus and Bacillus* spores - microbial methods

All experiments with *G. stearothermophilus* spores were performed with commercially available *G. stearothermophilus* spore suspensions ATCC 7953 [Merck KGaA, Darmstadt, Germany or NAMSA, Northwood, Ohio, USA (product certification in Annex 1), simplified as Merck or NAMSA]. For the treatments spore suspensions with initial counts of $7 \cdot 10^7$ - $3 \cdot 10^8$ CFU mL^{-1} were centrifuged at 3450 g for 3 min, resuspended in sterile 0.01 - 0.05 M ACES or phosphate buffer (Merck KGaA, Darmstadt, Germany) to approximately 10^7 CFU mL^{-1} or 10^8 CFU mL^{-1}. Details for buffer or spore concentration can be found in the text. Both microscopic examination (Eclipse E400, Nikon Corporation, Tokyo, Japan) and plate counts before and after heating at 80 °C for 10 min indicated that the amount of germinated spores and vegetative cells in the spore suspension was negligible. No increase of the CFU mL^{-1} after 80 °C for 10 min was observed. Determination of survivors was measured using plate counts on Nutrient agar (Oxoid, Basingstoke, UK) following serial dilution in Ringer's solution. Colonies were counted after incubation at 55 °C for 72 h and 144 h. No significant differences between the two incubation times could be observed.

Spore inactivation at different pH-values were performed with a frozen spore pool (-80 °C) with initial counts of $7 \cdot 10^7$ - $3 \cdot 10^8$ CFU mL^{-1} to obtain a homogeneous spore resistance over the whole experimental time. For inactivation studies the thawed spore suspensions were resuspended in sterile buffer solutions at different initial pH-values (4.5 - 8) to approximately 10^7 CFU mL^{-1}. Buffer pH-value was adjusted with a pH measuring electrode (InLab 422, Mettler-Toledo, Schwerzenbach, Switzerland) and 0.1 M sodium hydroxide base solution.

Bacillus licheniformis spores (Food Science Australia FRRB 2785) isolated from a dairy product were resuscitated from frozen glycerol stock on nutrient agar (Oxoid, Basingstoke, UK) + 0.1% w/v starch (Ajax Finechem, Seven Hills, Australia) (NAS) and incubated at 37 °C for 19 h. A cell suspension of this culture was prepared in sterile distilled water (SDW), and inoculated (0.1 mL) onto the surface of a bed of nutrient agar with added minerals (Cazemier,

Wagenaars & ter Steeg, 2001) contained in cell culture flasks (650 mL vented, Greiner Bio-One GmbH, Frickenhausen, Germany), incubated at 37 °C for 7 days. Sporulation of more than 95% of culture cells was checked using phase contrast microscopy and spores were harvested (4000 g at 4 °C for 10 min and pellets collected in 5 mL SDW), washed (three times) and resuspended in chilled SDW. Aliquots, 1 mL, of washed spore suspension were snap-frozen in cryogenic vials (2 mL; Nalgene Cryowave, New York, USA) and stored at -80 °C. Spore counts were performed on thawed suspensions by spread plating (0.1 mL) appropriate dilutions in sodium chloride peptone solution (0.9 g NaCl and 0.1 g bacteriological peptone per L) on NAS, incubated at 37 °C for 24 h. The spore count of thawed suspensions was established as $1.05 \cdot 10^{10}$ CFU mL^{-1}. Microscopic examination indicated suspension homogeneity, with negligible spore agglomerates, germinated (dark phase) spores or vegetative cells. Determination of survivors was measured using plate counts on NAS following serial dilution in Ringer's solution. Colonies were counted after incubation at 37 °C for 24 h and 48 h. No significant differences between the two incubation times could be observed. In addition, high pressure treated samples were subsequently treated at 80 °C for 20 min in a water bath, in order to eliminate high pressure germinated and sensitized spores. A second plate count determination of survivors was conducted on these samples, and compared with the counts obtained by only high pressure processing.

For screening under the microscope (Eclipse E400, Nikon Corporation, Tokyo, Japan), *B. cereus* and *B. coagulans* spore suspensions were provided by an external company.

3.2. Biophysical analysis

G. stearothermophilus spore suspensions ATCC 7953 from Merck were analyzed by microscopy (Eclipse E400, Nikon Corporation, Tokyo, Japan) and with the MTS three-fold dynamic optical back-reflection measurement (3D ORM) Particle System Analyzer (Schwartz & Braun, 1999; Mathys et al., 2007b). For homogeneous samples the suspension was stirred during the measurement. The final computational analysis (WinORM 4.36, MTS GmbH Düsseldorf, Germany) resulted in the equivalence diameter of Gaussian spheres (µm) in the range

between 0.1 µm and 60 µm. Minimum of six measurements were averaged and further analyzed with Origin 7SR1 software (Origin Lab Corp., MA, USA).
G. stearothermophilus spore suspensions ATCC 7953 from NAMSA were analyzed with the Sysmex FPIA (Flow Picture Image Analysis) 3000 (Malvern Instruments Ltd., Worcestershire, UK) and the Multisizer 3 COULTER COUNTER (Beckman Coulter, Inc.). Original spore suspensions was 1:10 diluted in sterile filtered 0.05 M ACES buffer with pH 7, which led to a concentration of approx. 2 x 10^7 particles per mL. Using the FPIA 3000, cooled samples (1 mL) were analyzed with high power field (HPF) and two lenses, 10x in a range of 1.5 µm – 40 µm and 20x for 0.8 µm – 20 µm. The FPIA 3000 was calibrated by using 1 and 2 µm latex spheres (LTX5100A, LTX5200A latex microsphere suspensions, Duke Scientific Corporation, Palo Alto, California, USA). After calibration the CE diameter of the 1 µm latex spheres were measured as 1.056 + /- 0.03 µm (lens 20x) and 2.056 + / - 0.03 µm (lens 10x) for 2 µm latex spheres.
The Multisizer 3 COULTER COUNTER (Beckman Coulter, Inc., Fullerton, CA, USA) was used with two different aperture tubes. Sample volumes of 50 µL were analyzed with an aperture diameter of 30 µm, an aperture current of -400 µA in a range within 0.42 – 18 µm. Sample volumes of 100 µL were analyzed with an aperture diameter of 100 µm, an aperture current of - 1600 µA in a range within 2 – 60 µm. Minimum of 10 measurements were averaged and further analyzed with Origin 7SR1 software (Origin Lab Corp., MA, USA).

3.3. Modeling and analysis of the dissociation equilibrium shift

By using a computational routine (MathCAD 2001i Professional, MathSoft Engineering & Education, Inc., USA) and Planck's equation (Equation 2.24), the known temperature dependence of the acid dissociation constant for different buffer systems $K_a(T)$ up to 60 °C (Goldberg, Kishore & Lennen, 2002) was incorporated into Equation 2.32 for K_a by a separation approach. The temperature dependences of acid dissociation constants were interpolated and extrapolated after the last reference value (MathCAD 2001i Professional, MathSoft Engineering & Education, Inc., USA). The generation of iso-pK_a-lines and the presentation in the p-T-plane was arranged by the Origin 7SR1 software (OriginLab Corporation, USA).

The temperature dependence of the pH-value in 0.01 M ACES, phosphate buffer and different food (detailed ingredients see Annex 2) between 5 - 80 °C were measured with a switched off temperature compensation (pH-meter HI 9318, HANNA instruments GmbH, Kehl, Germany).

3.4. Thermal treatment

3.4.1. Glass capillaries

To achieve quasi-isothermal conditions, commonly thin-wall glass capillaries with an inner diameter of 1.0 mm and an outer diameter of 1.3 mm were used.
By using a numerical simulation (QuickField 5.2, Tera Analysis Ltd., USA), the non-isothermal heat transfer in the capillary was investigated. The following assumptions were made:

- all substances are homogeneous and isotropic,
- spore suspension has the behavior of water,
- at time t=0 the capillary is immersed in the heating medium,
- temperature of the suspension at time t = 0 is 0 °C,
- thermal conductivity and specific heat from the suspension as soon as kinematic viscosity and Prandl number (dimensionless number approximating the ratio of kinematic viscosity and thermal diffusivity; (Sucker & Brauer, 1976); (VDI, 1994)) from the heating medium are dependent of temperature, all other physical properties are independent of temperature.

The formulation for non-linear temperature fields is

$$\frac{1}{r}\frac{\partial}{\partial r}\left(\lambda(T) r \frac{\partial T}{\partial r}\right)+\frac{\partial}{\partial z}\left(\lambda(T)\frac{\partial T}{\partial z}\right)=-q(T)-c(T)\rho\frac{\partial T}{\partial t} \qquad (3.1)$$

for axisymmetric case, with heat conductivity as a function of temperature λ(T) (W K^{-1} m^{-1}), volume power of heat sources as a function of temperature q(T) (W m^{-3}), specific heat as a function of temperature c(T) (J kg^{-1} K^{-1}) and the density of the substance ρ (kg m^{-3}).
Because of axis symmetry just a quarter of the glass capillary geometry is necessary. According to Sucker and Brauer (1976) the outer heat transfer coefficient can be calculated. All necessary properties of the heating medium and

water are given (VDI, 1994). The assumed flow rate of the heating medium is 0.01 m s^{-1}. AR-glass has a thermal conductivity of 1.1 W K^{-1} m^{-1}, a specific heat of 860 J kg^{-1} K^{-1} and a density of 2500 kg m^{-3}.
For heat treatment a sample volume of 60 µL was filled into the sterile AR-glass capillaries of 10 mm length, 1.0 mm inner and 1.3 mm outer diameter (Kleinfeld Labortechnik GmbH, Gehrden, Germany). The capillaries were pre-cooled in an ice bath and heated in a thermostat (Huber GmbH, Offenburg, Germany) with silicon oil (M40.165.10, Huber GmbH, Offenburg, Germany) as heating medium. After the defined heating time, the samples were rapidly cooled in an ice bath again.

3.4.2. Septa steel tubes

Another useful method is the screw cap tube technique of Kooiman & Geers (1975). The spore suspension was put into sterilized stainless steel screw-cap tubes with septa (0.5 inch blue septa 6520, Alltech Associates Australia Pty Ltd, Baulkham Hills,). Triplicate steel tubes were placed into a pre-heated oil bath (Julabo TSB2 Labortechnik, GmbH, Selbach, Germany, with Julabo thermal M oil) and equilibrated to 121 °C. Using a 1 mL syringe (BD Luer Lock, Singapore) with spinal needles (BD Yale, 3 inch spinal needle, 22G, Madrid, Spain), 100 µL of spore suspension was injected into each of the pre-heated steel tubes, providing a concentration of approximately 10^8 CFU mL^{-1}. The isothermal hold time commenced from the time of inoculation. After holding times, steel tubes were removed from the oil bath and rapidly cooled to room temperature in an ice bath. The main disadvantage of the screw cap tube technique is the dilution effect (1:100), when the spore suspension is injected into the heated tube.

3.5. High pressure apparatuses

3.5.1. Multivessel Model U 111

The Multivessel high-pressure unit (Model U111, Unipress, Warsaw, Poland) was designed to conduct kinetic studies up to pressures of 700 MPa in a temperature

range of -40 to 140 °C (Arabas, Szczepek, Dmowki, Heinz & Fonberg-Broczek, 1999) by using a low viscous heat and pressure transferring liquid (silicone oil M40.165.10, Huber GmbH, Offenburg, Germany). All five pressure chambers (inner volume: 4 mL) made from beryllium copper alloy were separately connected to an oil driven intensifier (U111, Unipress, PL) by five high-pressure valves (SITEC, Maur/Zürich, Switzerland). A hydraulic pump (Mannesman Rexroth Polska Ltd, Warszawa, Poland) produced a pressure of 70 MPa on the low pressure side in the intensifier (fixed displacement, size 0.4 cm^3, multiplying factor 1:11). The pressure chambers were immersed in a silicon oil bath equipped with a thermostat (CC 245, Huber GmbH, Offenburg, Germany). Pressure build-up rate was adjusted to approximately 24 MPa s^{-1} and decompression rate was 50 - 166 MPa s^{-1}. A pressure transducer between the intensifier and vessels, and a K-type thermocouple in each chamber monitor (1 Hz) the pressure and temperature profile respectively during the treatment cycle. Further details of the equipment can be found in literature (Ardia, 2004).

3.5.2. Monovessel Model U 111

In some experiments where the pressure exceeded 700 MPa the Monovessel U111 (Model U111, Unipress, Warsaw, Poland) high pressure unit was used, which is similar in design to the Multivessel system, except the maximum pressure is 1000 MPa, vessel volume is 5 mL and a hand pump is used for pressure build-up. The pressure transmitting medium was Bis-(2 -ethylhexyl) sebacate (Nr. 84822, Fluka, Steinheim, Germany). The pressure chamber was immersed in a silicon oil (M40.165.10, Huber GmbH, Offenburg, Germany) bath equipped with a thermostat (cc2, Huber GmbH, Offenburg, Germany). A DasyLab data logger (Newport Electronics GmbH, Deckenpfronn, Germany) enabled the monitoring of pressure and temperature in the high pressure vessel with 1 Hz. Details of the equipment can be found in literature (Schlueter, Benet, Heinz & Knorr, 2004).

3.5.3. Stansted Mini Foodlab

The micro high pressure system "Stansted Mini Foodlab FBG 5620" (Stansted Fluid Power Ltd, Stansted, UK) consists of two main parts, the accumulator and the high pressure system including the PLC (Programmable logic controller) (Figure 3.1). The accumulator was filled with hydraulic oil and gaseous nitrogen. A plunger pump (TC10H/1212, Stansted Fluid Power Ltd; Stansted; UK) was used to generate various pre-pressures up to 60 MPa in the accumulator. The generated pre-pressure was responsible for the pressure compression rate up to the required working pressure.

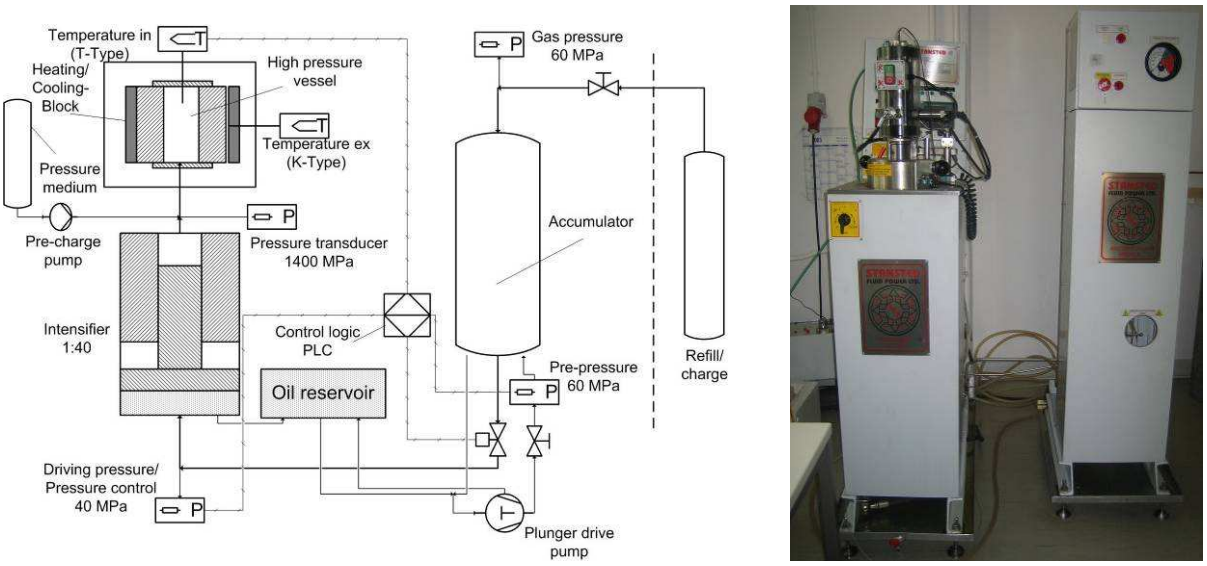

Figure 3.1: Stansted Mini Foodlab FBG 5620 high pressure unit with heating cooling system.

The high pressure unit had an internal intensifier, which is very adequate for sterilization processes under high pressure. The combination of accumulator and internal intensifier enabled the possibility of 350 MPa s^{-1} maximal pressure build-up rate and a maximal working pressure up to 1200 MPa. The whole pressure equipment was controlled by a PLC (FX1N-24MR, Mitsubishi Electric EUROPE B.V, Ratingen, Germany). The pressure build-up rate, dwell time, working pressure und decompression rate was entered via the control panel of the high pressure unit. The volume of the pressure cell was 198 µL. The tightness between pressure vessel and pressure unit is obtained without the use of sealing parts. A metal face-to-face connection between vessel and feed-injection system ensured

stable pressure conditions during the whole dwell time. By using a T-type thermocouple in the pressure vessel, it was possible to measure the temperature inside the vessel during a pressure cycle in a range of 5 °C and 140 °C.
Bis-(2 -ethylhexyl) sebacate (Nr. 84822, Fluka, Steinheim, Germany) was used as pressure transmitting medium. The pressure measurement of the control pressure at the low pressure side (FPG12400, Stansted Fluid Power Ltd., Stansted, UK) and of the pressure transducer (1400 MPa, EBM 6045-0514, EBM Brosa AG, Tettnang, Germany) was captured by pressure sensors with strain gauge. The transducer allowed the measuring of pressure inside the vessel during a pressure cycle. Both pressure sensors were calibrated over hydraulic control cycles.

3.5.4. HP equipment design and development

For temperature control of the 198 µL pressure cell, a heating cooling block was designed and built (Figure 3.2) for the Stansted Mini Foodlab high pressure equipment (German Institute of Food Technology DIL, Quackenbrück, Germany).

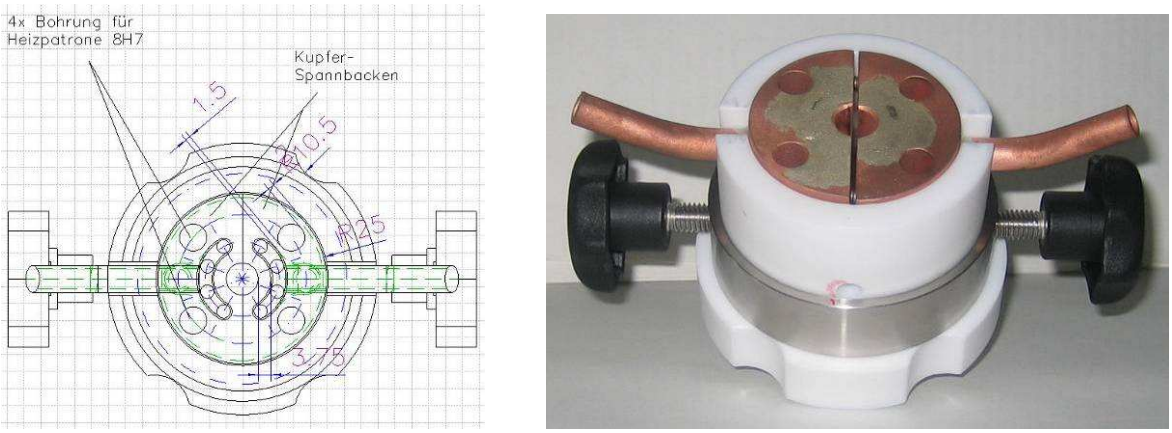

Figure 3.2: Heating cooling block (German Institute of Food Technology DIL, Quackenbrück, Germany).

The heating cooling bars were made of cupper because of the very quick heat transfer. To reduce the risk of material damages during heating and cooling, the block was manufactured in two bars. These bars are clamped with a stainless steal ring. The whole block is isolated with a Teflon plastic ring to minimize the heat transfer to the environment. Every heating cooling bar has four bore holes with an inner diameter of 0.4 mm for the cooling circuit and two bore holes with

0.8 mm diameter for the heating elements. All four heating elements together have a total power of 1600 W (Figure 3.2). Silicon oil (M60.115.05, Huber GmbH, Offenburg, Germany) with a temperature of 5 °C was used as medium for the cooling circuit. To measure the temperature directly at the outer pressure vessel wall, the heating cooling block had a small bore hole to fix a K-type thermocouple. The connected heating cooling system is shown in Figure 3.3.

Figure 3.3: Pressure vessel with connected heating cooling system.

A Keithley KPCI-3120 measuring board (Keithley Instruments, Inc, USA) with PCI-bus connection was used (Figure 3.4 A), to log the pressure and temperature data. This measuring board had analogue in- and outputs with a resolution of 12 bit and a maximal sampling rate of 225 kHz. Analogue input data can be logged in a range of -10 V to +10 V. To control analogue output units, the measuring board had two analogue output channels with an output signal of 0 V to 10 V. It was also possible to measure the analogue input data with 16 single-ended or pseudo-differential input channels, or with 8 differential input channels. The channels 49 to 72 are 32 digital channels. To calibrate the analogue in- and output channels, the operator can use the DriverLINX Software from Keithley (Keithley Instruments Inc., USA).

The output signal of the pressure sensor was griped prior to the PLC. The output signal was in the range of 4 - 20 mA. A T-type thermocouple and a K-type thermocouple was used to measure the temperature inside the high pressure vessel and on the outer vessel wall, respectively. The principle of measuring with thermocouple is based on the Seebeck-effect, providing an output signal in the range of µV. On this account thermocouple signal converters [DRF-TCK (K-type

thermocouple) and DRF-TCT (T-type thermocouple), Omega Engineering Inc., Connecticut, USA] were utilized to reach an output signal of 4 - 20 mA.
The measuring board was adjusted as differential voltage measuring to reduce the failure of measuring for data acquisition. Resistors with 270 Ω were used to convert the continuous current output signals of the pressure and temperature sensors into a voltage signal in the range of 0 - 10 V. All unimplemented analogue input channels of the measuring card were linked together and earthed via the ground channel of the board to reduce free electrical potentials on the card. The whole measuring assembly (Figure 3.4 A) was earthed through the system earth of one of the transformers.

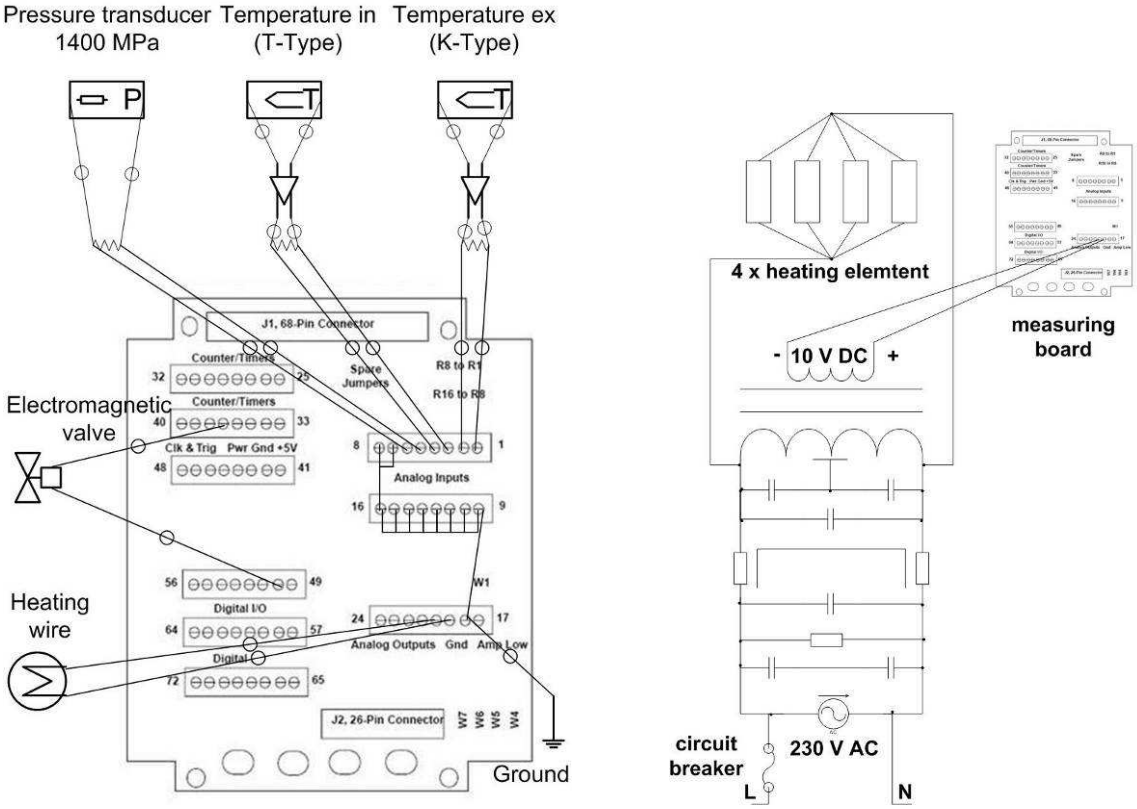

Figure 3.4: Design of the Keithley KPCI-3102 measuring board (A) (Keithley Instruments, Inc., USA) and assembly of the constructed power control for the heating elements (B).

A magnetic valve was implemented to control the cooling circuit. This valve required the digital signals “on” or “off” only. However, a simple on / off signal was inadequate to realize a quick and robust temperature control. Therefore it was necessary to construct a power controller for the heating wires (Figure 3.4

B), which allowed a continuous heating power regulation. Based on the used power controller (10PVC2425, Crydom Inc., San Diego, USA), which required a modulating input signal of 2 – 10 V DC, an analogues output channel of the measuring card was utilized to connect the power controller. The power control unit consisted of a power controller (10PVC2425, Crydom Inc., USA), a cooling element (SK89-75KLSSR1, RS Components GmbH, Germany), a modified computer power supply pack, an automatic circuit breaker (SH 200-C32A; RS Components GmbH; Germany), a computer case and four heating elements (type NSV, 230V, 400W,.Vulcanic GmbH, Hanau, Germany) (Figure 3.4 B).
The operated power controller is a power proportional controller. This controller opens up the possibility to regulate voltages up to 240 V AC and amperages up to 40 A with a simple 2 - 10 V DC voltage source. A cooling element to reduce the thermal load and an automatic circuit breaker (2CDs 211 001 R0324, ABB AG, Mannheim, Germany) was implemented, to guaranty the safety of the power controller. The heating elements were covered with heat-conductivity paste (189170-G0 heat-conductivity paste, -30 - +200 °C, Conrad Electronic SE, Germany) providing a better heat conduction. A computer-control of the heating–cooling block was necessary in order to achieve an ideal adiabatic heating and cooling, as well as isothermal conditions during dwell time in the high pressure vessel. This control software was created by TestPoint 4.0 (Capital Equipment Corp., MA, USA) and the flow chart is shown in Figure 3.5. The temperature control was realized by a digital PID-controller. As setpoint for temperature, the calculated adiabatic heating of water for the corresponding pressure and pre-heating conditions was used. The adiabatic heating of water based on a routine written in MathCAD 2001i Professional (MathSoft Engineering & Education, Inc., USA) and of sebacate based on experimental data from Ardia (2004) were implemented into the program. At the end of dwell times, the pressure vessel was automatically cooled by activation of the magnetic valve. With an online data acquisition rate of 5 Hz, the data from the thermocouples inside the pressure vessel and at the outer vessel wall, as well as the data from the drive pressure sensor were logged and graphically shown in the user interface (Figure 3.6). All data could also be exported to external programs to realize a fast and simple data analysis as well as documentation.

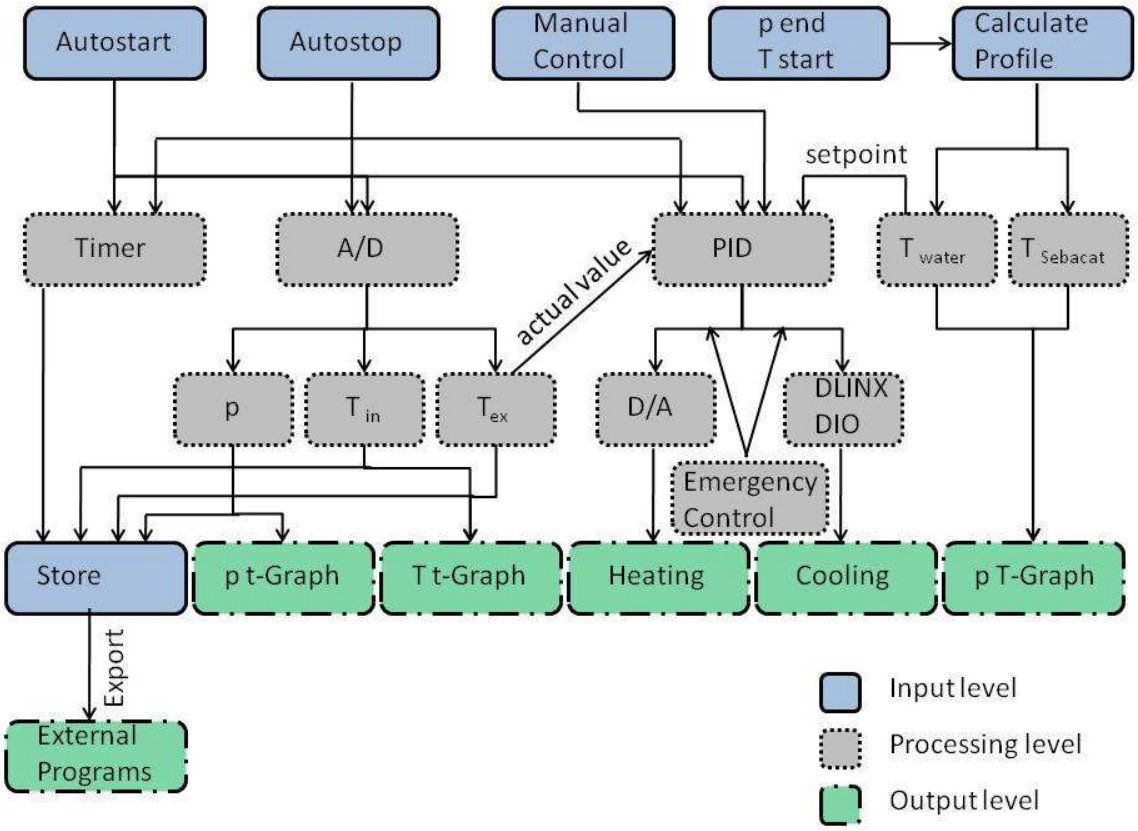

Figure 3.5: Developed temperature control concept as flow chart.

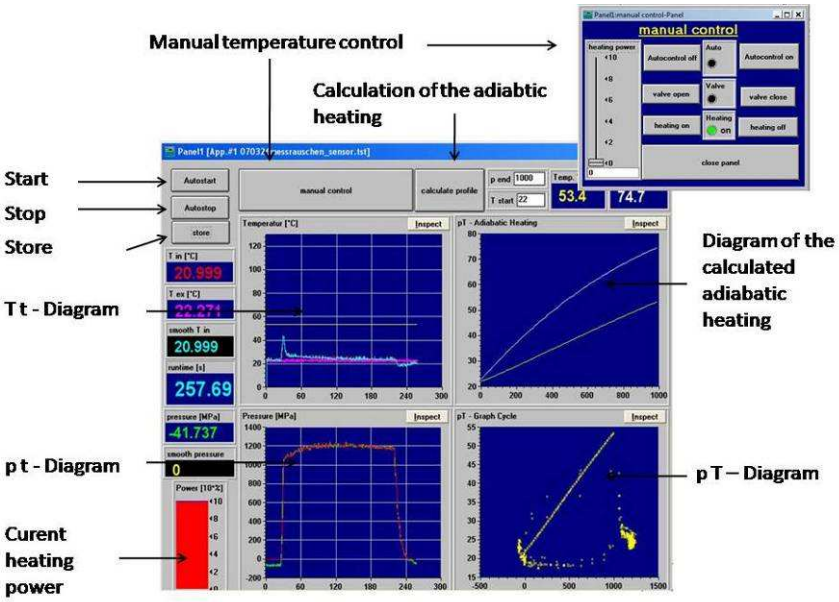

Figure 3.6: Designed user interface of the control and measurement software.

The automatic heating-cooling function was expanded with a manual temperature control (Figure 3.6). This control function provides the possibility to heat or cool the pressure cell manually or to change the setpoint temperature for the automatic heating. Furthermore the manual control panel was used in case of emergency to stop heating the vessel and cool it down. The written software also offered automatic emergency routines, to avoid extreme temperature conditions of more than 150 °C inside the pressure vessel,

The transient heat transfer via the pressure vessel, the pressure transmitting fluid (sebacate), the shrinking tube and spore suspension was calculated with an eighth of the vessel geometry analogue modeling of the heat transfer in glass capillaries (Chapter 3.4.1). For treatment, 100 µL spore suspension was filled in shrinking tubes of 55 mm length, 1.2 mm inner and 1.7 mm outer diameter (RT 375, Raychem GmbH, Ottobrunn, Germany). The high pressure vessel had a length of 80 mm, 2.5 mm inner and 10 mm outer diameter and was made of high maraging steel. A fixed temperature at the outer vessel wall was assumed for numerical simulation. At time t = 0 the outer wall of the high pressure vessel had reached the pre-heating temperature. All properties for the vessel, sebacate, shrinking tube and spore suspension are listed in Table 3.1. The temperature gradient (dT) between outer vessel wall and spore suspension had a maximum of 80 K.

Table 3.1: Material properties for numerical simulation of the transient heat transfer during pre-heating of the spore suspension prior pressure treatment

Medium	Thermal conductivity λ [W m^{-1} K^{-1}]	Specific heat c [J kg^{-1} K^{-1}]	Density ρ [kg m^{-3}]
Vessel	23.6	440	8100
Sebacate	13	460	913
Shrinking tube	0.165	1010	1545
Spore suspension	nonlinear*	nonlinear*	998

* nonlinear data based on NIST-data of water

3.6. High pressure treatment

3.6.1. Pressure treatment at different pH-values

Plastic tubes (CryoTube Vials, Nunc Brand Products, Roskilde, Denmark) were used as sample containers for pressure treatment studies. Spore suspensions were prepared as previously described in ACES or phosphate buffer and were initially at a temperature of 4 °C, achieved by pre-cooling of the filled plastic tube sample containers in ice. Pre-cooled samples were placed into pre-heated HP-vessels, immersed in the pre-heated pressure transmitting medium, and the vessel top-plugs closed. After reaching the calculated initial temperature, pressure build-up was commenced to the selected maximum pressure. Three different pressure treatments (500, 600 and 900 MPa) at 80 °C were used to inactivate *G. stearothermophilus* spores. All experiments at 900 MPa were performed with the Monovessel system. Pressure build-up rate was adjusted to 24 MPa s^{-1} at the Multivessel and 32 MPa s^{-1} at the Monovessel. Decompression rate was approximately 50 MPa s^{-1} at the Multivessel and 80 MPa s^{-1} at the Monovessel. No temperature peaks (> 80 °C) after pressure build-up were recorded during dummy runs with a K-type thermocouple in the sample plastic tube. Initial temperatures before compression were 55, 50 and 35 °C for 500, 600 and 900 MPa, respectively. Non-isothermal temperature profiles for the three different pressure treatments were a result of conduction (non-compression) heating of the pre-cooled plastic tube and compression heating of the sample when pressure was applied. At final pressure an isothermal phase with the final temperature (80 °C) followed. After decompression there was also a brief increase in sample temperature, as HP-vessel top-plugs were opened and samples were removed and cooled in ice.

3.6.2. Pressure treatment for flow cytometry analysis

Steel tubes with a steel moving piston system (Unipress, Warsaw, Poland), retrofitted to the unit, were used as sample containers to display a possible alternative to plastic tubes (CryoTube Vials, Nunc Brand Products, Roskilde,

Denmark). The main advantage is a leak-proof construction. However, the heat conductivity of steel (λ = 15 W m^{-1} K^{-1}) is much higher than that of plastic, which is indicated by faster temperature equalization of the pre-cooled sample volume after immersion in the pre-heated pressure transmitting medium (silicon oil, M40.165.10, Huber GmbH, Offenburg, Germany). By implementing a pre-pressurization step, it was possible to decrease the pressure come-up time, facilitating a smoother temperature profile where the retrofitted steel sample tubes were used (Figure 3.7). The pre-pressurization step consisted of allowing the pressure to build-up to 50 MPa before opening the high pressure (HP) valve to the pressure vessels.

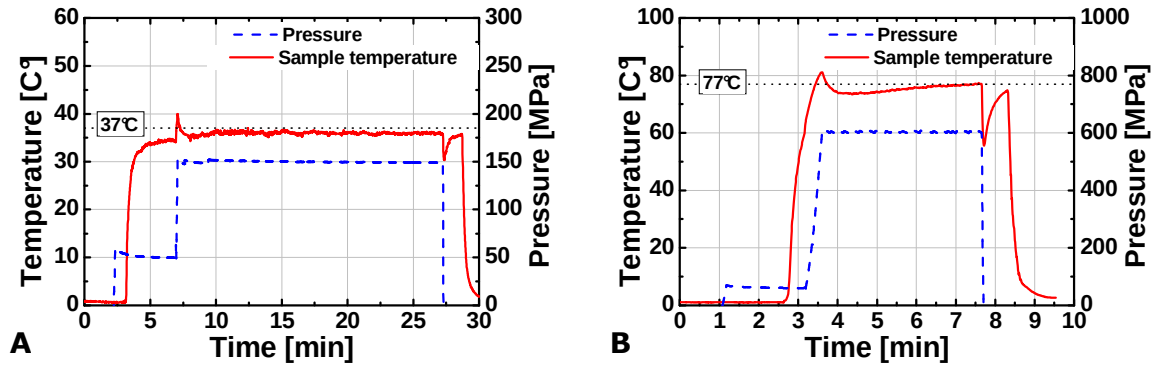

Figure 3.7: Pressure and sample temperature profiles of high pressure treated samples (nutrient broth), with pre-pressurization, in steel tubes; A) 150 MPa at 37 °C with 20 min hold time and B) 600 MPa at 77 °C with 4 min hold time.

Spore suspensions were initially at a temperature of 1 °C, achieved by pre-cooling of the filled steel tube sample containers in a salted ice slurry. Pre-cooled samples were placed into pre-heated HP-vessels, and the vessel top-plugs were closed. After reaching the calculated initial temperature, pressure build-up was commenced, and the HP-valve opened. Upon opening of the valve, the sample experienced an initial low pressure pulse, followed by continued compression to the selected maximum (hold) pressure (Figure 3.7). Decompression rate was 166 MPa s-1. Two different pressure / temperature combinations were used to treat *B. licheniformis* spores; a treatment at 150 MPa and 37 °C (hold temperature) for up to 20 min (Figure 3.7A) was employed with the aim of initiating spore germination, and a treatment at 600 MPa and 77 °C (hold temperature) for up to 4 min (Figure 3.7B) was employed with the aim of inactivating spores. A third treatment at 600 MPa and an initial temperature of

10 °C was evaluated and found to induce no apparent physiological changes in the spores. Non-isothermal temperature profiles for the two different pressure / temperature treatments are shown (Figure 3.7), and are a result of adiabatic heating of the sample combined with conduction (non-compression) heating of the steel tube, followed by a loss and then gain of temperature from the sample to and then from the steel tube and oil bath, respectively. After decompression there was also a small increase in the sample temperature, as the HP vessel top-plugs were opened and samples were removed and cooled.

3.6.3. Pressure treatment with Stansted Mini Foodlab

The spore suspension *G. stearothermophilus* ATCC 7953 (NAMSA, Northwood, Ohio, USA) was filled into shrinking tubes (RT 375, Raychem GmbH, Ottobrunn, Germany) with an inner diameter of 1.2 mm and an outer diameter of 1.7 mm. The shrinking tubes were hermetically sealed with a soldering iron and stored on crushed ice before treatment. The samples were inserted into the 198 µL cell and treated in a pressure range from 600 MPa to 1200 MPa under adiabatic conditions during compression and decompression, as well as isothermal conditions during dwell time. Prior to the compression phase, the sample was heated at initial temperature, which resulted in the desired processing temperatures of 90, 100, 110, 120 and 130 °C after compression. The whole vessel was automatically heated during the pressure build-up, simulating the adiabatic heat of compression of the sample. Once the pressure level was reached, the temperature of the system was stabilized at the processing temperature during dwell time and cooled automatically during decompression. After treatment the samples were stored on ice.

3.7. Physiological analysis with flow cytometry

Flow cytometry was performed using a FACS Calibur flow cytometer (BD Biosciences, San Jose, CA, USA) equipped with a 15 mW air-cooled 488 nm argon-ion laser. The operating software was BD CellQuest Pro (BD Biosciences). Isoton II (Coulter Corporation, Miami, FL, USA) was used as the sheath fluid.

Control (untreated) and treated samples were held on ice prior to flow cytometric assessment. Cooling (this study) or freezing (Black, Koziol-Dube, Guan, Wei, Setlow, Cortezzo et al., 2005) had no effect on the percentages of spores, determined by flow cytometry. Spore suspension aliquots, 15 µL, were added to 985 µL of freshly prepared fluorescent nucleic acid stain solution with 0.5 µM SYTO 16 (Invitrogen Australia Pty Limited,Mount Waverley, Australia; maximal values for the absorption and fluorescence emissions of the complex with DNA are observed at 488 and 518 nm, respectively) and 12 µM propidium iodide (PI, Invitrogen Australia Pty Limited; maximal values for the absorption and fluorescence emissions of the complex with nucleic acids are at 535 and 617 nm, respectively). The final concentration of the stained suspensions was approximately 10^6 CFU mL^{-1}. Suspensions were vigorously mixed and incubated in the dark at room temperature for 15 min prior to analysis. Data acquisition was set to 10,000 events, at a nominal flow rate of 1,000 events s^{-1}. To discriminate bacteria, the side scatter threshold level was adjusted manually to 307. The green emission from SYTO 16-staining (indicative of cortex hydrolysis) was collected through a 530 nm band-pass filter, and the red fluorescence from propidium iodide-staining (indicative of damage to the inner membrane) was collected through a 585 nm band-pass filter. Sheath fluid was allowed to pass through the fluidics system for at least 10 seconds between two consecutive samples. All measurements were repeated at least twice, with maximal 15 % variation of different populations between replicates.

3.8. Predictive modeling

3.8.1. Modeling of the log_{10}-reduction

The impact of spore agglomeration was discussed in Chapter 2.4.7 and calculated by Equation 2.47.

Isokineticity lines for pressure-temperature (p-T) diagrams were derived from kinetic analysis of the experimental inactivation data. The rate constants were regressively obtained (TableCurve 3D version 3, SPSS Inc., Chicago, IL, USA) by fitting the inactivation results with first- (n = 1) or n^{th}-order kinetics (TableCurve 2D version 4, SPSS Inc., Chicago, IL, USA).

For n[th]-order decay reactions Equation 2.38 was integrated,

$$\left(\frac{N}{N_0}\right) = \left(1 + k \cdot N_0^{(n-1)} \cdot t \cdot (n-1)\right)^{\frac{1}{1-n}} \quad (3.2)$$

and logarithmized:

$$\log_{10}\left(\frac{N}{N_0}\right) = \log_{10}\left(1 + k \cdot N_0^{(n-1)} \cdot t \cdot (n-1)\right)^{\frac{1}{1-n}} \quad (3.3)$$

The reaction order n in this equation was determined by minimizing the cumulative standard error (∑ SD) of fit over a wide range of reaction orders (1.0 - 1.45) (TableCurve 2D version 4, SPSS Inc., Chicago, IL, USA). After fixing the reaction order, the rate constants (k) were obtained regressively (TableCurve 2D version 4, SPSS Inc., Chicago, IL, USA). Empirical equations have often been suggested (Ardia, 2004; Ardia, Knorr, Ferrari & Heinz, 2004a; Margosch et al., 2006), to obtain a functional relationship of the rate constant in dependence on pressure and temperature k(p,T). Using a similar mathematical form of Equation 2.34 with a Taylor series expansion up to 3[rd] order terms,

$$\ln(k) = a + b \cdot p + c \cdot T + d \cdot p^2 + e \cdot T^2 + f \cdot p \cdot T + g \cdot p^3 + h \cdot T^3 + i \cdot p \cdot T^2 + j \cdot p^2 \cdot T \quad (3.4)$$

the rate constant can be adequately described [(Heinz & Knorr, 2002) and Chapter 2.2.2.4]. Replacing k in Equation 3.3 with Equation 3.4 and setting the reduction level (N/N_0) and treatment time *t* as constants, the functional relationship can be solved for p or T with MathCAD 2001i Professional (MathSoft Engineering & Education, Inc., USA).

The Weibullian Power Law (Equation 2.39) was used, to compare the experimental microbial reduction levels in ACES and PBS buffer. Non-isothermal temperature conditions as well as pressure come-up and release time were not considered in the Weibull model. The Weibull parameters b and n were dependent on the initial pH-value, obtained from regression analysis (TableCurve 2D version 4, SPSS Inc., Chicago, IL, USA) of the experimental kinetic data. The generation of inactivation graphs was arranged by the Origin 7SR1 software (Origin Lab Corp., Northampton, MA, USA).

3.8.2. Modeling of the inactivation mechanism

Flow cytometry data was analyzed using the free shareware program WinMDI (WinMDI 2.8, Joseph Trotter, USA). Data was visualized as density plots of FL1 (green fluorescence; SYTO 16) versus FL3 (red fluorescence, PI) with a smooth value of 2 and a display array resolution of 256 x 256 (262.1 KB). Values were plotted, gated and copied into MS PowerPoint (Microsoft Cooperation, USA). Gate values were analyzed with MS Excel (Microsoft Cooperation) and Origin 7SR1 software (Origin Lab Corp., Northampton, MA, USA). The three step model was suggested and fitted with the differential equation solver Berkeley Madonna (Version 8.0.1, R. I. Mackey & G.F. Oster, University of California at Berkeley, CA, USA). Similar models have been previously developed and analyzed by Heinz and Knorr (1996) for high pressure inactivation kinetics of *Bacillus subtilis* and Taub, Feeherry, Ross, Kustin and Doona (2003) for growth and death kinetics of *Staphylococcus aureus* in intermediate moisture bread. The mean deviations quoted, were determined using the Origin 7SR1 software to calculate the arithmetic means (for every treatment and medium) of the absolute deviations for the experimental values from the values predicted by the three step model and the arithmetic means (for every treatment) of the absolute deviations for the plate count values from the flow cytometer values. Correlation coefficients (R) were also calculated ($P < 0.005$ that $R = 0$).

4. Results and discussion

4.1. Impact of spore agglomeration

4.1.1. Agglomeration measurements

Different spore suspensions were investigated for agglomerations by microscopy. In all cases agglomerations can be observed as exemplified in Figure 4.1.

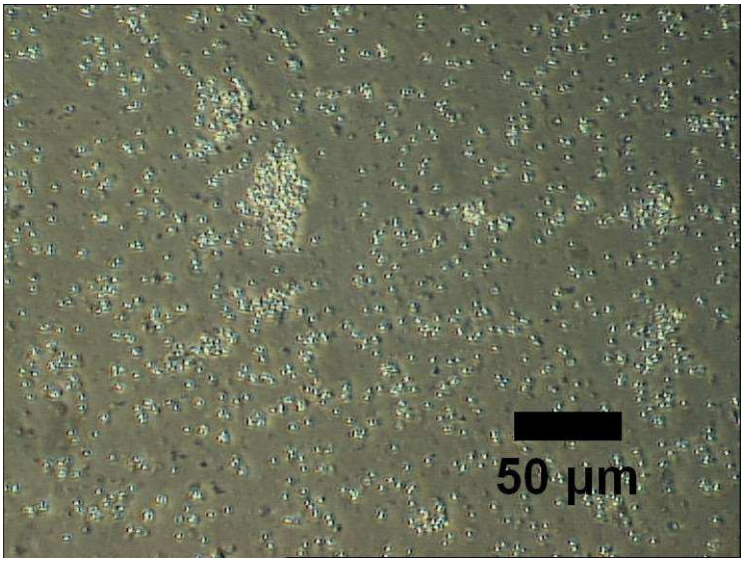

G. stearothermophilus (Merck)

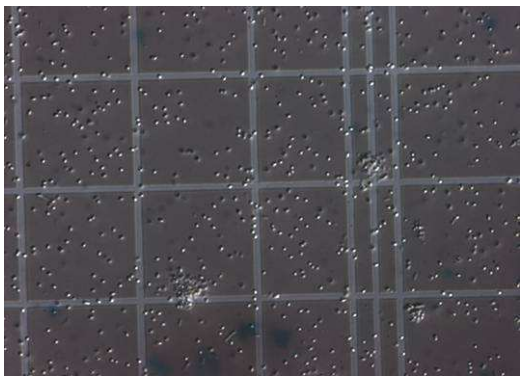

B. coagulans

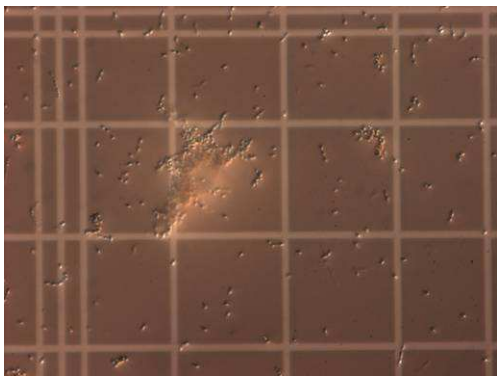

B. cereus

Figure 4.1: Largest observed agglomerations after screening of untreated spore suspensions with approximately 10^8 CFU mL^{-1} under microscopy and count chamber squares with 50 µm length under phase contrast.

Commercial *G. stearothermophilus* ATCC 7953 spore suspension (Merck) was investigated for agglomerations studies. Due to large agglomerates in the suspensions, it was impossible to count the total numbers of spores in such large clumps. The agglomerate size was not clearly visible under the microscope. Consequently a particle measurement was necessary.

The detailed geometry of *G. stearothermophilus* spores in a wet environment was imaged (Mönch, Heinz, Guttmann & Knorr, 1999) by transmission X-ray microscopy. After idealization to the spherical form, the assumed radius of the spores is 1.125 µm based on the X-ray microscopy determinations. In this model, the calculation of the volume V_{spore} (µm^3) and the cross-sectional area A_{spore} (µm^2) of one *G. stearothermophilus* spore was possible. The assumption for the agglomerate geometry was divided into three approaches. If all agglomerates are spheres, the volume V_A (µm^3) can be calculated with the measured diameter. The regular three-dimensional arrangements of spheres with the highest density are cubic close packing or hexagonal close packing. According to Kepler (1611) both arrangements have an average density of π($\sqrt{18}$)$^{-1}$. In the case of two dimensions the cross-sectional area A_A (µm^2) can be derived from the measured equivalence diameter. The honeycomb circle packing with a density of π($\sqrt{12}$)$^{-1}$ is the unique densest lattice sphere packing in two dimensions (Lagrange, 1773). For only one dimension, a chain formation with the product of spore diameter (µm) and spore number was supposed.

Therefore the maximum number of spores per agglomerate i can be expressed as:

$$i = \frac{\pi}{\sqrt{18}} \cdot \frac{V_A}{V_{spore}} \qquad (4.1)$$

for three-dimensions (3D model), with V_{spore} = 0.7455146 µm^3

$$i = \frac{\pi}{\sqrt{12}} \cdot \frac{A_A}{A_{spore}} \qquad (4.2)$$

for two-dimensions (2D model), with A_{spore} = 0.9940195 µm^2.

The number of spores in one dimension (1D model) can be calculated with the ratio between spore diameter and measured equivalence diameter.

With the help of the 3D ORM sensor the distribution of agglomerates can be specified. The spores per agglomerate can be derived from the distributions under different geometrical assumptions as shown in Figure 4.2.

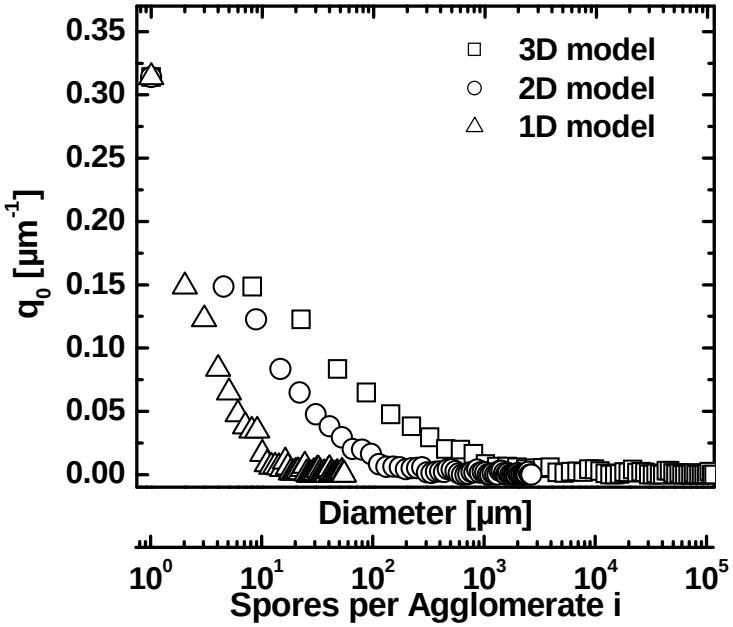

Figure 4.2: Agglomeration size distribution $q_0(i)$ of a *G. stearothermophilus* (Merck) spore suspension (0.05 M ACES, pH 7) with different geometrical assumptions for the agglomerates and an inset, which shows occurrences between 10^2-10^5 spores per agglomerate.

The different geometrical approaches showed large differences in number of spores per agglomerate. Comparing these results with the microscopic determinations (Figure 4.1), the best approximation to reality is located between the 2D and 3D model of the agglomerates. Therefore these models were the borderline cases for the geometry.

According to the common assumption and the microscopic images (Figure 4.1), the main population of the suspensions were single free spores. Agglomerates with up to 10^5 spores for the 3D model, a surprisingly huge number, were located in the suspension. It should be pointed out, that these agglomerates had a scarce occurrence. The inset in Figure 4.2 shows these low occurrences of agglomerates.

When the agglomeration distribution changed during the treatment, F_A can display an increase of the number of colony forming units because of disintegration. In this context, a so called "activation" could be explained. In the experimental part of the agglomeration model with F_A (15 min) at 121 °C = 1.04 (one experiment, 167 glass capillaries with a total sample volume of 10 mL), no

strong agglomeration or disintegration because of the treatment occurred. Therefore, the low increase of F_A is negligible and F_A was set to 1 for further calculations.

By using the 3D ORM sensor a minimum sample volume of 10 mL was required. Thermal inactivation studies in glass capillaries were performed with 60 µL sample volume. There was no volume for continuous analysis of the change in the agglomeration distribution.

4.1.2. Agglomeration model

A mechanistic model with first-order kinetics was used (Equation 2.47), to demonstrate the influence of the agglomeration on the thermal inactivation of *G. stearothermophilus*. After regressive derivation of the rate constants (Table 4.1), the experimental data (Figure 4.3) were modeled.

Table 4.1: Regression analysis of three-dimensional (3D) and two dimensional (2D) model to the experimental data (Figure 4.3)

Temperature [°C]	**Coefficient of determination R^2**	
	3D model	**2D model**
113	0.9942	0.9994
121	0.9973	0.9992
126	0.9922	0.9840
130	0.9891	0.9827

The regressive determination was necessary to derive the unknown slope of the end of the inactivation curves, which could not be correctly described by the last data plots. Small changes of the slope in the linear part could have large influence on the rate constant .

In Figure 4.3 the modeled survival curves and experimental plots are shown for different temperatures and two geometrical assumptions for the agglomerates.

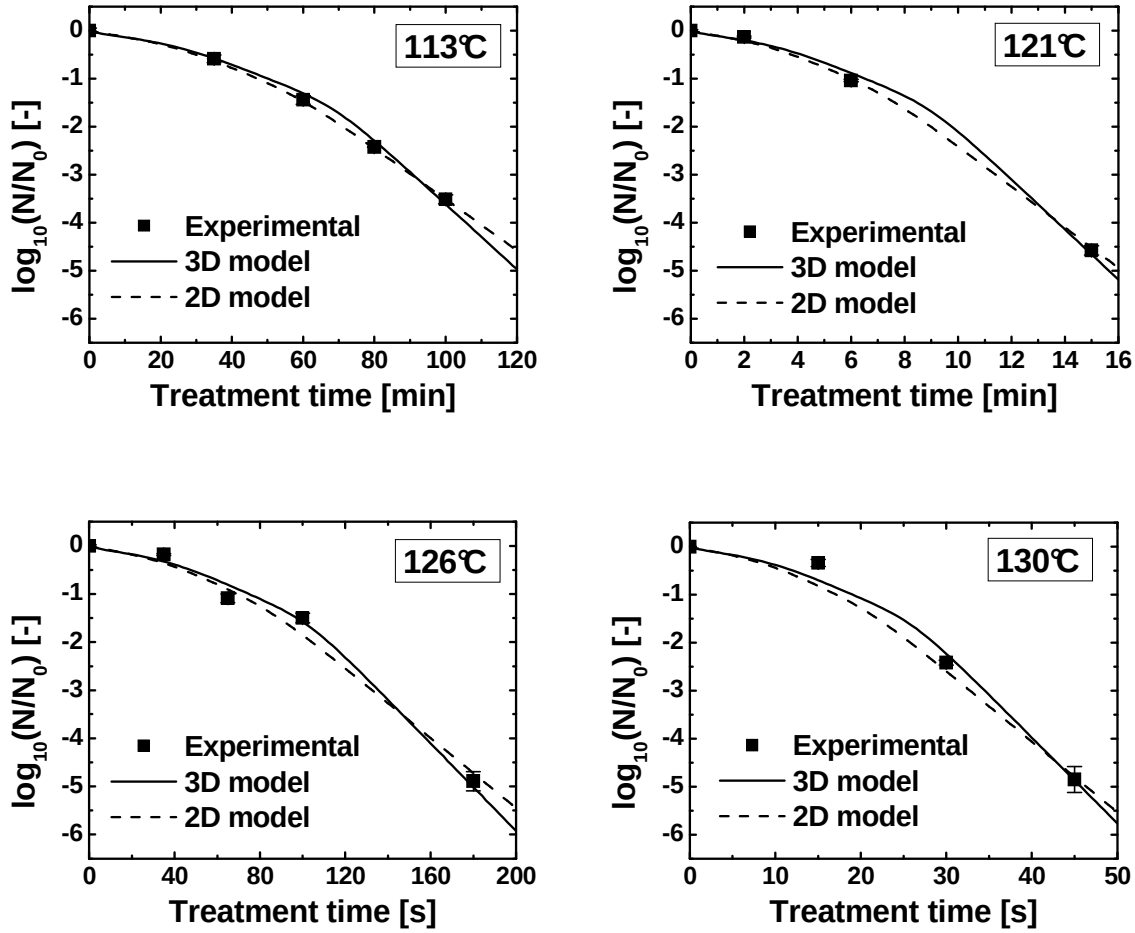

Figure 4.3: Experimental plots and isothermal, predicted data (lines) after thermal inactivation of *G. stearothermophilus* (Merck) spores in 0.05 M ACES (pH 7) with $D_{113°}$=885 s, $D_{121°}$=115 s, $D_{126°}$=22 s, $D_{130°}$=5.6 s for the three-dimensional (3D) model and $D_{113°}$=1125 s, $D_{121°}$=142 s, $D_{126°}$=27 s, $D_{130°}$=6.8 s for the two dimensional (2D) model.

After every heat treatment a shoulder formation of the survival curve could be observed. The three-dimensional approach resulted in a more distinct shoulder, due to the higher number of spores per agglomerate. From 126 °C to 130 °C this geometrical assumption gives a good description of the initial shoulder. However, the 2D model has shown a good correlation at 113 °C and 121 °C. Applying the isothermal model with the two borderline cases, the non-linear shoulder formation of the survival curves can be described up to 126 °C only.

4.1.3. Incorporation of non-isothermal conditions

Non-isothermal conditions have an increasing influence at high inactivation rates. Spore inactivation studies were performed with thin glass capillaries. Concerning the calculation of the temperature profile in a capillary Stern, Herlin and Procter (1952) have demonstrated that the heat penetration characteristic is equal to an infinite (length) cylinder. A common method is to measure the temperature with a fine wire thermocouple centered in the capillary tube (David & Merson, 1990), but it should be pointed out that the response time of the thermocouple must be subtracted. Olson and Schultz (1942) created tables for the numerical solution of the heating equations. Two borderline cases of the heat transfer mechanism for the capillary tube method were calculated from Haas, Behsnilian and Schubert (1996). In the first case the spore suspension is ideally mixed and in the second one no inner mixing is assumed. Because of changes in experimental designs and conditions, the determination of the temperature profile has to be adapted for practical experiments. In case of an ideally mixed suspension, the inner heat transfer coefficient is absent. After this assumption, the temperature from the inner layer of the glass wall to the center of the capillary profile is constant. Without any inner mixing the inner heat transfer coefficient has to be assessed for the heat transfer calculations. In general, a low but not ideal mixing gradient occurs. Hence it was assumed that the heat transfer from the inner layer to the center of the capillary profile can be approximated by thermal conductivity. The calculation of heat transfer in the capillary resulted in similar heating up times for all used final temperatures. In the case of 130 °C, the model for two different locations in the suspension is shown in Figure 4.4. The calculated outer heat transfer coefficient was 1598 W K^{-1} m^{-2} at this final temperature, with a kinematic viscosity of $3.01 \cdot 10^{-6}$ m^2 s^{-1} and a Prandl number (according to Sucker and Brauer, 1976) of 39.89 for the heating medium silicon oil. The biggest differences exist during the initial phase between zero and one second treatment time. For the ideal mixed case, the temperature on the inner layer of the glass wall would represent the whole thermal load. In the low mixed real case, the heat transfer from the glass wall to the suspension is replaced by the thermal conductivity of water. Some heating up times and D-values at different temperatures are given in Table 4.2.

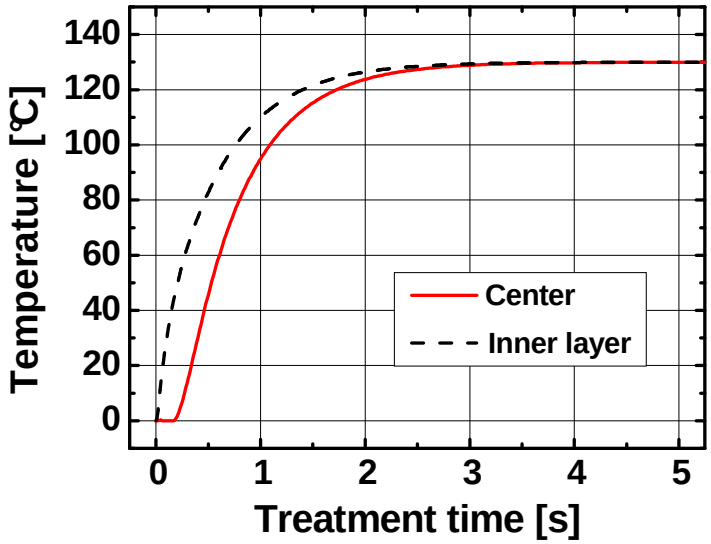

Figure 4.4: Heating of the suspension in glass capillaries with d_a=1.3 mm and d_i=1 mm at 130 °C in silicon oil at the center of the capillary profile and inner layer of the glass wall.

Table 4.2: Heating up time of the spore suspension in glass capillary at 130 °C final temperature with interpolated D-values from the isothermal calculation

Temperature [°C]	**D-value [s]**	**Heating up time [s]**	
	(3D model)	**Inner layer**	**Centre**
100	-	0.77	1.10
120	211.25	1.40	1.73
129	9.85	2.74	3.07
129.9	6.20	4.08	4.41
129.99	5.84	5.40	5.73
130	5.80	7.17	7.50

The suspension reached the final temperature in the capillary after about 7.5 seconds. David and Merson (1990) reported that 8.2 s were required for the sample to reach the final temperature in capillaries with similar geometry. Non-specified determinations resulted in a come-up time of 2.8 s (Abraham et al., 1990), but this value seems to be too small. It is well known that the ratio between heating up t_0 and holding time t_{real} plays a major role on the thermal load (Figure 4.5). The holding time t_{real} will be small at high temperatures,

because of the greater rate constants. Thus, the influence of the heating up process increases.

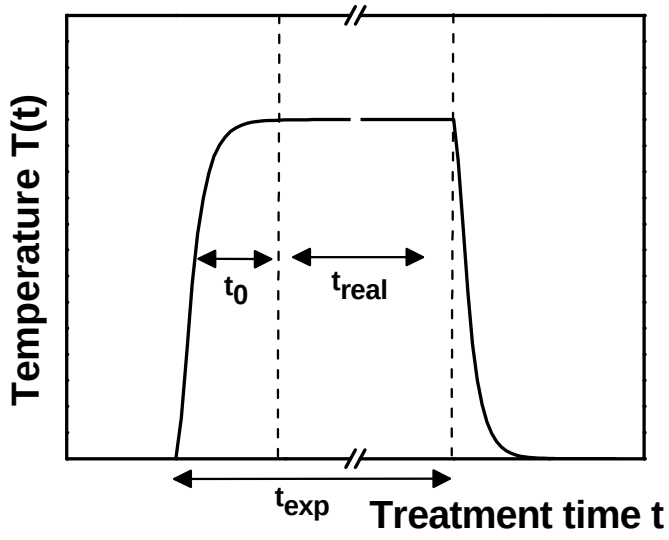

Figure 4.5: Temperature profile T(t) of the spore suspension in glass capillary with heating up time t_0, real holding time t_{real} and experimental holding time t_{exp}.

In order to estimate the influence of the non-isothermal temperature profile, a worst case scenario was assumed. The inhomogeneous temperature distribution during the heating made further calculations difficult. In any case, the biggest influence of the heating up time on the inactivation would be in the center of the capillary at a final temperature of 130 °C in the heating bath. By transforming the term $e^{-k \cdot t}$ from Equation 2.40 into term 2.44, the whole agglomeration model can be calculated under non-isothermal conditions. Term 2.44 can be solved easily, using the determined data for T(t) from the numerical calculation,. The modeling of inactivation of the largest possible agglomerate containing 10^5 spores at 130 °C showed differences between the isothermal and non-isothermal assumptions (Figure 4.6). Therefore the non-isothermal conditions were applied to the whole agglomeration model with three-dimensional geometry. The results are shown in Figure 4.7. It can be seen that there is just a small influence of the non-isothermal conditions. Nevertheless the initial shoulder formation was more distinct and the linear part had a higher slope. The influence of the non-isothermal conditions would increase at higher temperatures, because of the higher ratio between heating up and holding time (Figure 4.5).

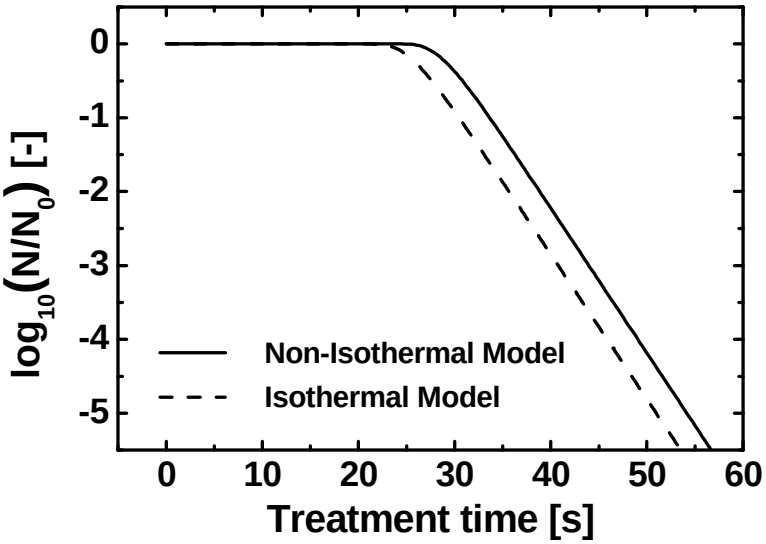

Figure 4.6: Comparison of isothermal and non-isothermal assumption in the agglomeration model for an agglomerate with 10^5 spores at 130 °C.

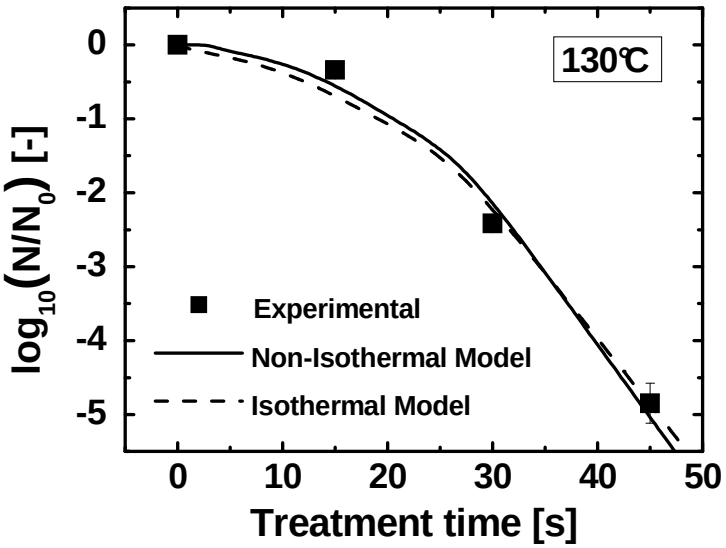

Figure 4.7: Comparison of isothermal (R^2 = 0.9891) and non-isothermal (R^2 = 0.9894) assumption in the agglomeration model with three-dimensional geometry of the agglomerates for *G. stearothermophilus* (Merck) spores suspension at 130 °C with z = 6.65 °C.

4.2. Impact of dissociation equilibrium shift

4.2.1. Modeling and analysis of the dissociation equilibrium shift

By measuring the pH-value in ACES and phosphate buffer between 10-80 °C (limit of the pH-electrode), the temperature dependence could be obtained in Figure 4.8. The quotient of both buffer systems (pH_{ACES} / pH_{PBS}) presents the pH-difference in ACES and phosphate buffer without the temperature dependence of the mV-signal during pH-measurement, which is explained by the Nernst equation (Nernst, 1889). Also other effects were removed by the division with pH_{PBS}. Phosphate buffer had a pH-value of 7.00 at 25 °C. This method offers a useful and simple tool for investigation of the temperature dependence differences of the pH-value in media up to 80 °C. In this case only the pH-values were measured and consequently the pH-shift, instead of dissociation equilibrium shift is discussed. The quotient (pH_{ACES} / pH_{PBS}) decreased with lower initial pH-values and consequently increased differences between pH and pK_a-value (Figure 4.8).

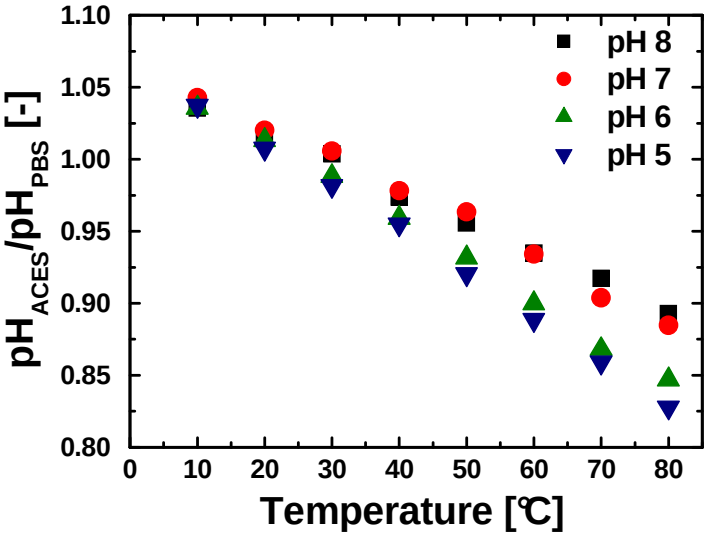

Figure 4.8: Measured temperature dependence differences (pH_{ACES}/pH_{PBS}) with different initial pH-values at 25 °C exemplified (pH 5, 6, 7, 8) in 0.01 M ACES and phosphate (PBS, 2nd) buffer between 10 - 80 °C.

For industrial applications such property changes of food matrices are important. Figure 4.9 shows in-situ pH shifts in food systems (milk, pea soup, baby mashed carrots with maize, herring with tomato sauce, detailed ingredients see Annex 2) and ACES buffer in dependence of temperature. To remove external effects, all data were divided by the pH-values of the temperature stable phosphate buffer. Hence, in Figure 4.9 pH-differences between food and phosphate buffer are shown. ACES buffer had the highest pH-shift and all other food systems had lower temperature dependences.

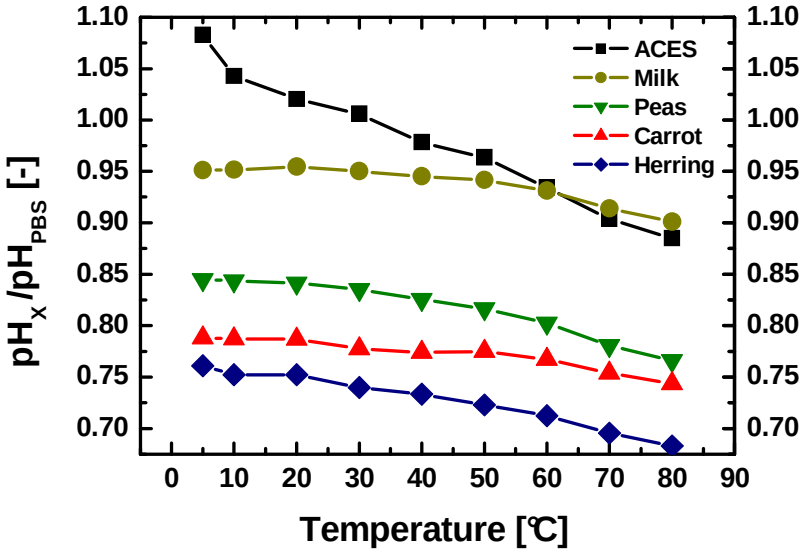

Figure 4.9: pH shift in food systems (x = milk, pea soup, baby mashed carrots with maize, herring with tomato sauce, detailed ingredients see Annex 2) and 0.01 M ACES buffer in dependence of temperature.

To investigate the temperature and pressure dependence of the dissociation equilibrium shift, different buffer systems were modeled. The p-T diagrams created by the calculated pK_a-value do show different changes with pressure and temperature (Figure 4.10).

Different initial temperatures and the adiabatic heating (dashed line) due to the pressure build-up process required the implementation of the specific temperature, respectively. These temperature dependences can be very high (Figure 4.8) and could compensate the advantages of the low isothermal pressure dependence.

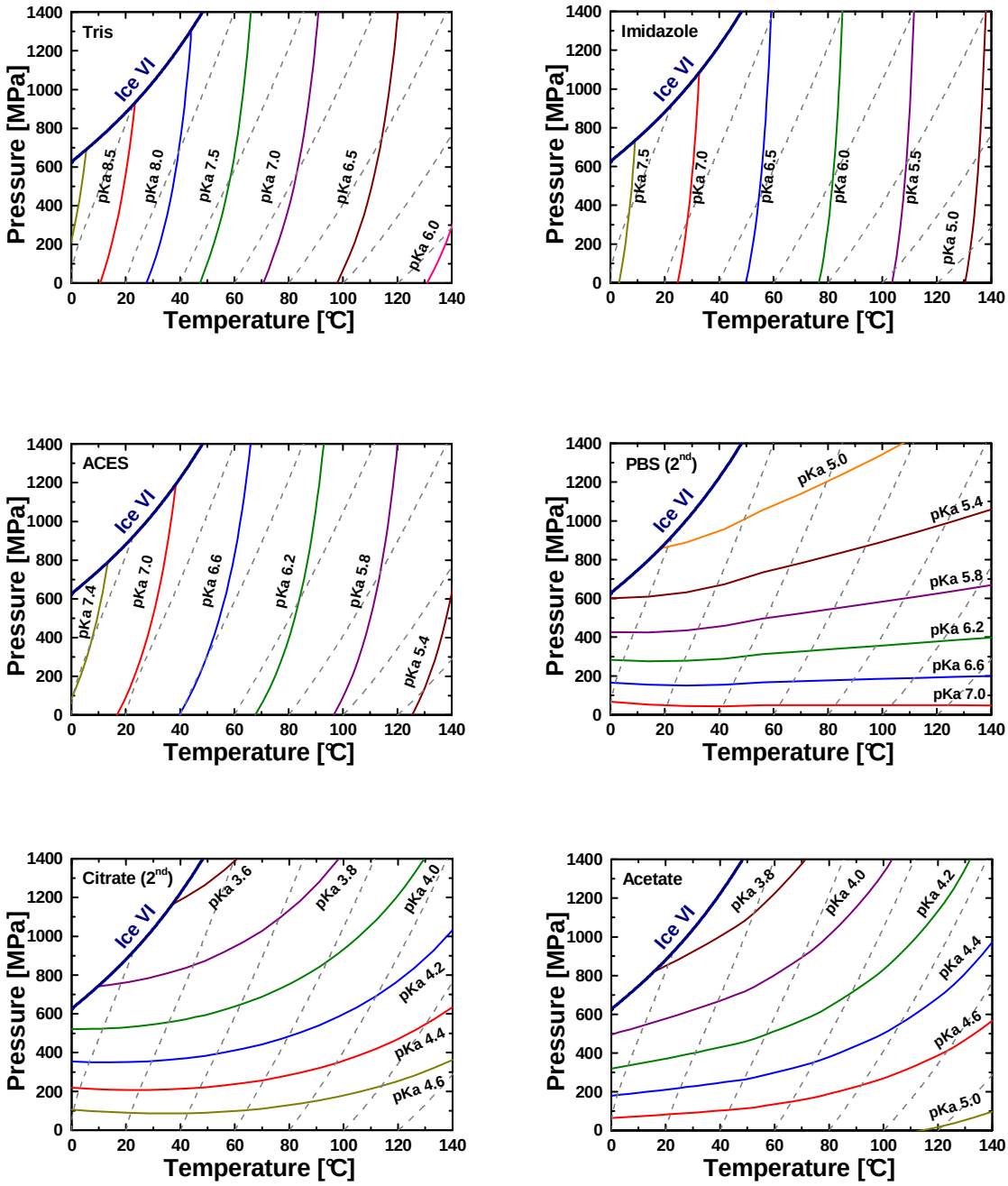

Figure 4.10: Modeling of the iso-pK_a-lines in different buffer systems under different p-T conditions with adiabatic lines (--) and phase transition line of pure water.

The diversity of iso-pK_a lines in buffer solutions resulted mainly from the different dissociation reactions (Equation 2.26 - 2.31) and consequently different standard molar enthalpies ($\Delta_r H^0$) or reaction volumes (ΔV). Table 4.3 summarizes the main important parameter for the dissociation equilibrium shift with pK_a-values,

standard molar enthalpies Δ_rH^0 and reaction volumes (ΔV) at 25 °C of the modeled buffer systems.

Table 4.3: pK_a-values, standard molar enthalpies (Δ_rH^0) from Goldberg et al. (2002) and reaction volumes (ΔV) at 25 °C of the modeled buffer systems with ΔV of Tris , ACES, Imidazole and Citrate (2^{nd}) (Kitamura and Itoh, 1987), ΔV of phosphate (2^{nd}) (Lo Surdo, Bernstrom, Jonsson & Millero, 1979) as well as ΔV of Acetate (Neuman, Kauzmann & Zipp, 1973), respectively

Buffer system	**pK_a at 25 °C**	**Δ_rH^0 in kJ mol^{-1}**	**ΔV in cm^3 mol^{-1}**
Tris	8.07	+ 47.4	+ 04.3
Imidazole	6.99	+ 36.6	+ 01.8
ACES	6.84	+ 30.4	+ 04.0
PBS (2^{nd})	7.19	+ 03.6	- 22.8
Citrate (2^{nd})	4.76	+ 02.2	- 12.3
Acetate	4.75	- 00.4	- 11.2

At atmospheric pressure and 25 °C, ACES has a pK_a of 6.84 and phosphate (2^{nd}) has a pK_a of 7.19 (Goldberg et al., 2002). Both buffer systems are adequately comparable, because of nearly equal buffer capacities of the pressure stable ACES and temperature stable phosphate. Therefore, practical experiments for the investigation of the different dissociation equilibrium shifts were performed with both buffer systems. At higher temperatures endothermic reactions are dominant. The equilibrium shifts in the direction of the products, because of the principle of Le Chatelier and Braun, where if a chemical system at equilibrium experiences a change; the equilibrium will shift in order to minimize that change. For example phosphate (2^{nd}) buffer with Δ_rH^0= + 3.6 kJ mol^{-1} has approximately a ten-fold smaller temperature dependence of the pK_a-value than ACES with Δ_rH^0= + 30.4 kJ mol^{-1}.

During the dissociation of ACES (Equation 2.27) there is no increased amount of charges to the product site, which is indicated by the positive reaction volume (ΔV = + 4 cm^3 mol^{-1}). Contrary, in phosphate (2^{nd}) buffer (Equation 2.29) the reaction in direction of the products produces more charges than backwards, which results in a smaller product volume and negative reaction volume (ΔV = -22.85 cm^3 mol^{-1}). Consequently, Planck's equation (Equation 2.24) represents also the principle of Le Chatelier and Braun. In reactions with negative reaction

volume an increase in pressure leads to an equilibrium shift in the direction of the products.

4.2.2. Spore inactivation at different initial pH-values

Thermal inactivation kinetics of *G. stearothermophilus* (Merck) spores for three different temperatures (114, 122 and 127 °C) were investigated considering a small influence of non-isothermal conditions due to the application of very thin glass capillaries. The logarithmic spore reductions (experimental and modeled data) in ACES and phosphate at different initial pH-values are presented in Figure 4.11 (114 - 127 °C). All relevant parameter and statistical results for the modeling are given in Annex 3.

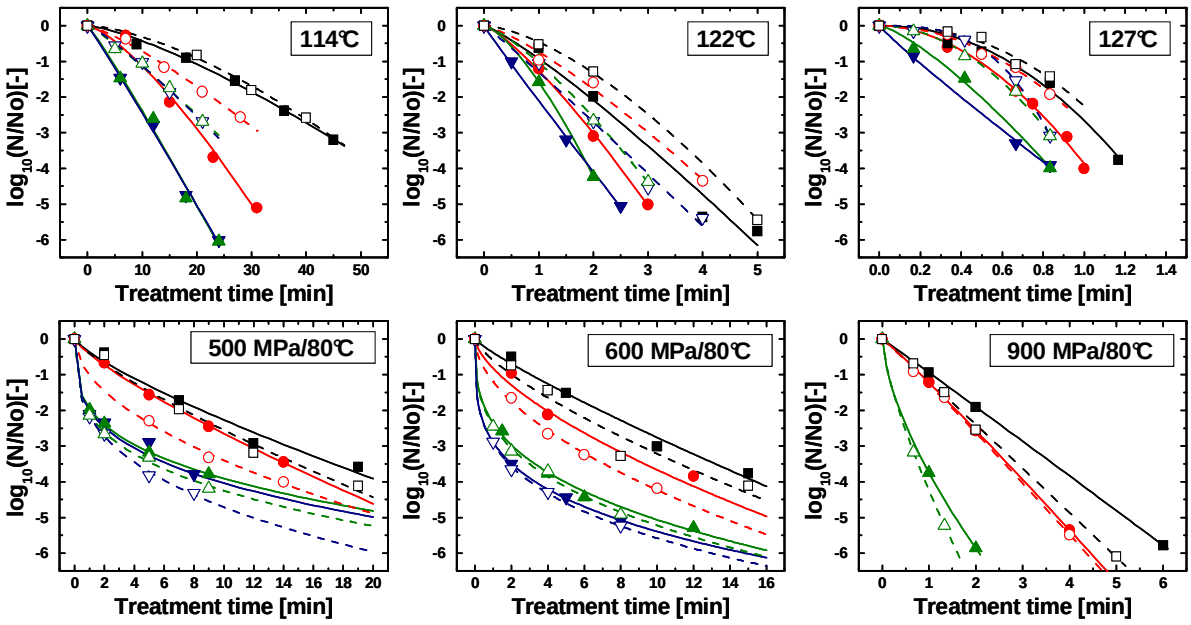

Figure 4.11: Thermal and pressure inactivation of *G. stearothermophilus* (Merck) after 114, 122, 127 °C and 500, 600, 900 MPa at 80 °C in ACES (-) and phosphate (--) buffer fitted with Weibullian power law and experimental data for different initial pH-value levels (detailed values in Annex 3), pH 8 (■, black), pH 7 (●, red), pH 6 (▲, green) and pH 5 (▼, blue), where closed symbols represented ACES and open symbols phosphate buffer.

It can be noticed, that with higher initial pH-values a lower reduction occurred. In contrast to phosphate buffer with the same initial pH-value, a higher inactivation was observed in ACES buffer. The highest $\log_{10}$ reduction was obtained at an initial pH-value of 5.

Pressure inactivation data were determined in two different high pressure units, because of the limited working pressure of up to 700 MPa of the Multivessel kinetic unit. All experimental and modeled kinetics are shown In Figure 4.11.
It is obvious that there is a different inactivation characteristic ("tailing") than after thermal treatment.
Similar to heat inactivation, a decrease of the initial pH-value resulted in higher inactivation rates for each pressure level considered. In contrast to thermal inactivation, the difference of the $\log_{10}$ reduction between both buffer systems did change (Figure 4.11).

4.2.3. Inactivation differences under heat and pressure

Figure 4.11 shows the different inactivation kinetics in both buffer systems. The modeled data from each individual buffer solution and treatment were subtracted (Figure 4.12) in order to give a more obvious presentation of the inactivation difference. By comparing the difference in $\log_{10}$ reduction ([$\log_{10}$(N/No)](PBS-ACES)) in phosphate and ACES, maximum values up to 3 $\log_{10}$ after thermal (114 °C, Figure 4.12) and 1.5 $\log_{10}$ after pressure treatment (900 MPa at 80 °C, Figure 4.12) were observed.

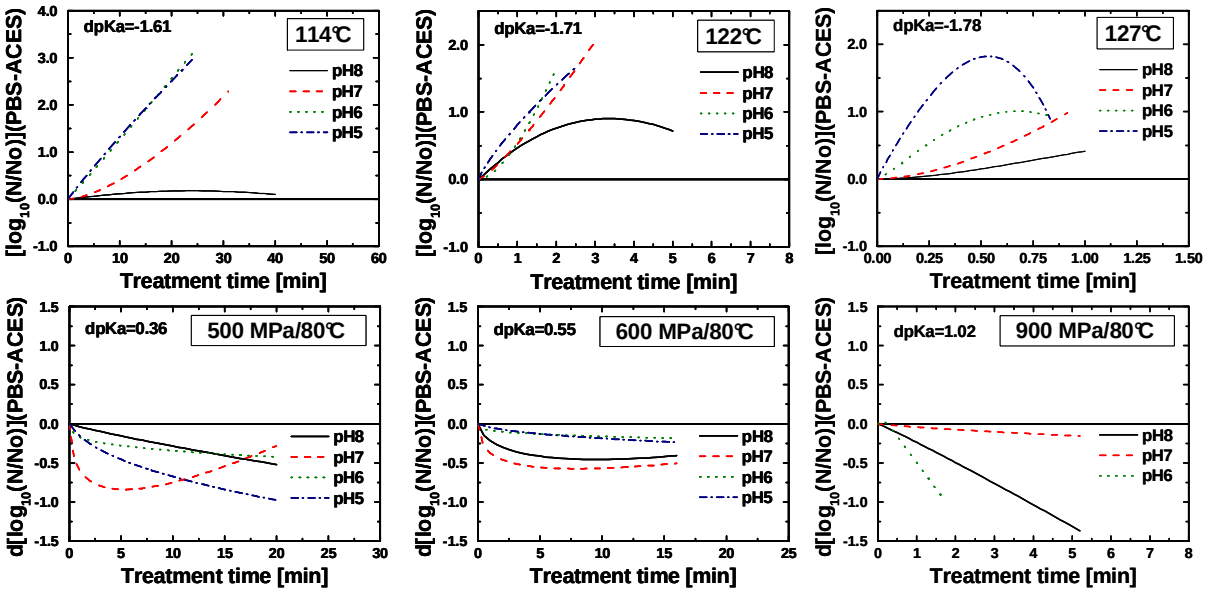

Figure 4.12: Difference in $\log_{10}$ reduction of *G. stearothermophilus* (Merck) spores in phosphate (PBS) and ACES ([$\log_{10}$(N/No)](PBS-ACES)) and in pK_a-shift [dpK_a (PBS-ACES)] after thermal and pressure treatment at different initial pH-values.

A significantly higher $\log_{10}$ reduction was detected after thermal inactivation in ACES buffer. Contrary, in all pressure treatments, a higher inactivation was obtained in phosphate buffer (Figure 4.12). These data indicated the different pK_a-shifts in buffer systems by heat and pressure. The variations of the initial pH-curves during thermal treatment in Figure 4.12 could be produced from different buffer capacities (analogue Figure 4.8). During pressure treatments (Figure 4.12) no trend between the initial pH-lines was observed. Direct comparison of different treatments and detailed amounts of pK_a-shifts is difficult because of the unknown temperature dependence of the pK_a-value at higher temperatures and especially various inactivation mechanisms, which were detected by different non-linear $\log_{10}$-reductions (shoulder and tailing).

4.3. Physiological mechanisms detected by flow cytometry

It is firmly held (Knorr, 1999), that spore inactivation is partly attributed to germination of a proportion of the spore population during the high pressure process. Recently, others have demonstrated the application of flow cytometry to the detection of spore germination by high pressure (Black et al., 2005) and Black et al. (2007c) reported the use of the green fluorescent nucleic acid dye SYTO 16 as an indicator of germination in pressure treated spores of *B. subtilis*. Dormant spores and decoated spores, where the spore outer membrane is lost, were not stained by SYTO 16. However, following hydrolysis of the spore cortex, the membrane-permeant SYTO 16 is able to cross the inner spore membrane and exhibit green fluorescence upon binding to nucleic acids in the spore core (Black et al., 2005). Therefore SYTO 16 has been designated as an indicator of the completion of spore germination (Black et al., 2007c) and used to demonstrate separation of dormant, pressure-germinated H_2O_2-inactivated and pressure-germinated spores by flow cytometry (Black et al., 2005).
In this study, the application of flow cytometry to assess the physiological response of *B. licheniformis* spores, after dual staining with SYTO 16 and propidium iodide (PI), was investigated.

4.3.1. Flow cytometry results

Spore populations with different fluorescence intensities were obtained after the different heat and pressure treatments (Figure 4.13 and Figure 4.14).

Comparison of untreated spores with those treated at 121 °C for 8 min showed a single population, with increased red (PI) and also green (SYTO 16) fluorescence, indicating that inactivation of bacterial spores by heat-only treatment was coincident with physical compromise of the inner membrane of the spore. Plate count results showed an approx. 6.5 $\log_{10}$ reduction after heat treatment at 121 °C for 8 min, indicating an effective spore kill. The observed increase in green fluorescence may be attributable to indiscriminate staining of membrane compromised, and presumably cortex hydrolyzed spores by membrane permeant SYTO 16, which is reported to stain only germinated (i.e. cortex hydrolyzed) spores (Gould, 1969; Ragkousi, Cowan, Ross & Setlow, 2000; Setlow, Loshon, Genest, Cowan, Setlow & Setlow, 2002).

No spore inactivation by high pressure processing alone, at 600 MPa and an initial temperature of 10 °C was observed using flow cytometry and plate count.

Four different populations could be identified by flow cytometry after high pressure treatment with 150 MPa at 37 °C for 10-20 min (Figure 4.13 and Figure 4.14); two kinetically increasing populations exhibiting SYTO 16 fluorescence were detected, confirming initial germination of spores by low-range high pressure, followed by a second physiological state change. At this pressure, as expected nutrient broth (Figure 4.14) was more favorable for germination than sodium citrate buffer (Figure 4.13). When the 150 MPa-treated spore populations were subsequently treated at 80 °C for 20 min, these two populations were eliminated, and there appeared to be an increase in the size of the population, presumed inactivated (PI stained), again demonstrating that thermal inactivation involves physical compromise of the inner spore membrane.

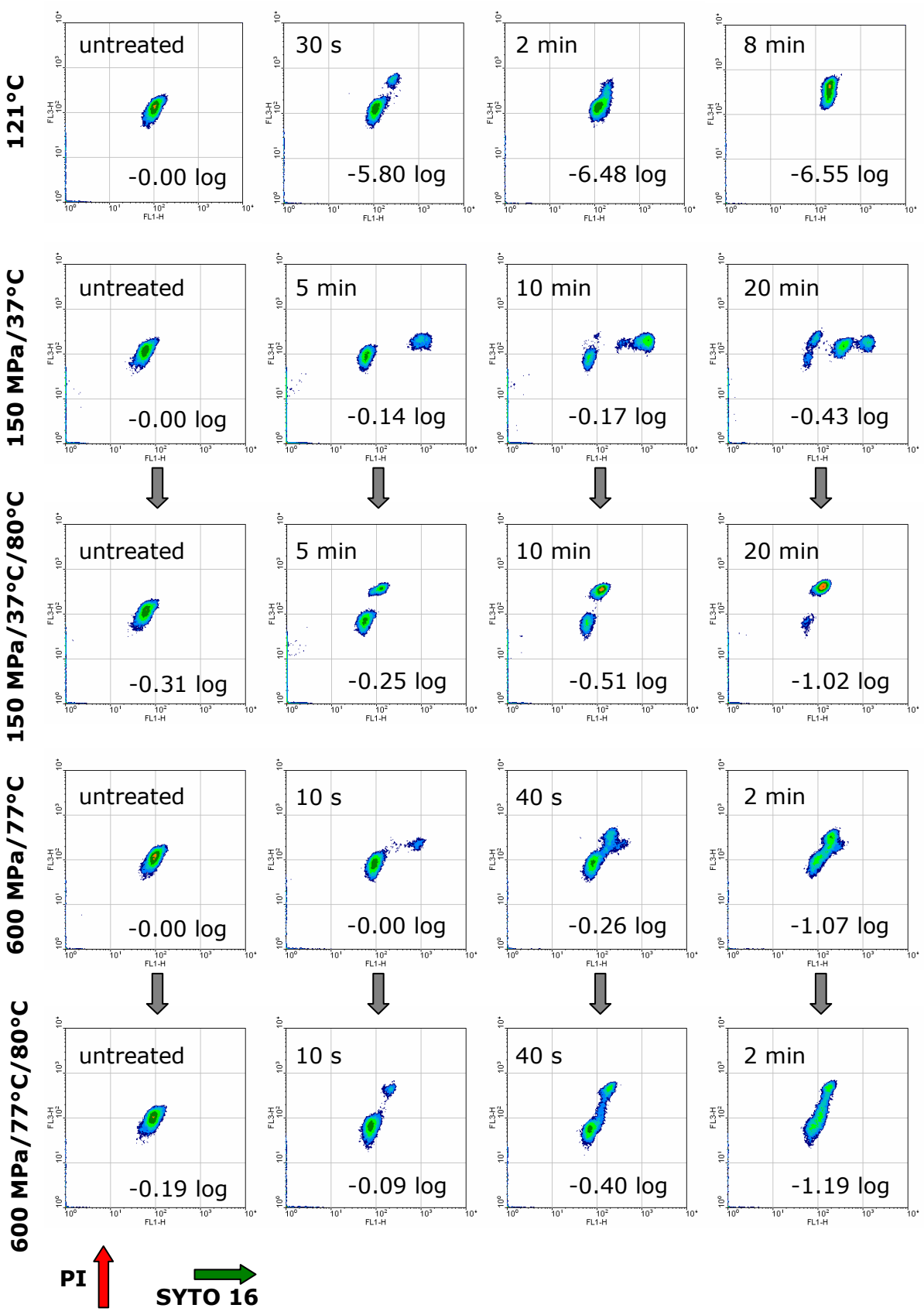

Figure 4.13: Representative flow cytometer density plot diagrams and plate count results from *B. licheniformis* spores in sodium citrate buffer (pH 7). Arrows represent the additional treatment at 80 °C for 20 min.

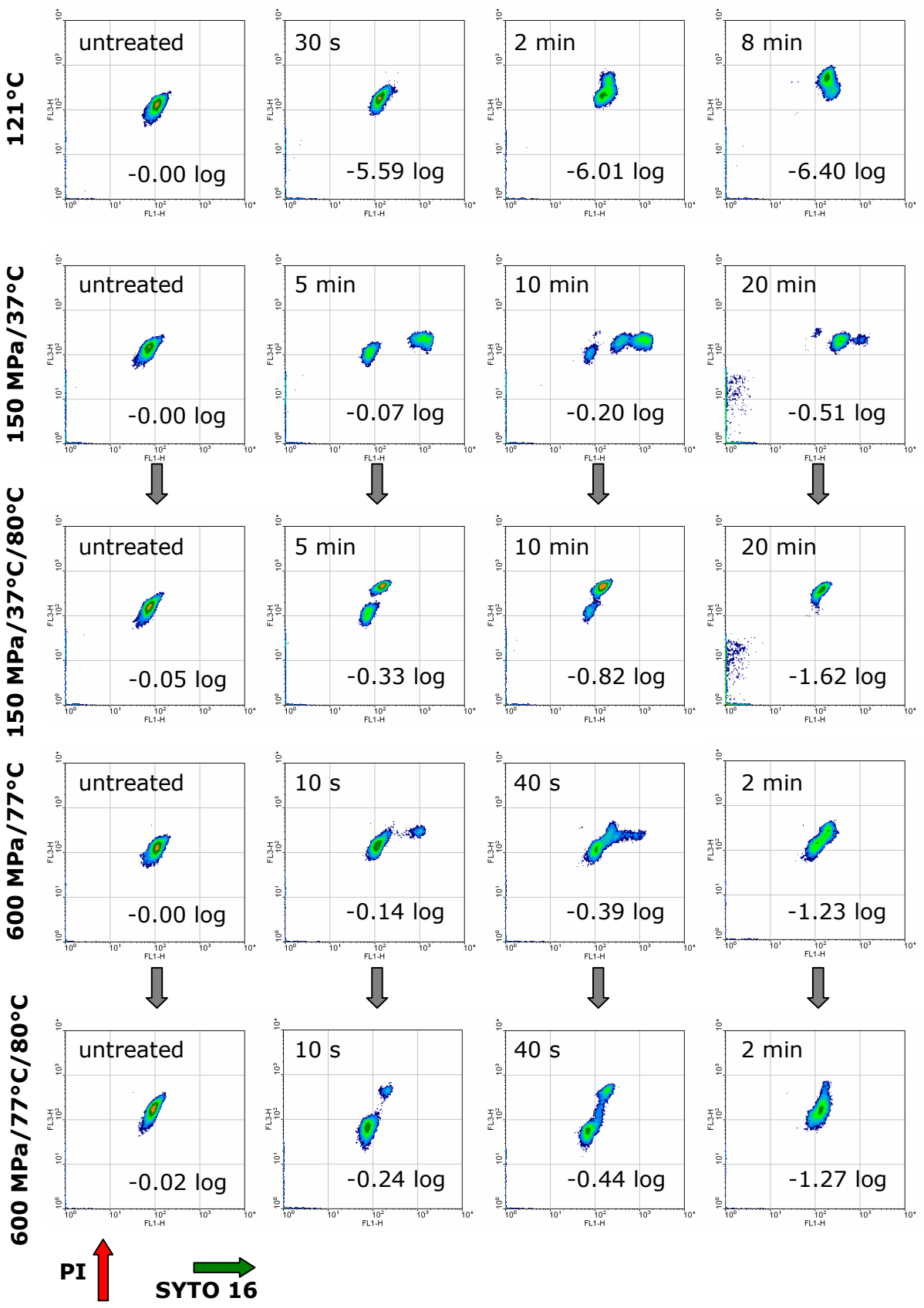

Figure 4.14: Representative flow cytometer density plot diagrams and plate count results from *B. licheniformis* spores in nutrient broth. Arrows represent the additional treatment at 80 °C for 20 min.

Following processing, at 600 MPa and 77 °C, conditions generally considered unsuitable for observation of spore germination (i.e. SYTO 16-only staining), the same four spore populations were observed as after processing at 150 MPa, but the discrimination of these four sub-populations notably decreased with increasing time under pressure, compared with the 150 MPa treated samples. Inactivation under these processing conditions proceeded rapidly, and apparently as a result of this, two of the defined sub-populations were only observed at very short pressure hold times. Subsequent heat treatment of the treated spores at 600 MPa and 77 °C still yielded two major sub-populations, but the staining intensity characteristics of the populations were different to those of dormant and inactivated sub-populations previously observed after heat-only treatment, and as a result were not as easily discriminated (Figure 4.13 and Figure 4.14). On the basis of the comparisons among different samples, a population assignment was made (Figure 4.15). Sub-population 1 was assigned as the dormant (culturable) spore sub-population, and sub-population 4 as the inactivated (non-culturable) spore sub-population. Results indicated that sub-population 2 represented the germinated (culturable, but heat sensitive) sub-population, and sub-population 3 a second, unknown heat-sensitive sub-population, of unknown culturability. Sub-population 2 is presumed to be cortex hydrolyzed spores with an intact inner membrane. The nature of sub-population 3 is difficult to presume and can not be defined.

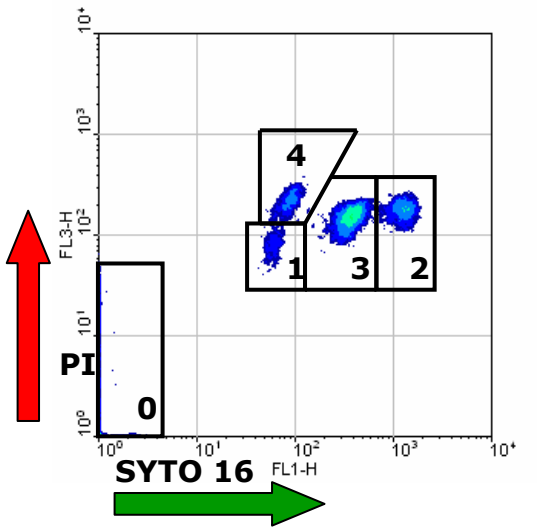

Figure 4.15: Sub-population assignment for density plot diagrams of *B. licheniformis* spores in sodium citrate buffer after treatment at 150 MPa at 37 °C for 20 min: (0 = noise), 1 = dormant, 2 = germinated, 3 = unknown, 4 = inactivated.

4.3.2. Three step model for physiological mechanisms under pressure

The work of Johnson and Zobell (1948) was found later to be due to a germinative effect of high pressure. Clouston & Wills (1969; 1970) and others (Gould, 1969; 1970; Gould & Sale, 1970; Gould et al., 1970) showed that comparably low pressures below 200 MPa can trigger spore germination which was detectable by common indicators. By using *in situ* scanning of the optical density of *Bacillus subtilis* during pressure treatment Heinz and Knorr (1998) demonstrated maximum germination rate optima in the range of 100 - 200 MPa.
Using the sub-population assignment described, a three step model of inactivation based on a series of chemical reactions with associated rate constants k_i (i =1, 2, 3) is suggested. The whole model includes: a germination step ($N_1 \rightarrow N_2$), an unknown step ($N_2 \rightarrow N_3$) and finally the inactivation step ($N_3 \rightarrow N_4$). The velocity v_i of each step is related to the rate constants k_i of the reaction and the concentration of the participating entities N_j (j =1, 2 ,3 ,4). Equation 4.3-4.6

$$dN_1/dt = -k_1 N_1 = -v_1 \quad (4.3)$$

$$dN_2/dt = k_1 N_1 - k_2 N_2 = v_1 - v_2 \quad (4.4)$$

$$dN_3/dt = k_2 N_2 - k_3 N_3 = v_2 - v_3 \quad (4.5)$$

$$dN_4/dt = k_3 N_3 = v_3 \quad (4.6)$$

represent a differential equation system of these assumptions in which changes in the species concentrations, (N_j) with time (t) proceed according to the velocities v_i of the reactions that form or remove them. After a multiparameter fit of the whole differential equation system with the sub-population values from each individual population, all three rate constants were obtained. The predictive three step model for the physiological mechanism of inactivation under pressure shows a good correlation with the experimental results (mean deviations, Figure 4.16 A = 0.033, Figure 4.16 B = 0.035, Figure 4.16 C = 0.041, Figure 4.16 D = 0.033; correlation coefficients R Figure 4.16 A = 0.986, Figure 4.16 B = 0.985, Figure 4.16 C = 0.991, Figure 4.16 D = 0.993).

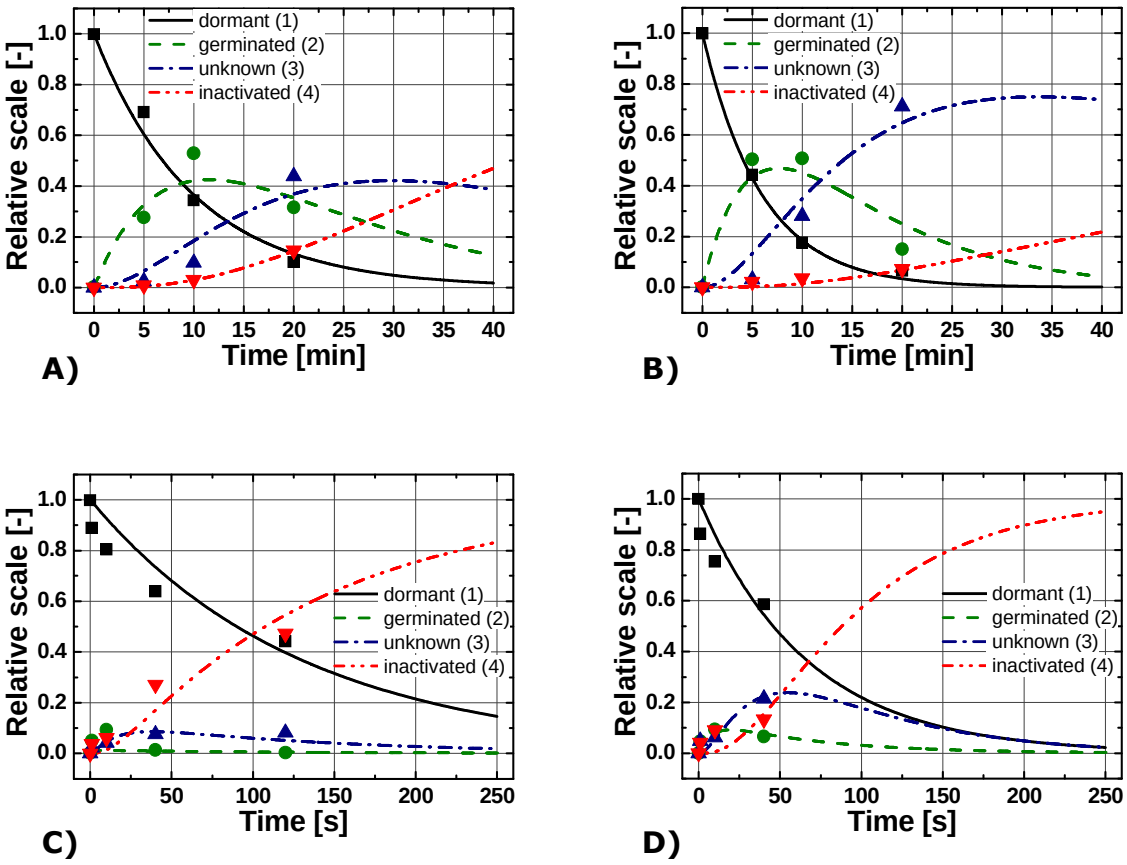

Figure 4.16: Heterogeneous population distribution in a predicted three-step-model (N1→N2→N3→N4, lines) for *B. licheniformis* spores after pressure treatment at (A) 150 MPa at 37 °C in sodium citrate buffer or (B) nutrient broth or (C) 600 MPa at 77 °C in sodium citrate buffer or (D) nutrient broth fitted with experimentally determined flow cytometric measurements; dormant (■), germinated (●), unknown (▲) and inactivated (▼) (mean deviation Fig. 4A = 0.033, 4B = 0.035, 4C = 0.041, 4D = 0.033; R Fig. 4A = 0.986, 4B = 0.985, 4C = 0.991, 4D = 0.993).

Especially for treatment at 150 MPa and 37 °C, transitions in small detection ranges could be adequately described. The modeling enables the assessment of the continuous population distribution and an extrapolation of the experimental data. Variations between the model and experimental data occurred because of partial overlap of some sub-populations. Comparing inactivation in nutrient broth and sodium citrate buffer, a higher germination and lower inactivation rate were observed in nutrient broth after treatment at 150 MPa and 37 °C (Figure 4.16).

At 600 MPa and 77 °C (Figure 4.16 C and Figure 4.16 D) it seems that the rate constant k_1 was not constant, and other reactions might be involved. It is well known that different germination mechanisms dominate at different pressure ranges (Wuytack et al., 1998; Wuytack, 1999; Wuytack, Soons, Poschet &

Michiels, 2000; Paidhungat et al., 2002; Setlow, 2003; Black et al., 2005; Black et al., 2007c). At lower pressures between 100-200 MPa, spore's nutrient-germinant receptors are activated (Wuytack et al., 2000; Setlow, 2003), while at high pressures of 500-600 MPa opening of the Ca^{2+}-DPA channels occurs (Paidhungat et al., 2002) and results in an incomplete germination process at 600 MPa (Wuytack et al., 1998; Paidhungat et al., 2002).

4.3.3. Flow cytometry versus plate count data

Based on the previously-described sub-population assignment, the unknown and inactivated populations were defined as non-recoverable, and a comparison of the plate counts (CFU are recoverable cells) and flow cytometric 'recoverable' counts (FCM, dormant and germinated population) was made. For this comparison, adequate correlations for both sodium citrate buffer and nutrient broth after treatment at 150 MPa and 37 °C could be found (mean deviation of $\log_{10}(N/N_0) = 0.099$, correlation coefficient R for CFU versus FCM = 0.917 and for CFU 80 °C versus FCM 80 °C = 0.967; Figure 4.17 A).
However, for spores treated at 600 MPa and 77 °C, a correlation of flow cytometer and plate count results could only be obtained up to a 40 s treatment time (mean deviation of $\log_{10}(N/N_0) = 0.096$, correlation coefficient R for CFU versus FCM = 0.942 and for CFU 80 °C versus FCM 80 °C = 0.874; Figure 4.17 B). This was because during longer hold times it was not possible to distinguish clearly the inactivated and dormant populations in density plot diagrams. At 150 MPa, nutrient broth was more favorable for germination than sodium citrate buffer, which resulted in a higher $\log_{10}$ reduction during pressure and post-pressure thermal treatment (Figure 4.17).

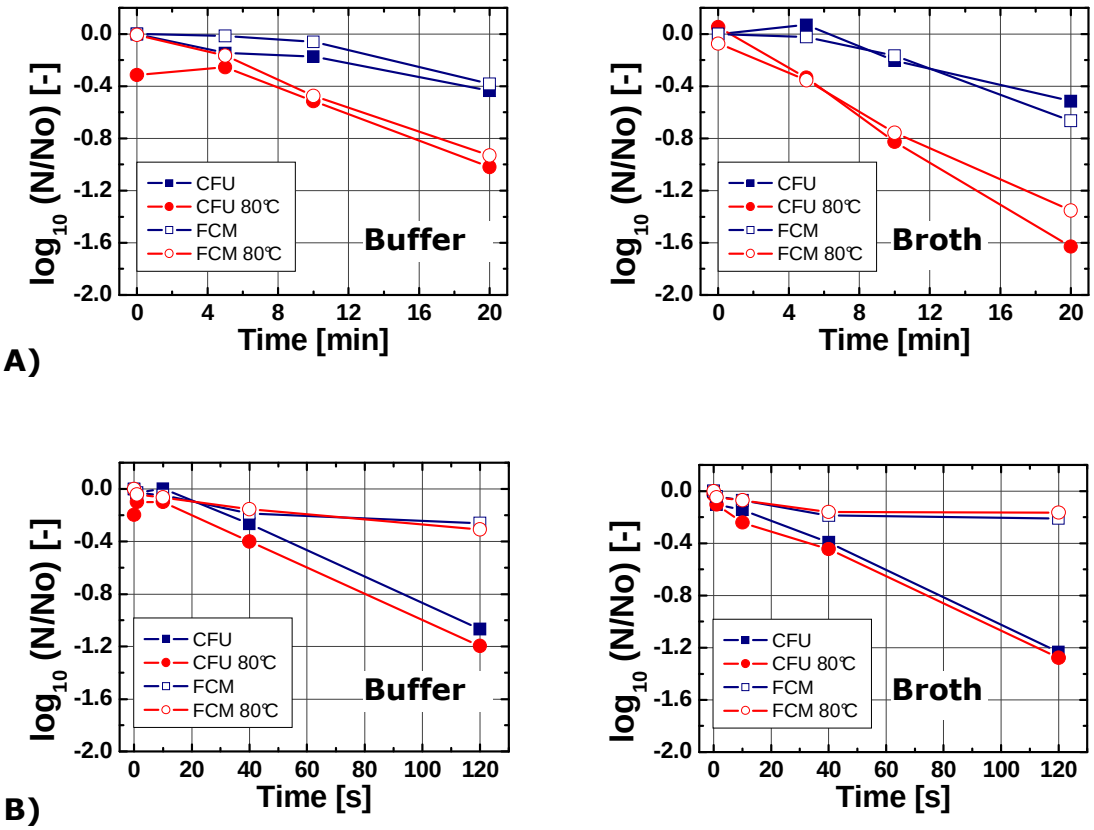

Figure 4.17: Flow cytometer (FCM) data versus plate count (CFU) results of *B. licheniformis* spores after pressure treatment with A) 150 MPa at 37 °C (mean deviation of $\log_{10}(N/N_0)$ = 0.099; R for CFU versus FCM = 0.917, R for CFU 80 °C versus FCM 80 °C = 0.967) and B) 600 MPa at 77 °C (up to 40 s; mean deviation of $\log_{10}(N/N_0)$ = 0.096; R for CFU versus FCM = 0.942, R for CFU 80 °C versus FCM 80 °C = 0.874) and after an additional thermal treatment (FCM 80 °C or CFU 80 °C) at 80 °C and 20 min holding time in sodium citrate buffer and nutrient broth.

4.4. Inactivation of *G. stearothermophilus* in the p-T landscape

4.4.1. Specification of *G. stearothermophilus* (NAMSA) spores

As presented in Chapter 4.1, spore agglomerations could have a strong impact on inactivation results. Particle analysis of *G. stearothermophilus* (NAMSA) spores suspension showed no significant spore agglomerations. Analyzing systems were proven by using latex microsphere suspensions. Latex spheres with 1 µm diameter resulted in a mean CE diameter of 1.05 ± 0.03 µm and 1.16 ± 0.32 µm by using the FPIA 3000 (20x lens) and Coulter Counter, respectively.

The investigation of *G. stearothermophilus* (NAMSA) spores with flow picture image analysis (10x lens) showed no larger CE diameters than 2.07 µm in a range within 1.5 µm – 40 µm (Figure 4.18).

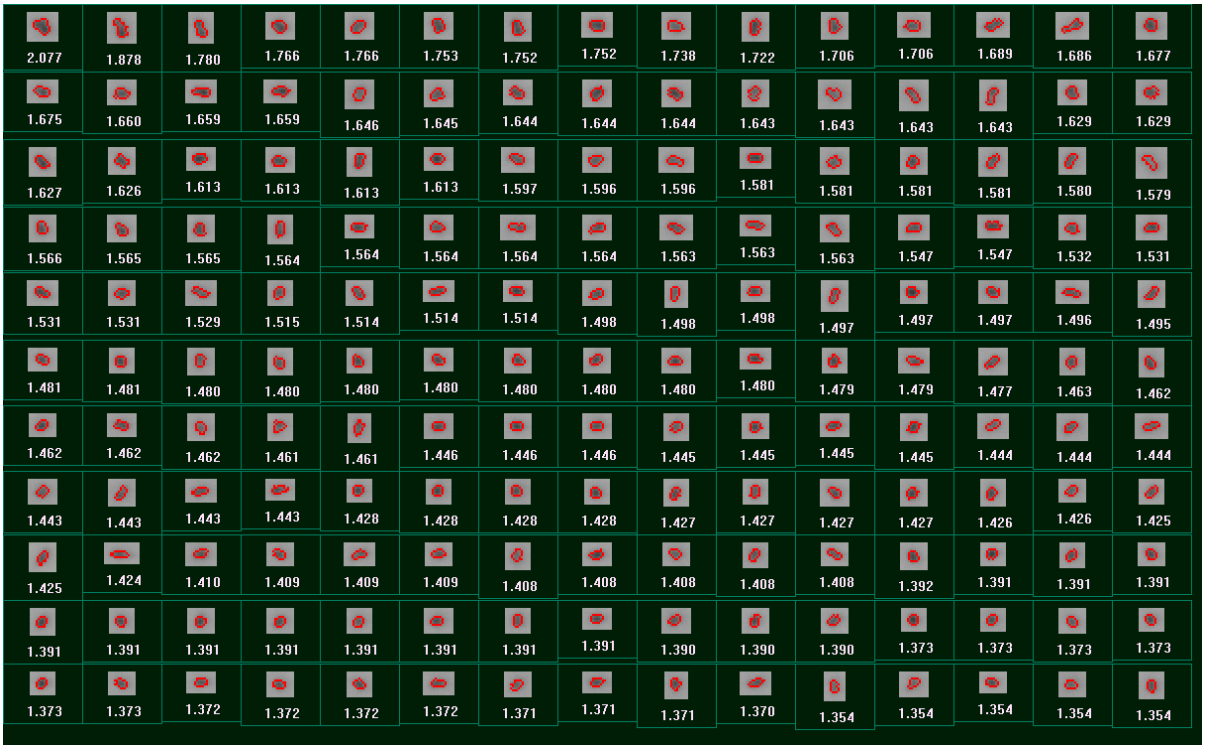

Figure 4.18: Particle images with CE diameter of *G. stearothermophilus* (NAMSA) spores suspended in sterile filtered 0.05 M ACES buffer (pH 7) measured with FPIA 3000 (A) (10x lens, HPF, range: 1.5 µm – 40 µm) with mean = 0.94 ± 0.10 µm. Pictures were sorted in descending order, where 2.077 µm was the largest observed particle.

Further analysis with both measuring devices and the lowest possible detection range resulted in two particle frequency distributions without significant spore agglomeration or larger particles (Figure 4.19).

The particle CE diameter distribution of *G. stearothermophilus* (NAMSA) spores showed no significant changes after high pressure and thermal treatment. However, the particle concentration detected was low and very less volume was available for particle analysis.

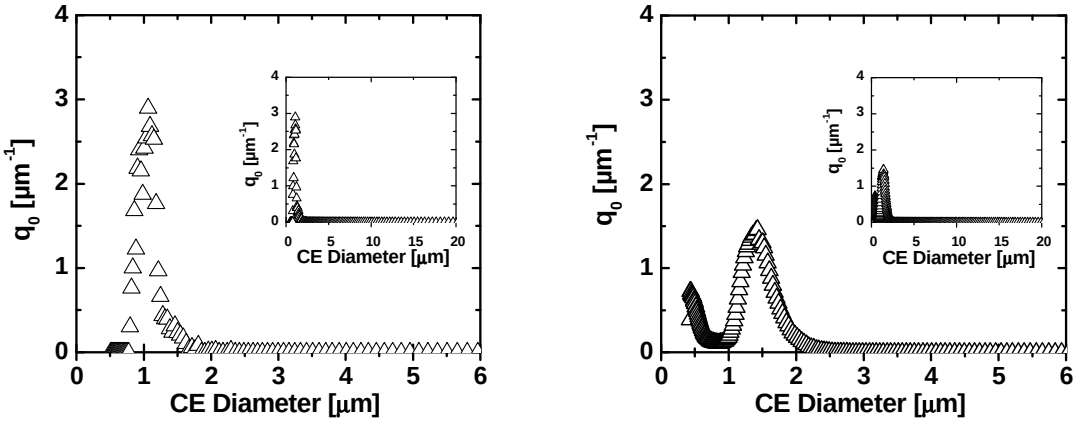

Figure 4.19: Particle CE diameter distribution of *G. stearothermophilus* (NAMSA) spores in sterile filtered 0.05 M ACES buffer (pH 7) measured with FPIA 3000 (A) (20x lens, HPF, range: 0.8 µm – 20 µm) with mean = 1.08 ± 0.18 µm and Coulter Counter (B) with mean = 1.35 ± 0.40 µm.

4.4.2. Process conditions

The developed temperature and process control enabled adequate inactivation experiments. However, the sample temperature could not be measured directly. For an optimal temperature control, it is essential that the initial temperature (prior to pressurization) is reached in the spore suspension. Consequently, a numerical simulation of the transient heat transfer via the pressure vessel, the pressure transmitting fluid (sebacate), the shrinking tube and spore suspension was necessary (data in Chapter 3.5.4). The transient heat transfer characteristic with dT max. = 80 K after 2 s treatment time T (2 s) is shown in Figure 4.20. The maximal temperature difference dT of 80 K ($T_{initial}$ =90 °C – $T_{cold\ vessel}$ =10 °C) represents the highest initial temperature prior to 600 MPa and a final temperature of 120 °C. The modeled heat source was located on the outer vessel wall and set to a non-transient source, because of software limitations. It can be noticed, that the shrinking tubes had an insulating effect (λ =0.16 W m^{-1} K^{-1}), which reduced the temperature loss during pressure build-up. The whole temperature profile T (t) of the inner vessel wall and of the spore suspension (location at red arrows) is presented in Figure 4.20 after numerical solving.

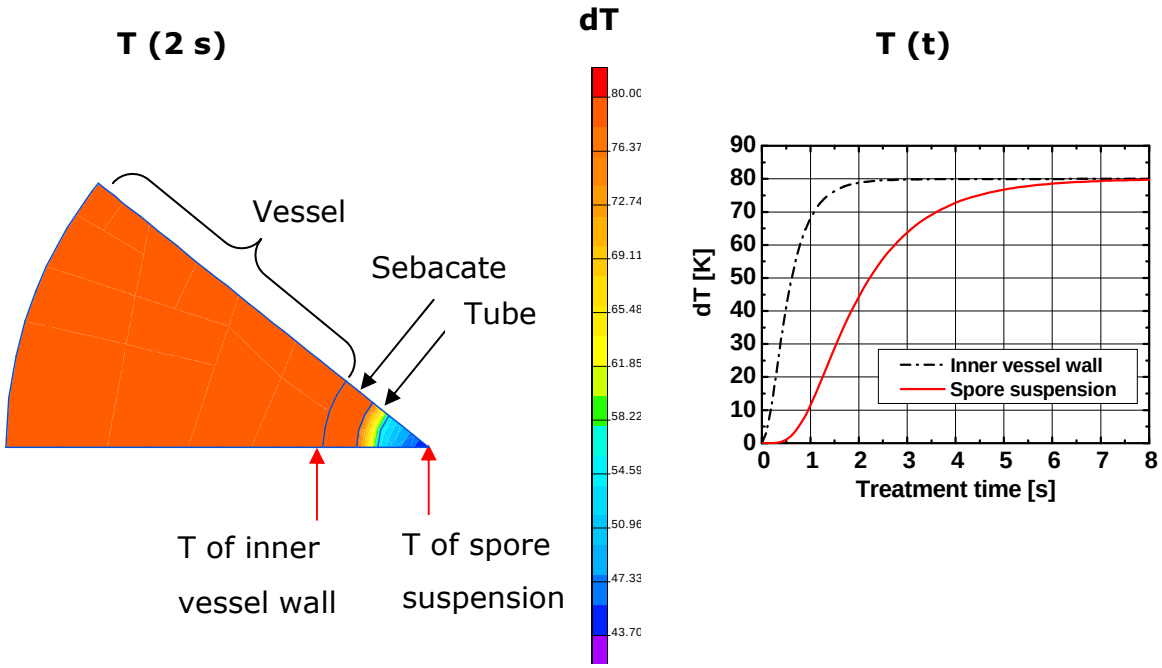

Figure 4.20: Pre-heating of spore suspension in the pressure vessel prior pressurization as transient heat transfer characteristic with dT max. = 80 K after 2 s treatment time T(1 s) and calculated temperature profile T(t) of inner vessel wall and spore suspension.

Numerical simulations of the pre-heating suggested, that after at least 8 s a homogeneous initial temperature in the spore suspension was reached. This resulted in the desired processing temperatures of 90, 100, 110 and 120 °C after compression. The modeling exemplified the heat transfer characteristic with a constant heat source at the outer vessel wall. A minimum pre-heating time was estimated with t < 8 s. Consequently, pressure build-up was set to commence 8 s after the thermocouple on the outer vessel wall (T_{ex} in Figure 3.1) reached the initial temperature. Longer times could have a little pre-treatment effect, while the effect on resistant spores was neglected. In contrast, shorter times could have an impact on spore inactivation, because they would lead to lower final temperatures during the first seconds of pressure holding.

By using the developed temperature control system, it was possible to perform inactivation experiments in a pressure range from 600 MPa to 1200 MPa under adiabatic conditions during compression and decompression, as well as isothermal conditions during dwell time as exemplified in Figure 4.21.

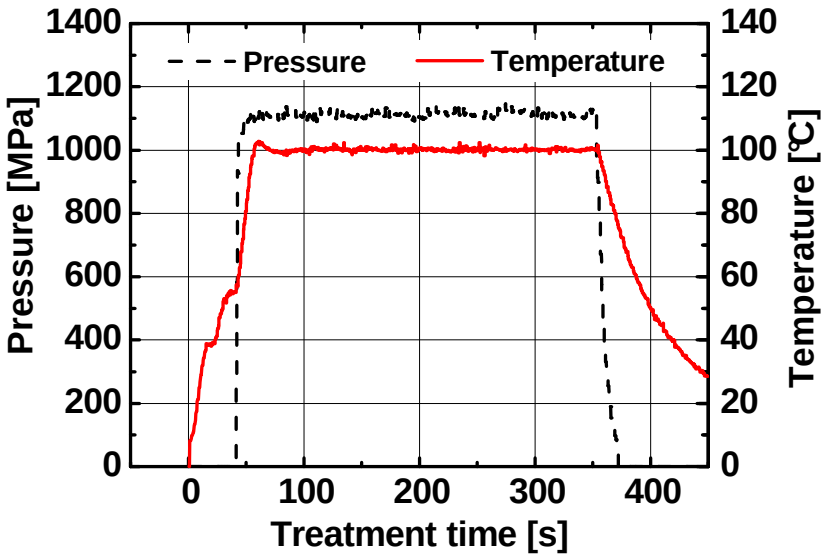

Figure 4.21: Measured pressure (black, dashed) and temperature on the outer vessel wall T_{ex} (red, line) profile at 1100 MPa, 100 °C final temperature and 300 s holding time.

4.4.3. Inactivation by heat and pressure

Thermal inactivation studies in glass capillaries with NAMSA *G. stearothermophilus* spores showed a linear $\log_{10}$ reduction (Figure 4.22). No shoulder formation, like with *G. stearothermophilus* spores from Merck, was observed.

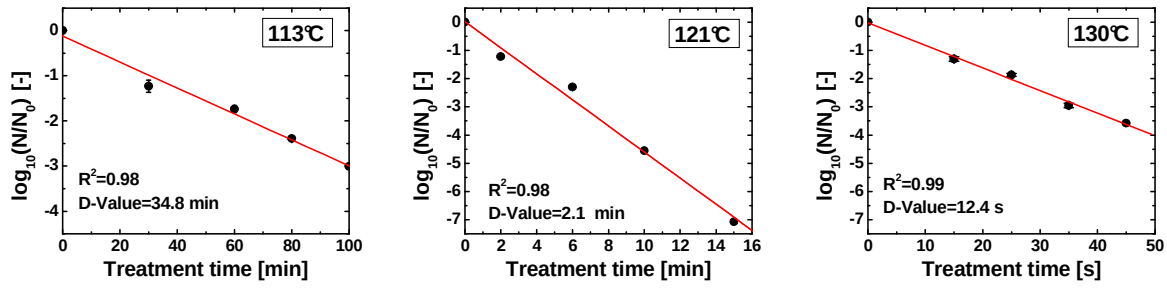

Figure 4.22: Thermal inactivation of *G. stearothermophilus* (NAMSA) spores in 0.05 M ACES buffer (pH 7) performed with glass capillaries with coefficients of determination R^2 and calculated D-values.

Similar to the functional relationship of temperature and rate constant k (Equation 2.15), a linear Arrhenius-type equation was used to fit the experimental rate constants k(T) in Equation 4.7,

$$\ln k(T) = -\frac{E_a}{R_m T} + A_0 \qquad (4.7)$$

with the regressions coefficients:

E_a = 389.470 ± 27.428 in [kJ/ mol]

A_0 = 114.60 ± 8.36.

The calculated rate constants in dependence of temperature are shown in Figure 4.23. A linear behavior enabled an adequate inter- and extrapolation. No significant inactivation differences in ACES and PBS buffer were observed, probably because of a higher resistance of the NAMSA spores.

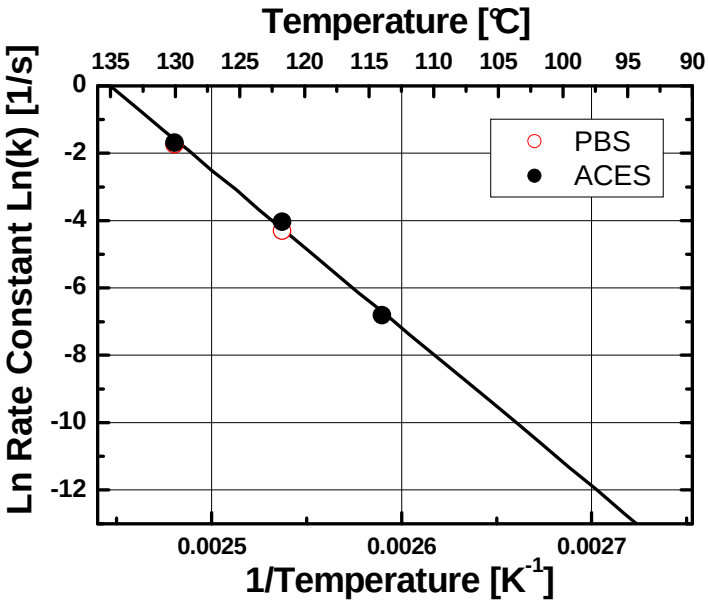

Figure 4.23: Natural logarithm of the rate constant ln(k) for thermal inactivation of *G. stearothermophilus* (NAMSA) spores in 0.05 M ACES (●) and phosphate (o) buffer (pH 7) in dependence of temperature (with extra- and interpolation line for ACES).

By using Equation 4.7, it is possible to calculate the temperature-time conditions to achieve a 7 $\log_{10}$ reduction of *G. stearothermophilus* (NAMSA) spores in 0.05 M ACES buffer (pH 7) (Figure 4.25). A z-value of 7.66 °C was calculated for the range 113 - 130 °C. Thermal inactivation in phosphate buffer resulted in a

z-value of 7.5 °C with similar D-values. The z-value of the NAMSA product certificate was defined as z = 7.4 °C (Annex 1).

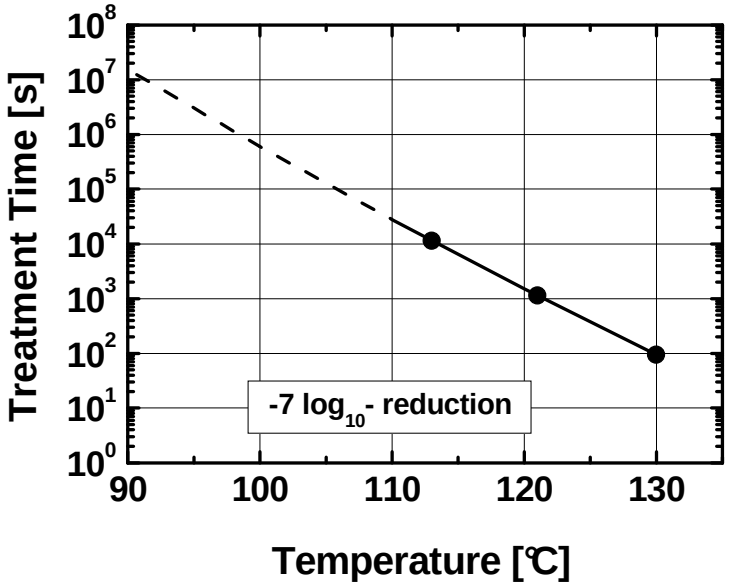

Figure 4.24: Temperature-time conditions to achieve a 7 $\log_{10}$ reduction of *G. stearothermophilus* (NAMSA) spores in 0.05 M ACES buffer (pH 7) with extra- and interpolation line.

All inactivation kinetics of *G. stearothermophilus* (NAMSA) spores in 0.05 M ACES buffer (pH 7) between 600 - 1200 MPa and 90 - 120°C are shown in Figure 4.25. The increase of temperature at constant pressure led to faster inactivation. Large reductions after pressure come-up time followed by immediate decompression were observed (1 s holding time). However, two pressure cycles with 1 s holding time at 800 MPa and 100 °C inactivated the same amount of *G. stearothermophilus* (NAMSA) spores as one cycle.

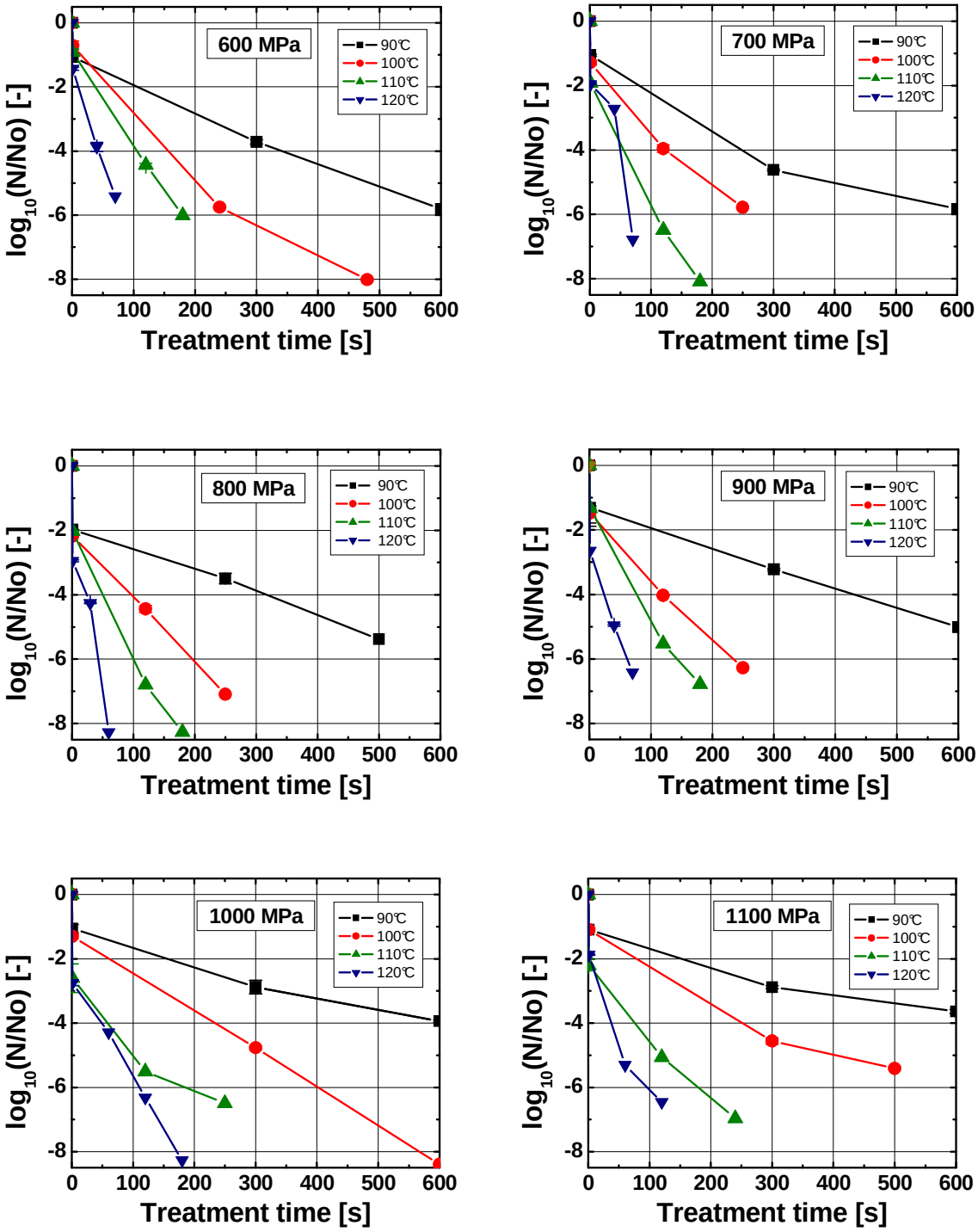

Figure 4.25: Inactivation of *G. stearothermophilus* (NAMSA) spores in 0.05 M ACES buffer (pH 7) at different pressure and temperature levels (detection limit ~ -7 $\log_{10}$).

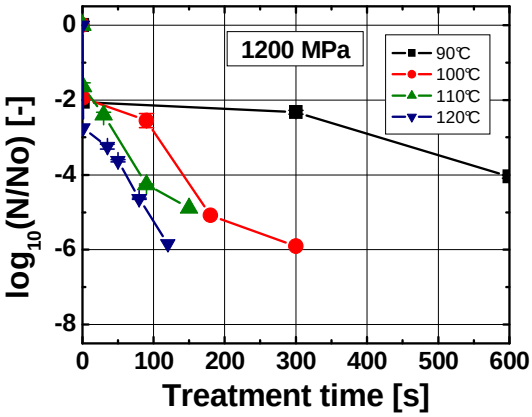

Figure 4.25: Inactivation of *G. stearothermophilus* (NAMSA) spores in 0.05 M ACES buffer (pH 7) at different pressure and temperature levels (detection limit ~ -7 $\log_{10}$) (continued).

4.4.4. Modeling of isokineticity lines in the p-T-landscape

Isokineticity lines in the pressure and temperature landscape (p-T diagram) are the most concise way of presenting the combined effects of pressure and temperature. A functional relationship (p, T) of the rate constant k needs to be found, when modeling isokinetic lines. Significant inactivations of up to -3 $\log_{10}$ after 1 s holding time complicated the modeling of the rate constants in Figure 4.25. However, after the initial drops in spore count nearly linear $\log_{10}$ reductions were observed. The simplest model approach for this problem is a first order kinetic (n = 1) after 1 s holding time using the CFU mL^{-1} after 1 s holding time N(1 s) as initial population N_0. In contrast to higher order decay reactions (Equation 3.3), one of the main advantages is that the first order model is not dependent on the initial population (Equation 2.36). After regression analysis (Annex 4, Annex 5), D-values in dependence of pressure and temperature were calculated (Figure 4.26). The rate constant k is the reciprocal of the D-value multiplied by 2.303 (Equation 2.36).

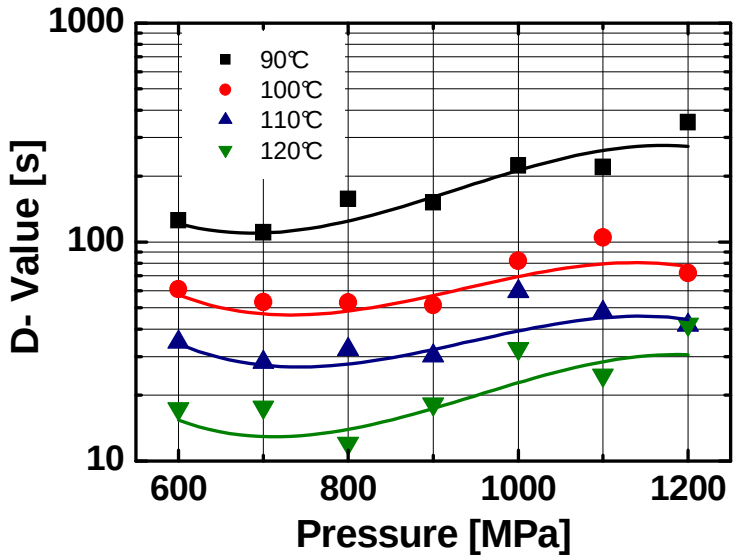

Figure 4.26: D-values (p, T) of *G. stearothermophilus* (NAMSA) spores suspended in 0.05 M ACES buffer (pH 7) with linear $\log_{10}$ reduction after pressure build-up with N(1 s) as initial population N_0.

Rate constants were modeled by a Taylor series polynom, limited to the 3rd order terms (Equation 3.4), which produced a satisfying fitting (Annex 5, Figure 4.26).

Using first order kinetics, just one p-T diagram for the whole kinetic data is necessary (Figure 4.27). The holding times of the isokineticity lines simply had to be multiplied by the same factor (Table 4.4), to increase the $\log_{10}$ reduction in the p-T diagram. This p-T diagram gives an overview and can be used for optimizations of sterilization processes at high isostatic pressure.

The simplified kinetic model produced an acceptable fitting of the experimental data (Figure 4.28).

Table 4.4: Transformation matrix for Figure 4.27

$\log_{10}$	Holding times of isokineticity lines in min						
-4	1	2	3	4	5	8	10
-2	0.5	1	1.5	2	2.5	4	5
-6	1.5	3	4.5	6	7.5	12	15
-8	2	4	6	7	10	16	20

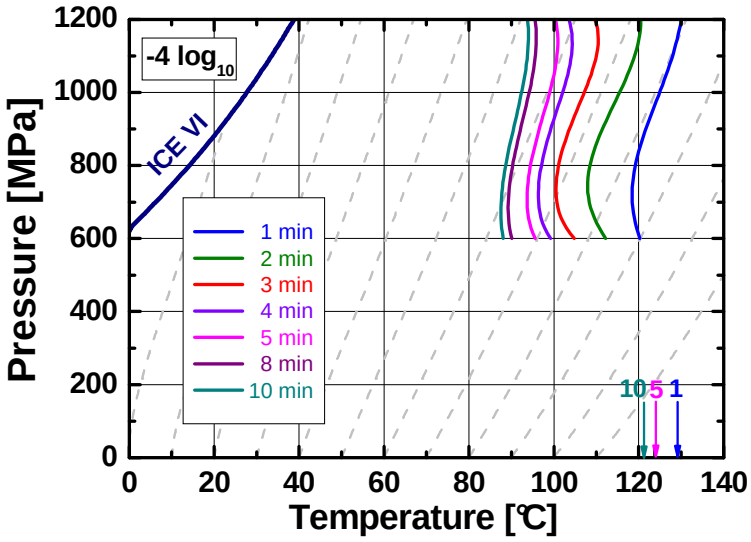

Figure 4.27: Isokineticity lines for a 4 $\log_{10}$ reduction of *G. stearothermophilus* (NAMSA) spores in the p-T landscape with adiabatic lines due to compression (--) of water. Inactivation (p,T) in ACES buffer (pH 7) is modeled with first order kinetics after pressure build-up with N(1 s) as initial population N_0. Data for thermal inactivation (in ACES) are shown as arrows with holding times in min.

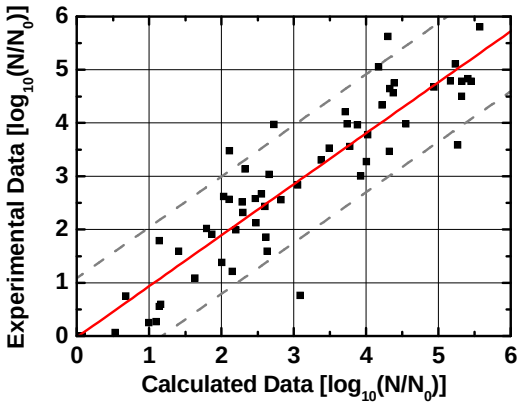

Figure 4.28: Comparison among calculated and experimental $\log_{10}$ reductions of *G. stearothermophilus* (NAMSA) spores in ACES buffer (pH 7) modeled with first order kinetics after pressure build-up with N(1 s) as initial population N_0 with 95 % prediction limit lines (dashed), R = 0.956 and SD = 0.55.

Alternatively, a biphasic inactivation model for kinetics in Figure 4.25 could be applied. However, the resistant sub-population [N(1 s)] varied from approximately 10^7 – 10^5 CFU mL^{-1} in comparison to the majority population [N_0 – N(1 s)] with approximately 10^8 CFU mL^{-1} (Figure 4.25). The rate constant of the majority population had to be very high, because of the $\log_{10}$ linear behavior after 1 s holding time. The main parameter was only the population distribution between resistant and sensitive population and not the rate constant of the majority population.

A semi-mechanistic model with incorporation of the empirically fitted $\log_{10}$ [N (1 s) / N_0] in dependence of pressure and temperature is suggested, in order to compare among $\log_{10}$ reductions after the whole process and during different holding times.

During calculation of Equation 3.3 it was necessary to remove the term $N_0^{(n-1)}$,

$$\log_{10}\left(\frac{N}{N_0}\right) = \log_{10}\left(1 + k' \cdot t \cdot (n-1)\right)^{\frac{1}{1-n}} \qquad (4.8)$$

because the initial population of the model N(1 s) varied in a range within approx. 10^7 – 10^5 CFU mL^{-1}. Therefore the specific rate constant k´ in Equation 4.8 represented an empirical parameter. All kinetic data were fitted with a 1.05 order decay reaction after regression analysis (Annex 4). The experimental $\log_{10}$ reductions after 1 s holding time and the calculated empirical rate constant k´in dependence of pressure and temperature are shown in Figure 4.29.

The differences of N(1 s) can be explained by different p-T combinations during pressure build up, represented by the adiabatic lines due to compression of water in the p-T diagrams. The $\log_{10}$ reductions after 1 s holding time (Figure 4.29 A) and the empirical rate constants (Figure 4.29 B) were fitted to a full third order Taylor series polynom, limited to the 3rd order terms (Equation 3.4). Regression coefficients and analysis can be found in Annex 6 and Annex 7. After additive implementation of the $\log_{10}$ reductions after 1 s holding time into Equation 4.8, the inactivation for the whole process including pressure build-up was modeled and the result is shown in Figure 4.30.

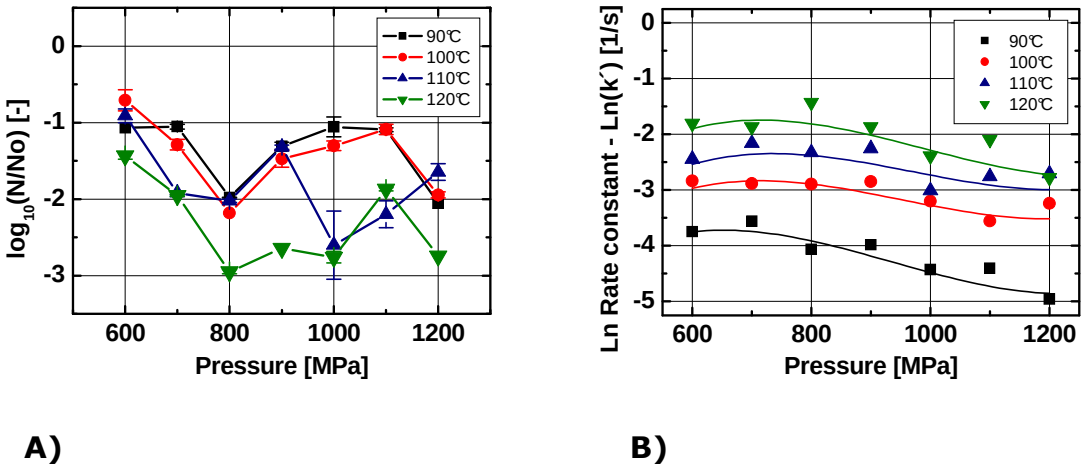

A) **B)**

Figure 4.29: $\log_{10}$[N (1 s) / N_0] (A) and empirical rate constant k´(p, T) (B) of *G. stearothermophilus* (NAMSA) spores suspended in 0.05 M ACES buffer (pH 7).

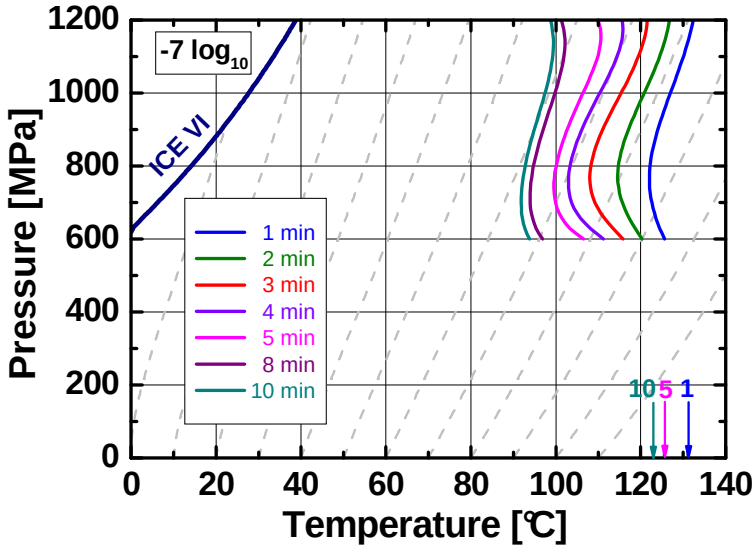

Figure 4.30: Isokineticity lines for a 7 $\log_{10}$ reduction of *G. stearothermophilus* (NAMSA) spores in the p-T landscape with adiabatic lines due to compression (--) of water. Inactivation (p,T) in ACES buffer (pH 7) is modeled for the whole process. Data for thermal inactivation (in ACES) are shown as arrows with holding times in min.

The model approach produced an acceptable fitting of the whole experimental data (Figure 4.31).

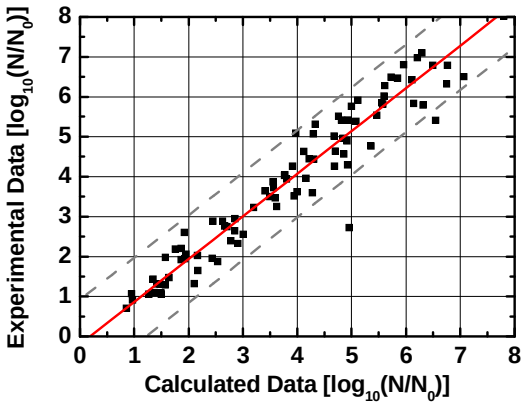

Figure 4.31: Comparison among calculated and experimental $\log_{10}$ reductions of *G. stearothermophilus* (NAMSA) spores in ACES buffer (pH 7) modeled for the whole inactivation process with 95 % prediction limit lines (dashed), R = 0.965 and SD = 0.54.

4.5. Discussion

Spore inactivation mechanisms and non-linear $\log_{10}$ reduction characteristics after thermal and pressure treatment have been discussed by many authors and different theories were developed. Some authors explained the initial lag phase (shoulder) after thermal inactivation with heat activation (Curran & Evans, 1945; Humphrey & Nickerson, 1961; Finley & Fields, 1962; Shull, Cargo & Ernst, 1963; Keynan, Evenchik, Halvorson & Hastings, 1964; Hyatt & Levinson, 1968; David & Merson, 1990). Humphrey and Nickerson (1961) explained the initial phase by a heat-induced initiator, which could be thought of as being divided in a less heat-labile and inactive state from which it would be freed by heat but eventually destroyed by further heating. Other authors (Keynan et al., 1964) assumed that heat or reducing agents change the tertiary structure of a protein responsible for the maintenance of the dormant state by reducing the disulfide linkages which stabilize the protein in a specific configuration.

A mathematical model was given by Shull et al. (1963), which was modified by Abraham et al. (1990). These authors suggested that the spore suspension contained an initial activated and dormant population of spores. The dormant population has to be activated before being destroyed by heat and the model based on the rate constant on the final linear part of the survival curve. In the performed experiments this model can not adequately describe the shoulder

formation, because of the high slope of the linear part and the consequential improbable population of dormant spores in the suspension. However, the mechanism of spore activation is not well understood (Paidhungat & Setlow, 2002).

Another theory from the biophysical point of view is given by Aiba and Toda (1966), Bueltermann (1997) and this work. Bueltermann (1997) investigated the agglomeration behavior of *G. stearothermophilus* (Merck) spore suspensions and described the shoulder formation after thermal inactivation by first-order inactivation kinetics when the agglomeration size was considered.

The results from Bueltermann (1997) could be supported in this study, but with a different measured particle distribution and incorporation of the spore packaging. Both studies proved the impact on non-isothermal conditions (Chapter 4.1.3) and found no or a very little effect on the shoulder formations (Figure 4.7). By using a Coulter Counter, Bueltermann (1997) found the maximum occurrence at approximately four spores per agglomerate, but also agglomerates with more than 100 spores occured in the same *G. stearothermophilus* (Merck) spore suspension. Reproducible particle analyses with different methods are one of the main challenges in this matter.

As mentioned, the reason for spore agglomerations may be the outer proteinaceous coat and / or the spore exosporium and consequently the specific hydrophobicity (Doyle et al., 1984; Wiencek et al., 1990). The pathogen *B. cereus* spores have the highest hydrophobicity (Wiencek et al., 1990; De Vries, 2006), which was also indirectly observed by the largest agglomerates under the microscope (Figure 4.1). Possiblity spore agglomerates were formed between stages VI – VII during cell lysis. However, going deeper into particle science there might be other important effects for spore agglomeration. In general, the higher the relationship between separative forces (e.g. gravity) and adhesive forces is, the higher the density of the agglomerates is (or: the smaller the porosity of the agglomerates). This relationship is smaller, the smaller the particles are. In aqueous solutions van der Waals adhesive forces are smaller than in gas atmosphere. Hence, agglomerates in aqueous solutions have a denser packaging or lower porosity. However, in aqueous solutions the main effects on separative forces are the zeta potential and Debye length according to the electrostatic double-layer (Schubert, 2007). In this context further research

is nesseary to find optimal packagings for a realistic spore count of a particular agglomerate.

To remove spore agglomerates, filtration of spore suspension can be possible (Feeherry, Munsey & Rowley, 1987; Furukawa, Noma, Yoshikawa, Furuya, Shimoda & Hayakawa, 2001). Unfortunately the pore size from the used filters was not given by the authors. Feeherry et al. (1987) found an initial shoulder after filtration of *G. stearothermophilus* spore suspension and supposed that the recovery of heat-injured spores could be an explanation for the curvilinear portion. After fictive filtration of the whole spore suspension with the smallest, practical applicable filter (4.5 µm pore size) calculated with Equation 4.9,

$$\log_{10}\frac{N(t)}{N_0} = \log_{10}\left(\sum_{i=1}^{15} q_0(i)\cdot p_i(t)\right) \qquad (4.9)$$

remain still maximal 15 spores in an agglomerate (2D model) with 4.5 µm equivalence diameter. Consequently survival curves of the used *G. stearothermophilus* (Merck) spores after thermal treatment would have a shoulder formation as well, because the high occurrences of middle sized agglomerates (Figure 4.2) had the main influence on the curvilinear form in this study. Complete disintegration of the agglomerates after ultrasonic treatment, dispersing in a tooth rim unit and addition of tensides failed (Bueltermann, 1997). Using the commercial sterilization indicator (NAMSA spore suspension, Annex 1), spore agglomeration could be avoided (Figure 4.18, Figure 4.19) in a very simple way. Unfortunately no detailed information about the spore production process was available. For the food industry the hydrophobicity and agglomeration behavior is of high importance, as possible reason for adhesion to surfaces, microbial "fouling" and non-$\log_{10}$-linear shoulder or also tailing formation. Aiba and Toda (1966) used a probabilistic agglomeration approach for the calculation of spore clump life span distribution and Furukawa et al. (2005) explained the non-linear tailing during heat treatment with the same relationship, but without detailed mathematical descriptions. The mentioned probabilistic agglomeration model and the work from Bueltermann (1997) as well as this study have the same basic mathematical approach.

Further descriptions for tailing formations discuss the population heterogeneity and the assumed existence of a spectrum of resistance with a super resistant sub-population (Peleg & Cole, 1998). In this study four distinct sub-populations

(dormant, germinated, unknown and inactivated; Figure 4.15) were detected by flow cytometry, which resulted in a heterogeneous population distribution of different physiological states during high pressure treatment at 150 MPa with 37 °C and 600 MPa at 77 °C (Figure 4.16).

The physiological state or "fitness" of cells encompasses both structural (i.e. changes to cortex and membrane) and functional (i.e. ability to be recovered by culture) factors as described by Bunthof (2002). In the current study membrane permeant SYTO 16 and membrane impermeant PI fluorescent dyes were used primarily to determine the structural properties of spores, with respect to cortex hydrolysis and membrane damage. Spores stained with SYTO 16, but not with PI, could exist in a number of different functional states, where "culturable" spores could be regarded as having the highest physiological fitness. Sublethally injured spores, that also stained with STYO 16 but not with PI, may prove to be functionally non-recoverable. Thus, the unknown functional fitness of spores stained with SYTO 16, but not with PI, may explain quantitative differences observed between the flow cytometric and plate count methods (Figure 4.17). A review of the major physiological states of non-growing microorganisms, including metabolically active-but-non-cultureable and viable-but-non-cultureable is given by Kell, Kaprelyants, Weichart, Harwood and Barer (1998). Nevertheless, sub-population 3 is still not definable. It might be possible that sub-population 3 represents a population with a hydrolyzed cortex and some damage to the inner membrane, thus allowing PI to enter the spores and partially displace SYTO 16 and reduce the observed green staining. SYTO 16 may also be quenched in sub-population 3 by fluorescence resonance energy transfer to PI, as has been reported for other SYTO dyes (Stocks, 2004).

Another theory is that sub-population 3 represented outgrowing spores. Hence, germinating spores, which have not fully recovered metabolism were highly permeable to SYTO 16 whereas outgrowing spores with a fully active metabolism were able to efflux some of the SYTO 16 and therefore appeared less fluorescent (Cronin & Wilkinson, 2007). However, it seemed that sub-population 3 was not culturable in this study, which is shown in Figure 4.13 and Figure 4.14 at 150 MPa, 37 °C and 10 - 20 min. The potential outgrowing spores were probably injured or had a too low physiological "fitness".

Previously, Black et al. (2005), using SYTO 16 staining only, obtained three sub-populations after pressure treatment (with and without pre-treatment in 98 % H_2O_2). The authors' histogram analysis showed incomplete discrimination of the sub-populations. In comparison, the applied two-color staining with SYTO 16 and PI has allowed for better discrimination of the sub-populations, and in addition the identification of sub-population 3. Comas-Riu and Vives-Rego (2002) also previously obtained a non-viable, membrane permeabilized sub-population stained with SYTO 13 and PI in aged spore cultures; such a physiological state may be ascribable to the observed sub-population 3.

From another point of view, the comparison of different methods within a 1 $\log_{10}$ (90%) detection range with highly concentrated cell suspensions will be subject to sources of error making quantitative comparison of the flow cytometric and plate count data more difficult. Other rapid and adequate reference methods to investigate spore germination are the measurements of the loss of refractility, optical density (Vary & Halvorson, 1965), dipicolinic acid release (Janssen, Lund & Anderson, 1958; Woese & Morowitz, 1958 and in more detail Heinz, 1997), respiratory activity with 5-cyano-2,3-diotolyl tertazolium chloride (Laflamme, Lavigne, Ho & Duchaine, 2004) or the Wirtz-Conklin staining technique (Hamouda, Shih & Baker, 2002). These methods have the same maximum detection range of 2 $\log_{10}$. Direct comparison between the analysis of DPA-release and flow cytometry has shown that flow cytometry is more accurate (Black et al., 2005).

In the work reported here, the greatest problem observed was the decrease in fluorescence, after high-temperature-high-pressure treatment at extended treatment times. This is most likely explained by a reduction in nucleic acid integrity resulting in a lower binding of fluorescent dyes. Density plots for samples treated at 600 MPa and 77 °C for 20 min, showing a 6.6 $\log_{10}$ reduction by plate counting were similar to those of untreated samples (i.e. Figure 4.13 and 4.14 „untreated") when assessed by flow cytometry. Comparing this observation with that of spores treated with heat only (121 °C, 8min; Figure 4.13 and 4.14), this may provide further evidence of a difference in the mechanisms of inactivation by heat and combined heat and HP processes.

Physiological studies could give more information about the detailed inactivation mechanism(s), but were performed mainly for vegetative cells. Smelt (1998)

investigated the high pressure induced increase of the membrane permeability because of phase transition of the cytoplasmic membrane from the physiological liquid-crystalline to the gel phase. Ulmer (2001) showed that lethal effects under high pressure resulted from the combination of damaged membrane transport systems and detrimental environmental parameters. High pressure treated vegetative cells lost the structural and functional integrity of the cytoplasmic membrane and were unable to maintain vital concentration gradients of ions and metabolites (Ulmer, 2001; Molina-Gutierrez, Stippl, Delgado, Gänzle & Vogel, 2002). After breakdown of the membrane permeability the difference between the internal and external pH-value could collapse or approach zero, resulting in loss of cell viability (Nannen & Hutkins, 1991). The internal pH is critical for the control of many cellular processes, such as ATP synthesis, RNA and protein synthesis, DNA replication, cell growth and it plays an important role in secondary transport of several compounds (Belguendouz, Cachon & Divie`s, 1997). It has a particularly inhibitory effect on membrane ATP-ase, a very important enzyme in the acid–base physiology of cells (Hoover, Metrick, Papineau, Farkas & Knorr, 1989). Setlow and Setlow (1980) measured the internal pH-value in dormant and germinated *Bacillus* spores at 6.3-6.4 and 7.3-7.5, respectively. On the base of these investigations it can be assumed that the intracellular shift of dissociation equilibriums and the loss of the ability of pH as well as pOH compensation could improve the inactivation of bacterial spores.

In this communication, it could be shown that the extracellular shift of the dissociation equilibriums affected the spore inactivation (Chapter 4.2). After thermal and pressure processing in two different temperature and pressure stable buffer systems, inactivation differences up to 3 $\log_{10}$ were detected. By using the pure empirical Weibullian Power Law, it was possible to model non-linear shoulder (thermal inactivation) and tailing (pressure inactivation) formation with one fundamental equation (Figure 4.11). The main advantage is the wide flexibility and adequate correlation of non-linear $\log_{10}$ reductions. This model approach was only used for the comparison of the impact of dissociation equilibrium shift in different buffer solutions on the inactivation (Figure 4.12) and not for mechanistic studies.

On the basis of thermodynamical equations, a simple model for the dissociation equilibrium shift in water and buffer systems was constructed. Modeling of the

discussed buffer solutions can be performed by using thermodynamical data in Goldberg et al.(2002) and Table 4.3. Experimental data with ACES and PBS buffer supported the suggested model. However, to verify and to evaluate the modeled data, in-situ measurements for the dissociation equilibrium shift have to be developed. Up to now such in-situ method is not available and no appropriate online measurement device exists.

Applying the above models, sensitive reactions such as cell inactivation or enzyme reactions can be better anticipated in planning experimental designs. Different buffer systems should be compared for thermal and pressure experiments. For optimal comparison, both buffer systems should have similar buffer capacities (pK_a). However, the main interest of the food industry is the pK_a- and / or pH-shift of real matrices, but surprisingly limited data exist in the literature. For skim milk, Schraml (1993) measured the pH-shift up to 88 °C (compare Figure 4.9). The dissociation of water and elimination of phosphate ions by crystallization of calcium phosphate decreased the pH-value in this case (Kessler, 1996). The crystallization led to a dissociation equilibrium shift of phosphoric acid, where by rearrangement of the equilibrium, phosphoric acid dissociated and more hydroxonium ions (H_3O^+) were generated (analogue Equation 2.29). Small changes of the pH-value could affect different reactions or inactivations in food matrices. Dannenberg (1986) found, that the so called "fouling" of skim milk on hot surfaces is drastically increased, when the pH-value was decreased from 6.6 to 6.5 - 6.4. A possible explanation could be increased protein aggregation, because of decreased electrostatic repulsion, when proteins approach their isoelectric point (Kessler, 1996). The isoelectric point is the pH-value at which a particular molecule or surface carries no net electrical charge. The complex matrix relations in skim milk during thermal processing provide ideas, how many relevant mechanisms might occur under high pressure high temperature processing. A review for different matrix effects is given in Chapter 2.5, but limited data exist.

Summarizing the discussed facts and data, for investigation of the detailed spore inactivation mechanism(s) in dependence of pressure and temperature a homogenous spore suspension in a very simple matrix with lowest possible changes in dependence of pressure and temperature had to proceed to constant process parameters, and if not possible to optimal controlled process parameters

(Chapter 4.4). The thermal inactivation of *G. stearothermophilus* (NAMSA) spores in ACES and PBS buffer showed linear $\log_{10}$ behavior and no typical shoulder formation, which could be found in agglomerated spore suspensions (Chapter 4.1). After high pressure processing nearly the same linear $\log_{10}$ behavior during holding pressure could be observed (Figure 4.25), which led to a fundamental first-order inactivation model in the p-T landscape (Figure 4.27). The strong come-up time reductions in Figure 4.25 were also reported by other authors (Margosch, Ehrmann, Gänzle & Vogel, 2004b; Rajan, Pandrangi, Balasubramaniam & Yousef, 2006b; Ahn et al., 2007) with *Clostridium* and *Geobacillus* spores. It has to be taken into account, that these literature data were generated without temperature control. Furthermore the strong come-up time reductions made flow cytometric assessments with a max. detection range of ~90 % impossible. To explain these strong come-up time reductions, a biphasic model was not adequate, because of varied N(1 s) and linear $\log_{10}$ behavior after 1 s holding time. It seemed that there were more sub-populations involved.

In Figure 4.25, most of the inactivation curves showed no tailing during high pressure holding times. A plausible and alternative explanation for tailing or leveling-off at longer treatment times could be incorporated spores in seal or plug-tube connections. These spores would have other matrix conditions, especially lower water activity, which lead to higher resistance (Pfeifer, 1992) and recontamination during opening of the treated samples. To avoid such "recontamination" the used shrink tubes in Chapter 4.4 had an air layer between spore suspension and seals. Shrink tubes were horizontally opened by a cut between seal and air layer, where no recontamination of sealed spores was possible.

Assuming a first-order kinetic model for thermal and pressure inactivation a universal p-T-diagram presented all kinetics (Figure 4.27), where all relevant data (p, T, t) for different D-concepts (e.g. 8 or 12 D concept) could be extracted. The come-up time reductions could represent a safety factor in this matter. The modeled isokineticy lines in Figure 4.27 have shown a pressure dependent behavior with an optimal inactivation around 750 MPa, a stabilization zone at >750 MPa and at longer holding times again an improved spore inactivation (~1100 MPa). Spore stabilization at ultra high pressure has been

reported by other authors (Ardia, 2004; Margosch et al., 2006; Patazca et al., 2006; Rajan et al., 2006a; Ahn et al., 2007), but only Ardia (2004) and Margosch et al. (2006) worked with ideal adiabatic process conditions and isothermal dwell times. Stabilization areas are possibly strain specific.

Ardia (2004) discussed the impact of the dissociation equilibrium shift in ACES and PBS buffer on the observed spore stabilization effects. The author found stabilization effects in three different buffer systems (PBS pH 7, ACES pH 7 and 6) and concluded that the dissociation equilibrium shift is not the main source of the phenomenon. As shown in Figure 4.32, relatively moderate differences of the dissociation equilibrium shift between both buffers would occur within the investigated experimental high pressure range in this study. During thermal inactivation there are much higher differences of the dissociation equilibrium shift, but no significant inactivation differences were observed with NAMSA spores (Figure 4.23), probably because of a high resistance to this matrix stress. Spores with lower resistance showed strong inactivation differences in both buffer systems (Figure 4.11). For further investigations in this matter in-situ measurements of the dissociation equilibrium shift would be necessary.

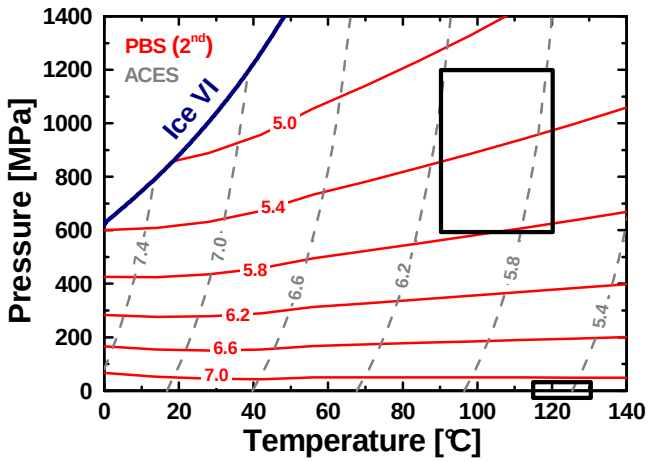

Figure 4.32: Modeled iso-pK_a-lines in ACES (--, gray) and phosphate (-, red) buffer under different p-T conditions with investigated experimental p-T range in this study (squares).

Using a semi-mechanistic model with the p-T diagram in Figure 4.30 it was possible to describe the whole inactivation kinetics. However, this p-T graph is dependent on the used HP unit. Reproducible inactivation results with different HP units can be generated by using the inactivation model without come-up time

reductions (Figure 4.27). Both p-T diagrams have the same isokineticity characteristics and 5 min holding time in Figure 4.30 is similar with 3 min holding time in Figure 4.27. The higher temperature dependence of isokineticity lines is better described with the semi-mechanistic model due to incorporation of the $\log_{10}$ reductions after 1 s holding time (Figure 4.30). Detailed studies about the spore inactivation mechanisms have to be performed with kinetics only dependent on treatment times, for example the first-order kinetic model in Figure 4.27. Using these isokineticy lines a hypothesized mechanism of spore inactivation is suggested. The whole assumptions are based on the germination model for *B. subtilis* (Setlow, 2003) in Figure 2.21 and literature data in Chapter 2.4.4. Opening of Ca^{2+}-DPA channels (Paidhungat et al., 2002) over 500 MPa is the start point, where a germination reaction without nutrients in buffer systems is possible. At this pressure and matrix conditions just a reduced amount of spore germination reactions would be possible as shown in Figure 4.33. Obviously the key factor for full cortex hydrolysis as well as core hydration and thus loss of resistance (Figure 2.20) is the activation of the main important CLEs, SleB and CwlJ (Figure 2.21). SleB is more resistant to wet heat than CwlJ (Moir, 2006), which makes the mechanism more complex. SleB and CwlJ are located in *B. subtilis* spores and for *G. stearothermophilus* similar enzymes are defined as CLE 1 and CLE 2 (Figure 4.33). Margosch et al. (2006) mentioned that the behavior of a single protein, which shows also stabilization areas under pressure, can hardly be described as determinative for inactivation unless it is required for a vital function (e.g. as a structural or protective component). In Figure 4.33 different reaction pathways are possible and two different enzymes with probably different activity or resistance distributions under a certain range of pressure-temperature conditions are involved. Heinz and Knorr (1998) assumed that pressure and temperature can trigger the CLE activities and cause inactivation of the same enzymes. Both competing reactions can also apply to many more catalyzed reaction steps requiring different enzymes each with an individual p-T behavior (Heinz & Knorr, 2002; Ardia, 2004). Hence, the CLE activity can be seen as functional relationship in dependence of p, T and t. Because of the high complexity of such systems, the whole generated lethal effects at constant temperature and holding time are defined as a lethal effect distribution in dependence of pressure (Figure 4.34).

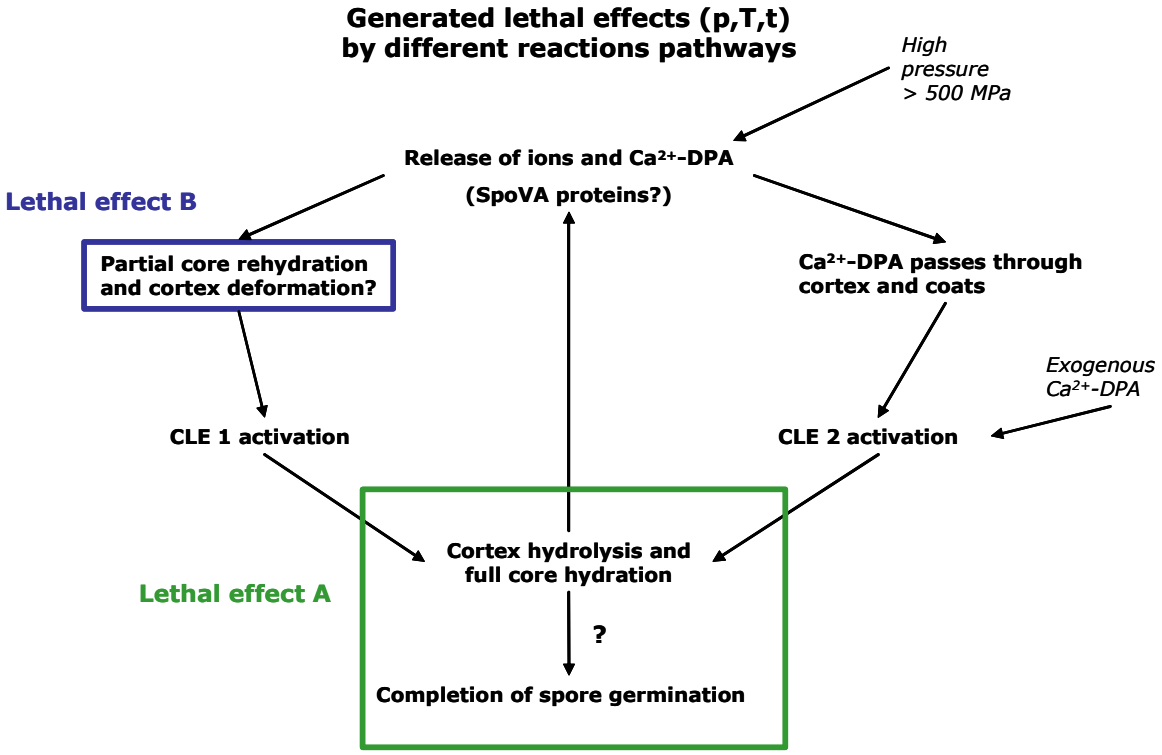

Figure 4.33: Different generated lethal effects by different germination reaction pathways at high pressures over 500 MPa according to Figure 2.21.

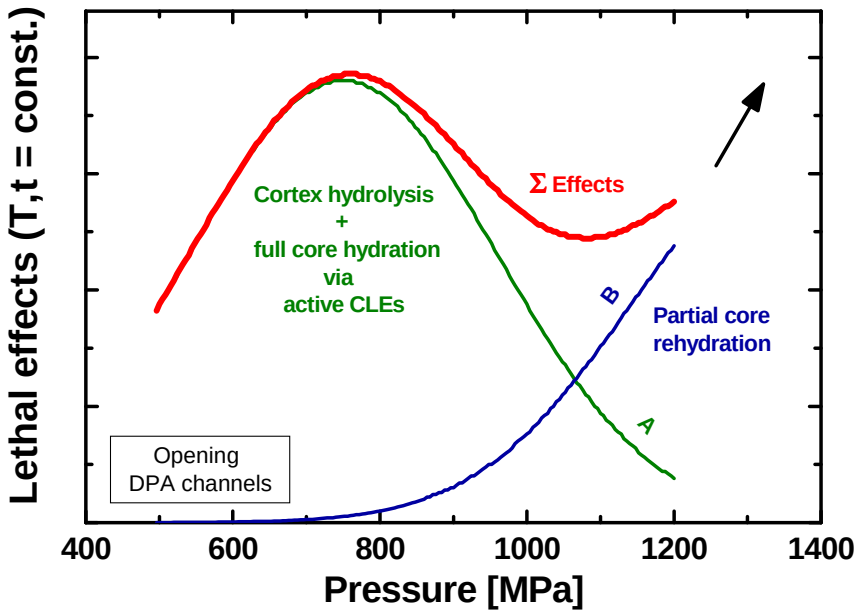

Figure 4.34: Hypothesized summed lethal effects at different pressure levels, constant temperature and constant holding time with different generated lethal effect distributions by different germination reactions (Figure 4.33). At around 500 MPa opening of the DPA channels occured, which enabled high pressure germination reactions. All inactivation effects resulted in the red cumulative distribution (∑ Effects) with a sensitive and stabilized zone.

In Figure 4.33, the lethal effect B during processing is produced by partial core rehydration and consequently higher water content with lowered resistance. The generated lethal effect distribution starts at very high pressures (Figure 4.34) and no CLEs are involved (Figure 4.33). It is assumed that this lethal effect is steadily increased by pressure, because of increased partial core rehydration and process intensity.

In Figure 4.27 both lethal effect distributions (A and B) at different pressure levels, constant temperature and constant holding time are shown. All summarized effects resulted in the red cumulative lethal effect distribution "∑ Effects", with a sensitive and stabilized zone. The produced lethal effects in dependence of pressure could be attributed to the isokineticy line for a 4 $\log_{10}$ reduction at approx. 105 °C with 3 min holding time in Figure 4.27. The cumulative lethal effects (∑ Effects) can be correlated with the applied temperature, where the difference between local maximum and minimum within 600-1200 MPa can be described with 10 K for this case. Furthermore, it can be assumed that at longer holding times the lethal effect due to partial core hydration increased, because of the lower difference between local maximum and minimum within 600-1200 MPa in Figure 4.27.

5. Conclusion and perspective

The mechanistic background of the inactivation of bacterial spores is still a topic of debate (Heinz & Knorr, 2002; Raso & Barbosa-Canovas, 2003; Setlow, 2003). The results of this study showed a significant impact of spore agglomerations on the thermal inactivation, which resulted in a shoulder formation of the survival curves (Figure 4.3). Several authors (Shull et al., 1963; Aiba & Toda, 1966; Abraham et al., 1990) found similar curvilinear parts in the survival curves of *Bacillus* spore suspensions after heat treatment, but there are different hypotheses to explain this phenomenon.

In this study the agglomeration size distribution in suspensions of *G. stearothermophilus* (Merck) spores was determined by using particle size analysis (3D ORM) (Figure 4.2). Thermal inactivation data have been modeled using first-order inactivation kinetics, superimposed by the agglomeration size (Equation 2.47). Since particle size analysis accurately yields the maximum length of an agglomerate, but provides no information on the packing density, two limiting cases have been discriminated in mathematical modeling: three-dimensional, spherical packing for maximum spore count and two-dimensional, circular packing for minimum spore count of a particular agglomerate. Thermal inactivation studies have been carried out in thin glass capillaries, where by using numerical simulations the non-isothermal conditions were modeled (Figure 4.4) and taken into account (Figure 4.7). It is shown that the lag phase often found in thermal spore inactivation (shoulder formation) can sufficiently be described by first-order inactivation kinetics when the agglomeration size is considered (Figure 4.3). The high occurrences of middle sized agglomerates (Figure 4.2) had the major impact on the curvilinear form in this study. Practical experiments are difficult in this context, because of the required defined separation of the agglomerates. Thus, it appears that agglomerations in spore suspensions need to be considered by modeling of the thermal and probably pressure inactivation. At present, no adequate mathematical model for the impact of agglomerations on tailing formations, typically for pressure inactivation, can be found.

It could be shown, that also matrix effects have a strong effect on mechanisms and inactivation studies, for example the dissociation equilibrium shift under high pressure and temperature. This change plays a major role in sensitive reactions e.g. inactivation of microorganisms and denaturation of proteins. Applying the suggested models, these sensitive reactions can be better anticipated in planning experimental designs. This preliminary study offers simple methods for basic assessment of the impact of pK_a-shift by heat-only (Figure 4.8, Figure 4.9) and combined high pressure thermal processing (Figure 4.10, Figure 4.11) with buffer solutions as possible reference. *G. stearothermophilus* spores suspended in ACES and phosphate buffer showed different $\log_{10}$ reductions, possibly because of varied pK_a-shifts (Figure 4.12). By using the Weibullian Power Law, it was possible to model pH-dependent non-linear shoulder and tailing formations with one fundamental equation. This study improves the comparison of spore inactivation data in the literature and offers explanations for possible variations in microbial reduction levels at similar treatment conditions.

For pressure treated spores, but not heat-only treated spores, four distinct populations were detected by flow cytometry (Figure 4.15). PI red fluorescent nucleic acid stain is membrane impermeant, and so was used to identify spores in which the inner cell membrane had been physically compromised. Spores were treated in sodium citrate buffer or in nutrient broth by either, heat-only at 121 °C or high pressure at 150 MPa (37 °C) to study spore germination, or by a combined high pressure and heat treatment at 600 MPa and 77 °C to investigate inactivation (Figure 4.13, Figure 4.14). Quantitative comparisons of spore germination and inactivation by the various treatments, in the two different systems (buffer, broth), were also made following recovery on microbiological media (Figure 4.17). On the basis of the kinetic flow cytometric and plate count discrimination of physiologically heterogeneous sub-populations, a simple model to describe the inactivation of *B. licheniformis* spores by high pressure, with and without heat, was constructed (Equation 4.3-4.6). The three step model of inactivation involving a germination step following hydrolysis of the spore cortex, an unknown step, and finally an inactivation step with physical compromise of the spore's inner membrane presented the time dependent heterogeneous population distribution during the process (Figure 4.16). This study offers a simple and very fast (within 20 min of processing) flow cytometric method for

the rapid assessment of the physiological state of spores following, high pressure, heat-only and combined high pressure and thermal processing. This high throughput method offers substantial benefits in acquiring large data sets, needed to predict and model bacterial spore inactivation by high pressure and heat, and to determine the stochastic nature of this inactivation. Thus great potential remains for research into the application of flow cytometry for the assessment of spore physiological response to various processes, including high pressure thermal processing.

It is well known, that spore inactivation is most successful at pressure levels above 600 MPa. The pressure range of 600 - 1200 MPa was investigated in more detail using an innovative high pressure unit. The equipment design allowed ideal adiabatic processes and isothermal dwell times. Inactivation studies were conducted with a high qualitative (no spore agglomerations), certified biological sterilization indicator (Annex 1). A first-order kinetic model for thermal and pressure inactivation led to a universal p-T diagram (Figure 4.27), delivering all relevant process parameters (p, T, t) for different D-concepts. Spore stabilization at ultra high pressures has been reported by other authors (Ardia, 2004; Margosch et al., 2006; Patazca et al., 2006; Rajan et al., 2006a; Ahn et al., 2007) and was also found in this study. Discrepancy in the stabilization p-T domain may be strain specific. However, this phenomenon requires further research to achieve a better understanding of the underlying mechanism. A plausible explanation was formulated using literature knowledge about the spore germination process in *B. subtilis* spores (Figure 4.33, Figure 4.34). Using the whole generated lethal effects at constant temperature and holding time by different germination reactions (Figure 4.33), it was possible to propose a hypothesized inactivation mechanism for different pressure levels, including a stabilization p-T domain. It was suggested that pressure at constant temperature and holding time can trigger the CLE activities and cause inactivation of the same enzymes. Germination reactions are initiated by opening of the DPA channels at pressures higher 500 MPa. At ultra-high pressure a lethal effect is induced by partial core hydration without any CLE activity. Summarizing all competing reactions as lethal effect, a cumulative lethal effect distribution in dependence of the applied pressure level could be generated (Figure 4.34). There is no doubt that these mechanisms need more clarification, especially the Ca^{2+}DPA release,

the specific CLE activity (p,T) in the spore matrix and the partial core hydration. Acquisition of this information would lead to a better understanding of the spore inactivation mechanism(s) and may improve sterilization concepts at high isostatic pressures.

Industrial relevance

To exemplify the industrial relevance of this study, the data generated of Chapter 4.4 were combined with industrial high pressure sterilization process charts (Figure 5.1 and 5.2). One of the few existing pilot systems is the Flow Pressure Systems QUINTUS (Food Press Type 35L-600) sterilization machine (Avure Technologies, Kent, WA, USA), which is described elsewhere in literature (Knoerzer et al., 2007). Pressure and temperature flow charts from two different processes with (10 L) and without (35 L) a Polytetrafluoroethylene (PTFE) carrier as insulation are shown in Figure 5.1 a and b (location 2 near top closure; Knoerzer et al., 2007). Using an insulating layer in the vessel, temperature decrease and inhomogeneities could be avoided. Alternative possibilities would be the use of a pressure transmitting medium with higher thermal conductivity, application of an internal heater or heating of the vessel wall to an appropriate temperature level which can minimize the temperature gradient (Ardia, 2004). In Figure 5.1 b the target inactivation level of -4 $\log_{10}$ can easily be varied (Table 4.4), because of a first order kinetic approach. Process conditions were 600 MPa final pressure, 90 °C initial temperature, 285 s dwell time and water as pressure transmitting medium (Knoerzer et al., 2007). Both processes are shown in Figure 5.1 a and b. Figure 5.1 b can be directly compared with the presented p-T diagrams of the main thermodynamical parameter in water (Chapter 2.2.2.1). Using the $F_{121.1\ °C}$-value concept (Equation 2.35) in Figure 5.1 c with $T(t)_p$ of the pressure holding times, $z_{600\ MPa}$ = 35.36 °C and $D_{121.1\ °C}$ = 13.52 s at 600 MPa (Annex 5), both processes can be adequately analyzed and compared. The high z-value at 600 MPa leads to a lower temperature dependence of the inactivation level, as normally expected with $z_{0.1\ MPa}$ = 10 °C. Literature data confirmed this fact (Figure 2.22). Because of the pressure dependence of the z-value, pre-heating as well as compression and decompression phase could not been incorporated. These process intensities can be considered as safety factor. Using the PTFE carrier a complete sterilization could be achieved (>12 D).

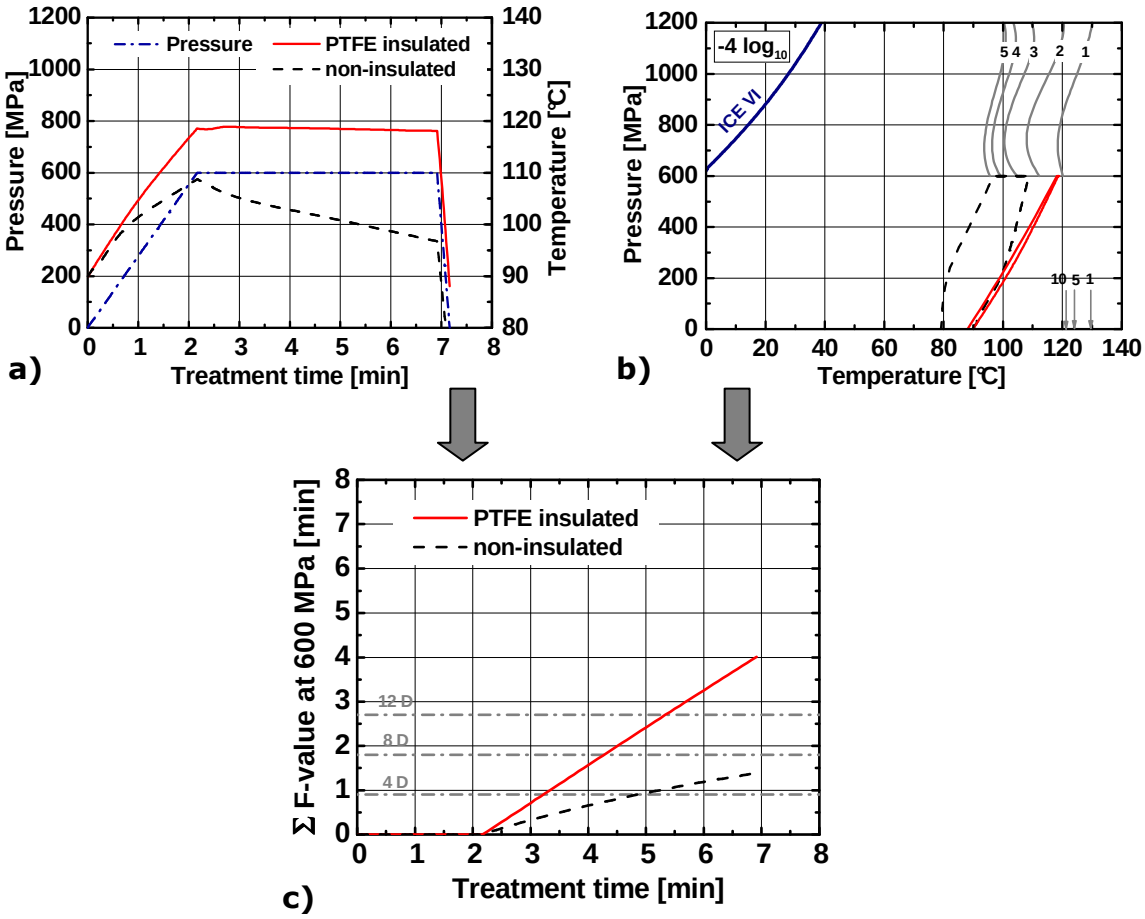

Figure 5.1: Industrial process analysis for a vertical 35 L vessel (--, black) and 10 L insulated volume (-, red) by using the F-value (c) (T_{ref} = 121.1 °C, $z_{600\ MPa}$ = 35.36 °C, $D_{121.1\ °C}$ = 13.52 s at 600 MPa) for pressure holding times $T(t)_p$. Pressure and temperature profiles (a) were taken from literature (Knoerzer et al., 2007). Inactivation profiles, D- and z–values (b) were generated in Chapter 4.4. The target inactivation level can be varied in Figure 5.1b by multiplying the dwell times of the isokineticity lines with the same factor.

An alternative process for a horizontal 55 L vessel (Uhde High Pressure Technologies GmbH, Hagen, Germany) is shown in Figure 5.2. The increase of the pressure level up to 700 MPa improved the sterilization effect (Figure 5.2 b). Temperatures were measured with K-type thermocouples in the non-insulated, water filled vessel (d_i = 200 mm) at the pressure water inlet and opposite plug (Nünnerich, P., 2008, Uhde High Pressure Technologies GmbH, Germany, personal communication). The distance from one thermocouple to the inner plug was 40 mm. Obviously process dwell times can be drastically decreased and a complete sterilization (12 D) can be achieved within 3 min dwell time at 700 MPa without any insulation.

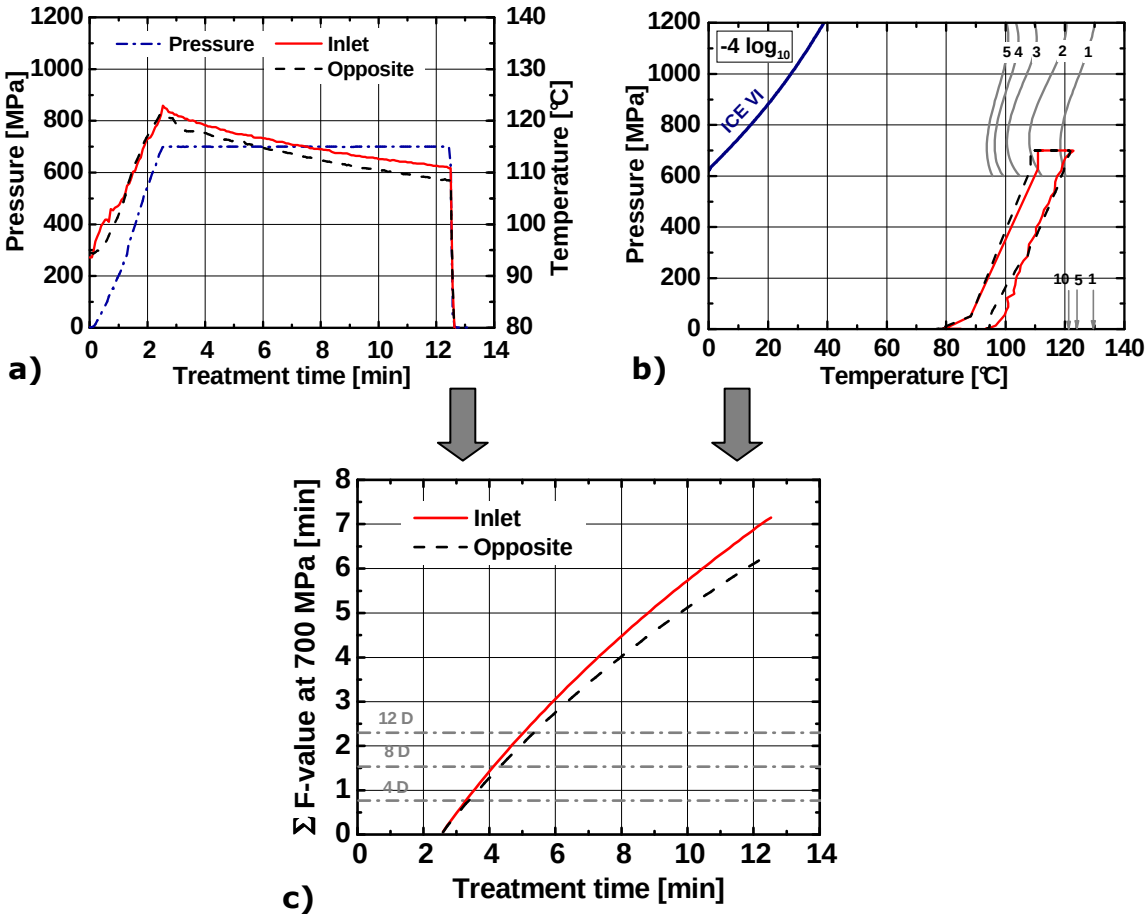

Figure 5.2: Industrial process analysis for a horizontal 55 L vessel by using the F-value (c) (T_{ref} = 121.1 °C, $z_{700\ MPa}$ = 37.45 °C, $D_{121.1\ °C}$ = 11.51 s at 700 MPa) for pressure holding times $T(t)_p$. Pressure and temperature profiles (a) for two different locations (inlet, opposite) were provided by Uhde High Pressure Technologies GmbH (Nünnerich, P., 2008, Germany, personal communication). Inactivation profiles, D- and z–values (b) were generated in Chapter 4.4. The target inactivation level can be varied in Figure 5.2b.

In conclusion, once the pressure and temperature conditions are known, it is possible to calculate the desired inactivation level and ensure the safety margins that are required for sterilized food with 4 D, 8 D or 12 D concepts. For the food industry, detailed inactivation studies with adequate strains in food matrices are necessary to formulate the desired and reproducible sterilization aim. Food safety and consumers health must be ensured in case-by-case studies demonstrating inactivation with realistic contamination levels in the respective food matrix and pilot plant. With an improved understanding of the spore inactivation mechanism it will be possible to assess the benefits of high pressure thermal sterilization with regards microbiological safety and stability.

Annex

Annex 1: Product certification for commercial *G. stearothermophilus* (NAMSA) spores

PRODUCT CERTIFICATION

This lot of product meets, where applicable, the accepted performance criteria specified in the USP and ANSI/AAMI/ISO/EN 11138-1.

LOT S75503 **REF**/Reorder Code: SUS-07
Organism: Geobacillus stearothermophilus
Derived from: ATCC# 7953
Biological Indicators For: Steam
Package contains: One vial (10 mL)

Storage: Refrigerated (2-8°C)
Keep away from high temperature, humidity and sterilants

Disposal:
Autoclave, steam at 121°C for not less than 30 minutes, or incinerate (standard microbial waste; non-pathogenic species)

Purity:
Examination on plate culture medium shows no evidence of contamination with other microorganisms.

Assayed Population (Post heat treatment):
2.4×10^{7} Spores/0.1 mL
2.4×10^{8} Spores/1.0 mL
Approximate size: Not Applicable
D-value: Fraction negative analysis after graded exposures

Steam (121°C)	2.4	minutes
	NA	minutes

Resistance Characteristics	Survival		Kill	
Steam	NS	minutes	NS	minutes
	NA	minutes	NA	minutes

z- value: 7.4 °C (based on 119 °C and 130 °C exposures)

Expiration: 09-05-25(YY-MM-DD)
D-value reproducible only when exposed and cultured under the exact conditions used to obtain results reported here. User should determine the suitability of the biological indicator for their particular use.

ATCC is registered trademark of American Type Culture Collection.
FOR INDUSTRIAL USE ONLY.
NS=Not Supplied
NA=Not Applicable

Annex 2: pH shift in real food systems (T)- Ingredients lists

Milk: Milsani UHT (Sachsenmilch AG, Germany), homogenized, 3.5 % fat, 3.7 % protein, 4.8 % carbohydrates

Pea soup: Maggi pea soup with bacon (Maggie GmbH, Germany), 4.5 % fat, 4.8 % protein, 8.0 % carbohydrates

Baby mashed carrots with maize: (Hipp GmbH & Co Vertriebs KG, Germany), 2.1 % fat, 1.3 % protein, 6.7 % carbohydrates

Herring with tomato sauce: (Produced for Kaiser Tengelmann AG, Germany), 60 % herring filet

Annex 3: Initial pH-value and Weibullian power law parameter (b, n) and R^2 for Figure 4.11

Treatment	Buffer system							
	ACES				Phosphate			
	pH	b	n	R^2	pH	b	n	R^2
114°C	7.9	0.020	1.330	0.99	7.9	0.009	1.528	0.98
	7.0	0.050	1.353	0.97	7.0	0.042	1.241	0.99
	6.0	0.199	1.080	0.99	6.0	0.083	1.136	0.99
	5.0	0.221	1.044	0.99	5.1	0.075	1.176	0.99
122°C	7.9	0.926	1.177	0.98	7.9	0.460	1.534	0.99
	7.1	1.265	1.258	0.99	7.2	0.738	1.274	0.99
	6.1	1.580	1.422	0.99	6.1	1.039	1.314	0.99
	5.1	2.112	0.959	0.99	5.1	1.304	1.053	0.99
127°C	7.9	4.7E-4	2.110	0.99	7.9	2.1E-4	2.265	0.97
	7.0	0.002	1.881	0.99	7.1	8.4E-4	1.974	0.96
	6.0	0.023	1.317	0.99	6.0	0.001	1.973	0.99
	5.1	0.106	0.925	0.99	5.0	2.3E-5	3.015	0.99
500 MPa/80°C	7.6	0.371	0.786	0.98	7.6	0.408	0.797	0.99
	6.9	0.421	0.800	0.99	6.8	1.012	0.526	0.99
	6.0	1.949	0.302	0.99	5.9	2.120	0.302	0.99
	5.5	2.005	0.304	0.98	5.5	2.157	0.339	0.99
600 MPa/80°C	8.0	0.383	0.857	0.99	8.2	0.597	0.731	0.96
	7.3	0.825	0.648	0.99	7.2	1.199	0.548	0.99
	6.0	2.356	0.332	0.99	6.0	2.437	0.331	0.99
	5.2	2.894	0.270	0.99	5.3	2.938	0.278	0.99
900 MPa/80°C	8.1	0.944	1.012	0.99	8.2	1.180	1.022	0.99
	6.9	1.224	1.064	0.99	7.1	1.265	1.057	0.99
	6.0	3.749	0.645	0.99	6.0	4.244	0.729	0.99

Annex 4: Regression analysis and identification of the reaction order n with the standard errors for specific pressure and temperature conditions as well as cumulative standard errors (Σ SD) of all fitted kinetics

p	T	Reaction order n									
[MPa]	[°C]	1	1.05	1.1	1.15	1.2	1.25	1.3	1.35	1.4	1.45
600	90	0.154	0.041	0.203	0.334	0.438	0.52	0.587	0.641	0.685	0.723
600	100	0.885	0.378	0.029	0.249	0.426	0.556	0.662	0.764	0.881	1.02
600	110	0.074	0.108	0.239	0.339	0.415	0.476	0.526	0.572	0.618	0.67
600	120	0.105	0.061	0.157	0.246	0.32	0.384	0.438	0.488	0.535	0.581
700	90	1.002	0.749	0.539	0.374	0.248	0.153	0.087	0.067	0.099	0.151
700	100	0.323	0.132	0.04	0.17	0.278	0.364	0.435	0.494	0.544	0.588
700	110	0.268	0.036	0.185	0.315	0.413	0.493	0.569	0.655	0.758	0.879
700	120	1.228	1.351	1.449	1.529	1.594	1.647	1.691	1.728	1.761	1.789
800	90	0.161	0.249	0.326	0.394	0.452	0.502	0.545	0.582	0.614	0.642
800	100	0.109	0.3	0.461	0.592	0.697	0.781	0.849	0.905	0.952	0.993
800	110	0.793	0.589	0.437	0.328	0.254	0.214	0.214	0.257	0.336	0.441
800	120	1.012	1.218	1.382	1.51	1.612	1.695	1.763	1.821	1.872	1.918
900	90	0.051	0.185	0.301	0.398	0.479	0.545	0.6	0.646	0.685	0.718
900	100	0.18	0.03	0.198	0.337	0.448	0.537	0.609	0.668	0.718	0.762
900	110	0.203	0.043	0.2	0.32	0.41	0.482	0.547	0.614	0.693	0.786
900	120	0.104	0.053	0.136	0.218	0.287	0.347	0.398	0.444	0.487	0.529
1000	90	0.197	0.133	0.074	0.022	0.027	0.068	0.104	0.137	0.165	0.19
1000	100	0.149	0.581	0.897	1.119	1.278	1.393	1.481	1.55	1.61	1.667
1000	110	0.636	0.48	0.341	0.224	0.13	0.062	0.054	0.097	0.143	0.187
1000	120	0.176	0.413	0.609	0.767	0.894	0.996	1.079	1.148	1.206	1.256
1100	90	0.335	0.269	0.208	0.153	0.104	0.061	0.024	0.015	0.042	0.067
1100	100	0.576	0.403	0.264	0.155	0.073	0.028	0.061	0.103	0.142	0.179
1100	110	0.406	0.19	0.027	0.14	0.252	0.342	0.415	0.475	0.529	0.579
1100	120	0.828	0.624	0.451	0.314	0.214	0.158	0.158	0.203	0.27	0.35
1200	90	0.459	0.485	0.508	0.53	0.55	0.568	0.585	0.601	0.615	0.628
1200	100	0.542	0.558	0.613	0.682	0.752	0.817	0.875	0.925	0.97	1.009
1200	110	0.316	0.238	0.198	0.208	0.251	0.307	0.364	0.419	0.469	0.515
1200	120	0.167	0.23	0.289	0.342	0.39	0.432	0.469	0.503	0.532	0.559
1200	130	0.5	0.521	0.541	0.558	0.575	0.59	0.604	0.617	0.629	0.64
Σ SD		11.939	10.648	11.302	12.867	14.261	15.518	16.793	18.139	19.56	21.016

Annex 5: Regression parameter and analysis for k(p,T) (Equation 3.4) in Figure 4.26 (n = 1). The D-value is the reciprocal of k(p,T) multiplied with 2.303 (Equation 2.36).

R^2=0.967, SD=0.190

Parameter	Value	SD
a	-89.9464804	32.39204626
b	-0.0093422	0.028560231
c	2.371466922	0.957748667
d	-4.25E-05	1.99E-05
e	-0.02490089	0.009652633
f	0.000897748	0.000377277
g	1.64E-08	6.46E-09
h	8.70E-05	3.25E-05
i	-3.94E-06	1.66E-06
j	-3.53E-08	9.16E-08

Annex 6: Regression parameter and analysis for k´(p,T) (Equation 3.4) in Figure 4.29 B (n = 1.05)

R^2=0.962, SD=0.208

Parameter	Value	SD
a	-96.7118043	35.51455199
b	-0.02396237	0.03131336
c	2.656534356	1.050073051
d	-2.92E-05	2.18E-05
e	-0.02741843	0.010583121
f	0.000945484	0.000413646
g	1.25E-08	7.09E-09
h	9.33E-05	3.56E-05
i	-3.87E-06	1.82E-06
j	-6.52E-08	1.00E-07

Annex 7: Regression parameter and analysis for $\log_{10}$ [N(1 s)/N_0] in dependence of pressure and temperature in Figure 4.29 A modeled with Equation 3.4, where ln(k) was replaced with $\log_{10}$ [N(1 s)/N_0]

R^2=0.782, SD=0.394

Parameter	Value	SD
a	3.011042264	67.22493811
b	-0.04543868	0.059272569
c	0.192481264	1.987666799
d	7.79E-05	4.1269e-05
e	0.001212225	0.020032623
f	-0.00049084	0.000782983
g	-3.95E-08	1.3414e-08
h	-6.56E-06	6.7449e-05
i	-4.66E-07	3.44981e-06
j	3.15E-07	1.90076e-07

Curriculum vitae and publication list

Alexander Mathys

Ph.D. Student, M.Eng Food Engineering

Address:

Technische Universität Berlin

Department of Food Biotechnology and
Food Process Engineering
Koenigin – Luise – Str. 22
14195 Berlin
Germany
Phone: +49 30 314 71248
Fax: +49 30 832 76 63
email: alexander.mathys@tu-berlin.de

Alexander Mathys

Wichertstrasse 41
10439 Berlin
Germany

Phone: +49 30 231 85969
Mobile: +49 179 148 0150
email: a.mathys@gmx.de

Biography

02/2006 – 07/2006: Visiting Researcher, CSIRO, Food Science Australia, P.O. Box 93, North Ryde 1670, NSW, Australia.

Since 01/2005 Ph.D. student at Berlin University of Technology, Prof. D. Knorr,

Thesis: Inactivation mechanisms of *Geobacillus* and *Bacillus* spores during high pressure thermal sterilization.

09/2004 M.Eng. (Dipl.-Ing.) Food Technology, Berlin University of Technology

Thesis: Influence of the membrane permeabilization of *L.bulgaricus* after freezing and thawing as measured by electro-optical and flow cytometry methods.

1998-2004 Studies of Food Technology at Berlin University of Technology

Date of birth June, 1st, 1979, Stralsund, Germany

Fields of interest

- High pressure processing
- Bacterial spores
- Modeling of kinetics and thermodynamic relationships/ parameters
- Development of high pressure units
- Biophysical and physiological analysis of microorganisms (e.g. FPIA, Coulter Counter, Flow cytometry)
- Fermentation of microorganisms

Eidesstattliche Erklärung

Ich erkläre an Eides Statt, daß die vorliegende Dissertation in allen Teilen von mir selbständig angefertigt wurde und die benutzten Hilfsmittel vollständig angegeben worden sind.

Weiter erkläre ich, daß ich nicht schon anderweitig einmal die Promotionsabsicht angemeldet oder ein Promotionseröffnungsverfahren beantragt habe.

Veröffentlichungen von irgendwelchen Teilen der vorliegenden Dissertation sind von mir wie folgt vorgenommen worden.

Berlin, 19.05.2008

Alexander Mathys

Peer-reviewed primary publications:

1. **Isbarn, S., Buckow, R., Mathys, A., Heinz, V., Knorr D. & Lehmacher, A. (in preparation).** Rotavirus inactivation by high pressure processing. *Applied and Environmental Microbiology*.
2. **Knorr D. and Mathys A. (accepted)**. High hydrostatic pressure. In: R. H. Stadler & D. Lineback. *Process-induced food toxicants and health risks*. John Wiley & Sons, Inc., New Jersey.
3. **Reineke K., Mathys A., Heinz V. & Knorr D. (accepted).** Temperature control for high pressure processes up to 1400 MPa. Journal of Physics: Conference Series.
4. **Mathys A., Heinz V. & Knorr D. (accepted).** New pressure and temperature effects on bacterial spores. Journal of Physics: Conference Series.
5. **Knorr D. & Mathys A. (accepted).** Ultra high pressure technology for innovative food processing. *Chemie Ingenieur Technik* (in German), Special Issue dedicated to Prof. Dr.-Ing. H. G. Kessler, in memoriam.
6. **Mathys, A., Kallmeyer, R., Heinz, V. & Knorr D. (2008).** Impact of dissociation equilibrium shift on bacterial spore inactivation by heat and pressure. *Food Control*, doi:10.1016/j.foodcont.2008.01.003.
7. **Mathys, A., Reineke K., Heinz, V. & Knorr D. (2008).** Gentle sterilization of food by high pressure treatment (in German). *Lebensmitteltechnik* 4/08, 68-69.
8. **Mathys, A., Chapman, B., Bull, M., Heinz, V. & Knorr D. (2007).** Flow cytometric assessment of *Bacillus* spore response to high pressure and heat. *Innovative Food Science & Emerging Technologies,* 8(4), 519-530.
9. **Mathys, A., Heinz, V., Schwartz, F. H. & Knorr D. (2007).** Impact of Agglomeration on the quantitative assessment of *Bacillus stearothermophilus* heat inactivation. *Journal of Food Engineering*, 81(2), 380-387.
10. **Toepfl, S., Mathys, A., Heinz, V. & Knorr D. (2006).** Review: Potential of emerging technologies for energy efficient and environmentally friendly food processing. *Food Review International*, 22(4), 405-423.

Other publications:

11. **Mathys A., Heinz V. & Knorr D. (2007**). High pressure assisted sterilization processes- Basics, mechanisms and challenges. *Chemie Ingenieur Technik* (in German) 79(9), 1422.
12. **Reineke K., Mathys A., Heinz V. & Knorr D. (2007).** Temperature control for high pressure processes up to 1400 MPa for gentile food sterilization. In: Proceedings (in German) of *GDL Congress "Food Technology 2007"*, VDI Verlag.
13. **Wiezorek T., Mathys A., Angersbach A. & Knorr D. (2007).** Flow Picture Image Analysis (FPIA) of *Lactobacillus plantarum* cell length changes during fermentation. In: Proceedings (in German) of *GDL Congress "Food Technology 2007"*, VDI Verlag.
14. **Mathys A., Heinz V. & Knorr D. (2007**). Food Sterilization under pressure- Fundamentals, new insights and challenges. In: Proceedings of *LMC International Conference "Innovations in Food Technology"* 2007.
15. **Mathys A., Schwartz, F.H., Heinz V. & Knorr D. (2007).** Agglomerations in bacterial spore suspensions. In: Proceedings of *Partec International Congress on Particle Technology* 2007.
16. **Mathys A., Heinz V. & Knorr D. (2006).** Influences on quantitative assessment of heat and pressure spore inactivation. In: Proceedings of the *Food is Life International Conference* 2006.
17. **Mathys A., Heinz V., Schwartz F. H. & Knorr D. (2006).** Agglomerations in *G. stearothermophilus* spore suspensions- Impact on thermal inactivation. In: Proceedings of *Food Factory of the Future International* Conference 2006.
18. **Mathys A., Buckow, R., Heinz V., & Knorr D. (2006).** New Model for the pH-value in buffer systems up to 1000 MPa. In: Proceedings of *3rd International Meeting on High Pressure Engineering* 2006.

19. **Mathys A., Heinz V. & Knorr D. (2006).** Modeling of the pH-value in buffer systems up to 1000 MPa In: Proceedings of *Future of Food Engineering International* Conference 2006, CIGR Section VI.
20. **Mathys A., Heinz V. & Knorr D. (2005).** Theoretical calculation of the pH-values in buffers under high pressure. In: Proceedings of *IntradFood* - EFFoST *International* Conference 2005, Elsevier, London. 329-332.
21. **Mathys A., Heinz V. & Knorr D. (2005).** Calculation of the pH-value in buffer systems under pressure In: Proceedings (in German) of *GDL Congress "Food Technology 2005"*, VDI Verlag.

Presentations

Selected oral presentations at scientific meetings:

1. **Mathys A., Heinz V. & Knorr D. (2008**). High pressure sterilization- State of the art. Oral presentation at 4th *CEFood International Conference*, Cavtat, Croatia.
2. **Mathys A., Heinz V. & Knorr D. (2008**). Development of high pressure sterilization concepts based on mechanistic inactivation studies of bacterial spores. Oral presentation at *10th International Congress on Engineering and Food (ICEF 10)*, Vina del Mar, Chile.
3. **Mathys A., Heinz V. & Knorr D. (2008).** Sterilization under high pressure- New mechanistic inactivation studies and adiabatic process concepts. Oral presentation (in German) at *ProcessNet FA Sitzung "Lebensmittelverfahrenstechnik 2008"*, Weihenstephan, Germany.
4. **Reineke K., Mathys A., Heinz V. & Knorr D. (2008).** Sterilization under high pressure- New mechanistic inactivation studies and adiabatic process concepts. Oral presentation (in German) at *ProcessNet FA Sitzung "Lebensmittelverfahrenstechnik 2008"*, Weihenstephan, Germany.
5. **Mathys A., Heinz V. & Knorr D. (2007).** Temperature control for ideal adiabatic and isothermal process conditions in micro high pressure vessels. Oral presentation (in German) at *ProcessNet Congress "Jahrestagung 2007"*, Aachen, Germany.
6. **Mathys A., Heinz V. & Knorr D. (2007**). Food Sterilization under pressure- Fundamentals, new insights and challenges. Oral presentation at *LMC International Conference "Innovations in Food Technology"* Copenhagen, Denmark.
7. **Wiezorek T., Mathys A., Angersbach A. & Knorr D. (2007).** Flow Picture Image Analysis (FPIA) of *Lactobacillus plantarum* cell length changes during fermentation. Oral presentation (in German) at *GDL Congress "Food Technology 2007"*, Hamburg, Germany.
8. **Reineke K., Mathys A., Heinz V. & Knorr D. (2007).** Temperature control for high pressure processes up to 1400 MPa for gentile food sterilization. Oral presentation (in German) at *GDL Congress "Food Technology 2007"*, Hamburg, Germany.
9. **Mathys A., Heinz V. & Knorr D. (2007).** New pressure and temperature effects on bacterial spores. Oral presentation at *21st AIRAPT and 45th EHPRG International Conference on High Pressure Science and Technology* 2007, Catania, Italy.
10. **Knorr D. & Mathys A. (2007).** Pressure assisted thermal sterilization: Current state of the art. Oral presentation at *IFT Annual Meeting* 2007, Chicago, IL, USA.
11. **Mathys A., Heinz V. & Knorr D. (2007).** Pressure and temperature effects on bacterial spores- New insights and mechanisms. Oral presentation at *IFT Annual Meeting* 2007, Chicago, IL, USA.
12. **Mathys A., Heinz V. & Knorr D. (2007).** Agglomerations in bacterial spore suspensions. Oral presentation at *Partec International Congress on Particle Technology* 2007, Nuernberg, Germany.
13. **Mathys A., Heinz V. & Knorr D. (2007).** Sterilization under pressure- Basics and challenges. Oral presentation (in German) at *ProcessNet FA-Sitzung: „Hochdruckverfahrenstechnik" und „Mehrphasenströmmung"*, Baden-Baden, Germany.

14. **Mathys A., Chapman B., Bull M., Heinz V. & Knorr D. (2006).** Measuring the effect of high pressure thermal processing on bacterial spores. Oral presentation at *Third Innovative Food Centre Conference* 2006, Melbourne, Australia.
15. **Mathys A., Heinz V. & Knorr D. (2006).** pH-value in water and buffer systems under adiabatic conditions up to 1000 MPa. Oral presentation at the Fourth International Conference on *High Pressure Bioscience and Biotechnology* 2006, Tsukuba, Japan.
16. **Mathys A., Heinz V., Schwartz F. H. & Knorr D. (2006).** Agglomerations in *G. stearothermophilus* spore suspensions- Impact on thermal inactivation. Oral presentation at *Food Factory of the Future* Conference 2006, Gothenburg, Sweden.
17. **Mathys A., Heinz V. & Knorr D. (2006).** Modeling of the pH-value in buffer systems up to 1000 MPa Oral presentation at *Future of Food Engineering* Conference 2006, CIGR Section VI, Warsaw, Poland.
18. **Mathys A., Heinz V. & Knorr D. (2005).** Calculation of the pH-value in buffer systems under pressure. Oral presentation (in German) at *GDL Congress "Food Technology 2005*", Dresden, Germany.

Selected poster presentations at scientific meetings:

19. **Wiezorek T., Mathys A., Angersbach A. & Knorr D. (2008).** Flow Picture Image Analysis (FPIA) of *Lactobacillus plantarum* cell length changes for online fermentation control (in German) at *ProcessNet FA Sitzung "Lebensmittelverfahrenstechnik 2008*", Weihenstephan, Germany.
20. **Mathys A., Heinz V. & Knorr D. (2008).** Mechanistic inactivation studies of bacterial spores under pressure and temperature. Poster presentation at *Nonthermal Processing Division Meeting and Workshop* 2008, Portland, OR, USA.
21. **Mathys A., Heinz V. & Knorr D. (2007).** Pressure assisted thermal sterilization- Basics and challenges. Poster presentation at *EFFoST and EHEDG Joint International Conference "Food- New options for the industry"* 2007, Lisbon, Portugal.
22. **Reineke K., Mathys A., Heinz V. & Knorr D. (2007).** New sterilization concept under high pressure. Poster presentation at *EFFoST and EHEDG Joint International Conference "Food- New options for the industry"* 2007, Lisbon, Portugal.
23. **Reineke K., Mathys A., Heinz V. & Knorr D. (2007).** Temperature control for high pressure processes up to 1400 MPa. Poster presentation at *21st AIRAPT and* 45th *EHPRG International Conference on High Pressure Science and Technology* 2007, Catania, Italy.
24. **Mathys A., Heinz V. & Knorr D. (2007).** Sterilization processes under high pressure- Effects and mechanisms. Poster presentation (in German) at *ProcessNet FA-Sitzung: „Lebensmittelverfahrenstechnik*" 2007, Zurich, Switzerland.
25. **Mathys A., Heinz V. & Knorr D. (2006).** Influences on quantitative assessment of heat and pressure spore inactivation. Poster presentation at *Food is Life International Conference* 2006, Nantes, France.
26. **Mathys A., Buckow, R., Heinz V. & Knorr D. (2006).** New Model for the pH-value in buffer systems up to 1000 MPa. Poster presentation at *3rd International Meeting on High Pressure Engineering* 2006, Erlangen, Germany.
27. **Mathys A., Heinz V. & Knorr D. (2006).** Influences on high pressure sterilization processes. Poster presentation at *44th EHPRG International Conference* 2006, Prague, Czech Republic.
28. **Mathys A., Heinz V. & Knorr D. (2005).** pH-value in buffers under high pressure. Poster presentation at *Nonthermal Processing Division Meeting and Workshop* 2005, Wyndmoor PA, USA.
29. **Mathys A., Heinz V. & Knorr D. (2005).** Theoretical calculation of the pH-values in buffers under high pressure. Poster presentation at *IntradFood – EFFoST International Conference* 2005, Valencia, Spain.

Honors

1. Winner of the ICEF 10 (International Congress on Engineering and Food) Award for Young Food Engineers 2008 at the ICEF 10 congress in Vina del Mar, Chile (2000 USD).
2. Candidate for Germany at the Second European Workshop on Food Engineering and Technology (EFCE) 2008 in Paris, France.
3. Finalist for the George F. Stewart IFT International Research Paper Competition 2007 in Chicago, USA.

References

Abraham, G., Debray, E., Candau, Y. & Piar, G. (1990). Mathematical model of thermal destruction of *Bacillus stearothermophilus* spores. *Applied and Environmental Microbiology*, *56*(10), 3073-3080.

Ahn, J., Balasubramaniam, V. M. & Yousef, A. E. (2007). Inactivation kinetics of selected aerobic and anaerobic bacterial spores by pressure-assisted thermal processing. *International Journal of Food Microbiology*, *113*(3), 321-329.

Aiba, S. & Toda, K. (1966). Some analysis of thermal inactivation of bacterial-spore clump. *Journal of Fermentation Technology*, *44*, 301-304.

Alderton, G., Ito, K. A. & Chen, J. K. (1976). Chemical manipulation of the heat resistance of *Clostridium botulinum* spores. *Applied and Environment Microbiology*, *31*(4), 492-498.

Alper, T., Gillies, N. E. & Elkind, M. M. (1960). The sigmoid survival curve in radiobiology. *Nature*, *186*, 1062-1063.

Alsaad, M., Bair, S., Sanborn, D. M. & Winer, W. O. (1978). Glass transitions in lubricants: its relation to EHD lubrication. *Trans ASME, Journal of Lubrication Technology*, *100*, 404-417.

Ananta, E., Heinz, V., Schlüter, O. & Knorr, D. (2001). Kinetic studies on high-pressure inactivation of *Bacillus stearothermophilus* spores suspended in food matrices. *Innovative Food Science & Energing Technologies*, *2*, 261-272.

Anderson, W. A., McClure, P. J., Baird-Parker, A. C. & Cole, M. B. (1996). The application of a log-logistic model to describe the thermal inactivation of *Clostridium botulinum* 213B at temperatures below 121.1°C. *Journal of Applied Bacteriology*, *80*, 283-290.

Aoyama, Y., Shigeta, Y., Okazaki, T., Hagura, Y. & Suzuki, K. (2005a). Non-thermal inactivation of *Bacillus* spores by pressure-holding. *Food Science and Technology Research*, *11*(3), 324-327.

Aoyama, Y., Shigeta, Y., Okazaki, T., Hagura, Y. & Suzuki, K. (2005b). Germination and inactivation of *Bacillus subtilis* spores under combined conditions of hydrostatic pressure and medium temperature. *Food Science and Technology Research*, *11*(1), 101-105.

Arabas, J., Szczepek, J., Dmowki, L., Heinz, V. & Fonberg-Broczek, M. (1999). New technique for kinetic studies of pressure-temperature induced changes of biological materials. In H. Ludwig. *Advances in high pressure bioscience and biotechnology* (pp. 537-540). Springer, Berlin.

Ardia, A. (2004). *Process considerations on the application of high pressure treatment at elevated temperature levels for food preservation*. Ph.D thesis, Berlin, Berlin University of Technology, 94.

Ardia, A., Knorr, D., Ferrari, G. & Heinz, V. (2004a). Kinetic studies on combined high-pressure and temperature inactivation of *Alicyclobacillus acidoterrestris* spores in orange juice. *Applied Biotechnology, Food Science and Policy*, *1*(3), 169-173.

Ardia, A., Knorr, D. & Heinz, V. (2004b). Adiabatic heat modelling for pressure build-up during high-pressure treatment in liquid-food processing. *Food and Bioproducts Processing*, *82*(C1), 89-95.

Arrhenius, S. A. (1889). Über die Reaktionsgeschwindigkeit bei der Inversion von Rohrzucker durch Säuren. *Zeitschrift für physikalische Chemie*, *4*, 226-248.

Arroyo, G., Sanz, P. D. & Prestamo, G. (1997). Effect of high pressure on the reduction of microbial populations in vegetables. *Journal of Applied Microbiology*, *82*(6), 735-742.

ASME (1953). *Viscosity and density of over 40 lubricating fluids of known composition at pressures to 150000 psi and temperatures to 425 °F*. American Society of Mechanical Engineers, New York.

Balasubramanian, S. & Balasubramaniam, V. M. (2003). Compression heating influence of pressure transmitting fluids on bacteria inactivation during high pressure processing. *Food Research International*, *36*(7), 661-668.

Ball, C. O. (1923). Thermal process time for canned foods. *Bulletin of the National research council*, *7*(37), 76.

Barák, I. (2004). Sporulation in *Bacillus subtilis* and other bacteria. In A. E. Ricca & a. S. M. C. O. Henriques. *Bacterial spore formers: probiotics and emerging applications* (pp.). Horizon Bioscience, Wymondham, Norfolk UK.

Basset, J. & Macheboeuf, M. A. (1932). Etudes sur les effects biologiques des ultrapressions: resistance des bacteries, des diastases et des toxines aux pressions tres elevees. *Comptes Rendus de l'Academie des Sciences*, *195*, 1431-1433.

Belguendouz, T., Cachon, R. & Divie`s, C. (1997). pH homeostasis and citric acid utilization: differences between *Leuconostoc mesenteroides* and *Lactococcus lactis*. *Current Microbiology*, *35*, 233–236.

Bender, G. R. & Marquis, R. E. (1982). Sensitivity of various salt forms of *Bacillus megaterium* spores to the germinating action of hydrostatic pressure. *Canadian Journal of Microbiology*, *28*, 643-649.

Bender, M. A. & Gooch, P. C. (1962). The kinetics of X-ray survival of mammalian cells in vitro. *International Journal of Radiation Biology*, *5*, 133-145.

BfR (2001). Rare but dangerous: food poisoning from *Clostridium botulinum*. *Federal Institute for Risk Assessment*, *25/2001, 10.09.2001*.

Black, E. P., Koziol-Dube, K., Guan, D., et al. (2005). Factors influencing germination of *Bacillus subtilis* spores via activation of nutrient receptors by high pressure. *Applied and Environmental Microbiology*, *71*(10), 5879-5887.

Black, E. P., Huppertz, T., Kelly, A. L. & Fitzgerald, G. F. (2007a). Baroprotection of vegetative bacteria by milk constituents: a study of *Listeria innocua*. *International Dairy Journal*, *17*, 104–10.

Black, E. P., Setlow, P., Hocking, A. D., Stewart, C. M., Kelly, A. L. & Hoover, D. G. (2007b). Response of Spores to High-Pressure Processing. *Comprehensive Reviews in Food Science and Food Safety*, *6*, 103-119.

Black, E. P., Wei, J., Atluri, S., et al. (2007c). Analysis of factors influencing the rate of germination of spores of *Bacillus subtilis* by very high pressure. *Journal of Applied Microbiology*, *102*, 65–76.

Bridgman, P. W. (1911). Water in the liquid and five solid forms, under pressure. *Proc. Amer. Acad. of Arts and Sciences*, *47*, 441-558.

Bridgman, P. W. (1912). Water in the liquid and five solid forms under pressure. *Proc. Amer. Acad. of Arts and Sciences*, *47*(13), 439-558.

Bruins, M. E., Matser, A. M., Janssen, A. E. M. & Boom, R. M. (2007). Buffer selection for HP treatment of biomaterials and its consequences for enzyme inactivation studies. *High Pressure Research*, *27*(1), 101-107.

Bueltermann, R. (1997). *Untersuchungen zur Hitzeresistenz von Bakteriensporen und zum Pasteurisieren von oberflächlich verkeimten Lebensmitteln*. PhD thesis, Karlsruhe, University of Karlsruhe, 149.

Bunthof, C. J. (2002). *Flow cytometry, fluorescent probes, and flashing bacteria*. PhD thesis, Wageningen, The Netherlands, Wageningen University, 160.

Butz, P., Ries, J., Traugott, U., Weber, H. & Ludwig, H. (1990). Hochdruckinaktivierung von Bakterien und Bakteriensporen. *Die Pharmazeutische Industrie*, *52*, 487-491.

Cameron, M. S., Leonard, S. J. & Barrett, E. L. (1980). Effect of moderately acidic pH on heat resistance of *Clostridium sporogenes* spores in phosphate buffer and in buffered pea puree. *Applied and Environmental Microbiology*, *39*(5), 943-949.

Cano, R. J. & Borucki, M. K. (1995). Revival and identification of bacterial spores in 25- to 40-million-year-old Dominican amber. *Science*, *1060-1064*(5213), 1060-1064.

Capellas, M., Mor-Mur, M., Gervilla, R., Yuste, J. & Guamis, B. (2000). Effect of high pressure combined with mild heat or nisin on inoculated bacteria and mesophiles of goat's milk fresh cheese. *Food Microbiology*, *17*, 633-641.

Casolari, A. (1994). About basic parameters of food sterilization technology. *Food Microbiology*, *11*, 75-84.

Cazemier, A. E., Wagenaars, S. F. M. & ter Steeg, P. F. (2001). Effect of sporulation and recovery medium on the heat resistance and amount of injury of spores from spoilage bacilli. *Journal of Applied Microbiology*, *90*(5), 761-770.

Cerf, O. (1977). Tailing of survival curves of bacterial spores. *Journal of Applied Bacteriology*, *42*, 1-19.

Certes, A. (1884). Sur la culture, a l'abri des germes atmospheriques, des eaux et des sediments rapportes par les expeditions du "Travailleur" du "Talisman"; 1882-1883. *Comptes Rendus de l'Academie des Sciences*, *98*, 690-693.

Cheftel, J. C. (1992). Effects of high hydrostatic pressure on food constituents: An overview. In C. Balny, R. Hayashi, K. Heremans & P. Masson. *High Pressure and Biotechnology* (pp. 195-209). John Libbey Eurotext, Montrouge.

Chick, H. (1910). The process of disinfection by chemical agencies and hot water. *Journal of Hygiene*, *10*, 237-286.

Chlopin, G. W. & Tammann, G. (1903). Über den Einfluß hoher Drücke auf Mikroorganismen. *Zeitschrift für Hygiene und Infektionskrankheiten*, *45*, 171-204.

Clery-Barraud, C., Gaubert, A., Masson, P. & Vidal, D. (2004). Combined Effects of High Hydrostatic Pressure and Temperature for Inactivation of Bacillus anthracis Spores. *Applied and Environment Microbiology*, *70*(1), 635–637.

Clouston, J. G. & Wills, P. A. (1969). Initiation of germination and inactivation of *Bacillus pumilus* spores by hydrostatic pressure. *Journal of Bacteriology*, *97*(2), 684-690.

Clouston, J. G. & Wills, P. A. (1970). Kinetics of initiation of germination of *Bacillus pumilis* spores by hydrostatic pressure. *Journal of Bacteriology*, *109*, 550-559.

Cohn, F. (1872). Untersuchungen über Bakterien. In M. Müller. *Beiträge zur Biologie der Pflanzen 1, 1875 (Heft 1)* (pp. 127-224). J. U. Kern's Verlag, Breslau.

Comas-Riu, J. & Vives-Rego, J. (2002). Cytometric monitoring of growth, sporogenesis and spore cell sorting in *Paenibacillus polymyxa* (formerly *Bacillus polymyxa*). *Journal of Applied Microbiology*, *92*(3), 475-481.

Cowan, A. E., Koppel, D. E., Setlow, B. & Setlow, P. (2003). A soluble protein is immobile in dormant spores of *Bacillus subtilis* but is mobile in germinated spores: Implications for spore dormancy. *Proceedings of the National Academy of Sciences*, *100*, 4209–4214.

Craven, S. E. & Blankenship, L. C. (1987). Changes in the hydrophobic characteristics of *Clostridium perfringens* spores and spore coats by heat. *Canadian Journal of Microbiology*, *33*, 773-776.

Crawford, Y. J., Murano, E. A., Olson, D. G. & Shenoy, K. (1996). Use of high hydrostatic pressure and irradiation to eliminate *Clostridium sporogenes* in chicken breast. *Journal of Food Protection*, *59*(7), 711-715.

Cronin, U. P. & Wilkinson, M. G. (2007). The use of flow cytometry to study the germination of *Bacillus cereus* endospores. *Cytometry Part A*, *71A*(3), 143-153.

Crossland, B. (1995). The development of high pressure equipment. In D. A. Ledward, D. A. Johnston, R. G. Earnshaw & A. P. M. Hasting. *High Pressure Processing of Foods* (pp. 7-26). Nottingham University Press, Nottingham.

Curran, H. R. & Evans, F. R. (1945). Heat activation inducing germination in the spores of thermotolerant and thermophilic aerobic bacteria. *Journal of Bacteriology*, *49*(4), 335-346.

Dannenberg, F. (1986). *Zur Reaktionskinetik der Molkenproteindenaturierung und deren technologischer Bedeutung*. thesis, München, TU München- Weihenstephan, PhD thesis.

David, J. & Merson, R. L. (1990). Kinetic parameters for inactivation of *Bacillus stearothermophilus* at high temperatures. *Journal of Food Science*, *55*(2), 488-93.

De Heij, W., Van Schepdael, L., Van den Berg, R. & Bartels, P. (2002). Increasing preservation efficiency and product quality through control of temperature profiles in high pressure applications. *High Pressure Research*, *22*(3-4), 653 -657.

De Heij, W., Van den Berg, R. W., Van Schepdael, L., Hoogland, H. & Bijmolt, H. (2005). Sterilization-only better. *New Food*, (2), 56-61.

De Heij, W. B. C., Van Schepdael, L. J. M. M., Moezelaar, R., Hoogland, H., Matser, A. M. & Van den Berg, R. W. (2003). High-pressure sterilization: maximizing the benefits of adiabatic heating. *Food Technology*, *57*(3), 37-42.

De Vries, Y. P. (2006). *Bacillus cereus spore formation, structure, and germination*. PhD thesis, Wageningen, Wageningen University.

Debye, P. & Hueckel, E. (1923). Zur Theorie der Elektrolyte. I. *Physikalische Zeitschrift*, *24*, 185-206.

Distèche, A. (1959). pH Measurements with a Glass Electrode Withstanding 1500 kg/cm^2 Hydrostatic Pressure. *Review of Scientific Instruments*, *30*(6), 474-478.

Douki, T., Setlow, B. & Setlow, P. (2005). Photosensitization of DNA by dipicolinic acid, a major component of spores of *Bacillus* species. *Photochemical & Photobiological Sciences*, *4*, 591 - 597.

Doyle, R. J., Nedjat-Haiem, F. & Singh, J. S. (1984). Hydrophobic characteristics of *Bacillus* spores. *Current Microbiology*, *10*, 329-332.

Drude, P. & Nernst, W. (1894). Über Elektrostriktion durch freie Ionen. *Zeitschrift für Physikalische Chemie*, *15*(79).

DSMZ (2008). www. dsmz.de (download 13.02.2008).

Earnshaw, R. G., Appleyard, J. & Hurst, R. M. (1995). Understanding physical inactivation processes: combined preservation opportunities using heat, ultrasound and pressure. *International Journal of Food Microbiology*, *28*, 197-219.

Eklund, T. (1989). Organic acids and esters. In G. W. Gould. *Mechanisms of Action of Food Preservation Procedures* (pp. 161– 200). Elsevier Applied Science, London.

Errington, J. (2003). Regulation of endospore formation in *Bacillus subtilis*. *Nature Reviews Microbiology*, *1*, 117-126.

Esty, J. R. & Meyer, K. F. (1922). The heat resistance of the spores of *B. Botulinus* and allied anaerobes. *Journal of Infectious Diseases*, *31*, 650-663.

Eyring, H. (1935a). The activated complex in chemical reactions. *Journal of Chemical Physics*, *3*, 107-115.

Eyring, H. (1935b). The activated complex and the absolute rate of chemical reactions. *Chemical Reviews*, *17*, 65-77.

Fairhead, H., Setlow, B. & Setlow, P. (1993). Prevention of DNA damage in spores and in vitro by small, acid-soluble proteins from *Bacillus* species. *Journal of Bacteriology*, *175*, 1367-1374.

Farid, M. M. (2006). *Pressure assisted thermal sterilisation or pasteurisation method and apparatus*. New Zealand, patent, (PCT/NZ/2006/000069), AUCKLAND UNISERVICES LTD.

Farkas, J., Andrássy, É., Simon, A. & Mészáros, L. (2003). Effects of Pasteurizing Levels of High Hydrostatic Pressure on *Bacillus subtilis* luxAB Spores. *Acta Alimentaria*, *32*(4), 1588-2535.

Feeherry, F. E., Munsey, D. T. & Rowley, D. B. (1987). Thermal inactivation and injury of *Bacillus stearothermophilus* spores. *Applied and Environmental Microbiology*, *43*, 365-370.

Fernández, A., Salmerón, C., Fernández, P. Z. & Martínez, A. (1999). Application of a frequency distribution model to describe the thermal inactivation of two strains of *Bacillus cereus*. *Trends in Food Science & Technology*, *10*, 158-162.

Fernandez, P. S., Gomez, F. J., Ocio, M. J., Rodrigo, M., Sanchez, T. & Martinez, A. (1995). D values of *Bacillus stearothermophilus* spores as a function of pH and recovery medium acidulant. *Journal of Food Protection*, *58*(6), 628-632.

Finley, N. & Fields, M. L. (1962). Heat activation and heat-induced dormancy of *Bacillus stearothermophilus* spores. *Applied and Environmental Microbiology*, *10*(3), 231-236.

Fornari, C., Maggi, A., Gola, S., Cassara, A. & Manachini, P. (1995). Inactivation of Bacillus endospores by high-pressure treatment. *Industria Conserve*, *70*(3), 259-265.

Fujii, K., Ohtani, A., Watanabe, J., Ohgoshi, H., Fujii, T. & Honma, K. (2002). High-pressure inactivation of *Bacillus cereus* spores in the presence of argon. *International Journal of Food Microbiology*, *72*(3), 239-242.

Furukawa, S. & Hayakawa, I. (2000). Investigation of desirable hydrostatic pressure required to sterilize *Bacillus stearothermophilus* IFO 12550 spores and its sterilization properties in glucose, sodium chloride and ethanol solutions. *Food Research International*, *33*, 901-905.

Furukawa, S., Noma, S., Yoshikawa, S., Furuya, H., Shimoda, M. & Hayakawa, I. (2001). Effect of filtration of bacterial suspensions on the inactivation ratio in hydrostatic pressure treatment. *Journal of Food Engineering*, *50*, 59-61.

Furukawa, S., Noma, S., Shimoda, M. & Hayakawa, I. (2002). Effect of initial concentration of bacterial suspensions on their inactivation by high hydrostatic pressure. *International Journal of Food Science and Technology*, *37*, 573-577.

Furukawa, S., Shimoda, M. & Hayakawa, I. (2003). Mechanism of the inactivation of bacterial spores by reciprocal pressurization treatment. *Journal of Applied Microbiology*, *94*, 836–841.

Furukawa, S., Narisawa, N., Watanabe, T., et al. (2005). Formation of the spore clumps during heat treatment increases the heat resistance of bacterial spores. *International Journal of Food Microbiology*, *102*(1), 107–111.

Gao, Y., Ju, X. & Jiang, H. (2006a). Analysis of reduction of *Geobacillus stearothermophilus* spores treated with high hydrostatic pressure and mild heat in milk buffer. *Journal of Biotechnology*, *125*(3), 351-360.

Gao, Y., Ju, X. & Jiang, H. (2006b). Studies on inactivation of *Bacillus subtilis* spores by high hydrostatic pressure and heat using design of experiments. *Journal of Food Engineering*, *77*(3), 672-679.

Garcia-Graells, C., Masschalck, B. & Michiels, C. W. (1999). Inactivation of *Escherichia coli* in milk by high-hydrostatic-pressure treatment in combination with antimicrobial peptides. *Journal of Food Protection*, *62*, 1248– 1254.

Gola, S., Foman, C., Carpi, G., Maggi, A., Cassara, A. & Rovere, P. (1996). Inactivation of bacterial spores in phosphate buffer and in vegetable cream treated with high

pressures. In R. Hayashi & C. Balny. *High pressure bioscience and biotechnology* (pp. 253-259). Elsevier, Amsterdam, Lausanne, New York, Oxford, Shannon, Tokyo.

Goldberg, R. N., Kishore, N. & Lennen, R. M. (2002). Thermodynamic quantities for the ionization reaction of buffers. *Journal of Physical and Chemical Reference Data*, *31*(2), 231-370.

Gonzalez, I., Lopez, M., Mazas, M., Gonzales, J. & Bernardo, A. (1995). The effect of recovery conditions on the apparent heat resistance of *Bacillus cereus* spores. *Journal of Applied Bacteriology*, *78*, 548-554.

Gould, G. W. (1969). Germination. In G. W. Gould & A. Hurst. *The bacterial spore* (pp. 397-444). Academic. Press, London, England.

Gould, G. W. (1970). Germination and the problem of dormancy. *Journal of Applied Bacteriology*, *33*, 34-49.

Gould, G. W. & Sale, A. J. H. (1970). Initiation of germination of bacterial spores by hydrostatic pressure. *Journal of General Microbiology*, *60*, 335.

Gould, G. W., Stubbs, J. M. & King, W. L. (1970). Structure and composition of resistant layers in bacterial spores coats. *Journal of General Microbiology*, *60*, 347-355.

Gruber, T. M. & Gross, C. A. (2003). Multiple sigma subunits and the partitioning of bacterial transcription space. *Annual Review of Microbiology*, *57*, 441-466.

Guidi-Rontani, C., Weber-Levy, M., Labruyere, E. & Mock, M. (1999). Germination of *Bacillus anthracis* spores within alveolar macrophage. *Molecular Microbiology*, *31*, 9-17.

Haas, J., Behsnilian, D. & Schubert, H. (1996). Determination of the heat resistance of bacterial spores by the capillary tube method. I. Calculation of two borderline cases describing quasi-isothermal conditions. *LWT - Food Science and Technology*, *29*, 197-202.

Haldenwang, W. G. (1995). The sigma factors of *Bacillus subtilis*. *Annual Review of Microbiology*, 1-30.

Hamann, S. D. (1982). The influence of pressure on ionization equilibria in aqueous solutions. *Journal of Solution Chemistry*, *11*(1), 63-68.

Hamouda, T., Shih, A. Y. & Baker, J. R. (2002). A rapid staining technique for the detection of the initiation of germination of bacterial spores. *Letters in Applied Microbiology*, *34*(2), 86-90.

Hartmann, C. (2002). Numerical simulation of thermodynamic and fluid-dynamic processes during the high pressure treatment of fluid food systems. *Innovative Food Science & Emerging Technologies*, *3*, 11-18.

Hartmann, C. & Delgado, A. (2002). Numerical simulation of convective and diffusive transport effects on a high pressure induced inactivation process. *Biotechnology and Bioengineering*, *79*(1), 94-104.

Hartmann, C., Delgado, A. & Szymczyk, J. (2003). Convective and diffusive transport effects in a high pressure induced inactivation process of packed food. *Journal of Food Engineering*, *59*, 33-44.

Hartmann, C. & Delgado, A. (2004). Numerical simulation of the mechanics of a yeast cell under high hydrostatic pressure. *Journal of Biomechanics*, *37*, 977–987.

Hauben, K. J. A., Wuytack, E. Y., Soontjens, C. C. F. & Michiels, C. W. (1996). High-Pressure Transient Sensitization of *Escherichia coli* to Lysozyme and Nisin by Disruption of Outer-Membrane Permeability. *Journal of Food Protection*, *59*, 350-355.

Hauben, K. J. A., Bernaerts, K. & Michiels, C. W. (1998). Protective effect of calcium on inactivation of *Escherichia coli* by hydrostatic pressure. *Journal of Applied Microbiology*, *85*, 678–84.

Hayakawa, I., Furukawa, S., Midzunaga, A., et al. (1998). Mechanism of inactivation of heat-tolerant spores of *Bacillus stearothermophilus* IFO 12550 by rapid decompression. *Journal of Food Science*, *63*(3), 371-374.

Hayakawa, K., Kanno, T., Tomito, M. & Fujio, Y. (1994a). Application of high pressure for spore inactivation and protein denaturation. *Journal of Food Science*, *59*, 159-163.

Hayakawa, K., Kanno, T., Yoshiyama, K. & Fujio, Y. (1994b). Oscillatory compared with continuous high pressure sterilization of *Bacillus stearothermophilus* spores. *Journal of Food Science*, *59*, 164-167.

Hayert, M., Perrier-Cornet, J.-M. & Gervais, P. (1999). A simple method for measuring the pH of acid solutions under high pressure. *The Journal of Physical Chemistry A*, *103*, 1785–1789.

Heinz, V. & Knorr, D. (1996). High pressure inactivation kinetics of *Bacillus subtilis* cells by a three-state-model considering distribution resistance mechanisms. *Food Biotechnology*, *10*(2), 149-161.

Heinz, V. (1997). *Wirkung hoher hydrostatischer Drücke auf das Absterbe- und Keimungsverhalten sporenbildender Bakterien am Beispiel von Bacillus subtilis ATCC 9372*. PhD thesis, Berlin, Berlin University of Technology, 142.

Heinz, V. & Knorr, D. (1998). High pressure germination and inactivation kinetics of bacterial spores. In N. S. Isaacs. *High pressure food science, bioscience and chemistry* (pp. 435-441). The Royal Society of Chemistry, Cambridge.

Heinz, V. & Knorr, D. (2002). Effects of high pressure on spores. In M. E. G. Hendrickx & D. Knorr. *Ultra high pressure treatments of foods* (pp. 77-114). Kluwer Academic/ Plenum Publishers, New York.

Heldman, D. R. & Newsome, R. L. (2003). Kinetic models for microbial survival during processing. *Food Technology*, *57*, 40-46.

Herdegen, V. & Vogel, R. F. (1998). Strategies for high pressure inactivation of endospore-forming bacteria. In N. S. Isaacs. *High pressure food science, bioscience and chemistry* (pp. 394-402). The Royal Society of Chemistry, Cambridge.

Heremans, K. (1982). High pressure effects on proteins and other biomolecules. *Annual Review of Biophysics and Bioengineering*, *11*, 1-21.

Hite, B. H. (1899). The effect of pressure in the preservation of milk - A preliminary report. *West Virginia Agricultural and Forestry Experiment Station Bulletin*, *58*, 15-35.

Hite, B. H., Giddings, N. J. & Weakley, C. E. (1914). The effect of pressure on certain microorganisms encountered in the preservation of fruits and vegetables. *West Virginia Agricultural and Forestry Experiment Station Bulletin*, *146*, 2-67.

Hölters, C., Sojka, B. & Ludwig, H. (1997). Pressure-induced germination of bacterial spores from Bacillus subtilis and Bacillus stearothermophilus. In K. Heremans. *High pressure research in the biosciences and biotechnology* (pp. 257-260). Leuven University Press, Leuven.

Hölters, C., van Almsick, G. & Ludwig, H. (1999). High pressure inactivation of anaerobic spores from *Clostridium pasteurianum*. In H. Ludwig. *Advances in high pressure bioscience and biotechnology* (pp. 65-68). Springer-Verlag, Berlin.

Hoover, D. G., Metrick, C., Papineau, A. M., Farkas, D. F. & Knorr, D. (1989). Biological effects of high hydrostatic pressure on food microorganisms. *Food Technology*, *43*(9), 99-107.

Humphrey, A. E. & Nickerson, J. T. R. (1961). Testing thermal death data for significant non-logarithmic behavior. *Applied Microbiology*, *9*(4), 282–286.

Hutton, M. T., Koskinen, M. A. & Hanlin, J. H. (1991). Interacting effects of pH and NaCl on heat resistance of bacterial spores. *Journal of Food Science*, *56*(3), 821-822.

Hyatt, M. T. & Levinson, H. S. (1968). Water vapor, aqueous ethyl alcohol, and heat activation of *Bacillus megaterium* spore germination. *Journal of Bacteriology*, *95*(6), 2090-2101.

Igura, N., Kamimura, Y., Islam, M. S., Shimoda, M. & Hayakawa, I. (2003). Effects of Minerals on Resistance of *Bacillus subtilis* Spores to Heat and Hydrostatic Pressure. *Applied and Environment Microbiology*, *69*(10), 6307–6310.

Islam, M. S., Inoue, A., Igura, N., Shimoda, M. & Hayakawa, I. (2006). Inactivation of Bacillus spores by the combination of moderate heat and low hydrostatic pressure in ketchup and potage. *International Journal of Food Microbiology*, *107*, 124 – 130.

Izuchi, M. & Nishibata, K. (1986). A high pressure rolling- ball viscometer up to 1 GPa. *Japanese Journal of Applied Physics*, *25*, 1091-1096.

Janssen, F. W., Lund, A. J. & Anderson, L. E. (1958). Colorimetric assay for dipicolinic acid in bacterial spores. *Science*, *127*, 26–27.

Jedrzejas, M. J. & Setlow, P. (2001). Comparison of the binuclear metalloenzymes diphosphoglycerate-independent phosphoglycerate mutase and alkaline phosphatase: their mechanism of catalysis by a phosphoserine intermediate. *Chemical Reviews*, *101*, 607-618.

Johnson, F. H. & Zobell, C. E. (1948). The retardation of thermal disinfection of *Bacillus subtilis* spores by hydrostatic pressure. *Journal of Bacteriology*, *57*, 353-358.

Kakugawa, K., Okazaki, T., Yamauchi, S., Morimoto, K., Yoneda, T. & Suzuki, K. (1996). Thermal inactivating behavior of *Bacillus stearothermophilus* under high pressure. In R. Hayashi & C. Balny. *High pressure bioscience and biotechnology* (pp. 171-175). Elsevier, Amsterdam, Lausanne, New York, Oxford, Shannon, Tokyo.

Kalchayanand, N., Sikes, T., Dunne, C. P. & Ray, B. (1994). Hydrostatic pressure and electroporation have increased bactericidal efficiency in combination with bacteriocins. *Applied and Environment Microbiology*, *60*(11), 4174-4177.

Kalchayanand, N., Sikes, A., Dunne, C. P. & Ray, B. (1998). Interaction of hydrostatic pressure, time and temperature of pressurization and Pediocin AcH on inactivation of foodborne bacteria. *Journal of Food Protection*, *61*, 425-431.

Kalchayanand, N., Dunne, C. P., Sikes, A. & Ray, B. (2003). Inactivation of bacterial spores by combined action of hydrostatic pressure and bacteriocins in roast beef. *Journal of Food Safety*, *23*(4), 219-231.

Kalchayanand, N., Dunne, C. P., Sikes, A. & Ray, B. (2004). Germination induction and inactivation of *Clostridium* spores at medium-range hydrostatic pressure treatment. *Innovative Food Science & Emerging Technologies*, *5*(3), 277-283.

Kell, D. B., Kaprelyants, A. S., Weichart, D. H., Harwood, C. R. & Barer, M. R. (1998). Viability and activity in readily culturable bacteria: a review and discussion of the practical issues. *Antonie van Leeuwenhoek*, *72*(2), 169-187.

Kellerer, A. M. (1987). Models of cellular radiation action. In R. G. Freeman. *Kinetics of Nonhomogeneous Processes* (pp.). John Wiley & Sons, New York.

Kepler, J. (1611). *Ioannis Kepleri S. C. Maiest. Mathematici Strena Seu De Niue Sexangula*. Gottfried Tampach, Francofurti ad Moenum.

Kessler, H. G. (1996). *Lebensmittel- und Bioverfahrenstechnik - Molkereitechnologie*. Verlag A. Kessler, Freising.

Keynan, A., Evenchik, Z., Halvorson, H. O. & Hastings, J. W. (1964). Activation of bacterial endospores. *Journal of Bacteriology*, *88*(2), 313-318.

Kitamura, Y. & Itoh, T. (1987). Reaction volume of protonic ionization for buffering agents. Prediction of pressure dependence of pH and pOH. *Journal of Solution Chemistry*, *16*(9), 715-725.

Kitsubun, P., Hartmann, C. & Delgado, A. (2005). Numerical Investigations of Process Heterogeneities during High Hydrostatic Pressure Treatment with Turbulent Inflow Conditions. *Proceedings in Applied Mathematics and Mechanics*, *5*, 573–574.

Knoerzer, K., Juliano, P., Gladman, S., Versteeg, C. & Fryer, P. (2007). A computational model for temperature and sterility distributions in a pilot-scale high-pressure high-temperature process. *American Institute of Chemical Engineers Journal*, *53*(11), 2996-3010.

Knorr, D. (1999). Novel approaches in food-processing technology: new technologies for preserving foods and modifying function. *Current Opinions in Biotechnology*, *10*, 485-491.

Knorr, D., Heinz, V. & Buckow, R. (2006). High pressure application for food biopolymers. *Biochimica et Biophysica Acta*, *1764*, 619–631.

Koch, R. (1876). Untersuchungen ueber Bakterien V. Die Aetiologie der Milzbrand-Krankheit, begruendent auf die Entwicklungsgeschichte des *Bacillus Anthracis*. *Beiträge zur Biologie der Planzen*, *2*, 277-310.

Kooiman, W. J. & Geers, J. M. (1975). Simple and accurate technique for the determination of heat resistance of bacterial spores. *Journal of Applied Bacteriology*, *38*(2), 185-9.

Koutchma, T., Guo, B., Patazca, L. & Parisi, B. (2005). High pressure-High temperature sterilization: From kinetic analysis to process verification. *Journal of Food Process Engineering*, *28*, 610–629.

Krebbers, B., Matser, A. M., Koets, M., Bartels, P. & van den Berg, R. (2002). High pressure-temperature processingf as an alternative for preserving basil. *High Pressure Research*, *22*(3), 711-714.

Krebbers, B., Matser, A. M., Hoogerwerf, S. W., Moezelaar, R., Tomassen, M. M. M. & Van den Berg, R. (2003). Combined high-pressure and thermal treatments for processing of tomato puree: Evaluation of microbial inactivation and quality parameters. *Innovative Food Science & Emerging Technologies*, *4*(4), 377-385.

Laflamme, C., Lavigne, S., Ho, J. & Duchaine, C. (2004). Assessment of bacterial endospore viability with fluorescent dyes. *Journal of Applied Microbiology*, *96*(4), 684-692.

Lagrange, J. L. (1773). Recherches d´arithmetique. *Nouv. Mem. Acad. Roy. Sc. Belle Letteres. Oeuvres III*, 265-312.

Larson, W. P., Hartzell, T. B. & Diehl, H. S. (1918). The effect of high pressures of bacteria. *Journal of Infectious Diseases*, *22*, 271-279.

Lea, D. E. (1955). *Action of radiations on living cells*. Cambridge University Press, New York.

Lee, E. L. & Gilbert, C. A. (1918). On the application of the mass law to the process of disinfection - being a contribution to the 'mechanistic theory' as opposed to the 'vitalistic theory'. *Journal of Physical Chemistry*, *22*, 348-372.

Lee, S., Dougherty, R. H. & Kang, D. (2002). Inhibitory Effects of High Pressure and Heat on *Alicyclobacillus acidoterrestris* Spores in Apple Juice. *Applied and Environment Microbiology*, *68*(8), 4158–4161.

Lee, S., Chung, H. & Kang, D. (2006). Combined treatment of high pressure and heat on killing spores of *Alicyclobacillus acidoterrestris* in apple juice concentrate. *Journal of Food Protection*, *69*(5), 1056-1060.

Lo Surdo, A., Bernstrom, K., Jonsson, C. A. & Millero, F. J. (1979). Molal volume and adiabatic compressibility of aqueous phosphate solutions at 25°C. *Journal of Physical Chemistry*, *83*(10), 1255-1262.

Loewick, J. A. M. & Anema, P. J. (1972). Effect of pH on the heat resistance of *Clostridium sporogenes* in minced meat. *Journal of Applied Bacteriology*, *56*, 193–199.

Lopez-Pedemonte, T. J., Roig-Sague´s, A. X., Trujillo, A. J., Capellas, M. & Guamis, B. (2003). Inactivation of spores of Bacillus cereus in cheese by high hydrostatic pressure with the addition of nisin or lysozyme. *Journal of Dairy Science*, *86*, 3075–3081.

Loshon, C. A., Genest, P. C., Setlow, B. & Setlow, P. (1999). Formaldehyde kills spores of *Bacillus subtilis* by DNA damage and small, acid-soluble spore proteins of the α/β-type protect spores against DNA damage. *Journal of Applied Microbiology*, *87*, 8-14.

Ludwig, H., van Almsick, G. & Sojka, B. (1996). High pressure inactivation of microorganisms. In R. Hayashi & C. Balny. *High pressure bioscience and biotechnology* (pp. 237-244). Elsevier Science B. V., Amsterdam.

Mallidis, C. G. & Drizou, D. (1991). Effect of simultaneous application of heat and pressure on the survival of bacterial spores. *Journal of Applied Bacteriology*, *71*, 285-288.

Margosch, D., Gänzle, M. G., Ehrmann, M. A. & Vogel, R. F. (2004a). Pressure Inactivation of Bacillus Endospores. *Applied and Environment Microbiology*, *70*(12), 7321–7328.

Margosch, D., Ehrmann, M. A., Gänzle, M. G. & Vogel, R. F. (2004b). Comparison of pressure and heat Resistance of *Clostridium botulinum* and other endospores in mashed carrots. *Journal of Food Protection*, 2530-2537.

Margosch, D., Ehrmann, M. A., Buckow, R., Heinz, V., Vogel, R. F. & Gänzle, M. G. (2006). High-pressure-mediated survival of *Clostridium botulinum* and *Bacillus amyloliquefaciens* endospores at high temperature. *Applied and Environment Microbiology*, *72*(5), 3476-3481.

Marquis, R. E. (1997). Oxidative killing of bacterial spores under pressure. In K. Heremans. *High pressure research in the biosciences and biotechnology* (pp. 229-232). Leuven University Press, Leuven.

Marshall, W. L. & Franck, E. U. (1981). Ion product of water substance, 0–1000 °C, 1–10,000 bars New International Formulation and its background. *Journal of Physical and Chemical Reference Data*, *10*(2), 295-304.

März, A. (2003). *Method for inactivating micro-organisms using high pressure processing*. USA, patent, (09/845,412).

Masschalck, B., Van Houdt, R. & Michiels, C. W. (2001). High pressure increases bactericidal activity and spectrum of lactoferrin, lactoferricin and nisin. *International Journal of Food Microbiology*, *64*(3), 325-332.

Masschalk, B. R., Van Houdt, R., Van Haver, E. G. R. & Michiels, C. W. (2001). Inactivation of Gram-negative bacteria by lysozyme, denatured lysozyme and lysozyme derived peptides under high pressure. *Applied and Environment Microbiology*, *67*, 339–344.

Mathys, A., Chapman, B., Bull, M., Heinz, V. & Knorr, D. (2007a). Flow cytometric assessment of *Bacillus* spore response to high pressure and heat. *Innovative Food Science & Emerging Technologies*, *8*(4), 519–527.

Mathys, A., Heinz, V., Schwartz, F. H. & Knorr, D. (2007b). Impact of agglomeration on the quantitative assessment of *Bacillus stearothermophilus* heat inactivation. *Journal of Food Engineering*, *81*(2), 380-387.

Mathys, A., Kallmeyer, R., Heinz, V. & Knorr, D. (2008). Impact of dissociation equilibrium shift on bacterial spore inactivation by heat and pressure. *Food Control*, *doi:10.1016/j.foodcont.2008.01.003*.

Matser, A. M., Krebbers, B., van den Berg, R. W. & Bartels, P. V. (2004). Advantages of high pressure sterilisation on quality of food products. *Trends in Food Science & Technology*, *15*(2), 79-85.

Melly, E., Genest, P. C., Gilmore, M. E., et al. (2002). Analysis of the properties of spores of *Bacillus subtilis* prepared at different temperatures. *Journal of Applied Microbiology*, *92*, 1105–1115.

Meyer, R. S. (2000). *Ultra high pressure, high temperature food preservation process*. USA, patent, (PCT/US1999/002094).

Meyer, R. S., Cooper, K. L., Knorr, D. & Lelieveld, H. L. M. (2000). High-pressure sterilization of foods. *Food technology*, *54*(11), 67-72.

Meyer, R. S. (2001). *Ultra high pressure, high temperature food preservation process*. USA, patent, (09/490134).

Mills, G., Earnshaw, R. & Patterson, M. F. (1998). Effects of high hydrostatic pressure on *Clostridium sporogenes* spores. *Letters in Applied Microbiology*, *26*, 227-230.

Moerman, F., Mertens, B., Demey, L. & Huyghebaert, A. (2001). Reduction of *Bacillus subtilis*, *Bacillus stearothermophilus* and *Streptococcus faecalis* in meat batters by temperature-high hydrostatic pressure pasteurization. *Meat Science*, *59*(2), 115-125.

Moerman, F. (2005). High hydrostatic pressure inactivation of vegetative microorganisms, aerobic and anaerobic spores in pork Marengo, a low acidic particulate food product. *Meat Science*, *69*(2), 225-232.

Moir, A., Corfe, B. M. & Behravan, J. (2002). Spore germination. *Cellular and Molecular Life Sciences*, *59*, 403–409.

Moir, A. (2006). How do spores germinate? *Journal of Applied Microbiology*, *101*(3), 526-530.

Molina-Gutierrez, A., Stippl, V. M., Delgado, A., Gänzle, M. G. & Vogel, R. F. (2002). In Situ Determination of the Intracellular pH of *Lactococcus lactis* and *Lactobacillus plantarum* during Pressure Treatment. *Applied and Environmental Microbiology*, *68*(9), 4399-4406.

Mönch, S., Heinz, V., Guttmann, P. & Knorr, D. (1999). X-ray microscopy in food science. In *Proceedings of the International Conference on X-Ray Microscopy-XRM 99*, University of California, Berkeley, USA.

Morgan, S. M., Ross, R. P., Beresford, T. & Hill, C. (2000). Combination of hydrostatic pressure and lacticin 3147 causes increased killing of *Staphylococcus* and *Listeria*. *Journal of Applied Microbiology*, *88*(3), 414-420.

Morin, R. S. & Kozlovac, J. P. (2000). Biological Safety: principles and practices. In D. O. Fleming & D. L. Hunt. *Biological Safety: principles and practices* (pp. 261-272). ASM Press, Washington, D.C.

Murrell, W. G. & Wills, P. A. (1977). Initiation of *Bacillus* spore germination by hydrostatic pressure: Effect of temperature. *Journal of Bacteriology*, *129*(3), 1272-1280.

Nakayama, A., Yano, Y., Kobayashi, S., Ishikawa, M. & Sakai, K. (1996). Comparison of pressure resistances of spores of six *Bacillus* strains with their heat resistances. *Applied and Environmental Microbiology*, *62*(10), 3897-3900.

Nannen, N. L. & Hutkins, R. W. (1991). Proton-translocating adenosine triphosphatase activity in lactic acid bacteria. *Journal of Dairy Science*, *74*, 747–751.

Navani, S. K., Scholfield, J. & Kibby, M. R. (1970). A digital computer program for the statistical analysis of heat resistance data applied to *Bacillus stearothermophilus* spores. *Journal of Applied Bacteriology*, *33*(4), 609-620.

Nazina, T. N., Tourova, T. P., Poltaraus, A. B., et al. (2001). Taxonomic study of aerobic thermophilic bacilli: descriptions of *Geobacillus subterraneus* gen. nov., sp. nov. and *Geobacillus uzenensis* sp. nov. from petroleum reservoirs and transfer of *Bacillus stearothermophilus*, *Bacillus thermocatenulatus*, *Bacillus thermoleovorans*, *Bacillus kaustophilus, Bacillus thermoglucosidasius* and *Bacillus thermodenitrificans* to *Geobacillus* as the new combinations *G. stearothermophilus*, *G. thermocatenulatus, G. thermoleovorans, G. kaustophilus, G. thermoglucosidasius* and *G. thermodenitrificans*. *International Journal of Systematic and Evolutionary Microbiology*, *51*(2), 433-446.

Nernst, W. (1889). Die elektromotorische Wirksamkeit der Ionen. *Zeitschrift für Physikalische Chemie*, *4*(2), 129–181.

Neuman, R. C., Kauzmann, W. & Zipp, A. (1973). Pressure dependence of weak acid ionization in aqueous buffers. *The Journal of Physical Chemistry*, *77*(22), 2687-2691.

Nishi, K., Kato, R. & Tomita, M. (1994). Activation of *Bacillus* spp. spores by hydrostatic pressure. *Nippon Shokukin Kogyo Gakkaishi*, *41*(8), 542-549.

North, N. A. (1973). Dependence of equilibrium constants in aqueous solutions. *The Journal of Physical Chemistry*, *77*(7), 931-934.

Oh, S. & Moon, M. J. (2003). Inactivation of *Bacillus cereus* spores by high hydrostatic pressure at different temperatures. *Journal of Food Protection*, 599–603.

Okazaki, T., Yoneda, T. & Suzuki, K. (1994). Combined effects of temperature and pressure on sterilization of *Bacillus subtilis* spores. *Nippon Shokukin Kogyo Gakkaishi*, *41*(8), 536-541.

Okazaki, T., Kakugawa, K., Yamauchi, S., Yoneda, T. & Suzuki, K. (1996). Combined effects of temperature and pressure on inactivation of heat-resistant bacteria. In R. Hayashi & C. Balny. *High pressure bioscience and biotechnology* (pp. 415-418). Elsevier, Amsterdam, Lausanne, New York, Oxford, Shannon, Tokyo.

Okazaki, T., Kakugawa, K., Yoneda, T. & Suzuki, K. (2000). Inactivation behavior of heat-resistant bacterial spores by thermal treatments combined with high hydrostatic pressure. *Food Science Technology Research*, *6*, 204-207.

Olson, F. C. W. & Schultz, T. (1942). Temperatures in solids during heating or cooling. *Industrial and Engineering Chemistry*, *34*, 874-877.

Oxen, P. & Knorr, D. (1993). Baroprotective effects of high solute concentrations against inactivation of Rhodotorula rubra. *LWT - Food Science and Technology*, *26*, 220–223.

Paidhungat, M., Setlow, B., Daniels, W. B., Hoover, D., Papafragkou, E. & Setlow, P. (2002). Mechanisms of induction of germination of *Bacillus subtilis* spores by high pressure. *Applied and Environmental Microbiology*, *68*(6), 3172-3175.

Paidhungat, M. & Setlow, P. (2002). Spore germination and outgrowth. In J. A. Hoch, R. Losick & A. L. Sonenshein. *Bacillus subtilis and its Relatives: From Genes to Cells* (pp. 537-548). American Society for Microbiology, Washington, DC.

Palou, E., Lopez-Malo, A., Barbosa-Canovas, G. V., Welti-Chames, J. & Swanson, B. G. (1997). Combined effect of high hydrostatic pressure and water activity on *Zygosaccharomyces balii* inhibition. *Letters in Applied Microbiology*, *24*, 417–420.

Patazca, E., Koutchma, T. & Ramaswamy, H. S. (2006). Inactivation kinetics of *Geobacillus stearothermophilus* spores in water using high-pressure processing at elevated temperatures. *Journal of Food Science*, *71*(3), M110-M116.

Peleg, M. & Cole, M. B. (1998). Reinterpretation of microbial survival curves. *Critical Reviews in Food Science*, *38*(5), 353-380.

Perkins, J. (1820). On the compressability of water. *Philosophical Transactions of the Royal Society*, *110*, 324-329.

Perkins, J. (1826). On the progressive compression of water by a high degree of force, with trials on the effect of other fluids. *Philosophical Transactions of the Royal Society*, *116*, 541-547.

Pfeifer, J. (1992). *Einfluss der Wasseraktivität sowie des Milieus zwischen Dichtungen und Dichtflächen auf die Dichtflächen auf die Hitzinaktivierung von Mikroorganismen am Beispiel bakterieller Sporen*. PhD thesis, München, TU München- Weihenstephan.

Phillips, Z. E. & Strauch, M. A. (2002). *Bacillus subtilis* sporulation and stationary phase gene expression. *Cellular and Molecular Life Sciences*, *59*, 392-402.

Piggot, P. J. & Losick, R. (2002). Sporulation genes and intercompartmental regulation. In A. L. Sonenshein, J. A. Hoch & R. Losick. *Bacillus subtilis and its closest relatives: from genes to cells* (pp.). ASM Press, Washington D.C.

Piggot, P. J. & Hilbert, D. W. (2004). Sporulation of *Bacillus subtilis*. *Current Opinion in Microbiology*, *7*, 579-586.

Planck, M. (1887). Über das Prinzip der Vermehrung der Entropie. *Annalen der Physik*, *32*(462).

Powers, E. L. (1962). Consideration of survival curves and target theory. *Physics in Medicine and Biology*, *7*, 3-28.

Quinlan, R. J. & Reinhart, G. D. (2005). Baroresistant buffer mixtures for biochemical analyses. *Analytical Biochemistry*, *341*(1), 69-76.

Ragkousi, K., Cowan, A. E., Ross, M. A. & Setlow, P. (2000). Analysis of nucleoid morphology during germination and outgrowth of spores of *Bacillus* species. *Journal of Bacteriology*, *182*, 5556–5562.

Rajan, S., Ahn, J., Balasubramaniam, V. M. & Yousef, A. E. (2006a). Combined pressure-thermal inactivation kinetics of *Bacillus amyloliquefaciens* spores in egg patty mince. *Journal of Food Protection*, *69*(4), 853–860.

Rajan, S., Pandrangi, S., Balasubramaniam, V. M. & Yousef, A. E. (2006b). Inactivation of *Bacillus stearothermophilus* spores in egg patties by pressure-assisted thermal processing. *LWT - Food Science and Technology*, *39*(8), 844-851.

Raso, J., Palop, A., Bayarte, M., Condon, S. & Sala, F. J. (1995). Influence of sporulation temperature onthe heat resistance of a strain of *Bacillus licheniformis* (Spanish Type Culture Collection 4523). *Food Microbiology*, *12*, 357-361.

Raso, J., Barbosa-Cánovas, G. & Swanson, B. G. (1998a). Sporulation temperature affects initiation of germination and inactivation by high hydrostatic pressure of *Bacillus cereus*. *Journal of Applied Microbiology*, *85*, 17-24.

Raso, J., Gongora-Nieto, M. M., Barbosa-Canovas, G. V. & Swanson, B. G. (1998b). Influence of several environmental factors on the initiation of germination and inactivation of *Bacillus cereus* by high hydrostatic pressure. *International Journal of Food Microbiology*, *44*(1-2), 125-132.

Raso, J. & Barbosa-Canovas, G. V. (2003). Nonthermal Preservation of Foods Using Combined Processing Techniques. *Critical Reviews in Food Science and Nutrition*, *43*(3), 265–285.

Reddy, N. R., Solomon, H. M., Fingerhut, G. A., Rhodehamel, E. J., Balasubramaniam, V. M. & Palaniappan, S. (1999). Inactivation of *Clostridium botulinum* type E spores by high pressure processing. *Journal of Food Safety*, *19*, 277-288.

Reddy, N. R., Solomon, H. M., Tezloff, R. C. & Rhodehamel, E. J. (2003). Inactivation of *Clostridium botulinum* type A spores by high pressure processing at elevated temperatures. *Journal of Food Protection*, *66*, 1402–7.

Reddy, N. R., Tetzloff, R. C., Solomon, H. M. & Larkin, J. W. (2006). Inactivation of *Clostridium botulinum* nonproteolytic type B spores by high pressure processing at moderate to elevated high temperatures. *Innovative Food Science & Emerging Technologies*, *7*(3), 169-175.

Regnard, P. (1884). Effet des hautes pressions sur les animaux marins. *C.R. Séances Soc. Biol.*, *36*, 394-395.

Roberts, C. M. & Hoover, D. G. (1996). Sensitivity of *Bacillus coagulans* spores to combination of high hydrostatic pressure, heat, acidity and nisin. *Journal of Applied Bacteriology*, *81*, 363-368.

Rodriguez, A. C., Smerage, G. H., Teixeira, A. A. & Busta, F. F. (1988). Kinetic effects of lethal temperatures on population dynamics of bacterial spores. *Transaction of the ASAE*, *31*(5), 1594-1601.

Rodriguez, A. C., Larkin, J. W., Dunn, J., et al. (2004). Model of the inactivation of bacterial spores by moist heat and high pressure. *Journal of Food Science*, *69*(8), 367-373.

Rosin, P. & Rammler, E. (1933). The laws governing the fineness of powdered coal. *The Institute of Fuel*, *7*, 29-36.

Rovere, P., Gola, S., Maggi, A., Scaramuzza, N. & Miglioli, L. (1998). Studies on bacterial spores by combined high pressure-heat treatments: possibility to sterilize low acid foods. In N. S. Isaacs. *High pressure food science, bioscience and chemistry* (pp. 355-363). The Royal Society of Chemistry, Cambridge.

Rovere, P., Lonnerborg, N. G., Gola, S., Miglioli, L., Scaramuzza, N. & Squarcina, N. (1999). Advances in bacterial spores inactivation in thermal treatments under pressure. In H. Ludwig. *Advances in high pressure bioscience and biotechnology* (pp. 114-120). Springer-Verlag, Berlin.

Rovere, P. (2002). Industrial-scale high pressure processing of foods. In M. E. G. Hendrickx & D. Knorr. *Ultra High Pressure Treatments of Foods* (pp. 251-268). Kluwer Academic/ Plenum Publishers, New York.

Royer, H. (1895). *Archives de Physiologie Normale et Pathologique*, *7*(12).

Sale, A. J. H., Gould, G. W. & Hamilton, W. A. (1970). Inactivation of bacterial spores by hydrostatic pressure. *Journal of General Microbiology*, *60*, 323-334.

Sasagawa, A., Yamazaki, A., Kobayashi, A., et al. (2006). Inactivation of Bacillus subtils spores by a combination of hydrostatic high-pressure and pulsed electric field treatments. *The Review of High Pressure Science an Technology*, *16*(1), 45-53.

Schlueter, O., Benet, G. U., Heinz, V. & Knorr, D. (2004). Metastable states of water and ice during pressure supported freezing of potato tissue. *Biotechnology Progress*, *20*, 799-810.

Schraml, J. (1993). *Zum Verhalten konzentrierter Produkte bei der Belagbildung an heißen Oberflächen*. PhD thesis, München, TU München- Weihenstephan.

Schubert, H. (2007). Interaction Forces between Particles. In U. Bröckel, W. Meier & G. Wagner. *Product Design and Engineering: Best Practices* (pp. 5-32). Wiley-VCH, Weinheim.

Schwartz, F. H. & Braun, M. (1999). *Apparatus for measuring particle dimensions in fluids*. USA, patent, (09/089,478), Messtechnik Schwartz GmbH. Duesseldorf. Germany.

Scurrah, K. J., Robertson, R. E., Craven, H. M., Pearce, L. E. & Szabo, E. A. (2006). Inactivation of *Bacillus* spores in reconstituted skim milk by combined high pressure and heat treatment. *Journal of Applied Microbiology*, *101*(1), 172-180.

Setlow, B. & Setlow, P. (1980). Measurements of the pH within dormant and germinated bacterial spores. *Proceedings of the National Academy of Sciences*, *77*(5), 2474–2476.

Setlow, B., Melly, E. & Setlow, P. (2001). Properties of spores of *Bacillus subtilis* blocked at an intermediate stage of spore germination. *Journal of Bacteriology*, *183*, 4894-4899.

Setlow, B., Loshon, C. A., Genest, P. C., Cowan, A. E., Setlow, C. & Setlow, P. (2002). Mechanisms of killing of spores of *Bacillus subtilis* by acid, alkali, and ethanol. *Journal of Applied Microbiology*, *92*, 362–375.

Setlow, B., Atluri, S., Kitchel, R., Koziol-Dube, K. & Setlow, P. (2006). Role of dipicolinic acid in resistance and stability of spores of *Bacillus subtilis* with or without DNA-protective α/β-type small acid-soluble proteins. *Journal of Bacteriology*, *188*(11), 3740-3747.

Setlow, P. (2003). Spore germination. *Current Opinion in Microbiology*, *6*, 550–556.

Setlow, P. (2007). I will survive: DNA protection in bacterial spores. *Trends in Microbiology*, *15*(4), 172-180.

Seyderhelm, I. & Knorr, D. (1992). Reduction of *Bacillus stearothermophilus* spores by combined high pressure and temperature treatments. *Zeitschrift für Lebensmitteltechnologie und Verfahrenstechnik*, *43*(4), EFS 17-20.

Shearer, A. E. H., Hoover, D. G., Dunne, C. P. & Sikes, A. (2000). Bacterial spore inhibition and inactivation in foods by pressure, chemical preservatives, and mild heat. *Journal of Food Protection*, *63*(1503-1510).

Shigeta, Y., Aoyama, Y., Okazaki, T., Hagura, Y. & Suzuki, K. (2007). Hydrostatic pressure-induced germination and inactivation of *Bacillus* spores in the presence or absence of nutrients. *Food Science and Technology Research*, *13*(3), 193-199.

Shull, J. J., Cargo, G. T. & Ernst, R. R. (1963). Kinetics of heat activation and of thermal death of bacterial spores. *Applied Microbiology*, *11*, 485-487.

Simpson, R. K. & Gilmour, A. (1997). The effects of high hydrostatic pressure on Listeria monocytogenes in phosphate buffered saline and model food systems. *Journal of Applied Microbiology*, *83*, 181–188.

Smeller, L. (2002). Pressure-temperature phase diagram of biomolecules. *BBA - Biochimica et Biophysica Acta*, *1595*, 11-29.

Smelt, J. P. P. M. (1998). Recent advances in the microbiology of high pressure processing. *Trends in Food Science & Technology*, *9*, 152-158.

Sognefest, P., Hays, G. L., Wheaton, E. & Benjamin, H. A. (1948). Effect of pH on the thermal process requirements of canned foods. *Food Research*, *13*, 400–416.

Sojka, B. & Ludwig, H. (1994). Pressure-induced germination and inactivation of *Bacillus subtilis* spores. *Die Pharmazeutische Industrie*, *56*(7), 660-663.

Sojka, B. & Ludwig, H. (1997). Effect of rapid pressure changes on the inactivation of *Bacillus subtilis* spores. *Die Pharmazeutische Industrie*, *59*(5), 436-438.

Stern, J. A., Herlin, M. A. & Procter, B. E. (1952). An electric method for continuous determination of rapid temperature changes in thermal death-time studies. *Food Research*, *17*, 460-465.

Stewart, C. M., Dunne, C. P., Sikes, A. & Hoover, D. G. (2000). Sensitivity of spores of *Bacillus subtilis* and *Clostridium sporogenes* PA 3679 to combinations of high hydrostatic pressure and other processing parameters. *Innovative Food Science and Emerging Technologies*, *1*(1), 49-56.

Stippl, V. M., Delgado, A. & Becker, T. M. (2002). Optical method for the *in-situ* measurement of the pH-value during high pressure treatment of foods. *High Pressure Research*, *22*, 757–761.

Stippl, V. M., Delgado, A. & Becker, T. M. (2004). Development of a method for the optical in-situ determination of pH value during high-pressure treatment of fluid food. *Innovative Food Science & Emerging Technologies*, *5*, 285–292.

Stocks, S. M. (2004). Mechanism and use of the commercially available viability stain, *Bac*Light. *Cytometry Part A*, *61A*(2), 189-195.

Stragier, P. & Losick, R. (1996). Molecular genetics of sporulation in *Bacillus subtilis*. *Annual Review in Genetics*, *30*, 297-341.

Stumbo, C. R. (1948). Bacteriological considerations relating to process evaluation. *Food Technology*, *2*(2), 115-132.

Subramanian, A., Ahn, J., Balasubramaniam, V. M. & Rodriguez-Saona, L. (2006). Determination of spore inactivation during thermal and pressure-assisted thermal processing using FT-IR spectroscopy. *Journal of Agricultural and Food Chemistry*, *54*(26), 10300-10306.

Subramanian, A., Ahn, J., Balasubramaniam, V. M. & Rodriguez-Saona, L. (2007). Monitoring Biochemical Changes in Bacterial Spore during Thermal and Pressure-Assisted Thermal Processing using FT-IR Spectroscopy. *Journal of Agricultural and Food Chemistry*, *55*(22), 9311-9317.

Sucker, D. & Brauer, H. (1976). Stationärer Stoff- und Wärmetransport an stationär quer angeströmten Zylindern. *Wärme- und Stoffübertragung*, *9*, 1-12.

Taki, Y., Awao, T., Toba, S. & Mitsuura, N. (1991). Sterilization of *Bacillus* sp. spores by hydrostatic pressure. In R. Hayashi. *High pressure science for food* (pp. 217–24). San-Ei Pub. Co., Kyoto.

Taub, I. A., Feeherry, F. E., Ross, E. W., Kustin, K. & Doona, C. J. (2003). A Quasi-Chemical Kinetics Model for the Growth and Death of Staphylococcus aureus in Intermediate Moisture Bread. *Journal of Food Science*, *68*(8), 2530-2537.

Timson, W. J. & Short, A. J. (1965). Resistance of micro-organisms to hydrostatic pressure. *Biotechnology and Bioengineering*, *7*, 139-159.

Ting, E., Balasubramaniam, V. M. & Raghubeer, E. (2002). Determining thermal effects in high pressure processing. *Journal of Food Technolgy*, *56*(2), 31-35.

Toepfl, S., Mathys, A., Heinz, V. & Knorr, D. (2006). Review: Potential of emerging technologies for energy efficient and environmentally friendly food processing. *Food Reviews International*, *22*(4), 405 - 423.

Tyler, S. A. & Dipert, M. H. (1962). On estimating the constant of the "multi-hit" curve using a medium speed digital computer. *Physics in Medicine and Biology*, *7*, 201-212.

Ulmer, H. M. (2001). *Molecular mechanisms of the high pressure inactivation of beer spoiling Lactobacillus plantarum*. PhD thesis, Munich, Technische Universität München, 141.

Van Boekel, M. A. J. S. (2002). On the use of the Weibull model to describe thermal inactivation of microbial vegetative cells. *International Journal of Food Microbiology*, *74*(1-2), 139-159.

Van Opstal, I., Bagamboula, C. F., Vanmuysen, S. C. M., Wuytack, E. Y. & Michiels, C. W. (2004). Inactivation of *Bacillus cereus* spores in milk by mild pressure and heat treatments. *International Journal of Food Microbiology*, *92*(2), 227-234.

Van Schepdael, L., De Heij, W. & Hoogland, H. (2004). *Method for high-pressure preservation*. USA, patent, (10/433,418).

Vary, J. C. & Halvorson, H. O. (1965). Kinetics of germination of *Bacillus* spores. *Journal of Bacteriology*, *89*(5), 1340-1347.

VDI (1994). *VDI-Wärmeatlas*. VDI-Verlag GmbH, Düsseldorf.

Vepachedu, V. R., Hirneisen, K., Hoover, D. G. & Setlow, P. (2007). Studies of the release of small molecules during pressure germination of spores of *Bacillus subtilis*. *Letters in Applied Microbiology*, *45*(3), 342-348.

Vergne, P. (1990). New high pressure viscosity measurements on di(2-ethylhexyl) sebacate and comparison with pervious data. *High Temperatures -High Pressures*, *22*, 613-621.

Vergne, P. (1994). Candidate fluids for high-pressure piston standards:State of the art and possible trends. *Metrologia*, *30*, 669-672.

Vreeland, R. H. & Rosenzweig, W. D. (2000). Isolation of a 250 million-year-old halotolerant bacterium from a primary salt crysta. *Nature*, *407*(6806), 897-900.

Wang, S. T., Setlow, B., Conlon, E. M., et al. (2006). The forespore line of gene expression in *Bacillus subtilis*. *Journal of Molecular Biology*, *358*, 16–37.

Watanabe, T., Furukawa, S., Hirata, J., Koyama, T., Ogihara, H. & Yamasaki, M. (2003). Inactivation of *Geobacillus stearothermophilus* Spores by High-Pressure Carbon Dioxide Treatment. *Applied and Environment Microbiology*, *69*(12), 7124-7129.

Watson, H. E. (1908). A note on the variation of the rate of disinfection with change in the concentration of the disinfectant. *Journal of Hygiene*, *8*, 536.

Wiencek, K. M., Klapes, N. A. & Foegeding, P. M. (1990). Hydrophobicity of *Bacillus* and *Clostridium* Spores. *Applied and Environment Microbiology*, *56*(9), 2600-2605.

Wilson, D. C. (1974). High pressure sterilization. In *Proceedings of the IFT 34th Annual Meeting*, New Orleans, USA.

Wilson, M. J. & Baker, R. (2000). *High temperature/Ultra-high pressure sterilization of foods*. USA, patent, (08/572,656), Kal Kan Foods, Inc.

Wilson, M. J. & Baker, R. (2003). *High temperature/Ultra-high pressure sterilization of low acid foods*. UK, patent, (02080565.1), Kal Kan Foods, Inc.

Wisniewski, R., Machowski, P. & Komorowski, P. (1995). The influence of high pressure on the solidification (glass transition) of di(2-ethylhexyl) sebacate. *High Temperatures - High Pressures*, *25/26*, 75-79.

Woese, C. & Morowitz, H. J. (1958). Kinetic of the release of dipicolinic acid from spores of *Bacillus subtilis*. *Journal of Bacteriology*, *76*, 81-83.

Wright, A. M., Hoxey, E. V., Sope, r. C. J. & Davies, D. J. (1995). Biological indicators for low temperature steam and formaldehyde sterilization: the effect of defined media on sporulation, growth index and formaldehyde resistance of spores of *Bacillus stearothermophilus* strains. *Journal of Applied Bacteriology*, *79*(4), 432-8.

Wuytack, E., Peirsman, K. & Michiels, C. (1997). Properties of *Bacillus subtilis* mutant affected in spore germination under high hydrostatic pressure. In K. Heremans. *High pressure research in the biosciences and biotechnology* (pp. 261-264). Leuven University Press, Leuven.

Wuytack, E. (1999). *Pressure-induced germination and inactivation of Bacillus subtilis spores*. Dissertation thesis, Leuven, KU Leuven, 124.

Wuytack, E. Y., Boven, S. & Michiels, C. W. (1998). Comparative study of pressure-induced germination of *Bacillus subtilis* spores at low and high pressures. *Applied and Environmental Microbiology*, *64*(9), 3220-3224.

Wuytack, E. Y., Soons, J., Poschet, F. & Michiels, C. W. (2000). Comparative study of pressure- and nutrient-induced germination of *Bacillus subtilis* spores. *Applied and Environmental Microbiology*, *66*(1), 257-261.

Wuytack, E. Y. & Michiels, C. W. (2001). A study on the effects of high pressure and heat on *Bacillus* subtilis spores at low pH. *International Journal of Food Microbiology*, *64*(3), 333-341.

Zhang, J., Peng, X., Jonas, A. & Jonas, J. (1995). NMR study of the cold, heat, and pressure unfolding of ribonuclease A. *Biochemistry*, *34*(27), 8631-8641.

Zipp, A. & Kauzmann, W. (1973). Pressure denaturation of metmyoglobin. *Biochemistry*, *12*(21), 4217-4228.